Accelerating black objects and their holographic duals



Andrea Boido
St Cross College
University of Oxford

A thesis submitted for the degree of
Doctor of Philosophy
Trinity 2024

Abstract

This thesis is devoted to the study of several geometric aspects, as well as their role in the holographic context, of certain supersymmetric AdS solutions that are expected to describe the near-horizon region of accelerating black holes in 4d and accelerating black strings in 5d. In particular, these are $\mathrm{AdS}_3 \times Y_7$ solutions of type IIB supergravity, sourced by D3-branes, and $\mathrm{AdS}_2 \times Y_9$ solutions of 11d supergravity, sourced by M2-branes. Both Y_7 and Y_9 are total spaces of fibrations with codimension two Sasakian fibres over a two-dimensional orbifold known as spindle. The latter is topologically a two-sphere but has conical deficits angles parametrized by coprime integers $m_\pm \in \mathbb{N}$ whose physical effect is indeed to turn on the acceleration.

We exploit the formalism of geometric extremization together with a series of geometric methods to derive block formulas for many holographic observables of interest, including central charges, free energies, quantized fluxes, and probe brane actions. These allow us to recover previously known results for numerous explicit supergravity solutions and to significantly generalize them to various other compactifications.

For the AdS_3 solutions (with toric internal space) we give a general proof that our off-shell supersymmetric action agrees with an appropriate off-shell central charge in the dual field theory, establishing a very general exact result in holography.

For the AdS_2 solutions we provide a general geometric prescription for reproducing various physical quantities appearing in the matrix model arising from the large N limit of the localized partition function of the dual field theory. Here we focus on the non-accelerating case but we comment on how our results should be extended to the accelerating case too.

We illustrate our findings with many examples throughout, including an explicit solution obtained in 5d STU gauged supergravity and uplifted on a five-sphere.

Statement of Originality

This thesis is based on results from the following publications, to which the author contributed substantially:

[1] Andrea Boido, Juan Manuel Pérez Ipiña, James Sparks, *Twisted D3-brane and M5-brane compactifications from multi-charge spindles*, JHEP 07 (2021) 222, arxiv:2104.13287

[2] Andrea Boido, Jerome P. Gauntlett, Dario Martelli, James Sparks, *Entropy Functions For Accelerating Black Holes*, Phys.Rev.Lett. 130 (2023) 9, 091603, arxiv:2210.16069

[3] Andrea Boido, Jerome P. Gauntlett, Dario Martelli, James Sparks, *Gravitational Blocks, Spindles and GK Geometry*, Commun.Math.Phys. 403 (2023) 2, 917-1003, arxiv:2211.02662

[4] Andrea Boido, Alice Lüscher, James Sparks, *Matrix models from black hole geometries*, JHEP 05 (2024) 226, arxiv:2312.11640

A version of [1] appeared previously in the DPhil thesis of co-author Juan Manuel Pérez Ipiña.

Acknowledgements

The present thesis is the result of a very long journey, certainly a challenging one but also extremely rewarding. I come out of it as a much better physicist, with an enrichment of my scientific knowledge that is second only to my growth as a person. The experience of living abroad for the first time and in such a rich and diverse environment has been really invaluable. I couldn't be happier to have reached this milestone and I shall now take the time to thank everyone who made it possible.

First and foremost, my deepest gratitude goes to my supervisor, James Sparks. He is an exceptional researcher, and I cannot overstate how fortunate I feel to have had the privilege of being his student. Even during the busiest moments, he never failed to generously share his immense knowledge of mathematics and physics. His guidance, encouragement, and invaluable insights have been instrumental in the successful completion of this thesis.

I am also grateful to all the great people I collaborated with during these years, from senior researchers Jerome Gauntlett and Dario Martelli, to fellow PhDs Juan Ipiña and Alice Lüscher. Working with them has been a really enriching experience, and their knowledge, enthusiasm and dedication have been truly motivating. I would like to acknowledge Pieter Bomans, Davide Cassani, Chris Couzens, Pietro Ferrero, Enrico Marchetto, and Palash Singh too for fruitful exchange of ideas that helped me grow as a researcher. I am particularly thankful to Chris for his monumental patience and willingness to answer every single one of my numerous questions and provide feedback on much of my work.

I would like to sincerely thank everyone with whom I shared my daily life in the past four years, starting from my fellow PhD students and postdocs at the Mathematical Institute (too many to name) for all the moments of break from work as well as the shared experiences. Thank you also to all my friends from Padua and to the cineforum group, all the jokes and the conversations in our group chats have been invaluable for my mental health, especially during the Covid-19 pandemic. To my gaming friends Andrea Di Sarno and Andrea Fattarelli, thank you for the weekly escape and all the countless laughs that helped me unwind and recharge. And thank you to Matteo Alasio, Letizia Bergamasco, Marco Eterno, Morena Porzio, and Andrea Senacheribbe for their friendship and never-ending support.

A big thank you to my parents and all my closest family members. I couldn't have made it to where I'm now without the quiet and loving atmosphere I grew up in.

To 雨杉, your love, kindness, and support in these last few months made the process of writing up this thesis much less of a burden than it would have been otherwise. I can't thank you enough for this.

Finally, a special thank you to mathematics and physics. The last nine years of my life revolved around their study and the way I now look at the world around me is deeply shaped by them. They will keep accompanying me throughout my life.

Contents

1 Introduction **2**

1.1 The AdS/CFT correspondence and microstate counting 2

1.2 Geometric extremization principles 8

1.2.1 Extremization principles in field theory 9

1.2.2 Sasaki-Einstein volume minimization 9

1.2.3 GK extremization 13

1.3 Spindle: an overview 19

1.4 Outline of the thesis 21

2 The geometry of spindle solutions **24**

2.1 Fibrations over a spindle 24

2.1.1 Building the fibration 25

2.1.2 Twist and anti-twist 27

2.2 Explicit supergravity solution with $X_5 = S^5$ 30

2.2.1 Local 5d metric and uplift to IIB 30

2.2.2 Global analysis and general solution 32

2.2.3 Central charge and R-symmetry 36

3 Gravitational blocks **39**

3.1 Derivation of the general block formula 39

3.1.1 Gravitational block lemma 40

3.1.2 Gravitational block formula 42

3.2 Flavour and universal (anti-)twist 45

3.2.1 Flavour twist 45

3.2.2 Universal anti-twist 50

3.3 Examples 56

3.3.1 $\mathrm{AdS}_3 \times Y_7$ solutions with $X_5 = S^5$ 56

3.3.2 $\mathrm{AdS}_2 \times Y_9$ solutions with $X_7 = S^7$ . . . 59
3.3.3 $\mathrm{AdS}_2 \times Y_9$ solutions with $X_7 = V^{5,2}$ . . . 63

4 Toric perspective **66**
4.1 Review of toric geometry . . . 66
4.1.1 Toric cones . . . 66
4.1.2 The master volume . . . 68
4.1.3 GK extremization for toric Y_{2n+1} . . . 70
4.2 Toric geometry fibred over a spindle . . . 71
4.2.1 Toric data for Y_{2n+1} . . . 72
4.2.2 Relating the master volumes of Y_{2n+1} and X_{2n-1} . . . 75
4.2.3 Geometric extremization for $X_{2n-1} \hookrightarrow Y_{2n+1} \to \Sigma$ . . . 79
4.2.4 R-charges of baryonic operators . . . 82
4.2.5 The limit when $b_0 = 0$, $m_\pm = 1$ . . . 84

5 Holography - AdS_3 (toric) case **86**
5.1 Central charge from anomaly polynomial . . . 86
5.1.1 D3-brane anomaly polynomial . . . 86
5.1.2 c-extremization and superconformal R-symmetry . . . 89
5.2 Matching $\mathrm{AdS}_3 \times Y_7$ solutions with field theory . . . 89
5.2.1 4d $\mathcal{N} = 1$ SCFT on $\mathbb{R}^{1,1} \times \Sigma$ . . . 90
5.2.2 Matching with GK geometry . . . 92
5.2.3 New variables . . . 94
5.3 Example: $\mathrm{AdS}_3 \times Y_7$ solutions with $X_5 = T^{1,1}$ . . . 95

6 Holography - AdS_2 case **99**
6.1 3d $\mathcal{N} = 2$ Chern-Simons-matter theories . . . 99
6.1.1 Geometric engineering . . . 99
6.1.2 Topologically twisted matrix model . . . 106
6.2 Near-horizon geometry of non-accelerating black holes . . . 113
6.2.1 Fibrations over Σ_g . . . 113

6.2.2 Flavour twist . . . 115
6.2.3 Example: $X_7 = S^7$ . . . 116
6.3 Matrix model geometry . . . 118
6.3.1 Holography of free energies and R-charges . . . 119
6.3.2 M-theory circle moment map . . . 121
6.3.3 Eigenvalue density from geometry . . . 125
6.3.4 M2-branes and Wilson loops . . . 131
6.4 Matrix models on the spindle . . . 138
6.4.1 Shifted eigenvalue densities . . . 138
6.4.2 Connecting to the refined twisted index . . . 142
6.5 Matrix models from toric spaces . . . 145
6.5.1 Critical points and M2-branes . . . 145
6.5.2 Eigenvalue density . . . 146
6.5.3 Example: $C(X_7) = \mathbb{C} \times C(T^{1,1})$ . . . 150

7 Discussion and outlook **157**

A Appendices **161**
A.1 Delzant construction . . . 161
A.2 Fluxes from Kaluza-Klein reduction . . . 164
A.3 Matching GK geometry for $\mathrm{AdS}_3 \times Y_7$ with field theory . . . 169
A.3.1 $\mathscr{Z}$ as a function of $R_a^{\pm}$ . . . 170
A.3.2 Proof of baryonic extremization conditions . . . 174
A.3.3 $R_a^{\pm}$ as functions of b_2, b_3 . . . 179
A.4 BPS condition for M2-branes . . . 180

Bibliography **183**

Conventions

Throughout the thesis we will use a set of symbols whose meaning is implied. Here we present a list of these.

- $\mathrm{d}s_X^2$ denotes the local line element of the space X.
- More generally, $\mathrm{d}s_d^2$ denotes the local line element of a space of dimension d.
- vol_X denotes the volume form of the space X.
- $\mathrm{Vol}(X)$ denotes the total volume of the space X.
- $\mathcal{R}$ is used for the Ricci tensor (with indices) and for the Ricci scalar (without indices).
- $\star_d$ denotes the Hodge duality operator in d dimensions.
- $G_{(d)}$ denotes the effective Newton constant in d dimensions.
- Actions will be denoted with the letter I and suitable sub/superscripts - except for the GK supersymmetric action S_{SUSY}.
- Σ with no sub/superscripts always denotes a spindle with parameters $m_{\pm}$.

Clashes of nomenclature will be avoided as much as possible but there are a few instances where the same symbol is used for different objects. If unclear from the context, it will be made explicit on a case by case basis which object is intended.

Chapter 1

Introduction

1.1 The AdS/CFT correspondence and microstate counting

The celebrated *holographic principle*, along with its concrete realization through the *AdS/CFT correspondence*, is undeniably one of the most significant breakthroughs that theoretical physics experienced over the past few decades. The idea of relating gauge theories with a large number of colours (N) with string theory was put forward by 't Hooft [5] by looking at the topology of Feynman diagrams in $U(N)$ Yang-mills theory in the $N \to \infty$ limit. It was not until shortly after Polchinski's understanding of D-branes and their role in string theory [6] that Maldacena could successfully formulate the famous conjecture that CFTs arising as worldvolume theories on a stack of branes are dual to string theory/M-theory living in AdS backgrounds [7]. The duality was then refined in [8, 9], where the authors proposed concrete relations between observables in the two sides.

The basic idea of the AdS/CFT correspondance is to consider string theory/M-theory in the presence of a large number N of D/M-branes. In this regime, the branes are heavy enough that their backreaction on the geometry cannot be ignored and in particular the spacetime gets deformed in such a way that an AdS factor appears. Furthermore, string theory becomes weakly coupled and can be described purely in terms of *supergravity*, with the deformed geometry being one of its vacua *i.e.* a classical solution of the supergravity equations of motion. On the other hand, the same setup gives rise to a gauge theory with N colours living on the branes worldvolume, which in general is expected to be strongly coupled. One can then relate observables in supergravity with their counterparts in field theory and use one of the two sides to gain insights into the other and vice versa.[1] The "holographic" nature of the correspondence resides in the fact that the field theory lives in one dimension less than the AdS factor in the supergravity background, so that naively one may think the

[1] For a more in depth overview of the generalities of the AdS/CFT correspondence see *e.g.* [10–12].

former lives on the (conformal) boundary of AdS.

The standard example consists in considering a stack of N coincident D3-branes in type IIB theory in flat space. When N becomes large, the spacetime geometry originated by the branes is $\mathrm{AdS}_5 \times S^5$ which is a maximally supersymmetric solution of type IIB supergravity with N units of five-form F_5 flux. The worldvolume theory is 4d $\mathcal{N} = 4$ super-Yang-Mills (SYM) with gauge group $SU(N)$. Note that both sides preserve the maximum number of supercharges (32). Moreover, the global $SO(6)$ R-symmetry is geometrized via the correspondence to become the $SO(6)$ isometry of the internal 5-sphere, while the 4d conformal group $SO(2,4)$ precisely matches the isometry group of AdS_5. But the duality goes further than this, and numerous physical quantities can explicitly be matched: free energy, correlation functions, spectrum of primary operators, Wilson loops, etc. Similar constructions were studied for setups originating from M2/M5-branes in M-theory, leading to $\mathrm{AdS}_4 \times S^7$ and $\mathrm{AdS}_7 \times S^4$ backgrounds respectively, with dual field theory the 3d $\mathcal{N} = 8$ ABJM theory [13] and the non-lagrangian 6d $\mathcal{N} = (2,0)$ theory [14, 15].

Ever since the first appearance of the AdS/CFT correspondence, extending its applicability scope has been a major branch of research, motivated by the hope of being able to use it to gain insights into longstanding problems and learn new physics.[2] A huge literature on the classification of supersymmetric solutions of 10d/11d supergravity stemmed from this necessity, in particular after the pioneering works [16–18] where it was realized that the geometry of the internal space is highly constrained by the Killing spinors, whose existence is required by supersymmetry. Following these, a plethora of results appeared, describing many backgrounds with AdS factors in different dimensions with different combinations of fluxes turned on.

Of particular interest for this thesis are AdS_5 and AdS_3 backgrounds in type IIB supergravity supported by the RR five-form flux F_5 only and AdS_4 and AdS_2 backgrounds in 11d supergravity supported by the seven-form flux $G_7 = \star_{11} G_4$ only, with no fibration of the AdS factor over the internal manifold. The AdS_5 and AdS_4 backgrounds arise from respectively D3-branes and M2-branes sitting at the singular point of a Calabi-Yau cone of suitable dimension (CY_3 the former, CY_4 the latter) [19–21]. These are complex cones over

[2] For the purposes of this thesis we will limit ourselves to discussing setups originating from string theory.

Sasaki-Einstein spaces (SE) of which many examples are known, including a countably infinite class which was discovered precisely while looking at AdS backgrounds [22–26]. The resulting solutions look like $\mathrm{AdS}_5 \times X_5$ and $\mathrm{AdS}_5 \times X_7$, with X_5 and X_7 the SE manifolds that form the base of the CY cones, and preserve less supersymmetry (in particular at least 1/4 of it) compared to the above examples where the internal manifold is a sphere. The dual field theories were identified to be 4d $\mathcal{N} = 1$ SYM coupled to matter [19, 27–30] and 3d $\mathcal{N} = 2$ Chern-Simons-matter theories [31–34]. Instead, the AdS_3 and the AdS_2 backgrounds are obtained by partially wrapping the same branes on two-cycles of Calabi-Yau spaces with one more complex dimension (*i.e.* CY_4 and CY_5 respectively). The backreacted geometries take the form $\mathrm{AdS}_3 \times Y_7$ and $\mathrm{AdS}_2 \times Y_9$, with Y_7 and Y_9 both being *Gauntlett-Kim* spaces (GK) [35–37], and the dual field theories being 2d $\mathcal{N} = (0, 2)$ SCFTs (see e.g. [38, 39]) and 1d superconformal quantum mechanics.[3] The geometries of SE and GK spaces share many similarities and will be briefly reviewed in the next subsection 1.2 as they play a crucial role in the duality.

An important point to highlight is that a subset of the AdS_3 and AdS_2 solutions above are deeply related with parent AdS_5 and AdS_4 solutions in the following way. Consider for example the brane setup that gives rise to AdS_4 solutions *i.e.* M2-branes at the conical singularity of a CY_4; one can further wrap the branes on a compact two dimensional space Σ_2 and, provided supersymmetry can be preserved (more on this point shortly), end up with a configuration where topologically $\Sigma_2 \times \mathrm{CY}_4 \simeq \mathrm{CY}_5$ [4] which is precisely the one giving rise to one of the AdS_2 solutions above. This is realized on the field theory side as a compactification on Σ_2 of the parent 3d $\mathcal{N} = 2$ SCFT dual to $\mathrm{AdS}_4 \times X_7$ followed by flowing to the infrared to obtain the superconformal quantum mechanics in one dimension dual to $\mathrm{AdS}_2 \times Y_9$, where $Y_9 \simeq \Sigma_2 \times X_7$ topologically. A similar relationship exists between $\mathrm{AdS}_5 \times X_5$ solutions and $\mathrm{AdS}_3 \times Y_7$ solutions with the topology of the GK Y_7 being that of Σ_2 times the SE X_5. These are examples of the phenomenon known as *flow across dimensions* that is schematically represented in figure 1.1. The first instance where this kind of construction appeared was in [40], where the authors described D3-branes and M5-branes wrapping a constant curvature

[3] There is no precise understanding of the latter in a purely 1d picture. Most known examples start from 3d theories and further compactify these on two dimensional spaces - we will talk more about these shortly.

[4] In general CY_5 will be a non-trivial fibration rather than a direct product.

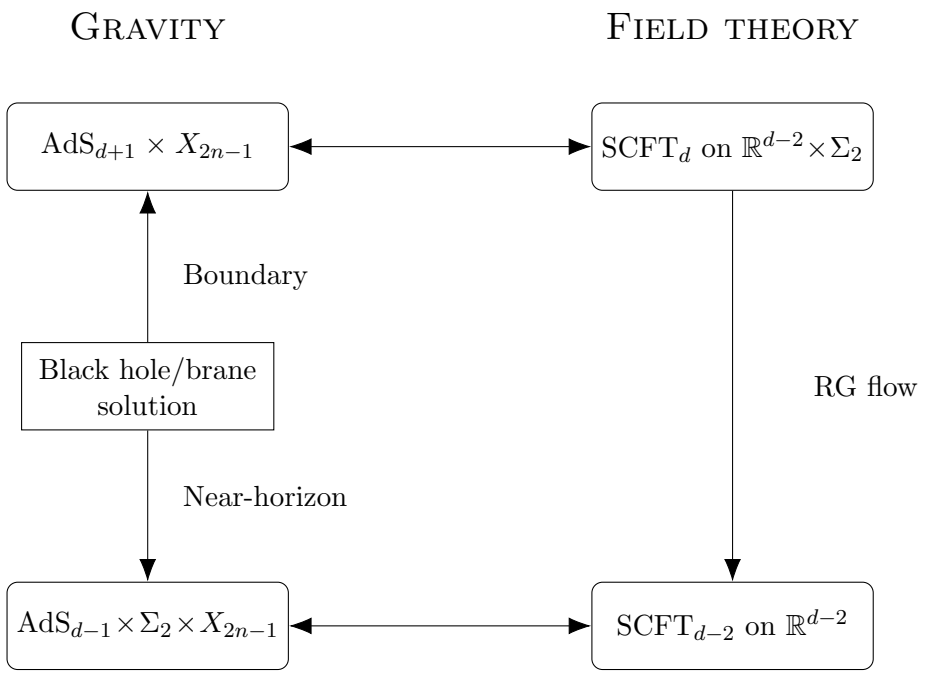


Figure 1.1: Flow across dimensions. For our purposes either $d = 3$ and $n = 4$ or vice versa.

Riemann surface Σ_g of genus $g > 1$. This work has subsequently been generalized in many directions, leading to a large literature on the subject. To cite a few examples, people considered branes wrapping higher dimensional compact spaces [41], Riemann surfaces with punctures [42], surfaces with non-constant curvature [43], etc.

The most widely used mechanism to preserve supersymmetry when wrapping branes on two-cycles is the *topological twist* [44, 45], which has the perk of being relatively simple and has by now been extensively studied.[5] In order to define a field theory on a compact space Σ_2 and preserve supersymmetry, the so-called Killing spinor equation (KSE) has to be satisfied. Schematically, it reads

$$(\nabla_\mu + (A_R)_\mu)\,\epsilon = (\partial_\mu + \omega_\mu + (A_R)_\mu)\,\epsilon = 0\,, \tag{1.1}$$

where ϵ is an off-shell spinor on Σ_2, A_R is a background R-symmetry gauge field, and ω_μ is the spin connection contracted with a suitable combination of flat space gamma matrices. The idea of the topological twist is to simply take the gauge field to be $(A_R)_\mu = -\omega_\mu$ so as

[5] For higher dimensional cycles another widely used approach is the one of [46].

to cancel all the "connection terms" and reduce (1.1) to the simple equation

$$\partial_\mu \epsilon = 0 \,, \tag{1.2}$$

which simply tells that ϵ is a section of a trivial bundle over Σ_2. For the following, it will be useful to note that requiring $(A_R)_\mu = -\omega_\mu$ imposes a condition on the magnetic flux Q_R through Σ_2

$$Q_R = \frac{1}{2\pi}\int_{\Sigma_2} \mathrm{d}A_R = -\frac{1}{2\pi}\int_{\Sigma_2} \mathrm{d}\omega = -\chi(\Sigma_2) \,, \tag{1.3}$$

where in the last step we used the Gauss-Bonnet theorem to read the Euler characteristic $\chi(\Sigma_2)$. Hence we obtain that a topological twist requires the magnetic flux of the background R-symmetry gauge field to be minus the Euler characteristic of the surface itself. In recent years however, a different mechanism to preserve supersymmetry was discovered [47, 48] and this thesis will be mostly focused on that. We will come back to this point in section 1.3.

The flow across dimensions is also intimately tied with another very fruitful application of the AdS/CFT correspondence: the statistical description of the thermodynamics of asymptotically AdS black holes. Ever since the seventies, black holes have been known to possess a temperature and an entropy [49–52]. In particular, their entropy $\mathscr{S}$ is proportional to the area of the event horizon, which suggests that the underlying microstates are localized there. Note how this is another realization of the holographic principle: the volume of space corresponding to the black hole is indeed described purely in terms of its boundary. The identification of such microstates from a statistical perspective has been a central question for many years and eventually it was possible to successfully give an answer for a certain class of asymptotically flat black holes thanks to string theory [53, 54]. Following these results, many extensions have been considered but it took almost twenty years to answer the same question in the case of asymptotically AdS black holes. After the failed attempt of [55] - already relying on the AdS/CFT correspondence - the first successful microscopic counting for AdS black holes was performed in [56]. There the authors considered supersymmetric and magnetically charged black holes in AdS_4 which can be uplifted to M-theory on S^7. These are solutions that interpolate between an AdS_4 boundary and an $\mathrm{AdS}_2 \times \Sigma_g$ near-horizon region,

with Σ_g a genus g Riemann surface. In this sense moving along the radial direction of the black holes correspond to moving along the RG flow that starts from 3d ABJM theory and flows to a superconformal quantum mechanics originating from putting the former theory on $\mathbb{R} \times \Sigma_g$ with a topological twist along Σ_g (see again figure 1.1). The microscopic degrees of freedom accounting for the entropy of the black holes are computed holographically via the Witten index of the superconformal quantum mechanics at the IR fixed point of the RG flow above, which in turn is given by the supersymmetric partition function of ABJM theory on $S^1 \times \Sigma_g$. Note the time direction has been Wick rotated to Euclidean signature and compactified to a circle in order to use supersymmetric localization, which allows to compute the exact partition function by arguing that it receives contributions from BPS configurations of the fields in the moduli space only [57, 58]. Following [56], many generalizations to different classes of AdS black holes and in different dimensions have been considered, some of which we will refer to later on in the thesis (see [59] for a nice review and a complete set of references).

In general, supersymmetric black holes are characterized by possessing an AdS_2 factor in their near-horizon geometry and many of them, once uplifted to 11d supergravity, are expected to belong to the class of $\mathrm{AdS}_2 \times Y_9$ solutions above, arising from parent $\mathrm{AdS}_4 \times X_7$ solutions in the sense of the flow across dimension. In this thesis we will be interested in solutions with an AdS_3 factor too, which instead correspond to supersymmetric black strings. The equivalent setup to the black holes above are black string in AdS_5 with horizon geometry given by $\mathrm{AdS}_3 \times \Sigma_g$ that can be uplifted to IIB supergravity on S^5. These realize holographically the RG flow between 4d SYM compactified on Σ_g and the IR fixed point given by a 2d $\mathcal{N} = (2, 0)$ SCFT [60,61]. The observables that mirrors the entropy in this case is the central charge c of the two dimensional field theory, which can be computed in gravity using the Brown-Henneaux formula [62] and correctly matched with the field theory result. Similarly to the black holes, in general, supersymmetric black strings have an AdS_3 factor in the near-horizon and many of them, once uplifted to type IIB supergravity, are expected to belong to the class of $\mathrm{AdS}_3 \times Y_7$ solutions above that are related to parent $\mathrm{AdS}_5 \times X_5$ solutions, and this is what we will be studying in this thesis.

Finally, let us point out that, aside the black holes and black strings constructed in gauged supergravities arising from consistent truncations of 10d/11d supergravity on spheres, not

many full-flow solutions are known in the literature, as most of the times solving the equations of motion is rather hard. An alternative approach that allows to compute observables associated to AdS background with different internal spaces is the one of *geometric extremization* which does not require knowing the full solution and which we review in some details in the next section.[6] The present thesis will make extensive use of this principle to detail various recent holographic results concerning AdS spaces which are obtained by compactifying branes on a two dimensional orbifold known as *spindle*, which can be naively thought as the horizon of accelerating black holes/strings. We will explain more in details the nature of this space in section 1.3, but first let us give a quick review of geometric extremization.

1.2 Geometric extremization principles

Finding explicit black hole/string solutions as described in the previous section is in general a hard task. The most used strategy is to construct these in 4d/5d gauged supergravities and then uplift them on a suitable internal space. However, except for a few cases, we lack consistent truncations of 10d/11d supergravity on most internal manifolds, and therefore this strategy become less viable. Even with a consistent truncation though, it is not guaranteed to be able to solve Einstein equations in closed form. The approach we will take here is to focus purely on their near-horizon geometry - which always contains an AdS factor - and allow for the corresponding solution to be "partially off-shell" in a sense that we will make precise momentarily. The observables of interest are then obtained by extremizing suitable algebraic functions over a certain set of unfixed parameters, which is a significantly simpler task compared to solving Einstein equations. The whole idea here is to mimic in gravity the extremization principles that give the exact superconformal R-symmetry in field theory first appeared for 4d $\mathcal{N} = 1$ SCFTs in [63] but then extended to SCFTs in other dimensions [56, 64, 65]. We review these ideas next.

[6] It has to be noted however, that this approach does not say anything on whether a certain solution should exist or not, it simply provides predictions assuming the first is true. In that sense, it is conjectural to some extent, though holography itself can provide evidence of its validity.

1.2.1 Extremization principles in field theory

Supersymmetric field theories all posses a global R-symmetry. In the case of minimal susy *e.g.* $\mathcal{N}=1$ in four dimensions, the R-symmetry group is $U(1)_R$.[7] However, in general the theory will possess other global $U(1)$ "flavour" symmetries, whose generators we label F_a. Now, the symmetry algebra does not uniquely determine the R-symmetry: if R_0 is a generator of $U(1)_R$, then

$$R = R_0 + \sum_a \Delta_a F_a \tag{1.4}$$

is a perfectly valid generator too, where Δ_a are arbitrary real parameters. Assuming the theory flows to a superconformal fixed point in the IR, the exact superconformal R-symmetry R^* will correspond to a particular choice of the parameters Δ_a^*. In [63] it was first argued that this choice amounts to extremizing a certain function $f(\Delta_a)$ *i.e.*

$$\left.\frac{\partial f(\Delta_a)}{\partial \Delta_a}\right|_{\Delta_a=\Delta_a^*} = 0\,. \tag{1.5}$$

The function f was identified to be one of the two central charges of 4d $\mathcal{N}=1$ SCFTs

$$a = \frac{3}{32}\left(3\,\mathrm{Tr}\,R^3 - \mathrm{Tr}\,R\right). \tag{1.6}$$

With slight differences, the same approach can be used to determine the superconformal R-symmetry in SCFTs in other dimensions, with the function f being a dimension specific observable, typically a central charge or the free energy *i.e.* minus the logarithm of the partition function. For an overview of these and relative references see table 1.1. In general it turns out that f is either a polynomial in the Δ_a or, at most, a sum of square roots of polynomials, so that the task of finding extrema reduces to solving algebraic equations.

1.2.2 Sasaki-Einstein volume minimization

Firstly, we describe how said extremization principle can be realized in gravity by looking at "empty" AdS solutions, in particular $\mathrm{AdS}_5 \times X_5$ solutions of type IIB supergravity arising

[7] If more susy is present, one can pick any Cartan subgroup of the R-symmetry group and follow the same reasoning.

d	Susy	Function $f(\Delta_a)$	Geometry	Field theory	Gravity
4	$\mathcal{N}=1$	Central charge a	$\mathrm{AdS}_5\times X_5$	[63]	[66, 67]
3	$\mathcal{N}=2$	Free energy	$\mathrm{AdS}_4\times X_7$	[64]	[66, 67]
2	$\mathcal{N}=(0,2)$	Central charge c	$\mathrm{AdS}_3\times Y_7$	[65]	[68]
1	$\mathcal{N}=1$	Free energy	$\mathrm{AdS}_2\times Y_9$	[56]	[68]

Table 1.1: Overview of extremization principles in holography. Note that the geometries indicated here are those we are interested in in this thesis but there are other possibilities that lead to the same classes of field theories *e.g.* $\mathrm{AdS}_5\times M_6$ solutions in M-theory.

from N D3-branes at the conical singularity of $C(X_5)$, and $\mathrm{AdS}_4\times X_7$ solutions of M-theory arising from N M2-branes at the conical singularity of $C(X_7)$. In both cases, the internal space X_{2n-1} is Sasaki-Einstein (see [69] for a review of SE geometry) and the cone $C(X_{2n-1})$ is Calabi-yau. However, following [66,67] we can go "off-shell" and consider $C(X_{2n-1})$ equipped with a Kähler, but not necessarily Ricci-flat, cone metric

$$\mathrm{d}s^2_{C(X_{2n-1})}=\mathrm{d}r^2+r^2\,\mathrm{d}s^2_{X_{2n-1}}\,. \tag{1.7}$$

When the cone (1.7) is Kähler the induced metric $\mathrm{d}s^2_{X_{2n-1}}$ on $X_{2n-1}=\{r=1\}\subset C(X_{2n-1})$ is by definition Sasakian (but not necessarily Einstein) and therefore comes equipped with a unit length Killing vector field ξ called *Reeb vector field*. In particular the metric on X_{2n-1} can be written as

$$\mathrm{d}s^2_{X_{2n-1}}=\tilde{\eta}^2+\mathrm{d}s^2_{2n-2}(\omega_S)\,, \tag{1.8}$$

where $\tilde{\eta}$ is the one-form dual to ξ, i.e. $\xi\lrcorner\,\tilde{\eta}=1$ (and $\xi\lrcorner\,\mathrm{d}\tilde{\eta}=0$). The metric (1.8) itself is transversely Kähler, with Kähler two-form ω_S and $\mathrm{d}\tilde{\eta}=2\omega_S$.[8] The transverse Kähler form on the base of the cone can be related with the Kähler form $\mathcal{J}$ on the cone itself in the following way

$$\mathcal{J}\equiv\frac{1}{2}\,\mathrm{d}(r^2\tilde{\eta})=r\,\mathrm{d}r\wedge\tilde{\eta}+r^2\,\omega_S\qquad\Longrightarrow\ \mathcal{J}\,\big|_{r=1}=\omega_S\,. \tag{1.9}$$

[8]The superscript in ω_S is meant to highlight that this Kähler two-form is such that the metric (1.8) is Sasakian.

The holomorphic $(n,0)$-form $\Psi_{(n,0)}$ on the cone $C(X_{2n-1})$ has charge n under ξ i.e.

$$\mathcal{L}_\xi \Psi_{(n,0)} = n\mathrm{i}\Psi_{(n,0)} \,. \tag{1.10}$$

We assume that X_{2n-1} has a $U(1)^s$ isometry with $1 \leq s \leq n$, and we call the corresponding generating vector fields ∂_{φ_i}, $i = 1, \ldots, s$, with the coordinates φ_i having period 2π. Note that the case $s = n$ corresponds to a toric cone. Having introduced the coordinates φ_i, we may parameterize the Reeb vector field ξ as

$$\xi = \sum_{i=1}^{s} b_i \, \partial_{\varphi_i} \,. \tag{1.11}$$

In particular, we choose the basis in (1.11) in such a way that $\Psi_{(n,0)}$ has charge 1 under ∂_{φ_1} and is uncharged under all other ∂_{φ_i}, so that (1.10) is achieved by setting $b_1 = n$.

The Killing vector field ξ in (1.11) implements geometrically $\mathrm{U}(1)_R$ symmetry of the dual field theory and therefore we may loosely identify the parameters b_i with the Δ_a in field theory - going in the details of this identification is out of this thesis purpose. In fact, it turns out that the field theory extremization described in the previous section is equivalent to extremizing the Sasakian volume $\mathrm{Vol}_S(X_{2n-1})$ as a function of b_i, fixing $b_1 = n$. The extremal value b_i^* brings the geometry on-shell and corresponds to a SE X_{2n-1} and in turn to a Ricci-flat cone $C(X_{2n-1})$.

1.2.2.1 AdS_5 solutions from D3-branes

Starting with $n = 3$, we place N D3-branes at the singular point $\{r = 0\} \in C(X_5)$. Including their backreaction and then taking the near-horizon limit, results in the associated AdS_5 backgrounds

$$\begin{aligned} \mathrm{d}s_{10}^2 &= L^2 \left(\mathrm{d}s_{\mathrm{AdS}_5}^2 + \mathrm{d}s_{X_5}^2 \right) \,, \\ F_5 &= 4L^4 \left(\mathrm{vol}_{\mathrm{AdS}_5} + \mathrm{vol}_{X_5} \right) . \end{aligned} \tag{1.12}$$

The constant length scale L is fixed by flux quantization via

$$L^4 = \frac{(2\pi\ell_s)^4 g_s\, N}{4\mathrm{Vol}_S(X_5)}\,, \tag{1.13}$$

where ℓ_s is the string length, g_s is the string coupling constant, $\mathrm{Vol}_S(X_5)$ is the volume of the Sasakian metric on X_5, and the integer flux N is

$$N = \frac{1}{(2\pi\ell_s)^4 g_s} \int_{X_5} F_5 \in \mathbb{N} \tag{1.14}$$

and gives the number of D3-branes.

The relevant observable for these solutions is the central charge of the dual 4d $\mathcal{N}=1$ SCFT, which computed in gravity is

$$a_{\mathrm{grav}}[\xi] = \frac{\pi}{8G_{(5)}} = \frac{\pi^3}{4\mathrm{Vol}_S(X_5)[\xi]}\, N^2\,. \tag{1.15}$$

Here $\mathrm{Vol}_S(X_5)[\xi]$ highlights the fact that the Sasakian volume of X_5 is a function of the Reeb vector field ξ [66, 67]. As anticipated, the 10d metric and five-form in (1.12) give an $\mathcal{N}=2$ supersymmetric solution to ten-dimensional supergravity precisely when the Sasakian metric $\mathrm{d}s^2_{X_5}$ is also Einstein, or equivalently when the Kähler cone metric (1.7) is also Ricci-flat, *i.e.* Calabi-Yau. In [66, 67] it was shown that such metrics precisely minimize the volume $\mathrm{Vol}(X_5)[\xi]$, as a function of ξ subject to the charge constraint (1.10) which fixes its normalization. It immediately follows that the extremal value of ξ then maximizes the holographic central charge a_{grav} in (1.15).

1.2.2.2 AdS_4 solutions from M2-branes

Instead, placing N M2-branes at the singular point $\{r=0\} \in C(X_7)$, including their back-reaction and then taking the near-horizon limit, results in the associated AdS_4 backgrounds

$$\begin{aligned} \mathrm{d}s^2_{11} &= L^2 \left(\tfrac{1}{4}\,\mathrm{d}s^2_{\mathrm{AdS}_4} + \mathrm{d}s^2_{X_7}\right)\,, \\ G_4 &= \tfrac{3}{8} L^3 \mathrm{vol}_{\mathrm{AdS}_4}\,. \end{aligned} \tag{1.16}$$

The constant length scale L is fixed by flux quantization via

$$L^6 = \frac{(2\pi\ell_p)^6 N}{6\mathrm{Vol}_S(X_7)}\,, \tag{1.17}$$

where ℓ_p is the eleven-dimensional Planck length, $\mathrm{Vol}_S(X_7)$ is the volume of the Sasakian metric on X_7, and the integer flux N is

$$N = \frac{1}{(2\pi\ell_p)^6}\int_{X_7} \star_{11} G_4 \in \mathbb{N} \tag{1.18}$$

and gives the number of M2-branes.

The relevant observable for these solutions is the holographically renormalized gravitational free energy

$$F_{\mathrm{grav}}[\xi] = \sqrt{\frac{2\pi^6}{27\mathrm{Vol}_S(X_7)[\xi]}}\, N^{3/2}\,, \tag{1.19}$$

Similar to before, the eleven-dimensional metric and four-form in (1.16) give an $\mathcal{N} = 2$ supersymmetric solution to eleven-dimensional supergravity when the Sasakian metric $\mathrm{d}s^2_{X_7}$ is also Einstein, which is when the Kähler cone metric (1.7) is also Ricci-flat. Again, such metrics minimize the volume $\mathrm{Vol}(X_7)[\xi]$, which means that the extremal value of ξ then maximizes the holographic free energy F_{grav} in (1.19).

1.2.3 GK extremization

Now we move to discuss solutions with AdS factors in lower dimensions, where the internal space Y_{2n+1} is equipped with a GK geometry [37]. In particular, we are interested in a class of supersymmetric $\mathrm{AdS}_3 \times Y_7$ solutions of type IIB string theory supported by D3-brane flux [35] and $\mathrm{AdS}_2 \times Y_9$ solutions of M-theory supported by M2-brane flux [36]. These include the geometries relevant for studying the near-horizon of the black holes/strings we are interested in. Similarly to before, in [68] solutions of this kind to the supergravity equations of motion were shown to be critical points of a certain finite-dimensional extremal problem for GK geometry, which we now review.

GK geometry [37] is defined on odd-dimensional Riemannian manifolds $Y = Y_{2n+1}$, of

dimension $2n+1$, where $n \geq 3$. The metric on Y_{2n+1} is equipped with a unit norm Killing vector field ξ, called the R-symmetry vector as it implements geometrically the $U(1)_R$ symmetry of the dual field theory. This has an analogous role to the Reeb vector field in (1.11) and that motivates the abuse of notation. Since ξ is nowhere vanishing, it defines a foliation $\mathcal{F}_\xi$ of Y_{2n+1}, and in local coordinates we may write

$$\xi = \frac{1}{\mathsf{c}}\,\partial_z\,, \qquad \eta = \mathsf{c}\,(\mathrm{d}z + P)\,, \tag{1.20}$$

where we have defined $\mathsf{c} \equiv \frac{1}{2}(n-2)$, and η is the Killing one-form dual to ξ. The metric on Y_{2n+1} then takes the form

$$\mathrm{d}s^2_{Y_{2n+1}} = \eta^2 + \mathrm{e}^B\,\mathrm{d}s^2_{2n}(J)\,, \tag{1.21}$$

where $\mathrm{d}s^2_{2n}$ is a Kähler metric transverse to $\mathcal{F}_\xi$ with Kähler two-form J, Ricci two-form $\varrho = \mathrm{d}P = \mathrm{d}\eta$, and a positive Ricci scalar $\mathcal{R} > 0$. The conformal factor e^B in (1.21) is determined completely by the Kähler form as

$$\mathrm{e}^B = \frac{\mathsf{c}^2}{2}\,\mathcal{R}\,. \tag{1.22}$$

The metric cone over Y_{2n+1} is by definition $C(Y_{2n+1}) \equiv \mathbb{R}_{>0} \times Y_{2n+1}$, with conical metric $\mathrm{d}s^2_{C(Y_{2n+1})} = \mathrm{d}r^2 + r^2\,\mathrm{d}s^2_{Y_{2n+1}}$. There is also an equivalent characterization of GK geometry in terms of the cone geometry [37]. For a GK geometry on Y_{2n+1} the cone has an integrable complex structure, and moreover we require it to be Gorenstein, which means that there exist a nowhere vanishing holomorphic $(n+1,0)$-form $\Psi_{(n+1,0)}$, which is closed $\mathrm{d}\Psi_{(n+1,0)} = 0$. In this sense $C(Y_{2n+1})$ is then Calabi-Yau, having vanishing first Chern class, although the conical metric $\mathrm{d}s^2_{C(Y_{2n+1})}$ is neither Kähler nor Ricci-flat. We also require that $\Psi_{(n+1,0)}$ has definite charge under ξ, satisfying

$$\mathcal{L}_\xi \Psi_{(n+1,0)} = \mathsf{i}\mathsf{c}^{-1}\,\Psi_{(n+1,0)}\,. \tag{1.23}$$

In particular this condition implies that ξ is a holomorphic vector field on $C(Y_{2n+1})$.

A GK geometry becomes "on-shell", satisfying the supergravity equations of motion in the string/M-theory applications described in sections 1.2.3.1 and 1.2.3.2, if the transverse Kähler metric satisfies the non-linear partial differential equation

$$\Box\mathcal{R} = \frac{1}{2}\mathcal{R}^2 - \mathcal{R}_{ab}R^{ab}\,, \tag{1.24}$$

where $\mathcal{R}_{ab}$ denotes the Ricci tensor for the Kähler metric, and $\Box$ is the Laplacian operator.

However, we will go again "off-shell" and we will not impose the PDE (1.24). Instead we follow [68] to setup another extremal problem. We assume $C(Y_{2n+1})$ comes equipped with a holomorphic $U(1)^{s+1}$ action, with $1 \leq s \leq n+1$. The case with the maximum number $s = n+1$ of $U(1)$ isometries corresponds to $C(Y_{2n+1})$ being a toric cone. We take corresponding generating vector fields ∂_{φ_μ}, $\mu = 0, 1, \ldots, s$, with each φ_μ having period 2π. Moreover, we choose this basis so that the holomorphic volume form has unit charge under ∂_{φ_1}, and is uncharged under $\partial_{\varphi_{\hat{\mu}}}$, $\hat{\mu} = 0, 2, \ldots, s$. Notice here that we have singled out the ∂_{φ_0} direction, as well as the ∂_{φ_1} direction. The reason for this notation will become clear later on in the thesis. Similarly to (1.11) we can then parametrize the R-symmetry vector as

$$\xi = \sum_{\mu=0}^{s} b_\mu\, \partial_{\varphi_\mu}\,, \tag{1.25}$$

where we may regard the coefficients as defining a vector $(b_\mu) = (b_0, b_1, b_2, \ldots, b_s) \in \mathbb{R}^{s+1}$.[9] Given the condition (1.23), we must then set

$$b_1 = \frac{1}{\mathsf{c}} = \frac{2}{n-2}\,. \tag{1.26}$$

A choice of ξ determines the foliation $\mathcal{F}_\xi$, and we then further choose a transverse Kähler metric with basic cohomology class $[J] \in H_B^{1,1}(\mathcal{F}_\xi)$. It will often be convenient to note from (1.20) that $\mathrm{d}\eta = \mathsf{c}\,\varrho = \frac{1}{b_1}\,\varrho$ where $[\varrho] \in H_B^{1,1}(\mathcal{F}_\xi)$ also defines a basic cohomology class.

[9] As is standard in the physics literature, b_μ here denotes both the vector, and the μ-th component of this vector. When this abuse of notation might lead to potential confusion, we write $(b_\mu) \in \mathbb{R}^{s+1}$ for the vector.

Given this data, we may define the following *supersymmetric action*[10]

$$S_{\rm SUSY}(\xi,[J]) \equiv \int_{Y_{2n+1}} \eta\wedge\varrho\wedge\frac{J^{n-1}}{(n-1)!}\,. \tag{1.27}$$

It is straightforward to show [68] that this is a positive multiple of the integral of the scalar curvature of the transverse metric $\mathcal{R}>0$ over Y_{2n+1}, and thus $S_{\rm SUSY}>0$ is a necessary condition for a regular on-shell solution. A necessary condition for the transverse Kähler metric to solve the PDE (1.24) is the constraint equation

$$\int_{Y_{2n+1}} \eta\wedge\varrho^2\wedge\frac{J^{n-2}}{(n-2)!}=0\,, \tag{1.28}$$

which is equivalent to imposing that the integral of (1.24) over Y_{2n+1} holds. We also impose the *flux quantization conditions*

$$\int_{\Sigma_\Upsilon} \eta\wedge\varrho\wedge\frac{J^{n-2}}{(n-2)!}=\nu_n\,\mathcal{N}_\Upsilon\,. \tag{1.29}$$

Here $\Sigma_\Upsilon\subset Y_{2n+1}$ are codimension two submanifolds, tangent to ξ, which form a basis for the free part of $H_{2n-1}(Y_{2n+1};\mathbb{Z})$, ν_n are certain real constants that are given in the physical cases of interest of $n=3$, $n=4$ in subsections 1.2.3.1, 1.2.3.2 below, and $\mathcal{N}_\Upsilon\in\mathbb{Z}$ are the quantized fluxes. For a given ξ, it is important to notice that the quantities (1.27), (1.28), (1.29) depend only on the basic cohomology classes $[J],[\varrho]\in H^{1,1}_B(\mathcal{F}_\xi)$, and not on the choice of Kähler metric itself.

The extremal problem then consists in extremizing the supersymmetric action (1.27), subject to imposing the constraints (1.28), (1.29), for fixed flux numbers $\mathcal{N}_\Upsilon$. Here the parameter space is the choice of ξ, parametrized by $(b_\mu)\in\mathbb{R}^{s+1}$ via (1.25), and the choice of transverse Kähler class. The number of constraints (1.28), (1.29) is the same as the number of transverse Kähler class parameters. Assuming one can eliminate the latter, the supersymmetric action (1.27) then effectively becomes a function only of b_μ and the flux numbers $\mathcal{N}_\Upsilon\in\mathbb{Z}$. There is currently no general theorem to this effect, but this is the

[10] GK geometries, even when partially off-shell as described, admit Killing spinors and in this sense are supersymmetric.

case in all known examples. The main result of [68] is that GK geometries that solve the PDE (1.24) are necessarily solutions to this extremal problem. Note that it is an important outstanding problem to determine sufficient conditions for when solutions of the extremal problem guarantee that one in fact has a GK geometry solving the PDE; for some further discussion see [68, 70].

1.2.3.1 AdS_3 solutions from D3-branes

Setting $n = 3$ in the above gives internal spaces Y_7 that are associated to supersymmetric solutions of type IIB supergravity of the form [35]

$$\begin{aligned} \mathrm{d}s_{10}^2 &= L^2\, \mathrm{e}^{-B/2} \left(\mathrm{d}s_{\mathrm{AdS}_3}^2 + \mathrm{d}s_{Y_7}^2 \right) , \\ F_5 &= -L^4 \left(\mathrm{vol}_{\mathrm{AdS}_3} \wedge F + *_{Y_7} F \right) . \end{aligned} \tag{1.30}$$

Here we have introduced the closed two-form

$$F \equiv -\frac{1}{c} J + \mathrm{d}(\mathrm{e}^{-B} \eta) \,, \tag{1.31}$$

where $\mathsf{c} = \frac{1}{2}(n-2) = \frac{1}{2}$, $\mathrm{d}s_{\mathrm{AdS}_3}^2$ denotes the unit radius metric on AdS_3, and $L > 0$ is a constant.

The fact that only the five-form flux F_5 in type IIB is non-zero implies that these solutions are in some sense supported only by D3-branes. This flux is properly quantized via (1.29), satisfying

$$\frac{1}{(2\pi \ell_s)^4 g_s} \int_{\Sigma_\Upsilon} F_5 = \mathcal{N}_\Upsilon \,, \tag{1.32}$$

provided we take the constant ν_3 to be

$$\nu_3 = \frac{2(2\pi \ell_s)^4 g_s}{L^4} \,. \tag{1.33}$$

Furthermore, the extremal value of the supersymmetric action (1.27) determines the central charge c_{sugra} of the dual field theory. In fact [68] introduced a "trial central charge" $\mathscr{Z}$,

defined by

$$\mathscr{Z} \equiv \frac{3L^8}{(2\pi)^6 g_s^2 \ell_s^8} S_{\rm SUSY} = \frac{12(2\pi)^2}{\nu_3^2} S_{\rm SUSY} \,, \tag{1.34}$$

and on-shell, *i.e.* after extremizing, one has has $\mathscr{Z}_{\rm os} = c_{\rm sugra}$.

1.2.3.2 AdS_2 solutions from M2-branes

Setting instead $n = 4$ gives internal spaces Y_9 that are associated to supersymmetric solutions of 11d supergravity of the form [36]

$$\begin{aligned} \mathrm{d}s_{11}^2 &= L^2 \, \mathrm{e}^{-2B/3} \left(\mathrm{d}s_{\mathrm{AdS}_2}^2 + \mathrm{d}s_{Y_9}^2 \right) \,, \\ G_4 &= -L^3 \, \mathrm{vol}_{\mathrm{AdS}_2} \wedge F \,, \end{aligned} \tag{1.35}$$

where F is again given by (1.31), but with now $\mathsf{c} = \frac{1}{2}(n-2) = 1$. Again $L > 0$ is a constant.

We may interpret the fact that the flux G_4 is zero when restricted to Y_9, as meaning there is only M2-brane flux, and no M5-brane flux, sourcing these solutions. The Hodge dual seven-form $\star_{11} G_4$ is properly quantized via (1.29), satisfying

$$\frac{1}{(2\pi\ell_p)^6} \int_{\Sigma_\Upsilon} \star_{11} G_4 = \mathcal{N}_\Upsilon \,, \tag{1.36}$$

provided we take the constant ν_4 to be

$$\nu_4 = \frac{(2\pi\ell_p)^6}{L^6} \,. \tag{1.37}$$

In this case we define a "trial entropy" $\mathscr{S}$ via

$$\mathscr{S} \equiv \frac{4\pi L^9}{(2\pi)^8 \ell_p^9} S_{\rm SUSY} = \frac{2(2\pi)^2}{\nu_4^{3/2}} S_{\rm SUSY} \,, \tag{1.38}$$

where the supersymmetric action is given by (1.27) with $n = 4$. When the $D = 11$ solution arises as the near horizon limit of a supersymmetric black hole, it was argued in [68] that the on-shell value, $\mathscr{S}_{\rm os}$, is the entropy of the black hole. More generally, one expects this quantity to be (minus) the logarithm of a supersymmetric partition function of the dual

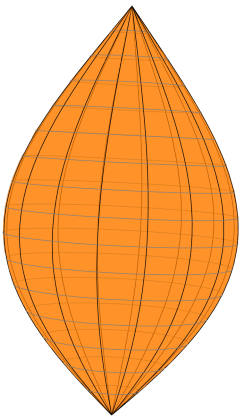


Figure 1.2: Pictorial representation of a spindle.

superconformal quantum mechanics, as argued earlier.

1.3 Spindle: an overview

A central role in this thesis will be played by the two-dimensional orbifold known as *spindle*. A spindle, which will be denoted with Σ throughout this thesis, is defined as the weighted complex projective line $\mathbb{WCP}^1_{[m_-,m_+]}$ with coprime integer weights $m_\pm > 0$. This is topologically a two-sphere S^2, but with conical deficit angles $2\pi\big(1-\frac{1}{m_\pm}\big)$ at the two poles (see figure 1.2). In particular, in [47, 48] it was first understood that branes wrapping Σ provide an interesting and novel setup for holography. In these works the authors built supergravity solutions interpreted as D3/M2-branes wrapping Σ which come with many peculiar features.

Firstly, it was discovered that the mechanism which allows to preserve supersymmetry is different from anything that was already known in the literature, and crucially it differs from the topological twist which we reviewed in section 1.1. It is now known that there are actually two topologically distinct mechanisms [71] that, among other things, differ in the total flux of the R-symmetry gauge field through Σ. These are known in the literature as *twist* and *anti-twist* and they correspond to

$$\text{Twist} \qquad Q_R = \frac{1}{2\pi}\int_\Sigma \mathrm{d}A_R = -\frac{m_+ + m_-}{m_+ m_-} = -\chi(\Sigma)\,, \tag{1.39}$$

$$\text{Anti-twist} \qquad Q_R = \frac{1}{2\pi}\int_\Sigma \mathrm{d}A_R = \frac{m_+ - m_-}{m_+ m_-} \neq -\chi(\Sigma)\,. \tag{1.40}$$

Note how the twist would be compatible with the condition (1.3) and indeed it is common to say that it is "topologically a topological twist". Moreover, if one formally sets $m_\pm = 1$ then the spindle turns into a two-sphere and the real topological twist is recovered. However, it turns out the mechanism is still quite distinct, as the Killing spinors on Σ are not sections of trivial bundles and we can build a bilinear out of them, which yields the Killing vector generating the azimuthal $U(1)_\Sigma$ symmetry of the spindle. The latter fact is true for the anti-twist too, but that is a completely different mechanism as confirmed also by (1.40).

Secondly, it is a general feature of all spindle solution that the R-symmetry Killing vector has a non-vanishing component along the $U(1)_\Sigma$ isometry. This is another novelty compared to earlier solutions with a Riemann surface Σ_g replacing the spindle, as in those there is never a mixing of the R-symmetry with isometries of the Riemann surface.[11] This has the direct consequence in geometry that the R-symmetry vector ξ as in (1.25) has one more parameter compared to the older Riemann surface solutions - the $\mu = 0$ component in (1.20).

Finally, many of the spindle solutions that are now known, and in particular all of those belonging to the class discussed in section 1.2.3, are completely smooth despite the spindle itself possessing orbifold singularities. This proves that such solutions are perfectly valid supergravity backgrounds and should not be discarded on the basis of having "unphysical singularities". The most relevant consequence is that when building solutions in lower dimensional supergravities that arise as consistent truncations of string theory or M-theory one should not automatically discard those that are singular as they might uplift to completely smooth geometries in 10d/11d.

There is by now a vast literature on spindles, with continued ongoing efforts to complement the understanding of such peculiar setups and their role within the AdS/CFT correspondence. Ever since the first two papers [47,48], many other explicit supergravity solutions arising from branes wrapping spindles appeared in the literature: D3-branes [1, 71, 73–76], M2-branes [71,77–81], M5-branes [1,71,82–85], D2-branes [84], D4-branes [83,86,87] and D6-branes [88]. Furthermore, some results concerning full black hole solutions with spindle horizon as well as a study of their thermodynamics and their general properties were carried on [2,77,89,90]

[11] For the $g = 0$ and $g = 1$ cases this has to be understood with the fact that the $U(1)$ R-symmetry cannot mix with the non-abelian isometries of the two-sphere and the torus ($SU(2)$ and $SL(2,\mathbb{Z})$ respectively) [72]. For the $g > 1$ case Σ_g does not have any isometries.

and the emergence of a gravitational blocks structure for holographic observables arising from spindle solutions was extensively discussed [3, 91, 92]. More recently there have been many efforts to better understand the partition function of field theories on the spindle, also called the *spindle index* [4, 93–95]. The discovery of spindle solutions also motivated the search for solutions with higher dimensional orbifolds and the study of their holographic duals [96–99] and some of the above solutions and results appeared recently as a playground for the development of equivariant localization techniques in supergravity [100–107]. Other solutions that are intimately related to the spindles are those containing a topological disc (which can be though of as a "half-spindle") which were identified as holographic duals of theories of class $\mathcal{S}$ [78, 108–115]; in fact it was recently discovered that spindles themselves are closely related to the latter [116]. Finally, another set of supergravity solutions that arise from the same local metric as spindles but that consider the non-compact sector are those of [117, 118], where the authors identified these as the holographic dual of SCFTs in the presence of defects.

In this thesis we will give an overview of the general geometric features of AdS_3 and AdS_2 solutions coming from D3/M2-branes wrapping a spindle and their role in a holographic context. In particular, such solutions belong to the classes introduced above in 1.2.3 with the internal GK manifold Y_{2n+1} being a fibration on the spindle Σ with Sasakian fibres X_{2n-1}, $n = 3, 4$. Motivated by the full flow solutions found in [48, 77], these geometries are conjecturally interpreted as the near-horizon limit of accelerating and magnetically charged black strings/holes, with the acceleration parameters given in terms of $m_{\pm}$, uplifted to 10d/11d supergravity on X_{2n-1} (for a more detailed discussion see also [2]). The geometric extremization approach detailed in section 1.2.3 allows us to make precise predictions for holographic observables for generic choices of X_{2n-1} and flavour twisting parameters. Matching with some known solutions and field theory computations corroborates the validity of the approach.

1.4 Outline of the thesis

Having covered some background and the motivations behind this thesis, we now anticipate what topics are discussed and how they are organized.

We start in chapter 2 by detailing the geometry of the total space Y_{2n+1} of a fibration with Sasakian fibres X_{2n-1} and a spindle Σ as a base. We build such fibration starting from local charts and then we make contact with earlier works, explaining how the two possibilities of twist and anti-twist differ. We then illustrate an example of such geometries by considering an explicit type IIB supergravity solution where the internal space is a general S^5 fibration over a spindle.

Chapter 3 follows with the derivation of one of the central results of this thesis: the gravitational block formula for the GK supersymmetric action. This allows to express many physical observables, including central charges and entropies, in terms of a sum of two contribution, the gravitational blocks, localized on the two poles of the spindle. We then use our findings to study particular cases where the geometry is simplified and the degrees of freedom in the extremization are reduced, namely the flavour twist and the universal twist.

Then in chapter 4 we discuss the case where the internal space is a toric cone. After introducing the toric machinery, we re-derive the block formula with an alternative approach based on toric geometry and we specify concretely all the relevant equations for the geometric extremization problem in terms of a "master volume". This is a fairly simple algebraic function of the linear vectors that encode all the information about a toric space and it turns out that any relevant quantity is a discrete sum over derivatives of this quantity.

The case of $\mathrm{AdS}_3 \times Y_7$ backgrounds of type IIB supergravity is discussed furtherly in chapter 5. In particular, for the toric case there is a known general prediction for the tentative central charge of the dual 2d $\mathcal{N} = (0, 2)$ SCFTs that we can match off-shell with our gravitational block formula. This provides a non-trivial general test of holography.

Instead, the holography of $\mathrm{AdS}_2 \times Y_9$ solutions is discussed in chapter 6. The dual field theory is now a superconformal quantum mechanics in 1d that comes from compactifying a 3d theory on a spindle. The free energy is computed as the large N limit of the localized partition function of the latter. Concretely this computation amounts to study a matrix model. Here we provide a concrete prescription to identify holographically many unexpected quantities in such matrix models with corresponding geometric duals and we demostrate the validity of our suggestion with a few examples.

We conclude with a short discussion and an outlook on the possibilities for related future

developments in chapter 7.

Chapter 2

The geometry of spindle solutions

In this chapter we describe in more details the geometry of the AdS_2 and AdS_3 backgrounds of section 1.2.3 in the special case where the internal space Y_{2n+1} takes the fibred form

$$X_{2n-1} \hookrightarrow Y_{2n+1} \xrightarrow{\pi} \Sigma\,, \tag{2.1}$$

where Y_{2n+1} projects under the projection map π to the two-dimensional orbifold $\Sigma = \mathbb{WCP}^1_{[m_-,m_+]}$, with Sasakian fibre X_{2n-1}.

Physically this corresponds to the following set-up. When the fibres X_{2n-1} are Sasaki-Einstein manifolds, taking $n = 3$, $n = 4$ leads to associated $\mathrm{AdS}_5 \times X_5$ and $\mathrm{AdS}_4 \times X_7$ solutions of type IIB supergravity and 11d supergravity, respectively. These are the near horizon limits of N D3-branes or N M2-branes placed at the Calabi-Yau cone singularities of $C(X_{2n-1})$, respectively. We may then interpret the fibration (2.1) as wrapping the D3-branes or M2-branes over Σ, as explained in section 1.1. The resulting low-energy effective theories on these wrapped branes, in dimensions 2 and 1 respectively, then flow to superconformal fixed points, with near horizon holographic duals given by $\mathrm{AdS}_3 \times Y_7$ and $\mathrm{AdS}_2 \times Y_9$, respectively.

We will firstly construct explicitly the fibration (2.1) and highlight its most relevant geometric features following [3]. After that, we will illustrate a concrete example of AdS_3 geometry by looking at the explicit supergravity solution considered in [1].

2.1 Fibrations over a spindle

Here we build explicitly the fibration (2.1) by gluing together the two local patches corresponding to the two poles of the spindle. We take general fibres where crucially ξ now has a component that is tangent to Σ, which means that the R-symmetry Killing vector mixes with the $U(1)_\Sigma$ isometry of the spindle.[1] The action of ξ on Σ is simply rotation about the poles,

[1] More precisely, $\pi_*\xi$ is a non-zero vector field on Σ.

which are orbifold points modelled locally by $\mathbb{C}/\mathbb{Z}_{m_\pm}$. We will also see how there exist two topologically distinct ways of preserving supersymmetry, which we call *twist* and *anti-twist*.

2.1.1 Building the fibration

We may construct a spindle Σ straightforwardly by gluing copies of $\mathbb{C}/\mathbb{Z}_{m_+}$ and $\mathbb{C}/\mathbb{Z}_{m_-}$, along their common S^1 boundary. The fibred geometries Y_{2n+1} that we are interested in may then be realized via a modification of this gluing construction.

We begin with the product $\mathbb{C}\times X_{2n-1}$, where X_{2n-1} will be the base of a Calabi-Yau cone $C(X_{2n-1})$ with $\dim_{\mathbb{C}} C(X_{2n-1}) = n$. The conical metric is $\mathrm{d}s^2_{C(X_{2n-1})} = \mathrm{d}r^2 + r^2\,\mathrm{d}s^2_{X_{2n-1}}$, with $r > 0$, and we denote by $\Psi_{(n,0)}$ the closed holomorphic $(n,0)$-form on $C(X_{2n-1})$. We also suppose that $C(X_{2n-1})$ is equipped with a holomorphic $U(1)^s$ action, with the Reeb vector field $\mathcal{J}(r\partial_r)$ generating a subgroup of this action, where $\mathcal{J}$ is the complex structure tensor of $C(X_{2n-1})$. We take a basis ∂_{ψ_i}, $i = 1,\ldots,s$, of holomorphic vector fields that generates the $U(1)^s$ action, such that the holomorphic volume form $\Psi_{(n,0)}$ has charge 1 under ∂_{ψ_1}, and is uncharged under ∂_{ψ_i}, $i = 2,\ldots,s$. The corresponding coordinates ψ_i on $X_{2n-1} = \{r = 1\} \subset C(X_{2n-1})$ here have period 2π.

Given this set-up, the space Y_{2n+1} may be constructed by taking $(\mathbb{C}\times X_{2n-1})/\mathbb{Z}_{m_+}$ and gluing it to $(\mathbb{C}\times X_{2n-1})/\mathbb{Z}_{m_-}$, where the local orbifold groups $\mathbb{Z}_{m_\pm}$ act on both $\mathbb{C}$ and the "fibres" X_{2n-1}. It then remains to specify this action, and also make precise how we glue. We may accomplish both together by first choosing two homomorphisms $h_\pm : U(1) \to U(1)^s$. This is equivalent to specifying integers $\alpha_i^\pm \in \mathbb{Z}$, $i = 1,\ldots,s$, so that explicitly

$$h_\pm(\omega) = (\omega^{\alpha_1^\pm},\ldots,\omega^{\alpha_s^\pm}) \in U(1)^s\,, \tag{2.2}$$

with $\omega \in U(1)$ a unit norm complex number. Given a point $(z,x) \in \mathbb{C}\times X_{2n-1}$, where $z \in \mathbb{C}$ and x is a point in X_{2n-1}, the $\mathbb{Z}_{m_\pm}$ orbifold actions are then defined by taking the generators $\Gamma_\pm$ to be

$$\Gamma_\pm(z,x) \equiv (\omega_\pm \cdot z, h_\pm(\omega_\pm)\cdot x) \in \mathbb{C}\times X_{2n-1}\,, \tag{2.3}$$

respectively. Here $\omega_\pm \equiv \mathrm{e}^{2\pi \mathrm{i}/m_\pm}$ are primitive $m_\pm$-th roots of unity, and the action of $h_\pm \in U(1)^s$ on the point $x \in X$ is via the assumed holomorphic $U(1)^s$ action on X_{2n-1}. Quotienting $\mathbb{C} \times X_{2n-1}$ by (2.3) then defines $(\mathbb{C} \times X_{2n-1})/\mathbb{Z}_{m_\pm}$.

The homomorphisms $h_\pm$ also specify diffeomorphisms $\Phi_\pm$ (which may be thought of as large $U(1)^s$ gauge transformations) of $S^1 \times X_{2n-1} \subset \mathbb{C} \times X_{2n-1}$, where $S^1 = \{z \in \mathbb{C} \mid |z| = 1\} \cong U(1)$ are the unit norm complex numbers. Specifically,

$$\Phi_\pm(z,x) \equiv (z, h_\pm^{-1}(z) \cdot x) \in S^1 \times X_{2n-1} \,. \tag{2.4}$$

Notice that the composition $\Phi_\pm \circ \Gamma_\pm \circ \Phi_\pm^{-1}$ maps $(z,x) \in S^1 \times X_{2n-1}$ to $(\omega_\pm \cdot z, x)$. Thus, after composing with the diffeomorphism $\Phi_\pm$, the quotient acts only on the z coordinate, showing that $(S^1 \times X_{2n-1})/\mathbb{Z}_{m_\pm} \cong S^1/\mathbb{Z}_{m_\pm} \times X_{2n-1} \cong S^1 \times X_{2n-1}$, which is the boundary of $(\mathbb{C} \times X_{2n-1})/\mathbb{Z}_{m_\pm}$. Both models then have the same boundary $S^1 \times X_{2n-1}$, and we glue these boundaries with the identity diffeomorphism, after reversing the orientation of $(\mathbb{C} \times X_{2n-1})/\mathbb{Z}_{m_-}$. This constructs the total space Y_{2n+1}.

We may make the above discussion more explicit by introducing coordinates. We write $z_\pm = |z_\pm| \mathrm{e}^{\mathrm{i}\hat{\phi}^\pm}$ as complex coordinates on each copy of $\mathbb{C}$, where $\hat{\phi}^\pm$ have period 2π before quotienting. The diffeomorphism/large gauge transformation (2.4) is then implemented by the coordinate transformation

$$\phi^\pm \equiv \hat{\phi}^\pm \,, \qquad \varphi_i^\pm \equiv \psi_i^\pm - \alpha_i^\pm \hat{\phi}_\pm \,. \tag{2.5}$$

Here $\psi_i^\pm$ are 2π-period angular coordinates on each copy of X_{2n-1}, and $(\phi^\pm, \varphi_i^\pm)$ are the new angular coordinates on each copy of $S^1 \times X_{2n-1}$. It follows that on the quotients $(\mathbb{C} \times X_{2n-1})/\mathbb{Z}_{m_\pm}$ the $\phi^\pm$ have periods $2\pi/m_\pm$, respectively. The gluing is then accomplished by identifying (the minus sign due to the orientation change of the second copy)

$$\varphi \equiv m_+ \phi^+ = -m_- \phi^- \,, \tag{2.6}$$

so that φ is a 2π-period coordinate for the azimuthal direction of the spindle. The fibres X_{2n-1} are glued with the identity diffeomorphism, meaning we identify $\varphi_i^+ = \varphi_i^-$. We then

define $\varphi_i \equiv \varphi_i^+ = \varphi_i^-$ as the angular coordinates on the fibres X_{2n-1}.

2.1.2 Twist and anti-twist

The previous subsection gives a self-contained description for how to construct the fibration (2.1) over a spindle Σ. However, we may also make contact with the discussion in [71], which focused on $U(1)$ fibrations over a spindle, by focusing on the i-th factor of $U(1) \subset U(1)^s$. The corresponding pair of integers (α_i^+, α_i^-) specify a $U(1)$ orbibundle over the spindle base Σ.[2] One can introduce a corresponding connection one-form A_i, and the discussion in [71] computes the total flux/Chern number

$$\frac{1}{2\pi}\int_\Sigma F_i = \frac{\alpha_i^-}{m_-} + \frac{\alpha_i^+}{m_+} = \frac{p_i}{m_+ m_-}\,, \tag{2.7}$$

where $F_i \equiv \mathrm{d}A_i$, and we have defined

$$p_i \equiv \alpha_i^- m_+ + \alpha_i^+ m_-\,. \tag{2.8}$$

Physically, these are interpreted as the magnetic charges of the black hole/string whose near-horizon is the geometry we are constructing and we will sometime refer to them as *flavour twisting parameters* in the following.

The complex line bundle over Σ that results is denoted $\mathcal{O}(p_i)$. In particular, different choices of $\alpha_i^\pm$ with the same p_i in (2.8) give isomorphic line bundles, as we shall see. Conversely, given a choice of $(p_1, \ldots, p_s) \in \mathbb{Z}^s$, we may specify the local model data above by first picking coprime integers $a_\pm$ satisfying

$$a_- m_+ + a_+ m_- = 1\,, \tag{2.9}$$

which exist by Bezout's lemma for coprime m_+, m_-, and then defining

$$\alpha_i^+ \equiv a_+ p_i\,, \qquad \alpha_i^- \equiv a_- p_i\,, \qquad i = 2, \ldots, s\,. \tag{2.10}$$

[2] This pair of integers was denoted $(m_N, -m_S)$ in [71], where recall we have without loss of generality set the variable $p = 0$ in [71], absorbing this into m_N or m_S. We also note that the analogue of the ψ_i coordinates here were denoted by χ (for a single $U(1)$) in [71].

These satisfy (2.8), by virtue of (2.9). Notice that here we treat the $i = 1$ direction differently, as discussed below. One can check that different choices in the above construction result in equivalent spaces Y_{2n+1}. Explicitly, given a solution $(a_+, a_-) \in \mathbb{Z}^2$ to (2.9), another solution is given by taking

$$a_+ \mapsto a_+ - \kappa m_+ \,, \qquad a_- \mapsto a_- + \kappa m_- \,, \tag{2.11}$$

where $\kappa \in \mathbb{Z}$ is arbitrary. Via (2.10) this in turn shifts $\alpha_i^\pm \to \alpha_i^\pm \mp \kappa p_i m_\pm \equiv \alpha_i^\pm \mod m_\pm$. It follows that different choices of κ lead to local models at each pole with equivalent quotient spaces $(\mathbb{C} \times X_{2n-1})/\mathbb{Z}_{m_\pm}$. Moreover, the fact that $\alpha_i^\pm/m_\pm$ change by $\mp\kappa p_i$, with opposite signs, then implies this change to each local model simply cancels in the gluing construction.

The $i = 1$ copy of $U(1)$ is special, as we chose the basis so that the holomorphic $(n, 0)$-form $\Psi_{(n,0)}$ on X_{2n-1} has charge 1 under this isometry. Equivalently, the Killing spinor associated to the GK geometry is charged under this direction. This was analysed in some detail in [71], with the conclusion that there are precisely two possibilities, called the *twist* and *anti-twist*:

$$\begin{aligned} \text{twist}: &\qquad \alpha_1^+ = -1 \,,\ \alpha_1^- = -1 \,, \\ \text{anti-twist}: &\qquad \alpha_1^+ = -1 \,,\ \alpha_1^- = +1 \,. \end{aligned} \tag{2.12}$$

It will be convenient for the remainder of the thesis to introduce a sign

$$\sigma \equiv \begin{cases} +1 & \text{twist} \\ -1 & \text{anti-twist} \end{cases} \qquad \Longrightarrow \qquad \alpha_1^- = -\sigma \,. \tag{2.13}$$

Via (2.8) we then have[3]

$$p_1 = -\sigma m_+ - m_- \,. \tag{2.14}$$

The twist case is "topologically a topological twist", meaning that it reduces to the usual topological twist on a smooth two-sphere S^2 in the limit $m_\pm \to 1$ [71]. Indeed, it arises

[3]Fixing the *overall* sign of p_1 here involves a choice of convention, which we have fixed in writing both (2.12) and (2.14). The result of [71] more generally fixes $|\alpha_1^\pm| = 1$, rather than (2.12), and it is the *relative* sign of α_1^+ and α_1^- that distinguishes the twist and anti-twist cases.

precisely when $C(X_{2n-1})$ fibred over Σ is also Calabi-Yau, in the sense that it admits a holomorphic $(n+1,0)$-form and one can perform an explicit construction by highlighting this perspective [3]. At present there is no similar geometric interpretation of the anti-twist.

For both the twist and the anti-twist, notice that defining $\partial_{\varphi_0} \equiv \partial_\varphi$, together with ∂_{φ_i}, $i = 1, \ldots, s$, these vector fields generate a $U(1)^{s+1}$ action on the total space Y_{2n+1}, where this basis then satisfies the conditions imposed in the general setup described in section 1.2.3. In particular, the holomorphic $(n+1,0)$-form $\Psi_{(n+1,0)}$ is *uncharged* under ∂_{φ_0}. Recall that the R-symmetry killing vector is given by (1.25) and note that if $b_0 \neq 0$ (which is true in general) then ξ has a component tangent to Σ, differently from the non-accelerating case where the spindle is replaced by a smooth Riemann surface Σ_g and $b_0 = 0$ [70, 119]. In terms of the coordinates introduced in the construction in section 2.1.1, it is helpful to note here that

$$\partial_{\varphi_0} \equiv \partial_\varphi = \pm \frac{1}{m_\pm} \partial_{\hat{\phi}^\pm} \pm \sum_{i=1}^{s} \frac{\alpha_i^\pm}{m_\pm} \partial_{\varphi_i} \,, \qquad \partial_{\varphi_i} = \partial_{\varphi_i^\pm} = \partial_{\psi_i^\pm} \,. \tag{2.15}$$

Later we will be particularly interested in the vector fields $\zeta_\pm$, that by definition rotate the normal directions to the fibres over the poles of the spindle; that is, the copies of $X_\pm \equiv X_{2n-1}/\mathbb{Z}_{m_\pm}$ located at $z_\pm = 0$, respectively, in the construction of section 2.1.1. These are given by $\zeta_\pm = \partial_{\hat{\phi}^\pm}$, and (2.15) immediately gives

$$\zeta_\pm \equiv \partial_{\hat{\phi}^\pm} = \begin{cases} m_+ \partial_{\varphi_0} + \partial_{\varphi_1} - \sum_{i=2}^{s} \alpha_i^+ \partial_{\varphi_i} \equiv \sum_{\mu=0}^{s} v_{+\mu} \partial_{\varphi_\mu} \\ -m_- \partial_{\varphi_0} + \sigma \partial_{\varphi_1} - \sum_{i=2}^{s} \alpha_i^- \partial_{\varphi_i} \equiv \sigma \sum_{\mu=0}^{s} v_{-\mu} \partial_{\varphi_\mu} \,, \end{cases} \tag{2.16}$$

where we have used (2.12) and (2.13) and we introduced vectors

$$(v_{+\mu}) = (m_+, 1, -\vec{\alpha}^+) \,, \qquad (v_{-\mu}) = (-\sigma m_-, 1, -\sigma \vec{\alpha}^-) \,, \tag{2.17}$$

where $\vec{\alpha}^\pm \equiv (\alpha_2^\pm, \ldots, \alpha_s^\pm)$.

For later use, we define $\xi_\pm$ to be the orthogonal projection of the R-symmetry vector ξ given in (1.25) onto directions tangent to the fibres over the two poles. These may then be

viewed as R-symmetry vectors for the fibres $X_\pm$. From (2.16) we have

$$\xi_\pm \equiv \xi \mp \frac{b_0}{m_\pm}\,\zeta_\pm = \sum_{i=1}^{s} b_i^{(\pm)}\partial_{\varphi_i}\,, \tag{2.18}$$

where we have defined the shifted vectors

$$b_i^{(+)} \equiv b_i - \frac{b_0}{m_+}v_{+i}\,, \qquad b_i^{(-)} \equiv b_i + \frac{b_0}{\sigma m_-}v_{-i}\,. \tag{2.19}$$

For later use we also note that via (2.8) we have

$$b_i^{(+)} - b_i^{(-)} = \frac{p_i}{m_+ m_-}\,b_0\,. \tag{2.20}$$

2.2 Explicit supergravity solution with $X_5 = S^5$

As a concrete example of the above construction, we illustrate the explicit supergravity solution which was studied in [1,73] and refined in [71]. We start from a family of supersymmetric AdS_3 solutions to 5d $U(1)^3$ gauged supergravity and uplift these on an S^5 internal space to corresponding $\mathrm{AdS}_3\times Y_7$ solutions of type IIB supergravity which fit in the description of the previous section. The local form of the 5d solutions was first presented in [120], where they were obtained from multi-charge superstar solutions in [121]. Shortly afterwards the same solutions were rediscovered in [122], where they arise as the uplifts of near-horizon limits of a family 5d unbalanced black ring solutions. However, here we perform a global analysis for the allowed values of the parameters in the solution, which is very different to the approach taken in [122] and [120]. Instead we follow the pioneering approach of [47].

2.2.1 Local 5d metric and uplift to IIB

We start considering 5d $U(1)^3$ gauged supergravity, whose action is given by

$$\begin{aligned} I_{\rm 5d} \;=\; \frac{1}{16\pi G_{(5)}}\int\Big\{\mathrm{d}^5x\sqrt{-\det g}\,\Big[\mathcal{R} + 4\sum_{I=1}^{3}(X_a)^{-1} - \frac{1}{2}\sum_{a=1}^{3}(X_a)^{-2}(\partial X_a)^2 \\ - \frac{1}{4}\sum_{a=1}^{3}(X_a)^{-2}(F_a)^2\Big] - F_a\wedge F_a\wedge A_a\Big\}. \end{aligned} \tag{2.21}$$

Here A_a, $a = 1, 2, 3$, are the three $U(1)$ gauge fields with field strengths $F_a = \mathrm{d}A_a$, and the scalars X_a satisfy the constraint $X_1 X_2 X_3 = 1$. We set the gauge coupling constant to 1.

Our starting point is the following supersymmetric AdS_3 solution to this theory [122]:

$$\begin{aligned} \mathrm{d}s_5^2 &= H(x)^{1/3}\left[\mathrm{d}s^2_{\mathrm{AdS}_3} + \frac{1}{4P(x)}\mathrm{d}x^2 + \frac{P(x)}{H(x)}\mathrm{d}\phi^2\right], \\ A_a &= \frac{x-\alpha}{x+3K_a}\mathrm{d}\phi\,, \qquad\qquad X_a = \frac{H(x)^{1/3}}{x+3K_a}\,. \end{aligned} \tag{2.22}$$

Here $\mathrm{d}s^2_{\mathrm{AdS}_3}$ a unit radius metric on AdS_3, the metric functions are the polynomials

$$\begin{aligned} H(x) &\equiv (x+3K_1)(x+3K_2)(x+3K_3) = x^3 + 3c_1 x + c_2\,, \\ P(x) &\equiv H(x) - (x-\alpha)^2\,, \end{aligned} \tag{2.23}$$

and α, K_a are constants, with the latter satisfying the constraint $K_1 + K_2 + K_3 = 0$. In the first line of (2.23) we have introduced the elementary symmetric polynomials for the parameters K_a, namely $c_1 = 3(K_1K_2 + K_2K_3 + K_1K_3)$, $c_2 = 27K_1K_2K_3$.

Any solution of 5d $U(1)^3$ gauged supergravity may be uplifted (locally) on S^5 to a solution of type IIB supergravity [121].[4] The 10d metric and the self-dual five-form are

$$L^{-2}\mathrm{d}s^2_{10} = W^{1/2}\mathrm{d}s^2_5 + W^{-1/2}\sum_{a=1}^{3}(X_a)^{-1}\left[\mathrm{d}\mu_a^2 + \mu_a^2(\mathrm{d}\phi_a + A_a)^2\right] \tag{2.24}$$

$$\begin{aligned} L^{-4}F_5 = (1+\star_{10})\Big\{ & 2\sum_{a=1}^{3}[(X_a)^2\mu_a^2 - WX_a]\,\mathrm{vol}_5 + \frac{1}{2}\sum_{a=1}^{3}(X_a)^{-1}\star_5 \mathrm{d}X_a\wedge\mathrm{d}(\mu_a^2) \\ & + \frac{1}{2}\sum_{a=1}^{3}(X_a)^{-2}\mathrm{d}(\mu_a^2)\wedge(\mathrm{d}\phi_a + A_a)\wedge\star_5 F_a\Big\}\,. \end{aligned} \tag{2.25}$$

Here we have introduced an arbitrary length scale parameter $L > 0$ which will be fixed via flux quantization later. We have also introduced the warp function

$$W = \sum_{a=1}^{3}\mu_a^2 X_a > 0\,. \tag{2.26}$$

[4] Whenever $A^{(1)} = A^{(2)}$ and $X^{(1)} = X^{(2)}$ the 5d solution can also be uplifted on the Maldacena-Nunez solution [40] to 11d supergravity, resulting in a metric which is interpreted as the near-horizon limit of M5-branes wrapping a Riemann surface times a spindle (see [1] for more details and [85] for a generalization to the BBBW class of solutions [123]).

Finally, $\{\mu_a, \phi_a\}$ form a system of polar coordinates on $S^5 \subset \mathbb{R}^2 \oplus \mathbb{R}^2 \oplus \mathbb{R}^2$, where correspondingly $\sum_{a=1}^3 \mu_a^2 = 1$ and the angular coordinates ϕ_a each have period 2π.

Applying the uplifting formula (2.24) to the AdS_3 solution (2.22) gives rise to the following warped $\mathrm{AdS}_3 \times Y_7$ metric

$$\mathrm{d}s_{10}^2 \;=\; L^2\, W^{1/2} H(x)^{1/3} \left(\mathrm{d}s_{\mathrm{AdS}_3}^2 + \mathrm{d}s_{Y_7}^2\right) , \tag{2.27}$$

where the seven-dimensional metric on Y_7 is

$$\mathrm{d}s_{Y_7}^2 \;=\; \frac{\mathrm{d}x^2}{4P(x)} + \frac{P(x)}{H(x)}\mathrm{d}\phi^2 + \sum_{I=1}^{3} \frac{x+3K_a}{W H(x)^{2/3}} \left[\mathrm{d}\mu_a^2 + \mu_a^2 \left(\mathrm{d}\phi_a + \frac{(x-\alpha)}{x+3K_a}\mathrm{d}\phi\right)^2\right] . \tag{2.28}$$

One can verify that this is the same metric as that given in section 5.2 of [120], where we identify their coordinates and parameters, in terms of those presented here, as $w = x - \alpha$, $z = -2\phi$, $q_a = \alpha + 3K_a$. In particular, reference [120] also shows that the solution is supersymmetric, with the dual 2d CFT having $(0,2)$ supersymmetry. By also noticing that (2.27) takes exactly the form (1.30) we can conclude that the solution illustrated here belongs to the general class described in section 1.2.3.1. The Killing vectors ∂_{ϕ_a} together with ∂_ϕ implement the $U(1)^{s+1}$ isometry of Y_7 with $s = 3$, albeit in a different basis from the one introduced before (1.25). In the next subsection we will see that Y_7 here is an S^5 fibration over a spindle and therefore is a particular instance of the geometry described in section 2.1 with $X_5 = S^5$ and we will identify the change of coordinates that relates the two bases above.

2.2.2 Global analysis and general solution

Given a local $\mathrm{AdS}_3 \times Y_7$ solution of the form (2.28), one would like to choose the parameters α, K_a and ranges of coordinates so as to obtain a smooth metric on a compact internal space Y_7. An analysis of this was carried out in [120] (see also [122]), where one looks at the degeneration loci of Killing vector fields on Y_7, which are constant linear combinations of the four vector fields ∂_ϕ and ∂_{ϕ_a}. We instead follow the approach of [47], first obtaining a 5d $\mathrm{AdS}_3 \times \Sigma$ solution. We then appropriately quantize the $U(1)^3$ gauge field fluxes so as to obtain a regular fibration of S^5 over this five-dimensional solution.

We begin then with the 5d metric in (2.22), which we rewrite as

$$\mathrm{d}s_5^2 \;=\; H(x)^{1/3}\left(\mathrm{d}s^2_{\mathrm{AdS}_3}+\mathrm{d}s^2_{\Sigma}\right)\,, \tag{2.29}$$

with the two-dimensional surface Σ having coordinates x, ϕ. In order for the metric to have the correct signature and be non-singular we would like to choose the parameters so that $H(x) > 0$ is strictly positive, and similarly $P(x) \geq 0$. In order that Σ forms a compact surface without boundary, we furthermore assume that $x \in [x_1, x_2]$ lies between two roots of the polynomial $P(x)$ in (2.23). In a certain regime of parameters, that we make explicit below, we find that the three roots x_1, x_2, x_3 of $P(x)$ are all real, and we then take $x_1 < x_2 < x_3$ so that $P(x) \geq 0$ for $x \in [x_1, x_2]$. Defining $\varrho_i = 2(x - x_i)^{1/2}$ for $i = 1, 2$ we find that as $x \to x_i$ the metric on the two-dimensional surface Σ approaches

$$\mathrm{d}s^2_{\Sigma} \;\simeq\; \frac{1}{4|P'(x_i)|}\left(\mathrm{d}\varrho_i^2+\kappa_i^2\varrho_i^2\,\mathrm{d}\phi^2\right)\,,\qquad \text{where}\quad \kappa_i \;\equiv\; \left|\frac{P'(x_i)}{x_i-\alpha}\right|\,,\quad i\;=\;1,2\,. \tag{2.30}$$

As for the solution in [47], it is not possible to remove both conical singularities at the roots $x = x_i$ by making a single choice $\Delta\phi$ of the period for ϕ. Instead we impose

$$\Delta\phi \;=\; \frac{2\pi}{\kappa_1 m_-} \;=\; \frac{2\pi}{\kappa_2 m_+}\,, \tag{2.31}$$

where $m_\pm \in \mathbb{N}$ and $\gcd(m_-, m_+) = 1$. The resulting surface Σ is then a spindle, with conical deficit angles $2\pi\left(1-\frac{1}{m_\mp}\right)$ at the poles $x = x_1$, x_2.

It turns out that, while $x_2 - \alpha < 0$ always, the sign σ of $x_1 - \alpha$ determines whether the twist or the anti-twist is realized. One may check that the second equality in (2.31) may be written as

$$\frac{\sigma m_+}{m_-} \;=\; \left(\frac{x_2-\alpha}{x_1-\alpha}\right)\left(\frac{-1+2x_1+x_2}{-1+x_1+2x_2}\right)\,, \tag{2.32}$$

where the roots x_1, x_2 satisfy the equations

$$\begin{aligned} 2\alpha+3c_1 \;&=\; x_1+x_2-x_1^2-x_2^2-x_1x_2\,,\\ c_2 \;&=\; \alpha^2+x_1^2x_2+x_1x_2^2-x_1x_2\,, \end{aligned} \tag{2.33}$$

and we have eliminated x_3 via the relation $x_1 + x_2 + x_3 = 1$. We also need the fluxes of the gauge field strengths $F_a = \mathrm{d}A_a$ through the surface Σ. Using (2.22) we compute

$$\mathfrak{p}_a \equiv \frac{1}{2\pi}\int_\Sigma F_a = \frac{(x_2 - x_1)(\alpha + 3K_a)}{(x_1 + 3K_a)(x_2 + 3K_a)}\frac{\Delta\phi}{2\pi}\,. \tag{2.34}$$

As explained in [47, 48], the appropriate quantization condition on these fluxes is

$$\mathfrak{p}_a \equiv \frac{\tilde{p}_a}{m_+ m_-}\,, \qquad \text{where} \quad \tilde{p}_a \in \mathbb{Z}\,. \tag{2.35}$$

Specifically, the circles parametrized by ϕ_a inside the internal space $S^5 \subset \mathbb{C}^3$ then give a well-defined orbifold circle fibration over Σ. Moreover, provided the integers $\tilde{p}_a$ are coprime to both of $m_\pm$, the total space of this fibration is smooth.[5] This leads to a fibration like (2.1) where $X_5 = S^5$ and the twisting is determined by the integers $\tilde{p}_a$.

At this stage we have a three-parameter family of solutions, determined by the constants α, K_2, K_3, where the roots x_1, x_2 obey (2.33). We would like to express the solution in terms of the more physical flux parameters $\tilde{p}_a$ and $m_\pm$, the ratio of the latter determined via (2.32). It turns out to be convenient to express quantities in terms of two of the three fluxes, say $\tilde{p}_2$ and $\tilde{p}_3$. After some work, it is possible to solve the three equations (2.32), and (2.33) for α, K_2, K_3, x_1, and x_2 in terms of $m_\pm$, $\tilde{p}_2$, and $\tilde{p}_3$. We find the rather unwieldy expressions

$$\begin{aligned}
x_1 \;=\; & \frac{1}{\mathcal{D}}\Big\{(\tilde{p}_2^2 + \tilde{p}_2\tilde{p}_3 + \tilde{p}_3^2)^2 + 3m_-\tilde{p}_2\tilde{p}_3(\tilde{p}_2 + \tilde{p}_3) + 2(\sigma m_+ + m_-)(\tilde{p}_2 + \tilde{p}_3)(\tilde{p}_2^2 + \tilde{p}_3^2) \\
& \qquad + (m_+^2 + m_-^2)(\tilde{p}_2^2 + \tilde{p}_3^2) + \sigma m_+ m_-(3\tilde{p}_2^2 + 4\tilde{p}_2\tilde{p}_3 + 3\tilde{p}_3^2) + 3m_-^2\tilde{p}_2\tilde{p}_3 \\
& \qquad\qquad + \sigma m_+ m_-(\sigma m_+ + m_-)(\tilde{p}_2 + \tilde{p}_3)\Big\}\,, \\
K_2 \;=\; & \frac{1}{3\mathcal{D}}\Big\{3\tilde{p}_3^2(\tilde{p}_2 + \tilde{p}_3)^2 - (\tilde{p}_2^2 + \tilde{p}_2\tilde{p}_3 + \tilde{p}_3^2)^2 - 2(\sigma m_+ + m_-)(\tilde{p}_2^2 - 2\tilde{p}_3^2)(\tilde{p}_2 + \tilde{p}_3) \\
& \qquad + 2\sigma m_+ m_-\tilde{p}_2\tilde{p}_3 - (m_+^2 + 3\sigma m_+ m_- + m_-^2)(\tilde{p}_2^2 - 2\tilde{p}_3^2) \\
& \qquad\qquad - \sigma m_+ m_-(\sigma m_+ + m_-)(\tilde{p}_2 - 2\tilde{p}_3)\Big\}\,, \\
x_2 \;=\; & x_1\,(\sigma m_+ \leftrightarrow m_-)\,, \qquad\qquad K_3 \;=\; K_2\,(\tilde{p}_2 \leftrightarrow \tilde{p}_3)\,,
\end{aligned} \tag{2.36}$$

[5] See appendix A of [48] for a detailed discussion of this.

where we have defined the denominator term

$$\mathcal{D} \equiv 3\left[(\sigma m_+ + m_-)(\tilde{p}_2 + \tilde{p}_3) + \sigma m_+ m_- + \tilde{p}_2^2 + \tilde{p}_2\tilde{p}_3 + \tilde{p}_3^2\right]^2 . \tag{2.37}$$

The parameter α may then be determined from the first equation in (2.33). The third flux is computed to be

$$\mathfrak{p}_1 = -\frac{\sigma m_+ + m_- + \tilde{p}_2 + \tilde{p}_3}{m_+ m_-} , \tag{2.38}$$

which notice also satisfies the quantization condition (2.35). We then also have

$$\mathfrak{p}_1 + \mathfrak{p}_2 + \mathfrak{p}_3 = -\frac{\sigma m_+ + m_-}{m_+ m_-} , \tag{2.39}$$

which agrees with the general expression for the R-symmetry flux through a spindle (1.39) and (1.40). Recalling that in the general construction in section 2.1.1 we had $p_1 = -\sigma m_+ - m_-$, it is then clear that

$$\mathfrak{p}_a = \frac{1}{m_+ m_-} \left\{p_1 - (p_2 + p_3), p_2, p_3\right\} . \tag{2.40}$$

We now have all the elements to express the coordinates ϕ and ϕ_a in terms of the basis φ_μ introduced in 1.2.3 and furtherly specified in 2.1.1. Firstly, note that from [37, 120] we know that the Killing spinor on Y_7 has unit charge under the Lie derivative along ∂_ϕ. However, by definition it has to be uncharged under the Lie derivative along ∂_{φ_0}. In order to obtain this, recall that this Killing spinor arises as a tensor product of the 5d Killing spinor with a spinor on the internal S^5. In particular, the latter has charge $\frac{1}{2}$ under each of the three vector fields ∂_{ϕ_a} generating the $U(1)^3$ isometry of the fibre $X_5 = S^5$. Since a gauge transformation of the A_a precisely leads to a phase rotation in the corresponding Killing spinor, which has unit charge under each A_a, this may be achieved via the gauge/coordinate transformation

$$\tilde{\phi}_a = \phi_a + \tfrac{2}{3}\,\phi , \qquad \tilde{A}_a = A_a - \tfrac{2}{3}\,\mathrm{d}\phi , \tag{2.41}$$

which ensures that $\mathrm{d}\phi_a + A_a = \mathrm{d}\tilde{\phi}_a + \tilde{A}_a$. Then we can define

$$\varphi_0 \equiv \frac{2\pi}{\Delta\phi}\,\phi , \tag{2.42}$$

so that $\Delta\varphi_0 = 2\pi$. Finally, from the fluxes (2.40) we can conclude that

$$\varphi_1 = \tilde{\phi}_1 + \tilde{\phi}_2 + \tilde{\phi}_3 \,, \qquad \varphi_2 = \tilde{\phi}_2 \,, \qquad \varphi_3 = \tilde{\phi}_3 \,, \tag{2.43}$$

and likewise the gauge fields $\tilde{A}_a$ are related to the A_i introduced above (2.7).

To conclude this section, we provide some inequalities among the parameters to ensure that our assumptions on the roots of $P(x)$ (*i.e.* $x_1 < x_2 < x_3$, $x_2 - \alpha < 0$, and $\sigma(x_1 - \alpha) > 0$) are all satisfied, and hence the solutions are physical. We find

$$\text{Twist:} \qquad \text{two } \mathfrak{p}_a > 0 \,, \tag{2.44}$$

$$\text{Anti-twist:} \qquad \mathfrak{p}_a > 0 \,, \quad a = 1, 2, 3 \,. \tag{2.45}$$

Note that (2.44) implies the third $\mathfrak{p}_a$ is negative while (2.45) implies $m_+ > m_-$.[6]

2.2.3 Central charge and R-symmetry

These AdS_3 solutions are, via the AdS/CFT correspondence, dual to 2d $(0,2)$ SCFTs. The central charge of these CFTs is computed in gravity using the standard formula [62]

$$c = \frac{3L}{2G_{(3)}} \,, \tag{2.46}$$

where $G_{(3)}$ is the effective Newton constant in three dimensions. In turn the latter is computed via dimensional reduction on Y_7, and is given by [68]

$$\frac{1}{G_{(3)}} = \frac{L^7}{G_{(10)}} \int_{Y_7} W^2 H(x)^{4/3} \, \mathrm{vol}_{Y_7} = \frac{\pi^3 L^7 \Delta\phi}{2G_{(10)}} (x_2 - x_1) \,, \tag{2.47}$$

where we have explicitly evaluated the integrals over S^5 and the spindle Σ. The ten-dimensional Newton constant is given by

$$G_{(10)} = \frac{(2\pi)^7 g_s^2 \, \ell_s^8}{16\pi} \,, \tag{2.48}$$

[6] In [71] they found $m_+ > m_-$ also in the twist case but it turns out that one can swap the labels m_+ and m_-, therefore accessing the case $m_+ < m_-$.

and therefore the central charge (2.46) reads

$$c \,=\, \frac{3L^8\Delta\phi}{32\pi^3 g_s^2\,\ell_s^8}\,(x_2-x_1)\,. \tag{2.49}$$

In order to obtain a good string theory solution we must also quantize the flux of the closed five-form (2.25) through five-cycles in the ten-dimensional spacetime. The only five-cycle in our solution is the S^5 fibre itself; integrating F_5 over it, we find the total flux is

$$N \,\equiv\, \frac{1}{(2\pi\ell_s)^4 g_s}\int_{S^5} F_5 \,=\, \frac{L^4}{4\pi\ell_s^4\,g_s}\,. \tag{2.50}$$

Eliminating L in the central charge (2.49) using this last equation then gives

$$c \,=\, \frac{3}{2\pi}\Delta\phi\,(x_2-x_1)N^2\,. \tag{2.51}$$

Finally, substituting the solution (2.36) into (2.51), we find the remarkably simple expression

$$c_{\rm sugra} = \frac{6m_-^2 m_+^2\,\mathfrak{p}_1\mathfrak{p}_2\mathfrak{p}_3}{m_+^2+m_-^2-m_+^2m_-^2(\mathfrak{p}_1^2+\mathfrak{p}_2^2+\mathfrak{p}_3^2)}\,N^2\,. \tag{2.52}$$

Note that upon setting $\mathfrak{p}_1=\mathfrak{p}_2=\mathfrak{p}_3=\frac{m_+-m_-}{3m_+m_-}$ and $\sigma=-1$ we recover precisely the anti-twist result of [47], where they considered a special case of our setup.

The $U(1)$ R-symmetry of the dual 2d $(0,2)$ field theory is realized in the gravity solution as a Killing vector field ξ of the $\mathrm{AdS}_3\times Y_7$ gravity solution. In particular, from [37, 120] we can read off that this vector field is simply

$$\xi \,=\, \partial_\phi \,=\, \sum_{a=1}^{3}\frac{\partial\tilde{\phi}_a}{\partial\phi}\,\partial_{\tilde{\phi}_a}+\frac{\partial\varphi_0}{\partial\phi}\,\partial_{\varphi_0} \,=\, \frac{2}{3}\sum_{a=1}^{3}\partial_{\tilde{\phi}_a}+\frac{2\pi}{\Delta\phi}\,\partial_{\varphi_0}\,, \tag{2.53}$$

where we used (2.41) and (2.42).

Note that ∂_{φ_0} generates the $U(1)_\Sigma$ isometry of the spindle. The gauge transformation (2.41) leads to a phase $\mathrm{e}^{\mathrm{i}(\tilde{\phi}_1+\tilde{\phi}_2+\tilde{\phi}_3)/2}$ in the Killing spinor on Y_7, but this is now invariant

under $U(1)_\Sigma$. We may then identify the Killing vector field on S^5

$$\xi_{\rm 4d} \,=\, \frac{2}{3}\sum_{a=1}^{3}\partial_{\tilde{\phi}_a}\,, \tag{2.54}$$

with the superconformal $\mathcal{N}=1$ R-symmetry before compactification of the theory on Σ, and from (2.53) hence write

$$\xi \,=\, \xi_{\rm 4d} - \frac{2m_+m_-(\sigma m_+ - m_-)}{m_+^2+m_-^2-m_+^2m_-^2(\mathfrak{p}_1^2+\mathfrak{p}_2^2+\mathfrak{p}_3^2)}\,\partial_{\varphi_0}\,. \tag{2.55}$$

Equation (2.55) states that the 4d $U(1)$ R-symmetry mixes with $U(1)_\Sigma$ in flowing to the 2d $U(1)$ R-symmetry in the IR, as we described in general in section 2.1.

We shall recover both (2.52) and (2.55) from a dual field theory calculation in section 5.1, as well as taking a geometric extremization approach in section 3.3.1.

Chapter 3

Gravitational blocks

In this chapter we will study the extremal problem described in section 1.2, in the special case that the internal space Y_{2n+1} takes the fibred form illustrated in chapter 2. The case where the spindle is replaced by a smooth Riemann Σ_g surface of genus g, and where the R-symmetry vector ξ is tangent to toric fibres X, was studied in [70, 119]. Here we are interested in generalizing this set-up by taking $\Sigma = \mathbb{WCP}^1_{[m_-,m_+]}$ to be a spindle.

The main result of this chapter will be that the supersymmetric action (1.27), together with the associated constraint (1.28) and flux quantization conditions (1.29), *localize* to integrals over the fibres $X_\pm$ over the poles of the spindle.[1] We refer to these contributions as *gravitational blocks*, since they generalize similar (conjectured) formulas that have already appeared in the literature – see [73,77,86,89,124–126]. As well as deriving these gravitational block formulas, we will also relate physical quantities in the parent 4d and 3d field theories on the D3-branes and M2-branes, respectively, to physical quantities in the compactified 2d and 1d theories in the IR. In turn, this will allow us to prove certain relations in holography. We then specify our results to the particular cases of the flavour twist and the universal anti-twist, which correspond to considering further assumptions on the geometry of the internal space. Finally, we illustrate our findings by applying the block formula to a few concrete examples of Sasakian fibres X_{2n-1}.

3.1 Derivation of the general block formula

Let us start by deriving the central result of this chapter, the gravitational block formula. This will constitute the backbone of almost all the other results in this thesis as it allows to reduce quantities computed on the total space Y_{2n+1} to sum of quantities computed on the fibres over the poles, which are typically easier.

[1] In general these fibres will be topologically $X_\pm \equiv X_{2n-1}/\mathbb{Z}_{m_\pm}$, rather than copies of the generic fibre X_{2n-1}, as we will explain in section 2.1.1 below.

3.1.1 Gravitational block lemma

To begin with, we state a geometric lemma which will be exploited in the our derivation of the block formula for the supersymmetric action and whose proof will be the main object of this subsection

$$\int_{Y_{2n+1}} \eta \wedge \varrho \wedge \Gamma = \frac{2\pi b_1}{b_0} \left(m_+ \int_{X_+} \eta \wedge \Gamma - m_- \int_{X_-} \eta \wedge \Gamma \right) . \tag{3.1}$$

Here Y_{2n+1} is a GK geometry fibering over a spindle Σ, as in (2.1), where the fibres over the two poles of the spindle are respectively $X_\pm \cong X_{2n-1}/\mathbb{Z}_{m_\pm}$, with the quotient given by (2.3). The orientations of $X_\pm$ here are those naturally induced via the Stokes' theorem argument we introduce shortly, but we note that these may not agree with the natural orientation induced by the complex structure on $C(Y_{2n+1})$ (we shall return to discuss this later). The differential form Γ in is any closed form on Y_{2n+1} that is basic with respect to the foliation defined by R-symmetry vector ξ, which we recall is expressed in term of an explicit basis in (1.25); that is, $\mathcal{L}_\xi \Gamma = 0$, $\xi \lrcorner \Gamma = 0$.

Both the supersymmetric action (1.27) and constraint equation (1.28) take the form of the left hand side of (3.1), but so too does the flux quantization condition (1.29), for submanifolds $\Sigma_\Upsilon \subset Y_{2n+1}$ that themselves fibre over the spindle direction Σ. Here we provide a general differential-geometric proof for arbitrary fibre X_{2n-1}. Later in chapter 4 we will obtain an alternative proof for the case of toric X_{2n-1}.

We begin by noting that from $\varrho = b_1 \mathrm{d}\eta$, (3.1) is equivalent to

$$\int_{Y_{2n+1}} \eta \wedge \mathrm{d}\eta \wedge \Gamma = \frac{2\pi}{b_0} \left(m_+ \int_{X_+} \eta \wedge \Gamma - m_- \int_{X_-} \eta \wedge \Gamma \right) . \tag{3.2}$$

In section 2.1.1 we introduced on Y_{2n+1} a set of 2π-period coordinates φ_μ, $\mu = 0, \ldots, s$, which are globally well-defined away from the fixed points of the $U(1)^{s+1}$ action on Y_{2n+1}. In particular, φ_0 is a 2π-period coordinate for the azimuthal direction of the spindle Σ, while φ_i, $i = 1, \ldots, s$, are coordinates on the fibres X_{2n-1}. φ_0 is then well-defined on Σ, except at the poles. Each pole of the spindle is locally modelled as a quotient $\mathbb{C}/\mathbb{Z}_{m_\pm}$, where we introduced complex coordinates $z_\pm = |z_\pm| \mathrm{e}^{\mathrm{i}\hat{\phi}_\pm}$ on the covering space copies of $\mathbb{C}$. Via (2.5),

(2.6), we then have

$$\hat{\phi}_+ = \frac{1}{m_+}\,\varphi_0\,, \qquad \hat{\phi}_- = -\frac{1}{m_-}\,\varphi_0\,. \tag{3.3}$$

Given the above notation, we next define the one-form

$$\upsilon_0 \;\equiv\; \frac{\mathrm{d}\varphi_0}{2\pi}\,. \tag{3.4}$$

A priori this is a one-form on Σ that is well-defined except at the poles. We may then pull this back to a one-form $\pi^*\upsilon_0$ on Y_{2n+1}, which in an abuse of notation we simply refer to also as υ_0. The latter is correspondingly then well-defined on Y_{2n+1}, except at the fibres $X_\pm$ over the poles, *i.e.* precisely where we integrate on the right hand side of (3.2).

The form υ_0 is manifestly closed, but we must be careful at the poles. Indeed, if we take the standard complex coordinate $z = |z|\mathrm{e}^{\mathrm{i}\phi}$ on $\mathbb{C}$, where ϕ has period 2π, then $\upsilon \equiv \mathrm{d}\phi/2\pi$ is a smooth one-form on $\mathbb{C}\setminus\{0\}$. Its exterior derivative is a two-form that is zero on $\mathbb{C}\setminus\{0\}$, but we also have

$$\int_{S^1_\epsilon} \upsilon = 1\,, \tag{3.5}$$

where $S^1_\epsilon \equiv \{|z| = \epsilon\}$ is the circle of radius $\epsilon > 0$. We may then identify

$$\mathrm{d}\upsilon = \delta \;\equiv\; \delta(x,y)\,\mathrm{d}x\wedge\mathrm{d}y\,, \tag{3.6}$$

as a distribution-valued two-form, where $z = x + \mathrm{i}y$, and $\delta(x,y)$ is the usual Dirac delta function. More abstractly, $\mathrm{d}\upsilon = \delta$ is a delta function representative of the Poincaré dual to the origin $0 \in \mathbb{C}$. We then have

$$1 = \int_{D_\epsilon} \delta = \int_{D_\epsilon} \mathrm{d}\upsilon = \int_{S^1_\epsilon} \upsilon\,, \tag{3.7}$$

as in (3.5), where $D_\epsilon \equiv \{|z| \leq \epsilon\}$ is the disc of radius ϵ.

We may apply the above analysis to υ_0 on the spindle, where $\mathrm{d}\upsilon_0$ is zero except at the

poles of Σ. These are both orbifold singularities, where recall that we introduced a local model at each pole, starting with $\mathbb{C}\times X_{2n-1}$ and then quotienting by the $\mathbb{Z}_{m_\pm}$ action generated by (2.3). We may then identify

$$\mathrm{d}\upsilon_0 = m_+\delta_+ - m_-\delta_- \,. \tag{3.8}$$

Here the factors of $\pm m_\pm$ come from the corresponding factors in (3.3), and $\delta_\pm$ are defined precisely as in (3.6), in local coordinates $z_\pm$ for each covering space $\mathbb{C}$. Notice that the origin of $\mathbb{C}$ is fixed under the $\mathbb{Z}_{m_\pm}$ action generated by (2.3), so this group acts purely on the fibres X_{2n-1} over the origin in $\mathbb{C}\times X_{2n-1}$, meaning the fibres over the poles are $X_\pm = X_{2n-1}/\mathbb{Z}_{m_\pm}$. Using (3.8) we may then immediately write

$$\int_{Y_{2n+1}} \eta\wedge\mathrm{d}\upsilon_0\wedge\Gamma = m_+\int_{X_+}\eta\wedge\Gamma - m_-\int_{X_-}\eta\wedge\Gamma\,. \tag{3.9}$$

Here $\mathrm{d}\upsilon_0$ is zero except near to $X_\pm$, which are at the origins of each local model $(\mathbb{C}\times X_{2n-1})/\mathbb{Z}_{m_\pm}$. On the other hand, the delta functions in (3.8) precisely restrict the integral to these copies of $X_\pm$. Starting with the left hand side of (3.9), we may then integrate by parts, using the fact that $\mathrm{d}\Gamma = 0$, to obtain[2]

$$\int_{Y_{2n+1}} \eta\wedge\mathrm{d}\upsilon_0\wedge\Gamma = \int_{Y_{2n+1}} \upsilon_0\wedge\mathrm{d}\eta\wedge\Gamma = \int_{Y_{2n+1}} (\xi\lrcorner\upsilon_0)\,\eta\wedge\mathrm{d}\eta\wedge\Gamma\,. \tag{3.10}$$

Here in the last step we have used the fact that both $\mathrm{d}\eta$ and Γ are basic, so $\xi\lrcorner\mathrm{d}\eta = 0 = \xi\lrcorner\Gamma$, while $\xi\lrcorner\eta = 1$. On the other hand, from (1.25) we immediately have $\xi\lrcorner\upsilon_0 = b_0/2\pi$. Combining (3.10) with (3.9), we have thus proven (3.2).

3.1.2 Gravitational block formula

We can now use these results to refine the extremal problem discussed in section 1.2.3 for GK geometries of the fibred form (2.1). Specifically we want to reconsider the supersymmetric

[2]One can circumvent the use of delta functions by instead cutting out small neighbourhoods of $X_\pm$ in Y_{2n+1}, to obtain a manifold with two boundary components, $(S^1\times X_{2n-1})/\mathbb{Z}_{m_+}\sqcup(-S^1\times X_{2n-1})/\mathbb{Z}_{m_-}$, and then integrating $\upsilon_0\wedge\eta\wedge\Gamma$ over this boundary. The integral of υ_0 over the circle factors gives $m_\pm$, resulting in the right hand side of (3.9). Instead using Stokes' theorem, we have $\mathrm{d}\upsilon_0 = 0$ on the interior of the manifold with boundary, and the only contribution is the right hand side of (3.10).

action (1.27), the constraint equation (1.28) and the expression for the fluxes (1.29).

We first observe that the supersymmetric action (1.27) takes the form of (3.1), with $\Gamma = J^{n-1}/(n-1)!$ and hence we may write

$$\begin{aligned} S_{\rm SUSY} &= \frac{2\pi b_1}{b_0}\left(m_+\int_{X_+}\eta\wedge\frac{J^{n-1}}{(n-1)!} - m_-\int_{X_-}\eta\wedge\frac{J^{n-1}}{(n-1)!}\right) \\ &= \frac{2\pi b_1}{b_0}\left[m_+{\rm Vol}(X_+) - m_-{\rm Vol}(X_-)\right], \end{aligned} \tag{3.11}$$

where ${\rm Vol}(X_\pm)$ are the induced volumes of the fibres over the poles. Indeed, since $X_\pm \cong X_{2n-1}/\mathbb{Z}_{m_\pm}$, we have in both cases $m_\pm{\rm Vol}(X_\pm) = {\rm Vol}(X_{2n-1})$, although the induced volume forms for each copy of X_{2n-1} are in general different, and the volumes are different. We shall obtain an explicit formula for this for toric X_{2n-1} in section 4.2. As remarked after equation (3.1), the orientations of $X_\pm$ in (3.11) may not agree with those induced from the complex structure on $C(Y_{2n+1})$, and correspondingly the "volumes" ${\rm Vol}(X_\pm)$ will then be negative.

We next note that there are two preferred fluxes, $N^{X_\pm}$, associated with the fibres $X_\pm \cong X_{2n-1}/\mathbb{Z}_{m_\pm}$ at the north and south poles, respectively. Following (1.29) we define

$$\int_{X_\pm}\eta\wedge\varrho\wedge\frac{J^{n-2}}{(n-2)!} \equiv \nu_n\, N^{X_\pm}\,. \tag{3.12}$$

We can then apply (3.1) to the constraint equation (1.28). We set $\Gamma = \varrho\wedge\frac{J^{n-2}}{(n-2)!}$, so that the constraint becomes

$$m_+\int_{X_+}\eta\wedge\varrho\wedge\frac{J^{n-2}}{(n-2)!} - m_-\int_{X_-}\eta\wedge\varrho\wedge\frac{J^{n-2}}{(n-2)!} = 0\,. \tag{3.13}$$

Thus, the constraint equation simply relates the two fluxes $N^{X_\pm}$ in (3.12). It is convenient to then define $N\in\mathbb{Z}$ via

$$N \equiv m_+N^{X_+} = m_-N^{X_-} \tag{3.14}$$

Fixing an orientation on the fibres, without loss of generality we will take $N>0$, from which we also have $N^{X_\pm}>0$. Notice that since m_+ and m_- are assumed co-prime, this means that $N = m_+m_-\mathcal{N}_0$, where $\mathcal{N}_0\in\mathbb{N}$.

Before continuing, we now define the geometric R-charges for GK geometries of the fibred

form (2.1). The R-charges, $R_a^\pm$, are associated with certain supersymmetric submanifolds $S_a^\pm$ of dimension $(2n-3)$ in Y_{2n+1}. More precisely, these may be defined as follows. We begin with a set of $U(1)^s$-invariant codimension two submanifolds $S_a \subset X_{2n-1}$, whose cones are divisors in the Calabi-Yau cone X_{2n-1}.[3] These in turn define codimension four submanifolds $S_a^\pm \subset Y_{2n+1}$, as the copies of S_a in the fibres $X_\pm = X_{2n-1}/\mathbb{Z}_{m_\pm}$ over the two poles of the spindle. We then define

$$R_a^\pm \equiv \frac{4\pi}{\nu_n N^{X_\pm}} \int_{S_a^\pm} \eta \wedge \frac{J^{n-2}}{(n-2)!} \,. \tag{3.15}$$

For $\mathrm{AdS}_3 \times Y_7$ solutions when $n=3$, the latter are three-dimensional supersymmetric submanifolds in the fibres $X_5/\mathbb{Z}_{m_\pm}$ and the geometric R-charges are dual to the R-charges of baryonic operators associated with D3-branes wrapping these submanifolds. Similarly, for $\mathrm{AdS}_2 \times Y_9$ solutions when $n=4$, they are five-dimensional supersymmetric submanifolds in the fibres $X_7/\mathbb{Z}_{m_\pm}$ and the geometric R-charges are dual to the R-charges of baryonic operators associated with M5-branes wrapping these submanifolds. We emphasize that these supersymmetric submanifolds exist even in cases with $H^2(X_{2n-1},\mathbb{R}) \cong 0$, which we discuss further in section 3.2. We also note that there is again an issue of orientation on S_a and we will see later in the toric case that we have $R_a^+ > 0$ and $\sigma R_a^- > 0$.

We now compute the fluxes through another preferred class of $(2n-1)$-dimensional submanifolds $\Sigma_a \subset Y_{2n+1}$. Specifically, we consider Σ_a which are the total spaces of the supersymmetric submanifolds S_a of the fibres X_{2n-1} defined above, that are then fibred over the spindle Σ:

$$S_a \hookrightarrow \Sigma_a \to \Sigma \,. \tag{3.16}$$

The associated flux through this class of cycles is[4]

$$\int_{\Sigma_a} \eta \wedge \varrho \wedge \frac{J^{n-2}}{(n-2)!} \equiv \nu_n M_a \,, \tag{3.17}$$

[3] Later in section 4.2 we will take these to be precisely the toric divisors when $C(X_{2n-1})$ is a toric Calabi-Yau cone, with the index $a = 1, \ldots, d$ running over the number of facets d of the associated polyhedral cone in $\mathbb{R}^n$. But for now we may take a to be a general index, labelling any set of $U(1)^s$ invariant divisors in $C(X_{2n-1})$.

[4] We emphasize that the fluxes M_a are, in general, distinct from the fluxes $\mathcal{N}_\Upsilon$ in (1.29) – see (4.51). We also note that even when $H_{2n-3}(X_{2n-1},\mathbb{R}) = 0$, so that the homology classes of S_a in the fibres X_{2n-1} are necessarily trivial, it does not follow that the M_a are zero. Indeed, these are integrals of the flux over Σ_a, whose homology classes are generically non-trivial due to the fibration.

where $M_a \in \mathbb{Z}$. In a completely analogous fashion to how we derived the block formula (3.1), we can split the integral in (3.17) into two pieces as

$$\int_{\Sigma_a} \eta \wedge \varrho \wedge \frac{J^{n-2}}{(n-2)!} = \frac{2\pi b_1}{b_0} \left(m_+ \int_{S_a^+} \eta \wedge \frac{J^{n-2}}{(n-2)!} - m_- \int_{S_a^-} \eta \wedge \frac{J^{n-2}}{(n-2)!} \right), \tag{3.18}$$

where recall that $S_a^\pm$ are the copies of the S_a in the fibres over the north and south poles of the spindle, respectively. We thus conclude that these preferred fluxes are related to the R-charges associated to these submanifolds via

$$M_a = \frac{b_1}{2b_0} \left(R_a^+ - R_a^- \right) N \,. \tag{3.19}$$

3.2 Flavour and universal (anti-)twist

We can make further progress by making some additional assumptions on the GK geometry. In this section we first consider what we call *flavour twist* (called "mesonic twist" in the toric setting in [127]) followed by the *universal anti-twist*, which involves an additional assumption.

3.2.1 Flavour twist

First consider the special class of geometries where the fibre X_{2n-1} has no baryonic symmetries, *i.e.* $H^2(X_{2n-1}, \mathbb{R}) \cong 0$. The nomenclature comes from the fact that for $n = 3, 4$ the field theories dual to the associated $\mathrm{AdS}_5 \times X_5$ and $\mathrm{AdS}_4 \times X_7$ geometries then have no baryonic $U(1)$ flavour symmetries. For this case the transverse Kähler class of the GK geometry restricted to the fibres at the poles, $[J|_{X_\pm}]$, must necessarily be proportional to $[\varrho]$ and we can write

$$[J|_{X_\pm}] = \Lambda_\pm [\varrho|_{X_\pm}] \in H_B^2(\mathcal{F}_{\xi_\pm}) \,, \tag{3.20}$$

with $\Lambda_\pm \in \mathbb{R}$, and recall that $\xi_\pm$ are the R-symmetry vectors of the fibres $X_\pm$, introduced in (2.18).

We can also consider a more general class of geometries where we do not assume $H^2(X_{2n-1}, \mathbb{R}) \cong 0$, but nevertheless (3.20) is still satisfied. We call this the "flavour twist". We will see below that this corresponds to fixing the GK geometry Y_{2n+1}, including certain constraints on the

fluxes M_a, in terms of X_{2n-1}, $m_\pm$ and p_i.

Substituting (3.20) into the supersymmetric action (3.11) we obtain

$$\begin{aligned} S_{\rm SUSY} &= \frac{2\pi b_1}{b_0}\left(m_+\Lambda_+^{n-1}\int_{X_+}\eta\wedge\frac{\varrho^{n-1}}{(n-1)!} - m_-\Lambda_-^{n-1}\int_{X_-}\eta\wedge\frac{\varrho^{n-1}}{(n-1)!}\right) \\ &= \frac{\pi(2b_1)^n}{b_0}\left[m_+\Lambda_+^{n-1}\,{\rm Vol}_S(X_+) - m_-\Lambda_-^{n-1}\,{\rm Vol}_S(X_-)\right] . \end{aligned} \tag{3.21}$$

Here ${\rm Vol}_S(X_\pm)$ is the Sasakian volume, obtained from ${\rm Vol}(X_\pm)$ by setting $[J]=\frac{1}{2b_1}[\varrho]$, namely

$${\rm Vol}_S(X_\pm) = \frac{1}{(2b_1)^{n-1}}\int_{X_\pm}\eta\wedge\frac{\varrho^{n-1}}{(n-1)!} . \tag{3.22}$$

These Sasaki volumes can be considered to be functions of trial Reeb vectors $\xi_\pm$ tangent to $X_\pm$. In practice, ${\rm Vol}_S(X_\pm)$ can be computed by taking the expression for the Sasakian volume of the fibre manifold X_{2n-1} and taking the trial Reeb vector to be the orthogonal projection of the R-symmetry vector ξ on Y_{2n+1} onto the fibres over the poles. We should divide by $m_\pm$ in order to take into account the quotient, and hence we can write

$${\rm Vol}_S(X_\pm) = \frac{1}{m_\pm}\,{\rm Vol}_S(X_{2n-1})|_{\xi=\xi_\pm} = \frac{1}{m_\pm}\,{\rm Vol}_S(X_{2n-1})|_{b_i^{(\pm)}} . \tag{3.23}$$

Here ${\rm Vol}_S(X_{2n-1})|_{b_i}$ is the standard positive Sasaki volume on X_{2n-1} as a function of b_i (leading to a positive Sasaki-Einstein volume after extremization). We thus have

$$S_{\rm SUSY} = \frac{\pi(2b_1)^n}{b_0}\left[\Lambda_+^{n-1}\;{\rm Vol}_S(X_{2n-1})|_{b_i^{(+)}} - \Lambda_-^{n-1}\;{\rm Vol}_S(X_{2n-1})|_{b_i^{(-)}}\right] . \tag{3.24}$$

To make further progress, we now consider the expression for the flux quantization (3.12) through the fibres over the poles. Using the same type of argument we find

$$N^{X_\pm} = \frac{1}{\nu_n}\int_{X_\pm}\eta\wedge\varrho\wedge\frac{J^{n-2}}{(n-2)!} = \frac{(n-1)}{m_\pm}\,\frac{(2b_1)^{n-1}}{\nu_n}\,\Lambda_\pm^{n-2}\,{\rm Vol}_S(X_{2n-1})|_{b_i^{(\pm)}} , \tag{3.25}$$

and we also recall the constraint equation (3.14) given by $N=m_+N^{X_+}=m_-N^{X_-}$. We can therefore solve for $\Lambda_\pm$ in terms of N. After substituting into (3.24) we obtain an expression for the off-shell action as a function of the R-symmetry vector ξ given in (1.25) and the

integer N. At this point, we can set $b_1 = \frac{2}{n-2}$ and the extremization of the GK geometry with respect to the remaining components of b_μ can be carried out.

Before doing that we derive an expression for the geometric R-charges $R_a^\pm$, defined in (3.15). Recall that $S_a^\pm$ are the copies of the supersymmetric $(2n-3)$-dimensional submanifolds S_a in the fibres over the north and south poles of the spindle, respectively. We can express $R_a^\pm$ in terms of the Sasakian volume of the submanifolds $S_a^\pm$, defined as

$$\mathrm{Vol}_S(S_a^\pm) \equiv \frac{1}{(2b_1)^{n-2}} \int_{S_a^\pm} \eta \wedge \frac{\varrho^{n-2}}{(n-2)!} = \frac{1}{m_\pm} \mathrm{Vol}_S(S_a)|_{b_i^{(\pm)}} \ . \tag{3.26}$$

Here $\mathrm{Vol}_S(S_a)|_{b_i}$ is the standard positive Sasaki volume of the submanifold $S_a \subset X_{2n-1}$ as a function of b_i (leading to a positive result on the Sasaki-Einstein manifold after extremization). Hence, after eliminating $\Lambda_\pm$ using (3.25), we can conclude that

$$R_a^\pm = \frac{2\pi}{(n-1)b_1} \left. \frac{\mathrm{Vol}_S(S_a)}{\mathrm{Vol}_S(X_{2n-1})} \right|_{b_i^{(\pm)}} \ . \tag{3.27}$$

Notice that using (3.19) we can therefore write the fluxes in the form

$$M_a = \frac{\pi N}{(n-1)b_0} \left[\left. \frac{\mathrm{Vol}_S(S_a)}{\mathrm{Vol}_S(X_{2n-1})} \right|_{b_i^{(+)}} - \left. \frac{\mathrm{Vol}_S(S_a)}{\mathrm{Vol}_S(X_{2n-1})} \right|_{b_i^{(-)}} \right] . \tag{3.28}$$

This equation must be interpreted carefully. The fluxes M_a on the left hand side are integers, while on the right hand side for fixed X_{2n-1} this is a function of the spindle data $m_\pm$, the flavour twisting variables p_i, and the R-symmetry vector $(b_\mu) = (b_0, b_1, \ldots, b_s) \in \mathbb{R}^{s+1}$. Fixing X_{2n-1}, $m_\pm$ and p_i fixes the internal space Y_{2n+1}, while the extremization involves varying over the R-symmetry vector, which of course is not compatible with holding the M_a fixed in (3.28). However, the correct interpretation is to extremize the supersymmetric action, detailed below in (3.34), (3.36), to obtain the critical R-symmetry b_μ^*, and then use this to compute the associated fluxes for this flavour twist solution using (3.28); in this sense the GK geometry Y_{2n+1} and the fluxes M_a are fixed by X_{2n-1}, $m_\pm$ and p_i. A necessary and sufficient condition for this to make sense is that the right hand side of (3.28) is rational (hence integer for appropriate choice of N). On the other hand, this is guaranteed to be true if $(b_\mu^*) \in \mathbb{Q}^{s+1}$ is itself rational, as the Sasakian volumes are (up to overall powers of π which

cancel) rational functions of b_i with rational coefficients [67]. The fluxes are thus determined in this way for the flavour twist. We shall also expand upon this point in section 4.2.3, in the case that X_{2n-1} is toric.

We now return to the issue of signs. Recall that $N = m_+ N^{X_+} = m_- N^{X_-} > 0$ and hence from (3.25) we can conclude that for odd n we have $\Lambda_\pm \operatorname{Vol}_S(X_{2n-1})|_{b_i^{(\pm)}} > 0$ while for even n we have $\operatorname{Vol}_S(X_{2n-1})|_{b_i^{(\pm)}} > 0$. Next consider $\operatorname{Vol}(X_\pm)$:

$$\operatorname{Vol}(X_\pm) \equiv \int_{X_\pm} \eta \wedge \frac{J^{n-1}}{(n-1)!} = \frac{(2b_1)^{n-1}}{m_\pm} \Lambda_\pm^{n-1} \operatorname{Vol}_S(X_{2n-1})|_{b_i^{(\pm)}} \,. \tag{3.29}$$

Recalling our discussion in section 3.1.2, by considerations of the toric case (see (4.30)), the orientation on $X_\pm$ that we need to take are such that

$$\operatorname{Vol}(X_+) > 0 \,, \qquad \sigma \operatorname{Vol}(X_-) > 0 \,. \tag{3.30}$$

Thus, for odd n we have:

$$\Lambda_+ > 0, \quad \sigma\Lambda_- > 0, \qquad \operatorname{Vol}_S(X_{2n-1})|_{b_i^{(+)}} > 0, \quad \sigma \operatorname{Vol}_S(X_{2n-1})|_{b_i^{(-)}} > 0 \,, \tag{3.31}$$

while for even n we have:

$$\Lambda_+ > 0, \quad \sigma\Lambda_- > 0, \qquad \operatorname{Vol}_S(X_{2n-1})|_{b_i^{(+)}} > 0, \quad \operatorname{Vol}_S(X_{2n-1})|_{b_i^{(-)}} > 0 \,, \tag{3.32}$$

which fixes the sign ambiguity in solving (3.25).

We now further illustrate using the two cases of physical interest when $n = 3$ and $n = 4$. The case $n = 3$ is associated with $\mathrm{AdS}_3 \times Y_7$ solutions. From (3.25) and (3.31) we have

$$\Lambda_\pm = \frac{\nu_3 N}{8 b_1^2 \operatorname{Vol}_S(X_5)|_{b_i^{(\pm)}}} \,. \tag{3.33}$$

Using (3.24) we therefore find that the off-shell central charge (1.34) can be written

$$\mathscr{Z} = \frac{6\pi^3 N^2}{b_1 b_0} \left(\frac{1}{\operatorname{Vol}_S(X_5)|_{b_i^{(+)}}} - \frac{1}{\operatorname{Vol}_S(X_5)|_{b_i^{(-)}}} \right) = \frac{24}{b_0 b_1} \left(a_{\mathrm{grav}}[\xi_+] - a_{\mathrm{grav}}[\xi_-] \right) , \tag{3.34}$$

where in the last step we related $\mathscr{Z}$ to a sum of contributions corresponding to the 4d central charge (1.15) of the parent 4d field theory, dual to $\mathrm{AdS}_5 \times X_5$ solutions, evaluated on the projection of the R-symmetry vector tangent to the fibres. We should then set $b_1 = 2$ when carrying out the extremization.

We now consider the case of $n = 4$, associated with $\mathrm{AdS}_2 \times Y_9$ solutions. From (3.25) and (3.32) we now have

$$\Lambda_+ = \left[\frac{\nu_4 N}{24 b_1^3 \,\mathrm{Vol}_S(X_7)|_{b_i^{(+)}}}\right]^{1/2}, \qquad \Lambda_- = \sigma \left[\frac{\nu_4 N}{24 b_1^3 \,\mathrm{Vol}_S(X_7)|_{b_i^{(-)}}}\right]^{1/2} \tag{3.35}$$

The off-shell entropy (1.38) now reads

$$\mathscr{S} = \frac{8\pi^3 N^{3/2}}{3 b_0 \sqrt{6 b_1}} \left(\frac{1}{\sqrt{\mathrm{Vol}_S(X_7)|_{b_i^{(+)}}}} - \frac{\sigma}{\sqrt{\mathrm{Vol}_S(X_7)|_{b_i^{(-)}}}}\right) = \frac{4}{b_0 \sqrt{b_1}} \left(F_{\mathrm{grav}}[\xi_+] - \sigma\, F_{\mathrm{grav}}[\xi_-]\right) , \tag{3.36}$$

where in the last step we likewise wrote the $\mathscr{S}$ as a sum of free energies (1.19) of the parent 3d field theory, dual to $\mathrm{AdS}_4 \times X_7$ solutions, evaluated on the projection of the R-symmetry vector tangent to the fibres. We should then set $b_1 = 1$ when carrying out the extremization.

It is interesting to make a comparison with fibrations with no baryonic symmetries over round two spheres. To do this we want to consider the twist case, *i.e.* $\sigma = 1$, set $m_\pm = 1$ and take the limit $b_0 \to 0$. First observe that with $\sigma = 1$ we have

$$\lim_{b_0 \to 0} \frac{f(b_i^{(+)}) - f(b_i^{(-)})}{b_0} = -\sum_{i=1}^{s} \left(\frac{v_{+i}}{m_+} + \frac{v_{-i}}{m_-}\right) \frac{\partial f}{\partial b_i} = \sum_{i=1}^{s} \frac{p_i}{m_+ m_-} \frac{\partial f}{\partial b_i} , \tag{3.37}$$

where $f(b_i)$ is a generic function of the Reeb vector. Defining the operator $\nabla = -\sum_{i=1}^{s} \frac{p_i}{m_+ m_-} \frac{\partial}{\partial b_i}$ we thus have

$$\lim_{b_0 \to 0} \mathscr{Z} = -\frac{24}{b_1} \nabla\, a_{\mathrm{grav}}[\xi] , \qquad \lim_{b_0 \to 0} \mathscr{S} = -\frac{4}{\sqrt{b_1}} \nabla\, F_{\mathrm{grav}}[\xi] . \tag{3.38}$$

In these expressions one should take derivatives with respect to b_1 before setting $b_1 = 2$ or $b_1 = 1$, respectively. We also observe that after setting $m_\pm = 1$ the second equation in (3.38) is the same as equation (3.10) of [127], who considered the case of X_7 with no baryonic

symmetries fibred over a round two-sphere.

3.2.2 Universal anti-twist

The universal anti-twist case is associated with Sasaki-Einstein X_{2n-1} fibred over the spindle and, moreover, with the twisting in the fibration only along the Reeb Killing vector of the Sasaki-Einstein space. The first condition is achieved by imposing again the flavour twist condition (3.20) imposed in the previous subsection. However, in addition we demand that the fluxes, p_i, determining the fibration satisfy

$$p_i = \frac{p_1}{b_1^{(+)}} b_i^{(+)} = \frac{p_1}{b_1^{(-)}} b_i^{(-)} \,. \tag{3.39}$$

We need to check *a posteriori* that after extremization this is consistent with the p_i being integers, much as with the discussion of fluxes after equation (3.28). We comment on this further below. Note that (3.39) is consistent with (2.20) and, in particular, implies that the twisting parameters can be written as

$$p_i = \frac{p_1}{[b_1 + b_0(-a_- + \sigma a_+)]}\, b_i \,, \qquad i = 2, \ldots, s \,. \tag{3.40}$$

As we will see we shall need to set $\sigma = -1$, and thus just have the anti-twist case, as well as take the Sasaki-Einstein manifold X_{2n-1} to be quasi-regular.

Since the universal anti-twist is a special case of the previous subsection, we can carry over all of the previous results of section 3.2.1 and write, for general n,

$$S_{\rm SUSY} = \frac{\pi(\nu_n N)^{\frac{n-1}{n-2}}}{[2b_1(n-1)^{n-1}]^{\frac{1}{n-2}} b_0} \left[\frac{1}{[\mathrm{Vol}_S(X_{2n-1})|_{b_i^{(+)}}]^{\frac{1}{n-2}}} - \frac{k_n}{[\mathrm{Vol}_S(X_{2n-1})|_{b_i^{(-)}}]^{\frac{1}{n-2}}} \right] , \tag{3.41}$$

where $k_n = +1$ if n is odd and $k_n = \sigma$ if is n even. As usual, to extremize we should set $b_1 = 2/(n-2)$. To proceed we extremize first over b_i and then b_0. For the former, it is useful to use (3.39) to introduce a new variable

$$r_i \equiv \frac{n}{b_1^{(+)}}\, b_i^{(+)} = \frac{n}{b_1^{(-)}}\, b_i^{(-)} \,, \tag{3.42}$$

and we note that $r_1 = n$. We next recall that $\mathrm{Vol}_S(X_{2n-1})(r_i)$, as a function of the Reeb vector r_i, is homogeneous of degree $-n$ in r_i. Hence, we can write

$$\mathrm{Vol}_S(X_{2n-1})|_{b_i^{(\pm)}} = \left(\frac{b_1^{(\pm)}}{n}\right)^{-n} \mathrm{Vol}_S(X_{2n-1})|_{r_i} \ , \tag{3.43}$$

and after substituting into (3.41) we obtain

$$S_{\mathrm{SUSY}} = \frac{\pi(\nu_n N)^{\frac{n-1}{n-2}}}{[2b_1 n^n (n-1)^{n-1}]^{\frac{1}{n-2}} b_0} \frac{1}{[\mathrm{Vol}_S(X_{2n-1})|_{r_i}]^{\frac{1}{n-2}}} \left[(b_1^{(+)})^{\frac{n}{n-2}} - k_n\,(b_1^{(-)})^{\frac{n}{n-2}}\right]. \tag{3.44}$$

At this point we can set $b_1 = 2/(n-2)$ and proceed with the extremization. It is clear that extremizing over b_i is the same as extremizing over r_i. Thus, we immediately deduce that S_{SUSY} is extremized over b_i when $\mathrm{Vol}_S(X_{2n-1})|_{r_i}$ is extremized over r_i and, recalling that $r_1 = n$, this results in nothing but the Sasaki-Einstein volume *i.e.* $\mathrm{Vol}_{SE}(X_{2n-1})$. This leads to the off-shell action

$$S_{\mathrm{SUSY}} = \left(\frac{n-2}{4n^n(n-1)^{n-1}}\right)^{\frac{1}{n-2}} \frac{\pi(\nu_n N)^{\frac{n-1}{n-2}}}{\mathrm{Vol}_{SE}(X_{2n-1})^{\frac{1}{n-2}}} \frac{1}{b_0} \left[(b_1^{(+)})^{\frac{n}{n-2}} - k_n (b_1^{(-)})^{\frac{n}{n-2}}\right] , \tag{3.45}$$

with the extremization over b_0 still to be carried out. We will explicitly extremize over b_0 for the two cases of physical interest below and favourably compare with known results for explicit supergravity solutions.

For the geometric R-charges, from (3.27) and (3.42) we have

$$R_a^{\pm} = \frac{2\pi}{(n-1)b_1} \left.\frac{\mathrm{Vol}_S(S_a)}{\mathrm{Vol}_S(X_{2n-1})}\right|_{\frac{b_1^{(\pm)} r_i}{n}} , \tag{3.46}$$

where $\mathrm{Vol}_S(S_a)$ is the volume of S_a with respect to the Sasakian metric. Now $\mathrm{Vol}_S(X_{2n-1})(r_i)$ and $\mathrm{Vol}_S(S_a)(r_i)$ are homogeneous of degree $-n$ and $-(n-1)$ in r_i, respectively. Thus, by a similar scaling argument we deduce that after extremizing over b_i the off-shell R-charges, as a function of b_0, are given by

$$R_a^{\pm} = \frac{2\pi b_1^{(\pm)}}{n(n-1)b_1} \frac{\mathrm{Vol}_{SE}(S_a)}{\mathrm{Vol}_{SE}(X_{2n-1})} = \frac{b_1^{(\pm)}}{b_1} R_a \, , \tag{3.47}$$

where we introduced

$$R_a \equiv \frac{2\pi}{n(n-1)} \frac{\mathrm{Vol}_{SE}(S_a)}{\mathrm{Vol}_{SE}(X_{2n-1})} \,. \tag{3.48}$$

For $n = 3$ and $n = 4$ we have $R_a \equiv R_a^{\mathrm{4d}}$ and $R_a \equiv R_a^{\mathrm{3d}}$, respectively, where R_a^{4d} and R_a^{3d} are the R-charges associated with the $\mathrm{AdS}_5 \times SE_5$ and $\mathrm{AdS}_4 \times SE_7$ solutions, respectively. Note that combining (3.19) with (2.20), the equations above for $R_a^{\pm}$ allows us to find the fluxes (with $\sigma = -1$)

$$M_a = \frac{b_1}{2b_0}(R_a^+ - R_a^-)N = \frac{1}{2b_0}\,(b_1^{(+)} - b_1^{(-)})R_a N = \frac{m_+ - m_-}{2m_+m_-} R_a N \,, \tag{3.49}$$

and we also have (with $\sigma = -1$)

$$R_a^+ + R_a^- = \left(2 - \frac{b_0}{b_1}\chi\right) R_a \,, \tag{3.50}$$

where $\chi = (m_- + m_+)/(m_- m_+)$ is the orbifold Euler character of the spindle. In both (3.49), (3.50) we have set $\sigma = -1$, as it is needed for the universal anti-twist case. Note that in the special case that the SE space is toric, we have $\sum_a R_a = 2$ and hence we then also have (with $\sigma = -1$)

$$\frac{1}{2}\sum_a (R_a^+ + R_a^-) = 2 - \frac{b_0}{b_1}\,\chi \,. \tag{3.51}$$

Finally, we should return to the issue of everything being properly quantized. Combining (3.40) with (3.42) and evaluating on-shell, we have

$$p_i = \frac{p_1}{n}\, r_i^* \,, \tag{3.52}$$

where r_i^* is the critical Reeb vector for the Sasaki-Einstein metric on X_{2n-1}. The latter is thus necessarily quasi-regular, meaning that $(r_i^*) \in \mathbb{Q}^s$ is rational. One may then ensure that $p_i \in \mathbb{Z}$ in (3.52) by appropriately choosing $p_1 = m_+ - m_- \in \mathbb{Z}$, which is a constraint on the choice of spindle Σ. Note that a similar conclusion was reached for the universal twist solutions in [70], where there $b_0 = 0$ and $\Sigma = \Sigma_g$ is a smooth Riemann surface. In that case the universal twist requires an appropriate divisibility property for the genus g of the

Riemann surface. Such issues were also effectively discussed in [47] for the explicit $\mathrm{AdS}_3 \times Y_7$ universal anti-twist solutions described in the next subsection, where $\mathbb{Z}_k$ quotients along the Reeb $U(1)$ isometry of the Sasaki-Einstein metric on X_{2n-1} were also considered[5].

Finally, since the R-charges R_a are rational for rational Reeb vector r_i^*, one may ensure the fluxes M_a in (3.49) are integer by appropriately choosing N. Again, *cf.* the discussion of the universal twist in [70].

3.2.2.1 $\mathbf{AdS}_3 \times Y_7$ case

For the $n = 3$ case, from (1.34) and (3.45), we therefore have

$$\mathscr{Z} = \frac{\pi^3 N^2}{9\mathrm{Vol}(SE_5)} \frac{1}{b_0} \left[(b_1^{(+)})^3 - (b_1^{(-)})^3 \right] . \tag{3.53}$$

Notice that this expression is quadratic in b_0. If we extremize over b_0 we find that it is only in the anti-twist case, $\sigma = -1$, that we get a positive on-shell central charge. So, setting $\sigma = -1$ we find the extremal value

$$b_{0*} = \frac{3m_- m_+ (m_- + m_+)}{m_-^2 + m_- m_+ + m_+^2} . \tag{3.54}$$

We can express the on-shell central charge in terms of, $a_{4\mathrm{d}}$, the central charge of the 4d SCFT, which is given by (1.15) at the SE extremal point, to find

$$c_{\mathrm{grav}} = \mathscr{Z}_{\mathrm{os}} = \frac{4(m_+ - m_-)^3}{3m_- m_+ (m_-^2 + m_- m_+ + m_+^2)} a_{4\mathrm{d}} , \tag{3.55}$$

which is positive for $m_+ > m_-$. The results (3.55) and (3.54) are in precise alignment with the results (21), (22) for the explicit supergravity solutions constructed in minimal gauged supergravity in [47] (after identifying $m_\pm$ with $n_\mp$).

From (3.47), the (off-shell) geometric R-charges can be written in the form

$$R_a^\pm = \frac{1}{2} b_1^{(\pm)} R_a^{4\mathrm{d}} , \tag{3.56}$$

[5]For such quotients the effective $U(1)^s$ action is not the same as on the unquotiented space.

and hence

$$R_a^{\pm} = \pm \frac{(m_+ - m_-)(2m_{\pm} + m_{\mp})}{2(m_-^2 + m_- m_+ + m_+^2)} R_a^{4\mathrm{d}} \,, \tag{3.57}$$

where $R_a^{4\mathrm{d}}$ are the four-dimensional R-charges associated with the $\mathrm{AdS}_5 \times SE_5$ solution. Notice that with $R_a^{4\mathrm{d}} > 0$ and $m_+ > m_-$ we have $R_a^+ > 0$ and $R_a^- < 0$ as expected from the toric discussion later on.

3.2.2.2 $\mathbf{AdS}_2 \times Y_9$ case

For $n = 4$ using (1.38) and (3.45) we get the off-shell entropy

$$\mathscr{S} = \frac{N^{3/2}\pi^3}{6^{3/2}\mathrm{Vol}(SE_7)^{1/2}} \frac{1}{b_0} \left[(b_1^{(+)})^2 - \sigma (b_1^{(-)})^2 \right] , \tag{3.58}$$

which is to be extremized over b_0. If $\sigma = +1$ there are no extrema, so we again conclude that we again must have the anti-twist case with $\sigma = -1$.

We can express the off-shell result in terms of the four-dimensional Newton constant $G_{(4)}$ (in the conventions of [48]), defined by

$$\frac{1}{G_{(4)}} = \frac{2^{3/2}\pi^2}{3^{3/2}\mathrm{Vol}(SE_7)^{1/2}} N^{3/2} \,. \tag{3.59}$$

Recall that the free energy on the three-sphere, $\mathcal{F}_{S^3}$, of the 3d SCFT dual to the $\mathrm{AdS}_4 \times SE_7$ solution is given by (*cf.* (1.19))

$$\mathcal{F}_{S^3} = \frac{\pi}{2G_{(4)}} \,. \tag{3.60}$$

We then can express the off-shell entropy (with $\sigma = -1$) as

$$\mathscr{S} = \frac{\pi}{8G_{(4)}} \frac{1}{b_0} \left[(b_1^{(+)})^2 + (b_1^{(-)})^2 \right] . \tag{3.61}$$

Extremizing over b_0 (and setting $b_1 = 1$) we find two solutions but only one gives a positive

entropy. Focusing on this extremum we find

$$b_{0*} = \frac{\sqrt{2}\, m_- m_+}{\sqrt{m_-^2 + m_+^2}}\,, \tag{3.62}$$

with the associated on-shell entropy given by

$$\mathscr{S}_{\rm os} = \frac{\pi}{4G_{(4)}} \frac{\sqrt{2\,(m_-^2 + m_+^2)} - m_+ - m_-}{m_- m_+}\,. \tag{3.63}$$

This agrees with the entropy for the supersymmetric, accelerating and magnetically charged black holes that were constructed in minimal gauged supergravity in (1.1) of [48].

From (3.47), the (off-shell) geometric R-charges can be written in the form

$$R_a^{\pm} = b_1^{(\pm)} R_a^{\rm 3d}\,, \tag{3.64}$$

and hence

$$R_a^{\pm} = \frac{\sqrt{m_-^2 + m_+^2} - \sqrt{2}\, m_{\mp}}{\sqrt{m_-^2 + m_+^2}}\, R_a^{\rm 3d}\,, \tag{3.65}$$

where $R_a^{\rm 3d}$ are the four-dimensional R-charges associated with the $\mathrm{AdS}_4 \times SE_7$ solution. Notice that with $m_+ > m_-$ and $R_a^{\rm 3d} > 0$ we again have $R_a^+ > 0$ and $R_a^- < 0$ as expected.

Finally, as in [2] we can also make a comparison of the off-shell entropy (3.61) with an off-shell entropy function that was constructed in [48]. More specifically, [48] considered a complex locus of supersymmetric, accelerating and magnetically[6] charged black holes that were non-extremal and then holographically calculated the on-shell action I at the AdS_4 boundary. After suitable extremization I gives rise to the on-shell entropy. To make the connection, note that we can also write the off-shell action (3.61) with $b_1 = 1$ as

$$\mathscr{S} = \mp \frac{1}{2\mathrm{i} G_{(4)}} \left(\frac{\varphi^2}{\omega} + (G_{(4)} Q_m)^2 \omega \right)\,, \tag{3.66}$$

[6] In fact the calculation in [48] was carried out for a larger family of black hole solutions with additional electric charge and rotation.

with

$$(G_{(4)}Q_m) = \frac{m_- - m_+}{4m_-m_+}\,, \qquad \varphi = \frac{\chi(\Sigma)}{4}\,\omega \pm \pi\mathrm{i}\,, \qquad \omega = \mp 2\pi\mathrm{i}\,b_0\,, \tag{3.67}$$

and we see this is precisely the same as (4.41) of [89] with $\mathscr{S} = -I$, where ϕ and ω take the role of chemical potentials associated to electric charge and rotation. However, this relation comes with its own puzzles: I is an on-shell quantity for the AdS_4 black holes, while $\mathscr{S}$ is an off-shell quantity for the associated near horizon AdS_2 solutions. It is therefore hard to see how these might be related physically, although by construction both are "entropy functions", in the sense that extremizing both gives the same black hole entropy.

3.3 Examples

In this section we use the general results of the previous section to calculate some physical quantities for particular examples of $\mathrm{AdS}_3 \times Y_7$ and $\mathrm{AdS}_2 \times Y_9$ solutions. For the $\mathrm{AdS}_3 \times Y_7$ solutions we consider $X_5 = S^5$ and compare with results associated with the explicit supergravity solutions presented in section 2.2. For the $\mathrm{AdS}_2 \times Y_9$ solutions we consider $X_7 = S^7$, for which we can also compare with known supergravity results, as well as $X_7 = V^{5,2}$ for which explicit supergravity solutions are not known. Note that the cases $X_5 = S^5$ and $X_7 = S^7$ can also be treated with the toric methods that we develop in sections 4.1 and 4.2.

3.3.1 $\mathbf{AdS}_3 \times Y_7$ solutions with $X_5 = S^5$

Since $H^2(S^5, \mathbb{R}) \cong 0$ the case of $X_5 = S^5$ is an example with no baryonic symmetries, as in section 3.2. In our chosen basis the Sasakian volume of S^5 as a function of the Reeb vector can be written as

$$\mathrm{Vol}_S(S^5) = \frac{\pi^3}{b_2\,b_3\,(b_1 - b_2 - b_3)}\,. \tag{3.68}$$

As is well known there are three supersymmetric three-submanifolds S_a which are $U(1)^3$ invariant and associated with baryonic operators in $\mathcal{N} = 4$ SYM theory dual to $\mathrm{AdS}_5 \times S^5$.

The Sasakian volume of these submanifolds are given by

$$\mathrm{Vol}_S(S_1) = \frac{2\pi^2}{b_2\, b_3}\,, \qquad\qquad \mathrm{Vol}_S(S_a) = \frac{2\pi^2}{b_a\,(b_1 - b_2 - b_3)}\,, \quad a = 2,3\,. \tag{3.69}$$

It will be convenient below to briefly recall that we obtain the Sasaki-Einstein volume by setting $b_1 = 3$ in (3.68) and then extremizing over b_2, b_3. The extremal values are $b_2 = b_3 = 1$ with $\mathrm{Vol}_{SE}(S^5) = \pi^3$ and $\mathrm{Vol}_{SE}(S_a) = 2\pi^2$.

We now consider the GK geometry associated with the $\mathrm{AdS}_3 \times Y_7$ solutions. The off-shell central charge can be obtained from (3.34) and reads

$$\mathscr{Z} = \frac{6N^2}{b_1 b_0}\left[b_2^{(+)}b_3^{(+)}\left(b_1^{(+)} - b_2^{(+)} - b_3^{(+)}\right) - b_2^{(-)}b_3^{(-)}\left(b_1^{(-)} - b_2^{(-)} - b_3^{(-)}\right)\right]\,. \tag{3.70}$$

Similarly, the off-shell geometric R-charges are obtained from (3.27) and are given by

$$R_1^{\pm} = \frac{2}{b_1}\left(b_1^{(\pm)} - b_2^{(\pm)} - b_3^{(\pm)}\right), \qquad\qquad R_a^{\pm} = \frac{2b_a^{(\pm)}}{b_1}\,, \quad a = 2,3\,. \tag{3.71}$$

Observe that for this example, which is also toric, we have

$$\begin{aligned} \sum_{a=1}^{d} R_a^{\pm} &= \frac{2b_1^{(\pm)}}{b_1}\,, \\ \frac{1}{2}\sum_{a=1}^{d}\left(R_a^{+} + R_a^{-}\right) &= 2 - \frac{m_- - \sigma m_+}{m_+ m_-}\frac{b_0}{b_1}\,, \end{aligned} \tag{3.72}$$

in agreement with the general toric results (4.61), (4.63).

Recall that there are two preferred fluxes, $N^{X_\pm}$, associated with the fibres $X_\pm \cong S^5/\mathbb{Z}_{m_\pm}$ at the north and south poles, respectively, and from (3.14) we have $N \equiv m_+ N^{X_+} = m_- N^{X_-}$. There are no further cohomologically non-trivial five-form fluxes. However, we also have three five-form fluxes M_a defined as the integral of the five-form flux through the three submanifolds Σ_a, obtained as the three supersymmetric submanifolds S_a of S^5 fibred over the spindle, as in (3.17). Using (3.19) we obtain the following expression for the fluxes M_a:

$$\mathfrak{p}_a \equiv \frac{M_a}{N} = \frac{1}{m_+ m_-}\big\{p_1 - (p_2 + p_3), p_2, p_3\big\}\,, \tag{3.73}$$

where as usual, $p_1 = -\sigma m_+ - m_-$. For this example, we have $\sum_{a=1}^{d} M_a = \frac{p_1}{m_+ m_-} N$, which one can check is in agreement with the general result (4.48) for toric X_7. We also note that the variables $\mathfrak{p}_a$ we have introduced can be identified with the background magnetic fluxes of the dual $d = 4$ SCFT, in this case $\mathcal{N} = 4$ SYM theory, as we discuss in more detail in the toric setting in section 5.2.

To obtain the on-shell values for the central charge and R-charges we should set $b_1 = 2$ and then extremize $\mathscr{Z}$ over b_0, b_2 and b_3. The expression for $\mathscr{Z}$ is quadratic in b_0, b_2, b_3 and we find that the extremal values for b_0, b_2 and b_3 depend on the spindle data $m_\pm$, σ as well as $a_\pm$ (subject to (2.10)). Here we report only the critical value of b_0

$$b_0^* = -\frac{2m_+ m_-(\sigma m_+ - m_-)}{m_+^2 + m_-^2 - m_+^2 m_-^2(\mathfrak{p}_1^2 + \mathfrak{p}_2^2 + \mathfrak{p}_3^2)} \,. \tag{3.74}$$

Crucially, the on-shell values of $\mathscr{Z}$ and $R_a^\pm$ are independent of $a_\pm$. For the on-shell central charge we find

$$c_{\text{sugra}} \equiv \mathscr{Z}_{\text{os}} = \frac{6m_-^2 m_+^2 \mathfrak{p}_1\mathfrak{p}_2\mathfrak{p}_3}{m_-^2 + m_+^2 - m_-^2 m_+^2(\mathfrak{p}_1^2 + \mathfrak{p}_2^2 + \mathfrak{p}_3^2)} N^2 \,. \tag{3.75}$$

Note that the fluxes (3.73), the central charge (3.75), and the mixing parameter for the R-symmetry vector (3.74) perfectly agree with those obtained from the explicit supergravity solution presented in section 3.3 (respectively (2.40), (2.52), and (2.55)).

Starting with (3.27), the on-shell expressions for the R-charges can be written

$$\begin{aligned} R_a^+ &= -Cm_+ \left(\mathfrak{p}_1[\sigma + m_-\mathfrak{p}_1], \mathfrak{p}_2[\sigma + m_-\mathfrak{p}_2], \mathfrak{p}_3[\sigma + m_-\mathfrak{p}_3]\right) \,, \\ R_a^- &= -Cm_- \left(\mathfrak{p}_1[1 + m_+\mathfrak{p}_1], \mathfrak{p}_2[1 + m_+\mathfrak{p}_2], \mathfrak{p}_3[1 + m_+\mathfrak{p}_3]\right) \,, \end{aligned} \tag{3.76}$$

where

$$C = \frac{2m_- m_+}{m_-^2 + m_+^2 - m_-^2 m_+^2(\mathfrak{p}_1^2 + \mathfrak{p}_2^2 + \mathfrak{p}_3^2)} \,. \tag{3.77}$$

This is a new result which could be checked using the explicit supergravity solutions. Let us also observe that if we demand, on-shell, $c_{\text{sugra}} > 0$ as well as $R_a^+ > 0$ and $\sigma R_a^- > 0$ then we

find precisely the inequalities in (2.44) and (2.45). This serves as a check of the validity of the approach based on geometric extremization as well as our block formula.

Finally, we can prove a conjecture for the central charge stated in [73, 86]. To see this, observe that we can use (3.70), (3.71) to write the off-shell central charge as

$$\mathscr{Z} = \frac{3N^2}{b_0}\frac{2}{b_1}\left[\prod_{a=1}^{3}\left(\varphi_a + \mathfrak{p}_a\frac{b_0}{2}\right) - \prod_{a=1}^{3}\left(\varphi_a - \mathfrak{p}_a\frac{b_0}{2}\right)\right], \tag{3.78}$$

where

$$\varphi_a \equiv \frac{b_1}{4}\left(R_a^+ + R_a^-\right), \tag{3.79}$$

and $\sum_a \varphi_a = \frac{1}{2}(b_1^{(+)} + b_1^{(-)}) = b_1 - \frac{b_0}{2}\frac{m_- - \sigma m_+}{m_- m_+}$. This is then in agreement with [86] provided that we identify our $(m_\pm, \varphi_a, b_0, \mathfrak{p}_a)$ with their $(n_\mp, \varphi_a, -2\epsilon, -\mathfrak{n}_a)$.

3.3.2 $\mathbf{AdS}_2 \times Y_9$ solutions with $X_7 = S^7$

The $\mathrm{AdS}_2 \times Y_9$ solutions of 11d supergravity with $X_7 = S^7$ also has no baryonic symmetries *i.e.* $H^2(X_7, \mathbb{R}) \cong 0$. In our chosen basis, the Sasakian volume of S^7, as a function of the Reeb vector, is given by

$$\mathrm{Vol}_S(S^7) \;=\; \frac{\pi^4}{3\, b_2 b_3 b_4 (b_1 - b_2 - b_3 - b_4)}\,. \tag{3.80}$$

There are four supersymmetric five-submanifolds S_a, which are $U(1)^4$ invariant and associated with baryonic operators in the SCFT dual to $\mathrm{AdS}_4 \times S^7$. The Sasakian volumes of these supersymmetric submanifolds are given by

$$\mathrm{Vol}_S(S_1) \;=\; \frac{\pi^3}{b_2 b_3 b_4}\,, \qquad \mathrm{Vol}_S(S_a) \;=\; \frac{\pi^3 b_a}{b_2 b_3 b_4 (b_1 - b_2 - b_3 - b_4)}\,, \quad a = 2, 3, 4\,. \tag{3.81}$$

The SE volume can be obtained by setting $b_1 = 4$ and then extremizing (3.80) over b_2, b_3, b_4. The extremal point has $b_2 = b_3 = b_4 = 1$ with $\mathrm{Vol}_{SE}(S^7) = \frac{\pi^4}{3}$ and $\mathrm{Vol}_{SE}(S_a) = \pi^3$.

We now consider the GK geometry associated with $\mathrm{AdS}_2 \times Y_9$ solutions. The off-shell

entropy function can be obtained from (3.36) and takes the form

$$\mathscr{S} = \frac{8\pi N^{3/2}}{3b_0\sqrt{2b_1}}\Bigg[\sqrt{b_2^{(+)}b_3^{(+)}b_4^{(+)}\left(b_1^{(+)}-b_2^{(+)}-b_3^{(+)}-b_4^{(+)}\right)} - \sigma\sqrt{b_2^{(-)}b_3^{(-)}b_4^{(-)}\left(b_1^{(-)}-b_2^{(-)}-b_3^{(-)}-b_4^{(-)}\right)}\Bigg]\,. \tag{3.82}$$

The off-shell geometric R-charges are obtained from (3.27) and are given by

$$R_1^{\pm} = \frac{2}{b_1}\left(b_1^{(\pm)}-b_2^{(\pm)}-b_3^{(\pm)}-b_4^{(\pm)}\right)\,, \qquad R_a^{\pm} = \frac{2b_a^{(\pm)}}{b_1}\,, \quad a=2,3,4\,. \tag{3.83}$$

Observe that for this example, which is also toric, we have

$$\sum_{a=1}^{d} R_a^{\pm} = \frac{2b_1^{(\pm)}}{b_1}\,,$$
$$\frac{1}{2}\sum_{a=1}^{d}\left(R_a^{+}+R_a^{-}\right) = 2 - \frac{m_- - \sigma m_+}{m_+m_-}\frac{b_0}{b_1}\,, \tag{3.84}$$

in agreement with the general toric results (4.61), (4.63). Also, using (3.19) we can find the following expression for the preferred five-form fluxes M_a defined in (3.17).

$$\mathfrak{p}_a \equiv \frac{M_a}{N} = \frac{1}{m_+m_-}\big\{p_1-(p_2+p_3+p_4),\, p_2,\, p_3,\, p_4\big\}\,, \tag{3.85}$$

where, as usual, $p_1 = -\sigma m_+ - m_-$. For this example, we have $\sum_{a=1}^{d} M_a = \frac{p_1}{m_+m_-}N$, which one can check is in agreement with the general result (4.48) for toric X_7.

To obtain the on-shell values for $\mathscr{S}$ and $R_a^{\pm}$, we should set $b_1 = 1$ and then extremize (3.82) as a function of b_2, b_3, b_4, and b_0. Performing such a computation analytically with general fluxes is difficult due to the square roots. We will look at a simpler case when the fluxes are pairwise equal, *i.e.* $M_1 = M_2$ and $M_3 = M_4$, which amounts to setting

$$p_2 = \frac{1}{2}\left(p_1 - 2p_3\right)\,, \qquad p_4 = p_3\,. \tag{3.86}$$

This choice corresponds to considering fibrations of the S^7 that maintain $U(2)\times U(2) \subset SO(8)$ symmetry. Notice in passing that this implies that $p_1 = -\sigma m_+ - m_-$ must be even. Consistent

with this $U(2) \times U(2)$ symmetry we now make the further assumption that we can carry out the extremization over the locus

$$b_2 = \frac{1}{2}(b_1 - 2b_3) + \frac{b_0}{2}(\sigma a_+ - a_-)\,, \qquad b_4 = b_3\,, \tag{3.87}$$

which implies

$$b_2^{(\pm)} = \frac{1}{2}\,(b_1^{(\pm)} - 2b_3^{(\pm)})\,, \qquad b_4^{(\pm)} = b_3^{(\pm)}\,. \tag{3.88}$$

With these restrictions, the arguments of the square roots in (3.82) become perfect squares, so we obtain

$$\mathscr{S} \;=\; \frac{4\pi N^{3/2}}{3b_0\sqrt{2}}\left[\delta_+ b_3^{(+)}(b_1^{(+)} - 2b_3^{(+)}) - \delta_- b_3^{(-)}(b_1^{(-)} - 2b_3^{(-)})\right], \tag{3.89}$$

where $\delta_\pm$ are signs defined by

$$\delta_+ \equiv \text{sign}\left[b_3^{(+)}(b_1^{(+)} - 2b_3^{(+)})\right], \qquad \delta_- \equiv \sigma\,\text{sign}\left[b_3^{(-)}(b_1^{(-)} - 2b_3^{(-)})\right]. \tag{3.90}$$

We now need to extremize over b_0, b_3 with $b_1 = 2$. By an explicit calculation we find that when $\delta_+ = \delta_-$, (3.89) is linear in b_3, b_0 and so it does not have any extremum. Hence we set

$$\delta_+ = -\delta_- \equiv \delta\,. \tag{3.91}$$

We then find two different set of values for (b_0, b_3) that extremize the off-shell entropy (3.89). However, there are restrictions on $m_\pm$ and p_3 to ensure that the $\mathscr{S}_{\text{os}} > 0$, $R_a^+ > 0$, and $\sigma R_a^- > 0$. A detailed analysis of these conditions (see [3]) reveals that only the anti-twist case is possible and only with $\delta = 1$. In particular the critical R-symmetry vector is given by

$$b_0^* = \frac{2m_+m_-}{\mathcal{D}}\,, \qquad b_3^* = \frac{1}{4} - \frac{m_- + m_+ + 4p_3(1 - 2a_-m_+)}{4\mathcal{D}}\,, \tag{3.92}$$

with

$$\mathcal{D} = \sqrt{-16p_3^2 + 8p_3\,(m_+ - m_-) + (m_+ + m_-)^2}\,. \tag{3.93}$$

The on-shell entropy is

$$\mathscr{S}_{\rm os} = -\frac{\pi N^{3/2}}{3\sqrt{2}}\left(\frac{m_- + m_+ - \mathcal{D}}{m_- m_+}\right), \tag{3.94}$$

and the on-shell R-charges are

$$\begin{aligned} R_1^{\pm} = R_2^{\pm} &= \frac{1}{2} + \frac{1}{2\mathcal{D}}\left(m_{\pm} - 3m_{\mp} \mp 4p_3\right), \\ R_3^{\pm} = R_4^{\pm} &= \frac{1}{2} - \frac{1}{2\mathcal{D}}\left(m_+ + m_- \mp 4p_3\right). \end{aligned} \tag{3.95}$$

with the following condition required on the parameters

$$0 < p_3 < \frac{1}{2}\left(m_+ - m_-\right). \tag{3.96}$$

Note that (3.94) is consistent with the analysis of explicit supergravity solutions studied in [77][7] and in [79].[8] The expressions for the geometric R-charges (3.95) are a new result, which could, in principle, be compared with a calculation using the supergravity solutions.

Finally, we can prove a conjecture for the entropy stated in [86]. To see this observe that we can use (3.83) to write the off-shell entropy function (3.82)

$$\mathscr{S} = \frac{2\pi N^{3/2}}{3b_0\sqrt{2b_1}}\left[\sqrt{\prod_{a=1}^{4}(\varphi_a + \mathfrak{p}_a b_0)} - \sigma\sqrt{\prod_{a=1}^{4}(\varphi_a - \mathfrak{p}_a b_0)}\right], \tag{3.97}$$

where

$$\varphi_a \equiv \frac{b_1}{2}\left(R_a^+ + R_a^-\right), \tag{3.98}$$

and $\sum_a \varphi_a = b_1^{(+)} + b_1^{(-)} = 2b_1 - b_0\frac{m_- - \sigma m_+}{m_- m_+}$. This is then in agreement with [86] provided that we identify our $(m_\pm, \varphi_a, b_0, \mathfrak{p}_a)$ with their $(n_\mp, \varphi_a, -\epsilon, -\mathfrak{n}_a)$.

[7] The fluxes there are 2 times the fluxes here.

[8] For a detailed discussion of the matching see [3].

3.3.3 $\mathrm{AdS}_2 \times Y_9$ solutions with $X_7 = V^{5,2}$

We now consider an example of X_7 with no corresponding supergravity solution known. Specifically, this is the (non-toric) Sasaki manifold $V^{5,2} = SO(5)/SO(3)$, which still has no baryonic symmetries. This manifold has $SO(5) \times U(1)$ isometry, with maximal torus $U(1)^3$, and hence $s = 3$. The Sasakian volume can be computed using the Hilbert series method [127]

$$\mathrm{Vol}_S(V^{5,2}) = \frac{54\pi^4}{(b_1 - b_2)(b_1 + b_2)(b_1 - b_3)(b_1 + b_3)} \,. \tag{3.99}$$

There are five supersymmetric and $U(1)^3$ invariant five-submanifolds S_a, and are associated with baryonic operators in the SCFT dual to $\mathrm{AdS}_4 \times V^{5,2}$. Their Sasakian volumes read

$$\begin{aligned}
\mathrm{Vol}_S(S_1) &= \frac{b_1\pi^3}{(b_1 - b_2)(b_1 + b_2)(b_1 - b_3)(b_1 + b_3)} \,, \\
\mathrm{Vol}_S(S_2) &= \frac{\pi^3}{(b_1 - b_2)(b_1 + b_2)(b_1 + b_3)} \,, \quad \mathrm{Vol}_S(S_3) = \frac{\pi^3}{(b_1 + b_2)(b_1 - b_3)(b_1 + b_3)} \,, \\
\mathrm{Vol}_S(S_4) &= \frac{\pi^3}{(b_1 - b_2)(b_1 - b_3)(b_1 + b_3)} \,, \quad \mathrm{Vol}_S(S_5) = \frac{\pi^3}{(b_1 - b_2)(b_1 + b_2)(b_1 - b_3)} \,.
\end{aligned} \tag{3.100}$$

The Sasaki-Einstein volume can be obtained by setting $b_1 = 4$ and then extremizing (3.80) over b_2, b_3. The extremal point has $b_2 = b_3 = 0$ with $\mathrm{Vol}_{SE}(V^{5,2}) = \frac{27\pi^4}{128}$ and $\mathrm{Vol}_{SE}(S_a) = \frac{\pi^3}{64}$.

We now consider the GK geometry associated with $\mathrm{AdS}_2 \times Y_9$ solutions. The off-shell entropy function can be obtained from (3.36) and takes the form

$$\begin{aligned}
\mathscr{S} \;=\; \frac{4\pi N^{3/2}}{27 b_0 \sqrt{b_1}} \Bigg[& \sqrt{(b_1^{(+)} - b_2^{(+)})(b_1^{(+)} + b_2^{(+)})(b_1^{(+)} - b_3^{(+)})(b_1^{(+)} + b_3^{(+)})} \\
& - \sigma \sqrt{(b_1^{(-)} - b_2^{(-)})(b_1^{(-)} + b_2^{(-)})(b_1^{(-)} - b_3^{(-)})(b_1^{(-)} + b_3^{(+)})} \Bigg] \,.
\end{aligned} \tag{3.101}$$

The off-shell geometric R-charges are obtained from (3.27) and are given by

$$\begin{aligned}
R_1^{\pm} &= \frac{2}{3}\frac{b_1^{(\pm)}}{b_1} \,, \qquad R_2^{\pm} = \frac{2}{3}\frac{b_1^{(\pm)} - b_3^{(\pm)}}{b_1} \,, \qquad R_3^{\pm} = \frac{2}{3}\frac{b_1^{(\pm)} - b_2^{(\pm)}}{b_1} \,, \\
& R_4^{\pm} = \frac{2}{3}\frac{b_1^{(\pm)} + b_2^{(\pm)}}{b_1} \,, \qquad R_5^{\pm} = \frac{2}{3}\frac{b_1^{(\pm)} + b_3^{(\pm)}}{b_1} \,.
\end{aligned} \tag{3.102}$$

From (3.19) we obtain the fluxes

$$\mathfrak{p}_a \equiv \frac{M_a}{N} = \frac{1}{3m_+m_-}\big\{p_1,\, p_1-p_3,\, p_1-p_2,\, p_1+p_2,\, p_1+p_3\big\}\,, \tag{3.103}$$

with $p_1 = -\sigma m_+ - m_-$. Note that

$$M_1 + M_2 + M_5 = M_1 + M_3 + M_4 = \frac{p_1}{m_+m_-}\,N\,. \tag{3.104}$$

These equations play an analogous role to the general formula (4.48) for the toric case, that we discuss later. Indeed, both (4.48) and (3.104) may be interpreted in field theory as the condition that the superpotential is twisted via the line bundle $\mathcal{O}(p_1)$, where the flux terms on the left hand side correspond to the twistings of individual fields that appear in the superpotential. For $V^{5,2}$ (3.104) may be determined from the field theory dual worked out in [128], with particular fields being associated with particular divisors $C(S_a) \subset C(V^{5,2})$.

To obtain the on-shell values for $\mathscr{S}$ and $R_a^{\pm}$, we should set $b_1 = 1$ and then extremize (3.101) as a function of b_2, b_3 and b_0. As for the S^7 case, the case of general fluxes is involved, hence we will take $M_2 = M_3$ and $M_4 = M_5$, which holds when

$$p_2 = p_3\,. \tag{3.105}$$

This choice corresponds to considering fibrations of the $V^{5,2}$ that preserve $SU(2)\times SU(2)\times U(1) \subset SO(5)\times U(1)$ isometry. In this case the entropy (3.101) becomes symmetric under the exchange $b_2 \leftrightarrow b_3$, and we may assume that at the extremal point $b_2 = b_3$. With (3.105) and restricting to this locus we find that the (3.101) simplifies to

$$\mathscr{S} = \frac{4\pi N^{3/2}}{27b_0}\left[\delta_+(b_1^{(+)}-b_2^{(+)})(b_1^{(+)}+b_2^{(+)}) - \delta_-(b_1^{(-)}-b_2^{(-)})(b_1^{(-)}+b_2^{(-)})\right], \tag{3.106}$$

where the signs are defined as

$$\delta_+ \equiv \text{sign}\left[(b_1^{(+)}-b_2^{(+)})(b_1^{(+)}+b_2^{(+)})\right], \quad \delta_- \equiv \sigma\,\text{sign}\left[(b_1^{(-)}-b_2^{(-)})(b_1^{(-)}+b_2^{(-)})\right]. \tag{3.107}$$

Following an analysis similar to the one performed in the previous section, requiring $\mathscr{S}_{\rm os} > 0$ and $R_a^+ > 0$ and $\sigma R_a^- > 0$, we find that only the anti-twist case is possible and only with $\delta_+ = -\delta_- = 1$. The corresponding critical R-symmetry vector is given by

$$b_0^* = \frac{2m_+m_-}{\sqrt{2(m_+^2+m_-^2)-p_2^2}}\,, \qquad b_2^* = -\frac{p_2(a_+m_- - a_-m_+)}{\sqrt{2(m_+^2+m_-^2)-p_2^2}}\,, \tag{3.108}$$

and the on-shell entropy is

$$\mathscr{S}_{\rm os} = -\frac{8\pi N^{3/2}}{27 m_+m_-}\left[m_+ + m_- - \sqrt{2\left(m_-^2+m_+^2\right)-p_2^2}\right], \tag{3.109}$$

and the on-shell R-charges read

$$\begin{aligned} R_1^\pm &= \frac{2}{3} - \frac{4m_\mp}{3\sqrt{2(m_+^2+m_-^2)-p_2^2}}\,,\\ R_2^\pm = R_3^\pm &= \frac{2}{3} - \frac{2(2m_\mp \pm p_2)}{3\sqrt{2(m_+^2+m_-^2)-p_2^2}}\,,\\ R_4^\pm = R_5^\pm &= \frac{2}{3} - \frac{2(2m_\mp \mp p_2)}{3\sqrt{2(m_+^2+m_-^2)-p_2^2}}\,. \end{aligned} \tag{3.110}$$

The allowed values for the parameters are again

$$0 < p_2 < \frac{1}{2}\left(m_+ - m_-\right). \tag{3.111}$$

It is natural to conjecture that these are sufficient constraints on the parameters in order for the $\mathrm{AdS}_2 \times Y_9$ solutions to actually exist.

The equations above provide a prediction for the entropy and R-charges of a supersymmetric accelerating black hole with $\mathrm{AdS}_4 \times \Sigma$ horizon that uplifts on $V^{5,2}$ and there is currently no other known result we can match with.

Chapter 4

Toric perspective

Another possible way to proceed further and evaluate explicitly the volumes in the block formula (3.11), besides the flavour twist, is to take the fibres X_{2n-1} to be *toric*. Given that the spindle itself is toric, the total GK space Y_{2n+1} will be toric too. The advantage of dealing with toric spaces is that geometric quantities can be expressed in terms of sums over combinatorial data, the *toric data*, including integrals over the internal space or its cycles. There are many known examples of such spaces and their dual field theories are well understood [129–131], which further motivates the study of this case. In this chapter, after recalling the properties of toric cones and their role in GK extremization, we will give an alternative proof of the block formula for toric fibres and derive expressions for all the relevant quantities in terms of a single object, the *master volume*, which is an algebraic function of the free parameters specifying the R-symmetry vector ξ and the transverse Kähler class $[J]$.

4.1 Review of toric geometry

In this section we recall some general properties of toric cones, and in particular discuss their master volume $\mathcal{V}$ which plays a crucial role in GK extremization as it allows to extremize over the possible R-symmetry vectors ξ algebraically. Note that, although we will write explicit formulas for toric cones over a GK manifold Y_{2n+1} as in (1.21), most of these are also applicable to cones over Sasakian manifolds $C(X_{2n-1})$ as in (1.8). We will make sure to point out any exception. We follow [70, 119, 132], where further details can be found.

4.1.1 Toric cones

We begin with the cone $C(Y_{2n+1})$ as considered in section 1.2.3

$$\mathrm{d}s^2_{C(Y_{2n+1})} = \mathrm{d}r^2 + r^2 \mathrm{d}s^2_{Y_{2n+1}} \,. \tag{4.1}$$

We additionally require it to be toric, which happens when $s = n + 1$ so that Y_{2n+1} has $U(1)^{n+1}$ isometry, genereted by the Killing vector fields ∂_{φ_μ}, with φ_μ having period 2π. At each radius $r > 0$ sits a homothetic copy of Y_{2n+1}, with the original Y_{2n+1} embedded naturally at $r = 1$. We next define the moment map coordinates

$$y^\mu \equiv \tfrac{1}{2} r^2 \partial_{\varphi_\mu} \lrcorner \, \eta \ , \qquad \mu = 0, 1, \ldots, n \ . \tag{4.2}$$

These span the moment map polyhedral cone $\mathcal{C} \subset \mathbb{R}^{n+1}$, where the y^μ are Euclidean coordinates on $\mathbb{R}^{n+1}$. The polyhedral cone $\mathcal{C}$, which is convex, is determined by D vectors $v_{A\mu}$ with $A = 1, \ldots, D$ and for each A we have $(v_{A\mu}) \in \mathbb{Z}^{n+1}$. Specifically, these are inward pointing and primitive normals to the D facets of the cone and we have

$$\mathcal{C} = \left\{ (y^\mu) \in \mathbb{R}^{n+1} \ \Big| \ \sum_{\mu=0}^{n} y^\mu v_{A\mu} \geq 0 \ , \quad A = 1, \ldots, D \right\} \ . \tag{4.3}$$

If we change basis for the $U(1)^{n+1}$ action with an $SL(n+1, \mathbb{Z})$ transformation, then there is a corresponding $SL(n+1, \mathbb{Z})$ transformation on the moment map coordinates and hence on the toric data, *i.e.* the vectors $v_{A\mu}$. In our basis, satisfying (1.23), the Gorenstein condition implies that $v_{A\mu=1} = 1$ for all A.

Geometrically, $C(Y_{2n+1})$ fibres over the polyhedral cone $\mathcal{C}$. There is a trivial $U(1)^{n+1}$ fibration over the interior $\mathcal{C}_{\rm int}$ of $\mathcal{C}$, with the D normal vectors $v_{A\mu}$ to each bounding facet $\{\sum_{\mu=0}^{n} y^\mu v_{A\mu} = 0\} \subset \partial\mathcal{C}$ specifying which $U(1) \subset U(1)^{n+1}$ collapses along that facet. Each facet is also the image under the moment map of a toric divisor $\mathcal{D}_A$ in $C(Y_{2n+1})$, where $\mathcal{D}_A$ is a complex codimension one submanifold that is invariant under the action of the $U(1)^{n+1}$ torus. We define T_A to be the $U(1)^{n+1}$ invariant $(2n-1)$-cycle in Y_{2n+1} associated with the toric divisor $\mathcal{D}_A$ on the cone. Since $\dim H_{2n-1}(Y_{2n+1}, \mathbb{R}) = D - (n+1)$, the toric $(2n-1)$-cycles $[T_A] \in H_{2n-1}(Y_{2n+1}, \mathbb{Z})$ are not independent in $H_{2n-1}(Y_{2n+1}, \mathbb{Z})$, satisfying the $(n+1)$ relations

$$\sum_{A=1}^{D} v_{A\mu} [T_A] = 0 \ , \qquad \mu = 0, 1, \ldots, n \ . \tag{4.4}$$

The image of $Y_{2n+1} = \{r = 1\}$ under the moment map is the compact, convex n-

dimensional polytope

$$P = P(b_\mu) = \mathcal{C} \cap H(b_\mu)\,, \tag{4.5}$$

where we define the Reeb hyperplane as

$$H = H(b_\mu) \equiv \left\{ (y^\mu) \in \mathbb{R}^{n+1} \mid \sum_{\mu=0}^{n} y^\mu b_\mu = \tfrac{1}{2} \right\}. \tag{4.6}$$

4.1.2 The master volume

We first fix a choice of toric cone metric on the complex cone $C(Y_{2n+1})$. As described in the previous subsection, this allows us to introduce coordinates (y^μ, φ_μ) on $C(Y_{2n+1})$. For a fixed choice of such complex cone, with ξ given by (1.25), we would then like to study a general class of transversely Kähler metrics of the form (1.21) with generic J.

Of central interest is the "master volume" defined by

$$\mathcal{V}_{2n+1} \equiv \int_{Y_{2n+1}} \eta \wedge \frac{J^n}{n!}\,, \tag{4.7}$$

which is a function both of the vector ξ and the transverse Kähler class $[J] \in H^2_B(\mathcal{F}_\xi)$. Note that, while for metrics like (1.8) (with generic Kähler form $\omega \neq \omega_S$) the equivalent formula for $\mathcal{V}_{2n-1}$ is precisely $\mathrm{Vol}(X_{2n-1})$, for GK manifolds Y_{2n+1} this is not the case due to the presence of the conformal factor in front of the transverse Kähler metric in (1.21).

We can introduce $c_A \in H^2_B(\mathcal{F}_\xi)$ to be basic representatives of integral classes in $H^2(Y_{2n+1}, \mathbb{Z})$, which are Poincaré dual to the D toric divisors $\mathcal{D}_A$ on $C(Y_{2n+1})$. This allows us to parametrize the Kähler class with D real parameters λ_A

$$[J] = -2\pi \sum_{A=1}^{D} \lambda_A c_A \in H^2_B(\mathcal{F}_\xi)\,. \tag{4.8}$$

The c_A are not all independent and $[J]$ in fact only depends on $D - n$ of the D parameters $\{\lambda_A\}$, as we shall see shortly. It is also useful to note that the first Chern class of the foliation

can be written in terms of the c_A as

$$[\varrho] = 2\pi \sum_{A=1}^{D} c_A \in H^2_B(\mathcal{F}_\xi) \ . \tag{4.9}$$

For the X_{2n-1} case we see that in the special case in which $\lambda_A = -\frac{1}{2b_1}$ for all $A = 1, \dots D$ we recover the Sasakian Kähler class $[\tilde{\varrho}] = 2b_1[\omega_S]$ and the master volume $\mathcal{V}_{2n-1}$ reduces to the Sasakian volume $\mathrm{Vol}_S(X_{2n-1})$. The master volume (4.7) may be written as

$$\mathcal{V}_{2n+1} = \frac{(2\pi)^{n+1}}{|b|} \mathrm{Vol}_E(\mathcal{P}) \ , \tag{4.10}$$

where $|b| \equiv (\sum_{\mu=0}^{n} b_\mu b_\mu)^{1/2}$. The factor $(2\pi)^{n+1}$ arises by integrating over the torus $U(1)^{n+1}$, while $\mathrm{Vol}_E(\mathcal{P})$ is the Euclidean volume of the compact, convex n-dimensional polytope

$$\mathcal{P} = \mathcal{P}(b_\mu; \lambda_a) \equiv \left\{ (y^\mu) \in H(b_\mu) \ \ | \ \ \sum_{\mu=0}^{n} (y^\mu - y^\mu_*) v_{A\mu} \geq \lambda_A \ , \ A = 1, \dots, D \right\} \ , \tag{4.11}$$

with y^μ_* an arbitrary point in the Reeb hyperplane. Different choices for y^μ_* can be reabsorbed into a re-definition of the λ_A. It is convenient to take

$$(y^\mu_*) \equiv \left(0, \frac{1}{2b_1}, 0, \dots, 0\right) \in H \ . \tag{4.12}$$

Note that taking $\lambda_A = -\frac{1}{2b_1}$ the polytope $\mathcal{P}$ is the same as the initial P given in (4.5).

One may show that the master volume $\mathcal{V}_{2n+1}$ is homogeneous of degree n in the λ_A and of degree -1 in the b_μ. Moreover, it satisfies the important identity

$$\sum_{A=1}^{D} \left(v_{A\mu} - \frac{b_\mu}{b_1} \right) \frac{\partial \mathcal{V}_{2n+1}}{\partial \lambda_A} = 0 \, , \qquad \mu = 0, 1, \dots, n \, . \tag{4.13}$$

It follows from this, together with homogeneity, that the master volume is invariant under the "gauge" transformations

$$\lambda_A \ \to \ \lambda_A + \sum_{\mu=0}^{n} \gamma^\mu (v_{A\mu} b_1 - b_\mu) \, , \tag{4.14}$$

for arbitrary constants γ^μ. Since the transformation parametrized by γ^1 is trivial, we see that the master volume only depends on $D-n$ of the D parameters $\{\lambda_A\}$, as noted above.

For later purposes, it is also useful to note that we can compute easily integrals over T_A, the $(2n-1)$-dimensional and $U(1)^{n+1}$ invariant cycle in Y_{2n+1} associated with a toric divisor $\mathcal{D}_A$ on the cone and Poincaré dual to c_A. From (4.8) we have

$$\int_{T_A} \eta \wedge \tfrac{1}{(n-1)!} J^{n-1} = \int_{Y_{2n+1}} \eta \wedge \tfrac{1}{(n-1)!} J^{n-1} \wedge c_A = -\frac{1}{2\pi} \frac{\partial \mathcal{V}_{2n+1}}{\partial \lambda_A} \,. \tag{4.15}$$

We can obtain similar formulas for integrals over higher-dimensional cycles. For example, consider the codimension four cycle $T_{A_1A_2}$ that is Poincaré dual to $c_{A_1} \wedge c_{A_2}$

$$\int_{T_{A_1A_2}} \eta \wedge \tfrac{1}{(n-2)!} J^{n-2} = \int_{Y_{2n+1}} \eta \wedge \tfrac{1}{(n-2)!} J^{n-2} \wedge c_{A_1} \wedge c_{A_2} = \frac{1}{(2\pi)^2} \frac{\partial^2 \mathcal{V}_{2n+1}}{\partial \lambda_{A_1} \partial \lambda_{A_2}} \,. \tag{4.16}$$

It is possible to obtain very explicit formulas for the master volume in low dimensions in terms of $v_{A\mu}$, b_μ and λ_A. Specifically, in dimensions $n = 1, 2$ and 3 the relevant formulae for Y_3, Y_5 and Y_7 were derived in [132], [70] and [119], respectively.[1]

Finally, we note that the formulae in this section assume that the polyhedral cone $\mathcal{C}$ is convex, since we started the section with a cone that admits a toric Kähler cone metric. However, this convexity condition is, in general, too restrictive. Indeed, for applications to AdS_2 and AdS_3 solutions of interest many explicit supergravity solutions are known that are associated with "non-convex toric cones", as defined in [68], which in particular have toric data which do not define a convex polyhedral cone. Based on the consistent picture that has emerged, including recovering results for the known explicit supergravity solutions, it is expected that the key formulae in this section are also applicable to non-convex toric cones, and we will assume this is the case in the sequel.

4.1.3 GK extremization for toric Y_{2n+1}

When Y_{2n+1} is toric, the geometric extremization of section 1.2.3 for the associated GK geometry on Y_{2n+1} can be carried out using the master volume $\mathcal{V}_{2n+1}(b_\mu; \lambda_A)$. In order to

[1] Note that the minus sign in (2.23) of [119] should be a plus sign.

carry this out we need expressions for the off-shell supersymmetric action, the constraint equation and flux quantization conditions. These can all be expressed in terms of derivatives of the master volume as follows:

$$\begin{aligned} S_{\rm SUSY} &= -\sum_{A=1}^{D} \frac{\partial \mathcal{V}_{2n+1}}{\partial \lambda_A} \,, \\ 0 &= \sum_{A,B=1}^{D} \frac{\partial^2 \mathcal{V}_{2n+1}}{\partial \lambda_A \partial \lambda_B} \,, \\ \nu_n M_A &= -\frac{1}{(2\pi)} \frac{\partial S_{\rm SUSY}}{\partial \lambda_A} = \frac{1}{2\pi} \sum_{B=1}^{D} \frac{\partial^2 \mathcal{V}_{2n+1}}{\partial \lambda_A \partial \lambda_B} \,, \end{aligned} \tag{4.17}$$

with $M_A \in \mathbb{Z}$. The M_A are not all independent[2] and, as a consequence of (4.4), satisfy $(n+1)$ linear relations given by

$$\sum_{A=1}^{D} v_{A\mu} M_A = 0 \,, \qquad \mu = 0, 1, \ldots, n \,. \tag{4.18}$$

Notice that the $\mu = 1$ component in (4.18) is actually the constraint equation given in (4.17).

The geometric extremization principle that is to be implemented for the GK geometry on Y_{2n+1} is now simple to state. To obtain the on-shell supersymmetric action, we need to fix $b_1 = \frac{2}{n-2}$ and then extremize $S_{\rm SUSY}$ with respect to $b_0, b_2, \ldots, b_n$ as well as the $D-n$ independent λ_A, subject to the constraint equation and flux quantization conditions in (4.17).

4.2 Toric geometry fibred over a spindle

With the toric formalism of section 4.1 to hand, we now return to studying GK geometries Y_{2n+1} of the fibred form

$$X_{2n-1} \hookrightarrow Y_{2n+1} \longrightarrow \Sigma \,, \tag{4.19}$$

introduced in section 3.1, where now the fibres X_{2n-1} are toric Sasaki-Einstein manifolds and $\Sigma = \mathbb{WCP}^1_{[m_-,m_+]}$ is a spindle. There is then a toric $U(1)^n$ action on X_{2n-1}, and when

[2]Note that the M_A are a linear combination of the (independent) quantized fluxes $\mathcal{N}_\Upsilon$ in (1.29), which are associated with the flux through a basis for the free part of $H_{2n-1}(Y_{2n+1};\mathbb{Z})$.

combined with the azimuthal rotation symmetry of the spindle, this gives rise to a toric $U(1)^{n+1}$ action on Y_{2n+1}. We will utilize the toric geometry summarized in the previous section both for Y_{2n+1} and, with suitable notational changes, for the fibres X_{2n-1}. Our main goal is to relate the quantities appearing in the geometric extremal problem for Y_{2n+1} in section 1.2.3 to the master volume $\mathcal{V}_{2n-1}$ of the toric fibres X_{2n-1}.

4.2.1 Toric data for Y_{2n+1}

As described in section 3.1, the fibration of X_{2n-1} over Σ is specified by n integers $(p_i) = (p_1, \ldots, p_n)$.[3] These are effectively Chern numbers for the associated $U(1)^n$ fibration over Σ, and may be identified in terms of the local gluing data $\alpha_i^{\pm}$ of section 3.1 via (2.8). Moreover, as explained in section 2.1.2, we have from (2.14)

$$p_1 = -(\sigma m_+ + m_-) \ , \tag{4.20}$$

where $\sigma = \pm 1$ corresponds to the twist or anti-twist case. Recall here that we are using a basis for the $U(1)^n$ action on X_{2n-1} for which the holomorphic $(n,0)$-form $\Psi_{(n,0)}$ on the cone $C(X_{2n-1})$ is only charged with respect to the first $U(1)$. This $U(1)$, associated with the integer Chern number p_1 in (4.20), may then be viewed as a fiducial choice of Reeb action on the Calabi-Yau cone $C(X_{2n-1})$, which in the holographic context is dual to a fiducial choice of R-symmetry of the dual SCFT (*i.e.* not necessarily the superconformal R-symmetry). The remaining $U(1)^{n-1}$, associated with the integer Chern numbers

$$\vec{p} \equiv (p_2, \ldots, p_n) \, , \tag{4.21}$$

are dual to flavour symmetries.

The toric data for $C(Y_{2n+1})$ may be determined in terms of the toric data for $C(X_{2n-1})$, together with the spindle data $m_{\pm}$, and the fibration data p_i, σ. To begin, let v_{ai} with $a = 1, \ldots, d$ and $i = 1, \ldots, n$ be the toric data for $C(X_{2n-1})$, with $v_a \in \mathbb{Z}^n$ for each a. In the basis for the $U(1)^n$ action described above we have $v_a = (1, \vec{w}_a)$, with $\vec{w}_a \in \mathbb{Z}^{n-1}$ describing a

[3] Setting $m_+ = m_+ = 1$ is the case of the round S^2, which arises in [70] as a genus $g = 0$ Riemann surface case. We should identify p_i here with $-n_i$ there.

convex polytope. Following the discussion in section 3.1, the toric data for the cone $C(Y_{2n+1})$ is then given by $D = d+2$ vectors $v_{A\mu}$ with $A = +, -, a$ and $\mu = 0, 1, \ldots, n$ and $(v_{A\mu}) \in \mathbb{Z}^{n+1}$ for each A. Explicitly, in the basis of vector fields ∂_{φ_μ}, $\mu = 0, 1, \ldots, n$, generating the $U(1)^{n+1}$ action introduced in section 3.1, the $v_{A\mu}$ can be written

$$\begin{aligned} v_{+\mu} &= (m_+, v_{+i})\,, \qquad && \text{where} \quad v_{+i} \equiv (1, -a_+\vec{p})\ , \\ v_{-\mu} &= (-\sigma m_-, v_{-i})\,, \qquad && \text{where} \quad v_{-i} \equiv (1, -\sigma a_-\vec{p})\ , \\ v_{a\mu} &= (0, v_{ai})\,, \qquad && \text{where} \quad v_{ai} \equiv (1, \vec{w}_a)\ . \end{aligned} \tag{4.22}$$

Here, as in (2.9), the $a_\pm \in \mathbb{Z}$ satisfy

$$a_- m_+ + a_+ m_- = 1\ . \tag{4.23}$$

Recall that ∂_{φ_0} is a vector field on Y_{2n+1} that rotates the spindle direction, with the holomorphic $(n+1,0)$-form $\Psi_{(n+1,0)}$ on $C(Y_{2n+1})$ having charge zero under ∂_{φ_0}, while ∂_{φ_i} are vector fields that generate the toric $U(1)^n$ action on the fibres X_{2n-1}. This immediately leads to the result $v_{a\mu} = (0, v_{ai})$ in (4.22). Geometrically, the v_{ai} specify the d $U(1) \subset U(1)^n$ subgroups that fix d corresponding toric divisors in $C(X_{2n-1})$, and in $C(Y_{2n+1})$ there are then correspondingly d toric divisors, fixed by $U(1) \subset U(1)^{n+1}$ and specified by $v_{a\mu}$; more precisely, these are the d toric divisors of $C(X_{2n-1})$ fibred over Σ. On the other hand, in $C(Y_{2n+1})$ there are two additional toric divisors, fixed by the $U(1) \subset U(1)^{n+1}$ subgroups specified by $v_{\pm\mu}$. Geometrically, these are cones over the fibres $X_\pm = X_{2n-1}/\mathbb{Z}_{m_\pm}$ over the two poles of the spindle, and the vector fields $\zeta_+ = \sum_{\mu=0}^n v_{+\mu}\,\partial_{\varphi_\mu}$, $\zeta_- = \sum_{\mu=0}^n \sigma v_{-\mu}\,\partial_{\varphi_\mu}$ were determined in (2.16), (2.17).

Recall that the integers $a_\pm$ in (4.23) are unique only up to shifts

$$a_+ \ \mapsto\ a_+ - \kappa\, m_+\,, \qquad a_- \ \mapsto\ a_- + \kappa\, m_-\ , \tag{4.24}$$

where $\kappa \in \mathbb{Z}$ is arbitrary. The toric data $v_{A\mu}$ for Y_{2n+1} given in (4.22) *a priori* depends on the choice of $a_\pm$, but recall that we are free to make $SL(n+1,\mathbb{Z})$ transformations, corresponding

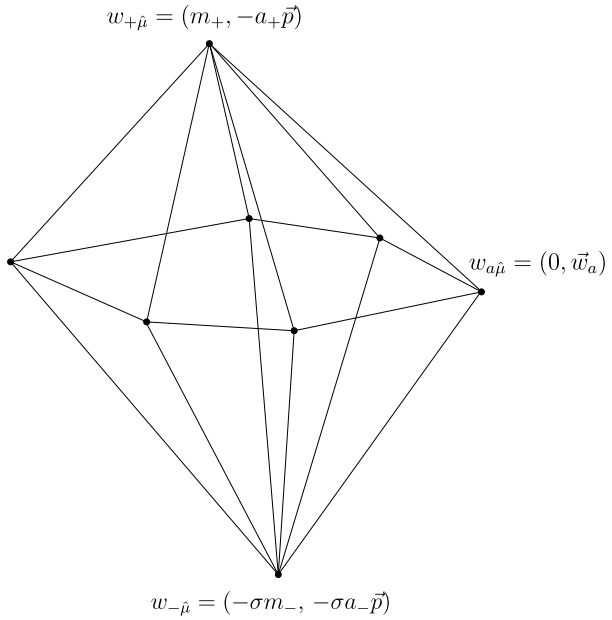


Figure 4.1: Toric data for a representative twist case ($\sigma = +1$) with $n = 3$, $d = 6$. The toric diagram is a suspension of the toric diagram for X_5, the two-dimensional polytope at height zero. For the anti-twist ($\sigma = -1$) notice that the figure is no longer convex (recall $m_\pm \in \mathbb{N}$).

to a change of basis for the torus $U(1)^{n+1}$. One can check that the matrix

$$M = \begin{pmatrix} 1 & 0 & 0 & \dots & 0 \\ 0 & 1 & 0 & \dots & 0 \\ \kappa p_2 & 0 & 1 & \dots & 0 \\ \vdots & \vdots & 0 & \ddots & \vdots \\ \kappa p_n & 0 & 0 & \dots & 1 \end{pmatrix} \in SL(n+1, \mathbb{Z}) \,, \tag{4.25}$$

acting on the μ index of $v_{A\mu}$, maps the vectors $v_{A\mu}$ in (4.22) to the same set of vectors with the replacements (4.24). The toric data we have presented is thus well-defined, with all choices of $a_\pm$ satisfying (4.23) describing the same toric geometry.

The toric data $v_{A\mu}$ for Y_{2n+1} is given by a "suspension" of those for X_{2n-1}, at least in the twist case. Dropping the $\mu = 1$ component in (4.22) we can define truncated vectors

$$w_{+\hat{\mu}} = (m_+, -a_+\vec{p}) \,, \quad w_{-\hat{\mu}} = (-\sigma m_-, -\sigma a_-\vec{p}) \,, \quad w_{a\hat{\mu}} = (0, \vec{w}_a) \,, \tag{4.26}$$

with $\hat{\mu} = 0, 2, \ldots, n$. In Figure 4.1 we have provided an illustration of the polytope that these vectors define for the twist case $\sigma = +1$, of dimension $n = 3$, $d = 7$. In particular, the two-dimensional polytope at height zero is the "toric diagram" for X_5, defined by the vectors $\vec{w}_a$; we see that the toric diagram for Y_7 is the suspension of this, adding two additional vectors $w_{\pm\hat{\mu}}$. For the anti-twist case $\sigma = -1$ the polytope is not convex.

That the toric data (4.22) describes a fibration (4.19) directly follows from our discussion in section 3.1. An alternative point of view is provided by utilizing the Delzant construction (see *e.g.* [27]), as discussed in appendix A.1.

4.2.2 Relating the master volumes of Y_{2n+1} and X_{2n-1}

We now show that we can relate the master volume $\mathcal{V}_{2n+1}$ for $C(Y_{2n+1})$, or more precisely certain derivatives of it, to the master volume $\mathcal{V}_{2n-1}$ associated with $C(X_{2n-1})$. Via (4.12), the defining condition for the $(n+1)$-dimensional Reeb hyperplane H given in (4.6) can be written in the form

$$\sum_{\mu=0}^{n} y^\mu b_\mu = \tfrac{1}{2} \quad \Leftrightarrow \quad y^0 b_0 + \sum_{i=1}^{n} (y^i - y^i_*) b_i = 0\,. \tag{4.27}$$

We now want to exploit the fact that the polytope $\mathcal{P}$ takes a special form, namely a "truncated prism" with upper and lower faces, $\mathcal{P}_\pm$, each of which is a polytope of one lower dimension specified by d vectors (see Figure 4.2). Specifically, these polytopes are defined by

$$\mathcal{P}_\pm \equiv \mathcal{P} \cap \left\{ \sum_{\mu=0}^{n} (y^\mu - y^\mu_*) v_{\pm\mu} = \lambda_\pm \right\}\,, \tag{4.28}$$

with $v_{\pm\mu}$ given in (4.22). Geometrically, these correspond to the $X_{2n-1}/\mathbb{Z}_{m_\pm}$ fibres over the two poles of the spindle, associated with orbifold singularities $\mathbb{Z}_{m_\pm}$, respectively, as described in section 3.1. The faces $\mathcal{P}_\pm$ of the truncated prism are the images of toric divisors $\mathcal{D}_\pm$ in $C(Y_{2n+1})$ under the moment map. We denote the corresponding $U(1)^{n+1}$ invariant $(2n-1)$-dimensional manifolds as $T_\pm$, which are copies of the fibre $T_\pm \equiv X_{2n-1}/\mathbb{Z}_{m_\pm}$ over the poles of the spindle. These submanifolds were denoted $X_\pm$ in section 3.1, and in particular in section 3.1.1, but as commented there we must be careful with orientations. From (4.15), the volume

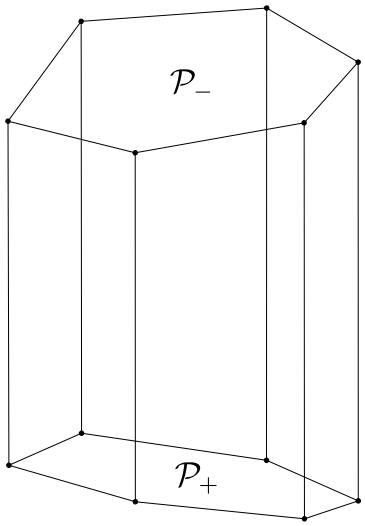


Figure 4.2: Toric polytope for a representative twist case with $n = 3$, $d = 6$.

of these manifolds are given by

$$\mathrm{Vol}(T_\pm) \equiv \int_{T_\pm} \eta \wedge \tfrac{1}{(n-1)!} J^{n-1} = -\frac{1}{2\pi} \frac{\partial \mathcal{V}_{2n+1}}{\partial \lambda_\pm} \ , \tag{4.29}$$

where the orientation on $T_\pm$ is induced from the complex structure and $\mathrm{Vol}(T_\pm) > 0$. We shall see later that these satisfy the homology relation $m_+[T_+] = \sigma m_-[T_-] \in H_{2n-1}(Y_{2n+1}, \mathbb{R})$, leading us to identify

$$T_+ = X_+ \, , \qquad T_- = \sigma X_- \, . \tag{4.30}$$

In particular, $\mathrm{Vol}(T_\pm)$ should always be positive for a *bona fide* GK geometry, where note that in section 3.1 (see also (3.30)) we then have $\mathrm{Vol}(X_-) = \sigma \mathrm{Vol}(T_-)$.

We now want to re-express $\mathrm{Vol}(T_\pm)$ in terms of master volume $\mathcal{V}_{2n-1}$ for the fibres X_{2n-1}. First consider T_+. We begin by noting that the volume of T_+ is obtained from the Euclidean volume of the $(n-1)$-dimensional polytope $\mathcal{P}_+$, where one imposes

$$\sum_{\mu=0}^{n} (y^\mu - y^\mu_*) v_{+\mu} = \lambda_+ \ , \qquad \sum_{\mu=0}^{n} (y^\mu - y^\mu_*) v_{a\mu} \geq \lambda_a \ . \tag{4.31}$$

Notice that since $v_{a\mu} = (0, v_{ai})$, this last inequality is exactly the same as the one for the

n-dimensional polytope:

$$\sum_{i=1}^{n}(y^i - y_*^i)v_{ai} \geq \lambda_a \ . \tag{4.32}$$

On the other hand, the first equation in (4.31) reads

$$y^0 m_+ + \sum_{i=1}^{n}(y^i - y_*^i)v_{+i} \ = \ \lambda_+ \ . \tag{4.33}$$

We can solve this for y^0 and then substitute into (4.27) to write the Reeb hyperplane condition in the form

$$\sum_{i=1}^{n}(y^i - y_*^i)\left(b_i - \frac{b_0}{m_+}v_{+i}\right) = -\frac{b_0}{m_+}\lambda_+ \ . \tag{4.34}$$

When $\lambda_+ = 0$, notice this is an n-dimensional Reeb hyperplane equation, where we have shifted the n-dimensional Reeb vector $b_i \to b_i - \frac{b_0}{m_+}v_{+i}$, which was already introduced in (2.19). We can also absorb the right hand side of (4.34) into a new y_*^i, which recall is an arbitrary point in the n-dimensional Reeb hyperplane. It is then convenient to make the shift

$$y_*^i \ \to \ y_*^i + \left(\frac{b_0}{m_+ b_1 - b_0}\lambda_+, 0, \ldots, 0\right) \equiv y_*^{(+)i} \ , \tag{4.35}$$

to then find that the two conditions (4.34) and (4.32), and hence (4.31) along with the Reeb hyperplane condition, can be written in the equivalent form:

$$\sum_{i=1}^{n}(y^i - y_*^{(+)i})b_i^{(+)} = 0 \ , \qquad \sum_{i=1}^{n}(y^i - y_*^{(+)i})v_{ai} \geq \lambda_a^{(+)} \ , \tag{4.36}$$

where we have also defined

$$b_i^{(+)} \equiv b_i - \frac{b_0}{m_+}v_{+i} \, , \qquad \lambda_a^{(+)} \equiv \lambda_a + \frac{b_0}{m_+ b_1^{(+)}}\lambda_+ \, . \tag{4.37}$$

Now (4.36) are precisely the conditions for specifying an $(n-1)$-dimensional polytope $\mathcal{P}_+$ associated with the fibre $X_{2n-1}/\mathbb{Z}_{m_+}$ sitting at the pole of the spindle with orbifold singularity $\mathbb{Z}_{m_+}$, as a function of the Reeb hyperplane vector $b_i^{(+)}$ and Kähler class parameters $\lambda_a^{(+)}$. If

$\mathcal{V}_{2n-1}(b_i;\lambda_a)$ denotes the master volume of X_{2n-1} as a function of Reeb vector b_i and Kähler class parameters λ_a, then the above analysis shows that

$$\mathrm{Vol}(T_+) = -\frac{1}{2\pi}\frac{\partial \mathcal{V}_{2n+1}}{\partial \lambda_+} = \frac{1}{m_+}\mathcal{V}^+_{2n-1}\,, \tag{4.38}$$

where we have defined

$$\mathcal{V}^+_{2n-1} \equiv \mathcal{V}_{2n-1}(b_i^{(+)};\lambda_a^{(+)})\,. \tag{4.39}$$

Here the factor of $1/m_+$ on the right hand side of (4.38) is because the corresponding fibre is not X_{2n-1}, but rather $T_+ = X_{2n-1}/\mathbb{Z}_{m_+}$.

A nearly identical analysis goes through for T_-, and we can summarize the final results for both cases as follows[4]

$$\begin{aligned}
\mathcal{V}^+_{2n-1} \equiv \mathcal{V}_{2n-1}(b_i^{(+)};\lambda_a^{(+)}) &= -\frac{m_+}{2\pi}\frac{\partial \mathcal{V}_{2n+1}}{\partial \lambda_+} = m_+\mathrm{Vol}(T_+)\,,\\
\mathcal{V}^-_{2n-1} \equiv \mathcal{V}_{2n-1}(b_i^{(-)};\lambda_a^{(-)}) &= -\frac{\sigma m_-}{2\pi}\frac{\partial \mathcal{V}_{2n+1}}{\partial \lambda_-} = \sigma m_-\mathrm{Vol}(T_-)\,,
\end{aligned} \tag{4.40}$$

where we have defined the shifted vectors

$$\begin{aligned}
b_i^{(+)} &= b_i - \frac{b_0}{m_+}v_{+i}\,, \qquad & \lambda_a^{(+)} &= \lambda_a + \frac{b_0}{m_+ b_1^{(+)}}\lambda_+\,,\\
b_i^{(-)} &= b_i + \frac{b_0}{\sigma m_-}v_{-i}\,, \qquad & \lambda_a^{(-)} &= \lambda_a - \frac{b_0}{\sigma m_- b_1^{(-)}}\lambda_-\,.
\end{aligned} \tag{4.41}$$

with $b_i^{(\pm)}$ already introduced in (2.19). From (4.40) we also immediately deduce that

$$\begin{aligned}
\frac{\partial^2 \mathcal{V}_{2n+1}}{\partial\lambda_+\partial\lambda_a} &= -\frac{2\pi}{m_+}\frac{\partial \mathcal{V}^+_{2n-1}}{\partial\lambda_a}\,, & \frac{\partial^2 \mathcal{V}_{2n+1}}{\partial\lambda_-\partial\lambda_a} &= -\frac{2\pi}{\sigma m_-}\frac{\partial \mathcal{V}^-_{2n-1}}{\partial\lambda_a}\,,\\
\frac{\partial^2 \mathcal{V}_{2n+1}}{\partial\lambda_+^2} &= -\frac{2\pi b_0}{m_+^2 b_1^{(+)}}\sum_{a=1}^{d}\frac{\partial \mathcal{V}^+_{2n-1}}{\partial\lambda_a}\,, & \frac{\partial^2 \mathcal{V}_{2n+1}}{\partial\lambda_-^2} &= +\frac{2\pi b_0}{m_-^2 b_1^{(-)}}\sum_{a=1}^{d}\frac{\partial \mathcal{V}^-_{2n-1}}{\partial\lambda_a}\,,\\
\frac{\partial^2 \mathcal{V}_{2n+1}}{\partial\lambda_+\partial\lambda_-} &= 0\,.
\end{aligned} \tag{4.42}$$

[4]As already remarked, the polytope $\mathcal{P}$ is convex only in the twist case with, with the anti-twist formulae-formally obtained from the twist formulae by setting $\sigma = -1$ in the toric data (4.22).

The last result is the statement that T_+ and T_- do not intersect, which is obvious geometrically as they are distinct fibres of a fibration. Since $\mathrm{Vol}(T_\pm) > 0$ we also note from (4.40) that $\mathcal{V}^+_{2n-1} > 0$ and $\sigma\mathcal{V}^-_{2n-1} > 0$.

We next consider the identity (4.13) satisfied by the master volume $\mathcal{V}_{2n+1}$. The $\mu = 1$ component of this vector equation is trivial. The $\mu = 0$ component, which will play a key role in a moment, can be written as

$$b_0 \sum_{a=1}^{d} \frac{\partial \mathcal{V}_{2n+1}}{\partial \lambda_a} = \Big(m_+ b_1 - b_0\Big) \frac{\partial \mathcal{V}_{2n+1}}{\partial \lambda_+} - \Big(\sigma m_- \, b_1 + b_0\Big) \frac{\partial \mathcal{V}_{2n+1}}{\partial \lambda_-} \,. \tag{4.43}$$

We do not explicitly write out the remaining components here.

4.2.3 Geometric extremization for $X_{2n-1} \hookrightarrow Y_{2n+1} \to \Sigma$

We now have all the ingredients to translate the geometric extremization procedure for Y_{2n+1}, summarized in section 4.1.3, in terms of the shifted master volumes on the fibres X_{2n-1}. We first consider the supersymmetric action. From the definition (4.17) and then using the identity satisfied by the master volume (4.43) we immediately have

$$\begin{aligned} S_{\mathrm{SUSY}} = -\sum_{A=1}^{D} \frac{\partial \mathcal{V}_{2n+1}}{\partial \lambda_A} &= -\frac{b_1}{b_0}\Big(m_+ \frac{\partial \mathcal{V}_{2n+1}}{\partial \lambda_+} - \sigma m_- \frac{\partial \mathcal{V}_{2n+1}}{\partial \lambda_-}\Big) \\ &= \frac{2\pi b_1}{b_0}\left[m_+ \mathrm{Vol}(T_+) - \sigma m_- \mathrm{Vol}(T_-)\right] , \end{aligned} \tag{4.44}$$

and we notice that the last expression is in exact alignment with the general result (3.1) that we proved earlier, taking into account the orientations in (4.30). Hence, using (4.40), we obtain the key result

$$S_{\mathrm{SUSY}} = \frac{2\pi b_1}{b_0}\left(\mathcal{V}^+_{2n-1} - \mathcal{V}^-_{2n-1}\right). \tag{4.45}$$

We next consider the fluxes on Y_{2n+1}. We denote these by $M_A = (M_+, M_-, M_a)$, which are the fluxes over the corresponding toric codimension two submanifolds $T_A \subset Y_{2n+1}$, where $T_A = (T_+, T_-, T_a)$. In particular

$$M_\pm \equiv \frac{1}{\nu_n} \int_{T_\pm} \eta \wedge \rho \wedge \frac{J^{n-2}}{(n-2)!} \,. \tag{4.46}$$

From (4.30) we take

$$M_+ = N^{X_+}\,, \qquad M_- = \sigma N^{X_-}\,, \tag{4.47}$$

where $N^{X_\pm} > 0$ were the fluxes introduced in section 3.1. The T_a may be identified with Σ_a in (3.16), and are the total spaces of toric codimension two submanifolds $S_a \subset X_{2n-1}$, fibred over the spindle Σ, with $a = 1, \ldots, d$. We first note that the linear relations satisfied by these fluxes given in (4.18) can be written in the equivalent form

$$\begin{aligned} m_+ M_+ &= \sigma m_- M_- \equiv N\,, \\ \sum_{a=1}^{d} M_a &= -\frac{\sigma m_+ + m_-}{m_+ m_-}\, N\,, \\ \sum_{a=1}^{d} \vec{w}_a M_a &= \frac{N}{m_+ m_-}\, \vec{p}\,, \end{aligned} \tag{4.48}$$

and these include the constraint equation $\sum_A M_A = 0$. The first line implies $m_+[T_+] = \sigma m_-[T_-] \in H_{2n-1}(Y_{2n+1}, \mathbb{R})$ that we mentioned earlier. As an aside notice that for the twist case the second line implies that some of the $M_a < 0$. We can also easily find expressions for the fluxes M_A in terms of $\mathcal{V}_{2n-1}$. Indeed from the expression for the M_A in terms of derivatives of $S_{\rm SUSY}$ given in (4.17) we immediately deduce

$$\begin{aligned} m_+ M_+ &= -\frac{1}{\nu_n}\frac{b_1}{b_1^{(+)}} \sum_{a=1}^{d} \frac{\partial \mathcal{V}^+_{2n-1}}{\partial \lambda_a}\,, \\ \sigma m_- M_- &= -\frac{1}{\nu_n}\frac{b_1}{b_1^{(-)}} \sum_{a=1}^{d} \frac{\partial \mathcal{V}^-_{2n-1}}{\partial \lambda_a}\,, \\ M_a &= -\frac{1}{\nu_n}\frac{b_1}{b_0}\left(\frac{\partial \mathcal{V}^+_{2n-1}}{\partial \lambda_a} - \frac{\partial \mathcal{V}^-_{2n-1}}{\partial \lambda_a} \right). \end{aligned} \tag{4.49}$$

The constraint equation can be recast in the form

$$\frac{1}{b_1^{(+)}} \sum_{a=1}^{d} \frac{\partial \mathcal{V}^+_{2n-1}}{\partial \lambda_a} = \frac{1}{b_1^{(-)}} \sum_{a=1}^{d} \frac{\partial \mathcal{V}^-_{2n-1}}{\partial \lambda_a}\,, \tag{4.50}$$

which ensures $m_+ M_+ = \sigma m_- M_- \equiv N$.

Due to the constraints (4.48), the set of toric fluxes $M_A = (M_+, M_-, M_a)$ is overdetermined, and it is sometimes convenient to instead work with a minimal set of unconstrained quantized fluxes $\mathcal{N}_\Upsilon$, as originally introduced in equation (1.29). We may make contact between the two descriptions using the results of appendix A.1. Here the index on $\mathcal{N}_\Upsilon$ may be identified as $\Upsilon = \hat{I} = 0, 1, \ldots, d-n$, labelling a basis for the free part of $H_{2n-1}(Y_{2n+1}, \mathbb{Z})$, while recall that $A = 1, \ldots, D = d+2$. We then have the general homology relation in toric geometry (see *e.g.* [129])

$$M_A = \sum_{\hat{I}=0}^{d-n} Q_{\hat{I}}^A \, \mathcal{N}_{\hat{I}} \,. \tag{4.51}$$

Written out explicitly using the charge matrix $Q_{\hat{I}}^A$, satisfying $\sum_{A=1}^{D} Q_{\hat{I}}^A \, v_{A\mu} = 0$, and deduced in appendix A.1, this reads

$$M_+ = m_- \, \mathcal{N}_0 \,, \qquad M_- = \sigma m_+ \, \mathcal{N}_0 \,, \qquad M_a = q_0^a \, \mathcal{N}_0 + \sum_{I=1}^{d-n} q_I^a \, \mathcal{N}_I \,. \tag{4.52}$$

Here q_I^a is the corresponding charge matrix for the toric fibres X_{2n-1}, satisfying $\sum_{a=1}^{d} q_I^a \, v_{ai} = 0$, and q_0^a satisfies $\sum_{a=1}^{d} q_0^a \, v_{ai} = p_i$, where recall the integers p_i determine the fibration of X_{2n-1} over Σ. Notice that the q_0^a are not unique and can be replaced with $q_0^a \to \sum_{I=1}^{d-n} c_I q_I^a$ where c_I are constants. In turn this shifts the "baryonic fluxes" $\mathcal{N}_I$, via $\mathcal{N}_I \to c_I \mathcal{N}_0$ showing that they are not unique either. We comment further on this in appendix A.2.

Given that in (4.48) we identify $m_+ M_+ = \sigma m_- M_- = N$, the first two equations in (4.52) allow us to identify

$$\mathcal{N}_0 = \frac{N}{m_+ m_-} \,. \tag{4.53}$$

Since $\mathcal{N}_0$ is required to be a positive integer (1.29), this shows that N is divisible by $m_+ m_-$, as commented earlier, below (3.14). The toric flux numbers M_a thus satisfy the last equation in (4.52). In appendix A.1 we further introduce the (non-unique) integers α_a^j that satisfy

$$\sum_{a=1}^{d} v_{ai} \, \alpha_a^j = \delta_i^j \,. \tag{4.54}$$

In terms of the gauged linear sigma model description, α_a^j is the charge of the a-th coordinate on $\mathbb{C}^d$ under the j-th $U(1)$ in the toric $U(1)^n$ action on the fibres X_{2n-1}. Using this, we may then write $q_0^a = \sum_{i=1}^n p_i \alpha_a^i$, and hence the last equation in (4.52) reads

$$M_a = \frac{N}{m_+ m_-} \sum_{i=1}^{n} p_i \alpha_a^i + \sum_{I=1}^{d-n} q_I^a \mathcal{N}_I \,. \tag{4.55}$$

This expresses the toric flux numbers M_a directly in terms of the "flavour fluxes" p_i, and a set of "baryonic fluxes" $\mathcal{N}_I$, one for each independent cycle, together with N and the toric data. Although as we comment further in appendix A.2, the $\mathcal{N}_I$ depend on an (arbitrary) choice of the α_a^j satisfying (4.54), and different choices lead to different $\mathcal{N}_I$.

Although we shall not work through the details, the flavour twist case of section 3.2 is obtained by imposing the condition (3.20), which in the toric setting amounts to set all the $\lambda_a \equiv \lambda$ to be equal in a particular gauge. To see this, from (4.8) and (4.9) we can write the transverse Kähler class for Y_{2n+1} in the form $[J] = -2\pi(\lambda_+ c_+ + \lambda_+ c_- + \lambda \sum_a c_a)$, while the first Chern class of the foliation is $[\rho] = 2\pi(c_+ + c_- + \sum_a c_a)$. In particular it is clear that (3.20) is satisfied on the toric fibres at the poles.

4.2.4 R-charges of baryonic operators

We now provide an expression for the geometric R-charges that are associated with certain supersymmetric cycles $T_{\pm a}$, $a = 1, \ldots, d$, of codimension four on Y_{2n+1}, which were introduced in section 3.1.2. Recall that these are defined as copies of $U(1)^n$ invariant codimension two submanifolds $S_a \subset X_{2n-1}$, whose cones are divisors in the Calabi-Yau cone X_{2n-1}, over each of the two poles of the spindle. In the notation of section 3.1 we have

$$T_{+a} = S_a^+ \,, \qquad T_{-a} = \sigma S_a^- \,, \tag{4.56}$$

precisely as in (4.30). In the case of $n = 3, 4$ the geometric R-charges are dual to the R-charges of baryonic operators associated with D3, M5-branes wrapping these cycles, respectively.

In section 4.1.2 we introduced $c_A \in H_B^2(\mathcal{F}_\xi)$ to be basic representatives of integral classes in $H^2(Y_{2n+1}, \mathbb{Z})$, which are Poincaré dual to the D toric divisors $\mathcal{D}_A$ on $C(Y_{2n+1})$. We write

$c_A = \{c_\pm, c_a\}$, with $c_\pm$ Poincaré dual to the divisors $\mathcal{D}_\pm$. The codimension four supersymmetric cycles $T_{\pm a}$ are then Poincaré dual to $c_\pm \wedge c_a$. Then using the result (4.16) in the definition of the R-charges (3.15) we deduce[5]

$$R_a^\pm \equiv \frac{4\pi}{\nu_n M_\pm} \int_{T_{\pm a}} \eta \wedge \frac{J^{n-2}}{(n-2)!} = \frac{1}{M_\pm} \frac{2}{\nu_n} \frac{1}{(2\pi)} \frac{\partial^2 \mathcal{V}_{2n+1}}{\partial \lambda_\pm \partial \lambda_a} \,. \tag{4.57}$$

Notice that these agree with the expressions defined in (3.15), with the different choices of orientation in the cycles in (4.56) cancelling due to the division by $M_\pm$ in (4.57), rather than $N^{X_\pm}$ in (3.15), where these are similarly related via (4.47). Since $M_+ > 0$ and $\sigma M_- > 0$ from the first line of (4.57) we have

$$R_a^+ > 0, \qquad \sigma R_a^- > 0 \,. \tag{4.58}$$

We will prove in a moment that these R-charges satisfy the identities

$$\sum_{a=1}^d R_a^+ v_{a\mu} \,=\, \frac{2}{b_1}\left(b_\mu - \frac{b_0}{m_+} v_{+\mu}\right), \qquad \sum_{a=1}^d R_a^- v_{a\mu} \,=\, \frac{2}{b_1}\left(b_\mu + \frac{b_0}{\sigma m_-} v_{-\mu}\right). \tag{4.59}$$

Using the results in the previous subsection we can now express the geometric R-charges in terms of $\mathcal{V}_{2n-1}$. Indeed using (4.42) we have

$$R_a^\pm = -\frac{1}{N} \frac{2}{\nu_n} \frac{\partial \mathcal{V}_{2n-1}^\pm}{\partial \lambda_a} \,. \tag{4.60}$$

In addition, using the expressions for the M_A given in (4.49) we immediately derive the result

$$\sum_{a=1}^d R_a^+ \,=\, 2 - \frac{2b_0}{b_1 m_+} \,, \qquad \sum_{a=1}^d R_a^- \,=\, 2 + \frac{2b_0}{b_1 \sigma m_-} \,, \tag{4.61}$$

and we also note that

$$R_a^+ - R_a^- = \frac{2b_0}{b_1} \frac{M_a}{N} \,, \tag{4.62}$$

[5]Note that the normalization of the geometric R-charges here is slightly different to what has appeared before in the literature. For example, setting $m_\pm = 1$, $\sigma = +1$ and $b_0 = 0$, we have the set-up associated with a Sasaki-Einstein space fibred over a sphere. In this case $M_\pm = N$ and the geometric R-charges here differ from those in [70, 119] by a factor of N.

agreeing with the general formula (3.19) derived earlier. It is also interesting to highlight that in the toric case, from (4.61) we can write

$$\frac{1}{2}\sum_{a=1}^{d}\left(R_a^+ + R_a^-\right) = 2 - \frac{m_- - \sigma m_+}{m_+ m_-}\frac{b_0}{b_1}\,. \tag{4.63}$$

Note that for the toric anti-twist case, with $\sigma = -1$, this expression is the same as what we saw in the universal anti-twist case in (3.51).

Observe that (4.61) is actually the $\mu = 1$ component of (4.59). Notice that the $\mu = 0$ component of (4.59) is trivially satisfied. Thus, to complete the proof of (4.59) we therefore just need to check the remaining components which read

$$\sum_{a=1}^{d} R_a^+ \vec{v}_a = \frac{2}{b_1}\vec{b}^{(+)}\,, \qquad \sum_{a=1}^{d} R_a^- \vec{v}_a = \frac{2}{b_1}\vec{b}^{(-)}\,. \tag{4.64}$$

Using the expressions for $R_a^\pm$ given in (4.60), we find that these are identities after using the fact that the $(2n-1)$-dimensional master volumes $\mathcal{V}_{2n-1}(\vec{b}^{(\pm)}; \lambda_a^{(\pm)})$ satisfy the identity

$$\sum_{a=1}^{d}\left(\vec{v}_a - \frac{\vec{b}^{(\pm)}}{b_1^{(\pm)}}\right)\frac{\partial \mathcal{V}^{\pm}_{(2n-1)}}{\partial \lambda_a} = 0\,, \tag{4.65}$$

which is the $(2n-1)$-dimensional version of (4.13).

4.2.5 The limit when $b_0 = 0$, $m_\pm = 1$

It is interesting to consider taking the limit $b_0 \to 0$ in the expressions for the geometric extremization problem above. In particular, if we set $m_\pm = 1$, and $\sigma = +1$ the spindle is then a two-sphere and we could expect to recover the results for GK geometry fibred over a Riemann surface of genus $g = 0$ with a topological twist as explained in 1.3. In particular, in this set-up there is no mixing of the R-symmetry vector with the $U(1)$ action on the two sphere and hence $b_0 = 0$.

We first note that setting $m_\pm = 1$ and taking the $b_0 \to 0$ limit of the off-shell supersym-

metric action (4.45) we find

$$\lim_{b_0\to 0} S_{\rm SUSY} = -2\pi b_1 \sum_{i=1}^{n}(-p_i)\frac{\partial \mathcal{V}_{2n-1}}{\partial b_i} - A\sum_{a=1}^{d}\frac{\partial \mathcal{V}_{2n-1}}{\partial \lambda_a}\,, \tag{4.66}$$

with $p_1 = -2$, and where we have defined

$$A \equiv -2\pi\,(\lambda_+ + \lambda_-)\,. \tag{4.67}$$

Note that in these expressions we should take derivatives before setting $b_1 = 2/(n-2)$. In addition, from (4.49) for the fluxes, in the $b_0 \to 0$ limit we obtain

$$\begin{aligned} N &= -\frac{1}{\nu_n}\sum_{a=1}^{d}\frac{\partial \mathcal{V}_{2n-1}}{\partial \lambda_a}\,, \\ M_a &= \frac{1}{\nu_n}\left[\frac{A}{2\pi}\sum_{b=1}^{d}\frac{\partial^2 \mathcal{V}_{2n-1}}{\partial\lambda_a\partial\lambda_b} + b_1\sum_{i=1}^{n}(-p_i)\frac{\partial^2 \mathcal{V}_{2n-1}}{\partial\lambda_a\partial b_i}\right]\,, \end{aligned} \tag{4.68}$$

and hence the constraint equation $\sum_A M_A = 0$ becomes in this limit

$$0 = -2\pi(-p_1)\sum_{a=1}^{d}\frac{\partial \mathcal{V}_{2n-1}}{\partial\lambda_a} + A\sum_{a,b=1}^{d}\frac{\partial^2 \mathcal{V}_{2n-1}}{\partial\lambda_a\partial\lambda_b} + 2\pi b_1\sum_{a=1}^{d}\sum_{i=1}^{n}(-p_i)\frac{\partial^2 \mathcal{V}_{2n-1}}{\partial\lambda_a\partial b_i}\,. \tag{4.69}$$

Finally, the R-charges (4.60) are given by

$$\lim_{b_0\to 0} R_a^{\pm} = -\frac{1}{N}\frac{2}{\nu_n}\frac{\partial \mathcal{V}_{2n-1}}{\partial\lambda_a}\,. \tag{4.70}$$

These are precisely the formulae derived in [70, 119], associated with a Sasaki-Einstein space fibred over a Riemann surface of genus $g = 0$, after taking into account that the R-charges differ by an extra factor of N as noted before, as well as identifying $-p_i$ here with n_i there.

We expect that setting $m_\pm = 1$ implies that we must have $b_0 = 0$ (which we assumed above). For the case $n = 3$ we can explicitly show that this is true later in section 5.2.3.

Chapter 5

Holography - AdS_3 (toric) case

This chapter will focus on the toric set up introduced in chapter 4 with $n = 3$. This is associated with $AdS_3 \times Y_7$ solutions of type IIB supergravity, where Y_7 is a toric GK geometry consisting of a fibration of a toric Sasaki-Einstein space X_5 over a spindle. Recall these solutions can be interpreted as being dual to the compactification on the spindle, with magnetic fluxes switched on, of the 4d $\mathcal{N} = 1$ SCFTs which are themselves dual to $AdS_5 \times X_5$ solutions. Here we focus on studying the field theory side of the AdS/CFT correspondence and we identify precise mappings with quantities computed in gravity for any such toric space.

5.1 Central charge from anomaly polynomial

Firstly, we illustrate how one can compute the central charge of 2d $\mathcal{N} = (0, 2)$ SCFTs dual to our $AdS_3 \times Y_7$ solutions via integration of the anomaly polynomial of parent 4d SCFTs compactified on Σ. For convenience we will focus on the case where $X_5 = S^5$, which is indeed a toric Sasaki-Einstein space and was considered in [1, 73]. In particular, we consider the SCFT dual to the explicit supegravity solution we presented in section 2.2, which arises from taking $\mathcal{N} = 4$ SYM theory, which is holographically dual to the $AdS_5 \times S^5$ vacuum of the 5d $U(1)^3$ gauged supergravity theory, and then compactifying it on the spindle Σ, with background fluxes for the $U(1)^3$ Abelian symmetry given by (2.35). We compute both the central charge and superconformal $U(1)$ R-symmetry using purely field theory methods, finding precise agreement with the supergravity results of section 2.2 and the geometric extremization carried out in section 3.3.1.

5.1.1 D3-brane anomaly polynomial

Generalizing the approach of [47], our starting point is the anomaly polynomial for $\mathcal{N} = 4$ SYM, with background gauge field fluxes F_a for the $U(1)^3 \subset SO(6)$ global symmetry group

of this theory. In the large N limit this anomaly polynomial reads (see, for example, [133])

$$\mathcal{A}_{4\mathrm{d}} \,=\, c_1(F_1)c_1(F_2)c_1(F_3)\frac{N^2}{2}\,. \tag{5.1}$$

Here $c_1(F_a)$ denote the first Chern classes of the $U(1)$ bundles with gauge field curvatures F_a, respectively. We want to compactify this theory on Σ, with fluxes given by (2.35), and compute the anomaly polynomial of the resulting 2d theory. For this we also need to take into account the $U(1)$ global symmetry in 2d, coming from the $U(1)_\Sigma$ isometry of Σ. Geometrically, this means that we want to compute the anomaly polynomial (5.1), where the six-manifold Z_6 on which it is defined is the total space of a Σ fibration over Z_4. We may achieve this by introducing a connection form $\mathcal{A}_\Sigma$ for $U(1)_\Sigma$, and replacing $\mathrm{d}\varphi_0 \to \mathrm{d}\varphi_0 + \mathcal{A}_\Sigma$. In doing so it is important that the 5d Killing spinor is independent of φ_0, which is true in the tilde gauge defined by (2.41). We thus introduce the connection one-forms on Z_6:

$$\mathscr{A}_a \,\equiv\, \left(\frac{x-\alpha}{x+3K_a}-\frac{2}{3}\right)\frac{\Delta\phi}{2\pi}(\mathrm{d}\varphi_0+\mathcal{A}_\Sigma) \,\equiv\, \rho_a(x)(\mathrm{d}\varphi_0+\mathcal{A}_\Sigma)\,, \qquad a\,=\,1,2,3\,, \tag{5.2}$$

which by construction restricts to the supergravity gauge field $\tilde{A}_a$ on each Σ fibre. We then compute the curvature

$$\mathscr{F}_a \,\equiv\, \mathrm{d}\mathscr{A}_a \,=\, \rho_a'(x)\,\mathrm{d}x\wedge(\mathrm{d}\varphi_0+\mathcal{A}_\Sigma)+\rho_a(x)\mathcal{F}_\Sigma\,, \tag{5.3}$$

where $\mathcal{F}_\Sigma = \mathrm{d}\mathcal{A}_\Sigma$. By construction the integral of $\mathscr{F}_a$ over a fibre Σ gives the flux $\mathfrak{p}_a$, as in (2.34). The curvature form $\mathscr{F}_a$ defines a $U(1)$ bundle $\mathcal{L}_a$ over Z_6 by taking $c_1(\mathcal{L}_a) = [\mathscr{F}_a/2\pi] \in H^2(Z_6,\mathbb{R})$. We also define $c_1(\Sigma) = [\mathcal{F}_\Sigma/2\pi] \in H^2(Z_4,\mathbb{Z})$. In the anomaly polynomial we then write

$$c_1(F_a) \,=\, \Delta_a\, c_1(R_{2\mathrm{d}}) + c_1(\mathcal{L}_a)\,, \tag{5.4}$$

where $R_{2\mathrm{d}}$ is the pull-back of a $U(1)$ bundle over Z_4. The trial R-charges Δ_a satisfy the constraint $\Delta_1+\Delta_2+\Delta_3 = 2$, which is equivalent to the superpotential (in $\mathcal{N}=1$ language) having R-charge 2.

The 2d anomaly polynomial is then obtained by integrating $\mathcal{A}_{4\mathrm{d}}$ in (5.1) over Σ:

$$\begin{aligned}\mathcal{A}_{2\mathrm{d}} &= \int_\Sigma \mathcal{A}_{4\mathrm{d}} = \frac{N^2}{2}\int_\Sigma c_1(F_1)c_1(F_2)c_1(F_3)\\ &= \frac{N^2}{2}\int_\Sigma \Big\{\Delta_1\Delta_2\Delta_3 c_1(R_{2\mathrm{d}})^3 + c_1(R_{2\mathrm{d}})^2\big[\Delta_2\Delta_3 c_1(\mathcal{L}_1) + \Delta_1\Delta_3 c_1(\mathcal{L}_2)\\ &\qquad + \Delta_1\Delta_2 c_1(\mathcal{L}_3)\big] + c_1(R_{2\mathrm{d}})\big[\Delta_3 c_1(\mathcal{L}_1)c_1(\mathcal{L}_2) + \Delta_2 c_1(\mathcal{L}_1)c_1(\mathcal{L}_3)\\ &\qquad + \Delta_1 c_1(\mathcal{L}_2)c_1(\mathcal{L}_3)\big] + c_1(\mathcal{L}_1)c_1(\mathcal{L}_2)c_1(\mathcal{L}_3)\Big\}\,.\end{aligned} \tag{5.5}$$

After a computation using the explicit functions $\rho_a(x)$ defined in (5.2), with the parameters there given in terms of the spindle integers and the fluxes in (2.36), we find the integral in (5.5) gives

$$\begin{aligned}\mathcal{A}_{2\mathrm{d}} &= \frac{N^2}{2}\Bigg\{\left[\frac{\tilde{p}_3\,\Delta_1\Delta_2}{\sigma m_+ m_-} + \frac{\tilde{p}_2\,\Delta_1\Delta_3}{\sigma m_+ m_-} + \frac{\sigma m_+ + m_- - \tilde{p}_2 - \tilde{p}_3}{\sigma m_+ m_-}\,\Delta_2\Delta_3\right] c_1(R_{2\mathrm{d}})^2\\ &\quad + \sum_{a=1}^{3}\frac{\Delta_a\, f_a(\sigma m_+, m_-, \tilde{p}_2, \tilde{p}_3)}{3m_+^2 m_-^2(-\sigma m_+ + m_-)}\, c_1(R_{2\mathrm{d}})c_1(\Sigma)\\ &\quad - \frac{g_1(\sigma m_+, m_-, \tilde{p}_2, \tilde{p}_3)\, g_2(\sigma m_+, m_-, \tilde{p}_2, \tilde{p}_3)}{9\sigma m_+^3 m_-^3(-\sigma m_+ + m_-)^2}\, c_1(\Sigma)^2\Bigg\}\,,\end{aligned} \tag{5.6}$$

where we have defined

$$\begin{aligned}f_1(\sigma m_+, m_-, \tilde{p}_2, \tilde{p}_3) &\equiv (\sigma m_+ + m_-)(2\tilde{p}_2^2 + \tilde{p}_2\tilde{p}_3 + 2\tilde{p}_3^2) - 2\sigma m_+ m_-(\tilde{p}_2 + \tilde{p}_3)\\ &\quad - (2\tilde{p}_2^2 - \tilde{p}_2\tilde{p}_3 + 2\tilde{p}_3^2)(\tilde{p}_2 + \tilde{p}_3)\,,\end{aligned} \tag{5.7}$$

$$\begin{aligned}f_2(\sigma m_+, m_-, \tilde{p}_2, \tilde{p}_3) &\equiv 2(m_+^2 + m_-^2)(\tilde{p}_2 + \tilde{p}_3) - (\sigma m_+ + m_-)(4\tilde{p}_2^2 + 7\tilde{p}_2\tilde{p}_3 + 2\tilde{p}_3^2)\\ &\quad - 2\sigma m_+ m_-(\sigma m_+ + m_- - 3\tilde{p}_2 - 2\tilde{p}_3) + \tilde{p}_2(2\tilde{p}_2^2 + 5\tilde{p}_2\tilde{p}_3 + 5\tilde{p}_3^2)\,,\end{aligned} \tag{5.8}$$

$$f_3(\sigma m_+, m_-, \tilde{p}_2, \tilde{p}_3) \equiv f_2(\sigma m_+, m_-, \tilde{p}_3, \tilde{p}_2)\,, \tag{5.9}$$

$$\begin{aligned}g_1(\sigma m_+, m_-, \tilde{p}_2, \tilde{p}_3) &\equiv (\sigma m_+ + m_-)(4\tilde{p}_2^2 + 13\tilde{p}_2\tilde{p}_3 + 4\tilde{p}_3^2) - 4(\sigma m_+ + m_-)^2(\tilde{p}_2 + \tilde{p}_3)\\ &\quad + 4\sigma m_+ m_-(\sigma m_+ + m_-) - 9\tilde{p}_2\tilde{p}_3(\tilde{p}_2 + \tilde{p}_3)\,,\end{aligned} \tag{5.10}$$

$$g_2(\sigma m_+, m_-, \tilde{p}_2, \tilde{p}_3) \equiv (\sigma m_+ + m_-)(\tilde{p}_2 + \tilde{p}_3) - \sigma m_+ m_- - (\tilde{p}_2^2 + \tilde{p}_2\tilde{p}_3 + \tilde{p}_3^2)\,.$$

5.1.2 c-extremization and superconformal R-symmetry

The coefficient of $\frac{1}{2}c_1(L_i)c_1(L_j)$ in the anomaly polynomial $\mathcal{A}_{2\mathrm{d}}$ is precisely $\mathrm{Tr}\,\gamma^3\mathcal{Q}_i\mathcal{Q}_j$, where the global symmetry $\mathcal{Q}_i$ is associated to the $U(1)$ bundle L_i over Z_4, and γ^3 is the 2d chirality operator. We know from c-extremization [65] that the 2d superconformal $U(1)$ R-symmetry extremizes the trial function

$$c_{\mathrm{trial}} \;=\; 3\,\mathrm{Tr}\,\gamma^3 R_{\mathrm{trial}}^2\,, \tag{5.11}$$

over the space of possible R-symmetries. Introducing $\mathcal{J}_\Sigma$ to be the generator of the global symmetry coming from the $U(1)_\Sigma$ isometry of the spindle, we can write

$$R_{\mathrm{trial}} \;=\; R_{2\mathrm{d}} + \varepsilon\,\mathcal{J}_\Sigma\,, \tag{5.12}$$

so that

$$c_{\mathrm{trial}} \;=\; 3\left(\mathrm{Tr}\,\gamma^3 R_{2\mathrm{d}}^2 + 2\varepsilon\,\mathrm{Tr}\,\gamma^3 R_{2\mathrm{d}}\mathcal{J}_\Sigma + \varepsilon^2\,\mathrm{Tr}\,\gamma^3\mathcal{J}_\Sigma^2\right)\,. \tag{5.13}$$

Next we can substitute for the traces using (5.6), and extremize over the trial R-charges ε, Δ_a, subject to the constraint $\Delta_1+\Delta_2+\Delta_3=2$. We find the extremal values to be

$$\varepsilon_* \;=\; -\frac{2m_+m_-(\sigma m_+ - m_-)}{m_+^2+m_-^2-m_+^2m_-^2(\mathfrak{p}_1^2+\mathfrak{p}_2^2+\mathfrak{p}_3^2)}\,,\qquad \Delta_1^* \;=\; \Delta_2^* \;=\; \Delta_3^* \;=\; \frac{2}{3}\,. \tag{5.14}$$

The central charge c in the large N limit, is then given by evaluating (5.11) on the superconformal R-symmetry with $\varepsilon=\varepsilon_*$ and $\Delta_a=\Delta_a^*$. We find

$$c \;=\; \frac{6m_-^2m_+^2\,\mathfrak{p}_1\mathfrak{p}_2\mathfrak{p}_3}{m_+^2+m_-^2-m_+^2m_-^2(\mathfrak{p}_1^2+\mathfrak{p}_2^2+\mathfrak{p}_3^2)}\,N^2\,. \tag{5.15}$$

This precisely matches the gravity computation (2.52), and moreover the R-symmetry (5.12) with $\varepsilon=\varepsilon_*$ and $\Delta_a=\Delta_a^*$ precisely matches its geometric dual (2.55).

5.2 Matching $\mathbf{AdS}_3\times Y_7$ solutions with field theory

We now proceed to determine the explicit map between the field theory variables involved in c-extremization and those appearing in the extremization of the GK geometry.

5.2.1 4d $\mathcal{N}=1$ SCFT on $\mathbb{R}^{1,1}\times\Sigma$

Consider the four-dimensional $\mathcal{N}=1$ SCFT that is associated with N D3-branes sitting at the apex of the Calabi-Yau 3-fold cone $C(X_5)$, with toric vectors v_{ai}, $a=1,\ldots,d$ and $i=1,\ldots 3$. Recall that the SCFT has, generically,[1] $U(1)^d$ symmetry with $U(1)^{d-3}$ baryonic symmetry associated with the number of independent three cycles $d-3=\dim H_3(X_5,\mathbb{R})$ on the Sasaki-Einstein manifold X_5. We then place the SCFT on a spindle with background magnetic fluxes for the $U(1)^d$ symmetry, associated with either a twist or an anti-twist to preserve supersymmetry. Assuming that the resulting field theory flows to a 2d $\mathcal{N}=(0,2)$ SCFT in the IR, we can extract the central charge, as well as the R-charges of the baryonic operators, using c-extremization as argued in the introduction 1.2.1. The extremization can be carried out in two stages by extremizing over the baryonic directions first. The resulting central charge after the first stage, which is still off-shell, is what can be matched with the off-shell gravitational computation, as we shall show in detail.

Let Δ_a be the trial R-charges of the fields that are associated with the toric divisors of $C(X_5)$ (see *e.g.* [129, 130]). The Δ_a satisfy the constraint

$$\sum_{a=1}^{d}\Delta_a=2\ , \tag{5.16}$$

which is equivalent to the statement that the superpotential has R-charge 2. We also turn on background magnetic fluxes for the $U(1)^d$ symmetry, with field strengths F_a given by

$$\mathfrak{p}_a=\frac{1}{2\pi}\int_\Sigma F_a\,, \tag{5.17}$$

where $\mathfrak{p}_a$ are integers divided by (m_+m_-). These may be viewed as twisting the associated fields into sections of $\mathcal{O}(\mathfrak{p}_a)$ over the spindle, where to preserve supersymmetry we have the constraint

$$\sum_{a=1}^{d}\mathfrak{p}_a=-\frac{\sigma m_++m_-}{m_+m_-}\ , \tag{5.18}$$

[1] In some cases this is enlarged to a non-Abelian symmetry.

associated with the twist and the anti-twist case when $\sigma = \pm 1$, respectively.

Now we consider the anomaly polynomial of these 4d $\mathcal{N} = 1$ SCFTs at large N, generalization of (5.1)

$$\mathcal{A}_{4\mathrm{d}} \;=\; \frac{N^2}{12} \sum_{a,b,c=1}^{d} (v_a, v_b, v_c)\, c_1(F_a) c_1(F_b) c_1(F_c)\,, \tag{5.19}$$

where (v_a, v_b, v_c) is the determinant of the 3×3 matrix with (v_{ai}), (v_{bi}), (v_{ci}) as columns. Integrating this in a similar fashion to what we did in the previous section 5.1, one can get the two-dimensional anomaly polynomial $\mathcal{A}_{2\mathrm{d}}$, and hence the trial central charge c_{trial}. In [73] this computation was carried out to find

$$c_{\mathrm{trial}} = \frac{3}{\varepsilon} \left(\sum_{a<b<c} (v_a, v_b, v_c)\, \Delta_a^+ \Delta_b^+ \Delta_c^+ - \sum_{a<b<c} (v_a, v_b, v_c)\, \Delta_a^- \Delta_b^- \Delta_c^- \right) N^2\,. \tag{5.20}$$

Here we introduced the "shifted" R-charges

$$\Delta_a^{\pm} \;\equiv\; \Delta_a \pm \frac{\varepsilon}{2} \left(\mathfrak{p}_a \pm \frac{r_a}{2} \frac{\sigma m_+ - m_-}{m_+ m_-} \right)\,, \tag{5.21}$$

where ε is a mixing parameter for the spindle $U(1)_\Sigma$ isometry and r_a are a set of arbitrary variables satisfying the constraint $\sum_{a=1}^{d} r_a = 2$. Different choices of r_a give different gauges, and so will drop out of final results. To see this, notice that the freedom we have is

$$r_a \;\mapsto\; r_a + \delta r_a\,, \qquad \text{with} \qquad \sum_{a=1}^{d} \delta r_a = 0\,. \tag{5.22}$$

On the other hand, from (5.21) we see that such a shift may be absorbed into the trial R-charges Δ_a via

$$\Delta_a \;\mapsto\; \Delta_a - \frac{\delta r_a}{2} \frac{\sigma m_+ - m_-}{m_+ m_-}\, \varepsilon\,, \tag{5.23}$$

and, moreover, this shift preserves the constraint (5.16). Notice that (5.16)–(5.21) imply

$$\sum_{a=1}^{d} \Delta_a^+ = 2 - \frac{\varepsilon}{m_+}\,, \qquad \sum_{a=1}^{d} \Delta_a^- = 2 + \frac{\varepsilon}{\sigma m_-}\,. \tag{5.24}$$

Associated with the $d-3$ baryonic directions, we can first impose a partial set of extremization conditions

$$\sum_{a=1}^{d} q_I^a \frac{\partial c_{\text{trial}}}{\partial \Delta_a} = 0 \ , \qquad I = 1, \ldots, d-3 \ , \tag{5.25}$$

where we recall that q_I^a are the kernel vectors for the toric data for $C(X_5)$ satisfying

$$\sum_{a=1}^{d} q_I^a \, v_{ai} = 0 \, . \tag{5.26}$$

which specifies the embedding $U(1)^{d-3} \subset U(1)^d$ (see appendix A.1). After solving these conditions, and substituting back into c_{trial}, one obtains an off-shell function, $c_{\text{trial}}|_{\text{baryonic}}$, of $d-(d-3)=3$ variables: we start with the $d+1$ variables $\Delta_1, \ldots, \Delta_d, \varepsilon$, with one constraint (5.16), and end up with (say) $\Delta_1, \Delta_2, \varepsilon$, where we have eliminated $\Delta_3, \ldots, \Delta_d$ using the constraints (5.25). After extremizing over the baryonic directions, the resulting $\Delta_a^{\pm}|_{\text{baryonic}}$ are then also functions of trial R-charges $\Delta_1, \Delta_2, \varepsilon$. The on-shell results are then obtained by further extremizing over $\Delta_1, \Delta_2, \varepsilon$.

5.2.2 Matching with GK geometry

Recalling (4.48), the rank of the gauge group N is identified on the gravity side via

$$N \equiv m_+ M_+ = \sigma m_- M_- \, . \tag{5.27}$$

Furthermore the background magnetic fluxes $\mathfrak{p}_a$ are identified on the gravity side via

$$\mathfrak{p}_a \equiv \frac{M_a}{N} \, , \tag{5.28}$$

where M_a characterize the quantized five-form flux through the d toric five-cycles on Y_7 associated with the toric divisors $\mathcal{D}_a$. Importantly, the second condition in (4.48) on the M_a implies that this identification is consistent with the field theory constraint (5.18) on the $\mathfrak{p}_a$. Note also from the third condition in (4.48), for consistency, we deduce that the background magnetic fluxes of the SCFT are related to the geometric data $\vec{p}$ which specifies the fibration

of the SE_5 over the spindle, via

$$\sum_a \vec{w}_a \, \mathfrak{p}_a = \frac{1}{m_- m_+} \, \vec{p}. \tag{5.29}$$

This particular relation may be understood in field theory as follows. Recall that turning on the magnetic flux $\mathfrak{p}_a$, the corresponding fields Z_a become sections of $\mathcal{O}(\mathfrak{p}_a)$ over the spindle Σ. On the other hand, in the gauged linear sigma model description of the fibres $C(X_5)$, the Z_a are also sections of non-trivial bundles over the fibres X_5, as they are (typically) charged under the baryonic $U(1)^{d-3}$ symmetries. However, from (5.26) one can verify that $\prod_{a=1}^d Z_a^{v_{ai}}$ are sections of trivial bundles on the fibres X_5, that moreover have charge δ_{ij} under the j-th toric $U(1) \subset U(1)^3$. The variables $\vec{p}$ then precisely describe the twisting of this i-th flavour direction over the spindle Σ, for $i = 2, 3$, which is the equality (5.29). A more detailed discussion of this may be found in appendix B of [119], albeit in the case that the spindle is replaced by a smooth Riemann surface of genus g.

We also make the identifications

$$\varepsilon = b_0 \, , \qquad\qquad \Delta_a^{\pm}\big|_{\text{baryonic}} = R_a^{\pm} \, , \tag{5.30}$$

where the notation on the left hand side means that we have already extremized over the baryonic directions *i.e.* imposed (5.25). We immediately notice that the conditions on the $\Delta_a^{\pm}|_{\text{baryonic}}$ arising from (5.24) are consistent with the conditions on the $R_a^{\pm}$ in (4.61). Observe that $R_a^{\pm}$ are functions of the trial R-symmetry vector (b_0, b_2, b_3) (with $b_1 = 2$, as required for a GK geometry) while the $\Delta_a^{\pm}|_{\text{baryonic}}$ are functions of trial R-charges $\Delta_1, \Delta_2, \varepsilon$, after extremizing over the baryonic directions.

The claim is that (5.30) gives the change of variables between field theory and GK geometry. Notice this is *a priori* over-determined, as there are $2d$ equations in (5.30), but only three independent variables. However, we can prove that the identification is consistent; the proof is somewhat involved so we have presented it in appendix A.3. We will also show there, using the key results of the previous section, that the off-shell trial central charge in gravity

obtained from (4.45) can be expressed in the form

$$\mathscr{Z} = \frac{3N^2 b_1^2}{4b_0} \sum_{a<b<c} (v_a, v_b, v_c) \left(R_a^+ R_b^+ R_c^+ - R_a^- R_b^- R_c^- \right) . \tag{5.31}$$

With the above dictionary, this is then in exact agreement with the field theory result (5.20).

5.2.3 New variables

In field theory, instead of using the variables Δ_a subject to the constraints (5.16) and (5.25) we can use a slightly different set of variables φ_a defined via

$$\varphi_a \equiv \frac{1}{2} (\Delta_a^+ + \Delta_a^-) = \Delta_a + \frac{\varepsilon}{4} \frac{\sigma m_+ - m_-}{m_+ m_-} r_a \,, \tag{5.32}$$

where we used (5.21) and we recall the gauge parameters satisfy $\sum_a r_a = 2$. The inverse relation is $\Delta_a^\pm = \varphi_a \pm \frac{\varepsilon}{2} \mathfrak{p}_a$. The constraints (5.16), (5.25) then become

$$\begin{aligned} \sum_{a=1}^{d} \varphi_a &= 2 + \frac{\varepsilon}{2} \frac{\sigma m_+ - m_-}{m_+ m_-} \,, \\ \sum_{b=1}^{d} \sum_{a=1}^{b} \sum_{c=1}^{d} q_I^a (v_a, v_b, v_c) \, (\varphi_b \mathfrak{p}_c + \varphi_c \mathfrak{p}_b) &= 0 \,, \end{aligned} \tag{5.33}$$

where we used (A.55) to get the second expression. We also highlight that while (v_a, v_b, v_c) is antisymmetric in b, c and $(\varphi_b \mathfrak{p}_c + \varphi_c \mathfrak{p}_b)$ is symmetric, the sum is not trivial due to middle summation running from $a = 1, \ldots, b$. The off-shell trial central charge (5.20) can be written in terms of the φ_a as:

$$c_{\text{trial}} = 3N^2 \sum_{a<b<c} (v_a, v_b, v_c) \left(\mathfrak{p}_a \varphi_b \varphi_c + \mathfrak{p}_b \varphi_a \varphi_c + \mathfrak{p}_c \varphi_a \varphi_b + \frac{\varepsilon^2}{4} \mathfrak{p}_a \mathfrak{p}_b \mathfrak{p}_c \right) . \tag{5.34}$$

These formulas generalize those of [73,86], who studied the case of $X_5 = S^5$, to arbitrary X_5. For general X_5, using the φ_a variables it is straightforward to show that when the spindle becomes a two-sphere, then necessarily $\varepsilon = 0$ (recall that in section 4.2.5 we assumed $\varepsilon = 0$). Indeed, setting $m_\pm = 1$ and $\sigma = +1$, both of the constraints (5.33) are independent of ε. Thus, the only ε dependence in c_{trial} is the quadratic dependence in the last term in (5.34)

and hence the extremal point will necessarily have $\varepsilon = 0$.

5.3 Example: $\mathbf{AdS}_3 \times Y_7$ solutions with $X_5 = T^{1,1}$

We now illustrate some of our formalism explicitly by considering the example when $X_5 = T^{1,1}$, the base of the conifold. The toric data for $T^{1,1}$ are specified by $d = 4$ vectors given by

$$v_{1i} = (1, \vec{w}_1) \ , \qquad v_{2i} = (1, \vec{w}_2) \ , \qquad v_{3i} = (1, \vec{w}_3) \, , \qquad v_{4i} = (1, \vec{w}_4) \, , \tag{5.35}$$

where

$$\vec{w}_1 = (0, 0) \ , \qquad \vec{w}_2 = (1, 0) \ , \qquad \vec{w}_3 = (1, 1) \, , \qquad \vec{w}_4 = (0, 1) \, . \tag{5.36}$$

There is a one-dimensional kernel q_1^a, satisfying $\sum_{a=1}^4 q_1^a \, v_{ai} = 0$, given by

$$q_1^a = (-1, 1, -1, 1) \ . \tag{5.37}$$

The toric data for the $T^{1,1}$ fibration over Σ is then given by $D = 6$ vectors as in (4.22):

$$v_{+\mu} = (m_+, 1, -a_+ \vec{p}) \, , \quad v_{-\mu} = (-\sigma m_-, 1, -\sigma a_- \vec{p}) \, , \quad v_{a\mu} = (0, 1, \vec{w}_a) \, , \tag{5.38}$$

where $\vec{p} = (p_2, p_3) \in \mathbb{Z}^2$ and $a_\pm \in \mathbb{Z}$ satisfy $a_- m_+ + a_+ m_- = 1$. The three integers $p_i = (p_1, p_2, p_3)$, with $p_1 = -(m_- + \sigma m_+)$, specify the fibration. There is a two-dimensional kernel $Q^A_{\hat{I}} = (Q^A_0, Q^A_1)$, satisfying $\sum_{A=1}^6 Q^A_{\hat{I}} \, v_{A\mu} = 0$ (see appendix A.1), given by

$$\begin{aligned} Q^A_0 \ &= \ (m_-, \sigma m_+, -(m_- + \sigma m_+) - p_2 - p_3, p_2, 0, p_3) \ , \\ Q^A_1 \ &= \ (0, 0, 1, -1, 1, -1) = (0, 0, q_1^1, q_1^2, q_1^3, q_1^4) \ . \end{aligned} \tag{5.39}$$

Using the vectors (5.38) we can obtain an explicit (and lengthy) expression for the master volume $\mathcal{V}_7$ for Y_7 using the formula given in (2.27) of [119]. The master volume $\mathcal{V}_7$ depends on just 3 of the 6 Kähler class parameters λ_A. We therefore solve the constraint equation and two of the flux quantization conditions in (4.17) for three of the λ_A. For example, we

can solve the constraint equation and the expressions for M_+ and M_1 for $(\lambda_+, \lambda_-, \lambda_1)$. The remaining Kähler class parameters $\lambda_2, \lambda_3, \lambda_4$ then drop out of any final formula. The flux vector M_A in (4.17) is now expressed in terms of M_+, M_1, p_2, p_3 and, in particular, we find $m_+ M_+ = \sigma m_- M_- \equiv N$. Instead of using these four variables, it is most illuminating to express the flux vector in terms of M_1, M_2, M_3, M_4 to obtain

$$M_A = \left\{ M_+, \frac{\sigma m_+}{m_-} M_+, M_1, M_2, M_3, M_4 \right\} , \qquad M_+ = -\frac{m_-}{m_- + \sigma m_+} \sum_{a=1}^{4} M_a \, . \tag{5.40}$$

We can further rescale the M_a by a factor of N and introduce $\mathfrak{p}_a$, which are to be identified with the background magnetic fluxes of the SCFT shortly, via

$$\mathfrak{p}_a \equiv \frac{M_a}{N} , \qquad \sum_{a=1}^{4} \mathfrak{p}_a = -\frac{m_- + \sigma m_+}{m_+ m_-} , \tag{5.41}$$

and also, from (5.29), we have the fibration data $\vec{p} = (p_2, p_3)$ is related to the $\mathfrak{p}_a$ via

$$p_2 = m_- m_+ (\mathfrak{p}_2 + \mathfrak{p}_3) , \qquad p_3 = m_- m_+ (\mathfrak{p}_3 + \mathfrak{p}_4) . \tag{5.42}$$

We can then obtain an expression for the off-shell central charge $\mathscr{Z}$ from (1.34), with $S_{\rm SUSY}$ given by (4.17). This is expressed in terms of $m_\pm$, $a_\pm$, $\mathfrak{p}_a$, b_0, b_1, b_2, b_3 and set $b_1 = 2$.

Equivalently, we can apply the block formulas for toric fibrations over Σ obtained in section 4.2, namely (4.45) and (4.49), obtaining the very same end results, which corroborates the validiy of our analysis.

The gravitational off-shell central charge $\mathscr{Z}$ obtained is quadratic in b_0, b_2, b_3 and after extremizing over these variables we find that on-shell it can be expressed as[2]

$$c_{\rm sugra} \equiv \mathscr{Z}_{\rm os} = \frac{3\,(m_- + \sigma m_+)^2 \sum_{a<b, c\neq a,b} \mathfrak{p}_a \mathfrak{p}_b \mathfrak{p}_c^2 \sum_{a<b<c} \mathfrak{p}_a \mathfrak{p}_b \mathfrak{p}_c}{(m_-^2 - \sigma m_- m_+ + m_+^2) \prod_{a<b} (\mathfrak{p}_a + \mathfrak{p}_b) - \sigma m_+ m_- \Theta} \, N^2 , \tag{5.43}$$

where we defined

$$\Theta \equiv \sum_{a<b, c\neq a,b} \mathfrak{p}_a \mathfrak{p}_b \mathfrak{p}_c^4 - 2 \sum_{a<b} \mathfrak{p}_a \mathfrak{p}_b \prod_c \mathfrak{p}_c \, . \tag{5.44}$$

[2]This corrects some typos in [73] who analysed this from field theory as explained below.

Notice that $a_\pm$ have dropped out of the final expression. The extremal values b_0, b_2, b_3 are lengthy and we do not give them here explicitly. With the master volume in hand, it is also straightforward to obtain explicit expressions for both the R-charges $R_a^\pm$ using (4.57). The on-shell expressions are expressed in terms of $m_\pm$ and $\mathfrak{p}_a$ as expected. One then determines the ranges of allowed parameters by imposing, on-shell, $c_{\rm sugra} > 0$, $R_a^+ > 0$ and $\sigma R_a^- > 0$.

Now $H^2(T^{1,1}, \mathbb{Z}) \cong \mathbb{Z}$, associated with there being a single baryonic $U(1)$ symmetry in the Klebanov-Witten field theory dual to $\mathrm{AdS}_5 \times T^{1,1}$. Thus, $H_5(Y_7, \mathbb{Z}) = \mathbb{Z}^2$ and there are two independent fluxes $\mathcal{N}_0, \mathcal{N}_1$. We can therefore express M_A in terms of $\mathcal{N}_0, \mathcal{N}_1$, given the spindle data $m_\pm, \sigma$ and the fibration data p_i. Recall from (4.53) we have $\mathcal{N}_0 = \frac{N}{m_+ m_-}$. Hence from (4.52), recalling the kernel (5.39), we can write

$$(M_1, M_2, M_3, M_4) = \frac{N}{m_+ m_-}(-(m_- + \sigma m_+) - p_2 - p_3, p_2, 0, p_3) + \mathcal{N}_1(1, -1, 1, -1)\,. \quad (5.45)$$

and $\mathcal{N}_1$ is the baryonic charge. As emphasized earlier, the definition of baryonic charge is not unique. In particular, for a given M_a, we could also write (4.52) as $M_a = (q_0^a + q_1^a \mathcal{N}_1/\mathcal{N}_0)\mathcal{N}_0$ and then using $\tilde{q}_0^a \equiv q_0^a + q_1^a \mathcal{N}_1/\mathcal{N}_0$ instead of q_0^a to define the baryonic charge, which still satisfies $\sum_{a=1}^d \tilde{q}_0^a\, v_{ai} = p_i$, we would conclude that the baryonic charge vanishes.

We can now compare with field theory. For the case of the anti-twist the relevant field theory calculations were carried out already in [73]; here we also include the twist case. We consider the quiver gauge theory dual to $\mathrm{AdS}_5 \times T^{1,1}$, with rank N gauge groups. This gauge theory has $U(1)^3 \times U(1)_B$ symmetry where $U(1)_B$ is a baryonic symmetry associated with the kernel (5.37). We now put this gauge theory on a spindle with background magnetic fluxes, parametrized by $\mathfrak{p}_a$, for the $U(1)^3 \times U(1)_B$ symmetry. The trial central charge is parametrized by Δ_a and from the general result (5.20) we find (setting all r_a to $\frac{1}{2}$ for simplicity)

$$\begin{aligned} c_{\rm trial} = N^2 \Bigg\{ & 3\Big[\mathfrak{p}_1(\Delta_2\Delta_3 + \Delta_2\Delta_4 + \Delta_3\Delta_4) + \mathfrak{p}_2(\Delta_1\Delta_3 + \Delta_1\Delta_4 + \Delta_3\Delta_4) \\ & + \mathfrak{p}_3(\Delta_1\Delta_2 + \Delta_1\Delta_4 + \Delta_2\Delta_4) + \mathfrak{p}_4(\Delta_1\Delta_2 + \Delta_1\Delta_3 + \Delta_2\Delta_3)\Big] \\ & - \varepsilon\, \frac{3(m_- - \sigma m_+)}{4 m_- m_+}(\mathfrak{p}_1(2 - \Delta_1) + \mathfrak{p}_2(2 - \Delta_2) + \mathfrak{p}_3(2 - \Delta_3) + \mathfrak{p}_4(2 - \Delta_4)) \\ & - \varepsilon^2 \Big[\frac{9(m_- + \sigma m_+)(m_- - \sigma m_+)^2}{64 m_-^3 m_+^3} - \frac{3}{4}(\mathfrak{p}_1\mathfrak{p}_2\mathfrak{p}_3 + \mathfrak{p}_1\mathfrak{p}_2\mathfrak{p}_4 + \mathfrak{p}_1\mathfrak{p}_3\mathfrak{p}_4 + \mathfrak{p}_2\mathfrak{p}_3\mathfrak{p}_4)\Big] \Bigg\}\,. \end{aligned} \quad (5.46)$$

The on-shell central charge calculated in field theory is obtained by extremizing with respect to Δ_a and ε, subject to $\sum_a \Delta_a = 2$. We can do this in two steps, first extremizing over the baryonic direction defined by $q_1^a \Delta_a = \Delta_1 - \Delta_2 + \Delta_3 - \Delta_4$, and then over the remaining three independent variables, which can taken to be, for example, $\Delta_1, \Delta_2, \varepsilon$. After the first step we get $c_{\rm trial}|_{\rm baryonic}$ as a function of $\Delta_1, \Delta_2, \varepsilon$ and we find that there is an exact agreement with the off-shell gravitational charge $\mathscr{Z}$, as a function of b_0, b_2, b_3. The dictionary between the two sets of variables is as described in section 5.2.2:

$$b_0 \,=\, \varepsilon\,, \qquad \mathfrak{p}_a \,=\, \frac{M_a}{N}\,, \qquad \Delta_a^{\pm}|_{\rm baryonic} \,=\, R_a^{\pm}\,, \tag{5.47}$$

as well as identifying N on each side. Explicitly, for this example we find

$$\begin{aligned} b_2 &= \frac{1}{\mathfrak{p}_1+\mathfrak{p}_2}\left[2\mathfrak{p}_2 - (\mathfrak{p}_2+\mathfrak{p}_3)\,\Delta_1 + (\mathfrak{p}_1+\mathfrak{p}_4)\,\Delta_2\right] + \frac{1}{2}\,\varepsilon(\mathfrak{p}_2+\mathfrak{p}_3) \\ &\quad \frac{1}{4}\varepsilon\left(\frac{m_- - \sigma m_+}{m_+ m_-}\right)\frac{(-r_2\mathfrak{p}_1 + (r_1-2)\mathfrak{p}_2 + r_1\mathfrak{p}_3 - r_2\mathfrak{p}_4)}{\mathfrak{p}_1+\mathfrak{p}_2} - a_+ m_- \varepsilon(\mathfrak{p}_2+\mathfrak{p}_3)\,, \\ b_3 &= 2 - \Delta_1 - \Delta_2 + \frac{1}{2}\,\varepsilon(\mathfrak{p}_3+\mathfrak{p}_4) - \frac{1}{4}\,\varepsilon(r_3+r_4)\left(\frac{m_- - \sigma m_+}{m_+ m_-}\right) - a_+ m_- \varepsilon(\mathfrak{p}_3+\mathfrak{p}_4)\,. \end{aligned} \tag{5.48}$$

Notice that the dictionary involves the parameters a_+. Recall that a_+ is only defined up the transformation given in (4.24). Making this shift in (5.48), and using (5.42), induces a transformation on the vector (b_0, b_1, b_2, b_3) which is precisely given by the $SL(4,\mathbb{Z})$ transformation in (4.25) with $b_2 \to b_2 + \kappa p_2 b_0$ and $b_3 \to b_2 + \kappa p_3 b_0$.

Chapter 6

Holography - AdS_2 case

This last chapter is devoted to the exploration of the holographic matching in the case of the $AdS_2 \times Y_9$ solutions, with Y_9 a GK space, which correspond to the near horizon limit of black holes in AdS_4. We start by taking a step back and introducing the 3d field theories dual to such black holes in the case where the acceleration is set to zero, namely when the spindle Σ inside Y_9 is replaced by a smooth Riemann surface Σ_g. This case was already studied extensively [70,119,127] but here we provide a novel geometric construction, inspired by some observations made in the empty AdS_4 case [134–136], that allows to push further the holographic dictionary. We illustrate our findings with a couple of examples, both toric and non-toric, and suggest a generalization to the accelerating case in section 6.4. The main reference is [4].

6.1 3d $\mathcal{N} = 2$ Chern-Simons-matter theories

6.1.1 Geometric engineering

Let us start by reviewing how one can construct 3d $\mathcal{N} = 2$ worldvolume theories for M2-branes in backgrounds $\mathbb{R}^{1,2} \times C(X_7)$. This is well-understood in cases where $C(X_7)$ may be appropriately viewed as a fibration over a Calabi-Yau three-fold $C(X_5)$, and there is a corresponding interpretation in terms of D2-branes in type IIA string theory. We will focus on two simple examples which illustrate the general features, where both describe M2-branes in quotients of flat spacetime $\mathbb{R}^{1,2} \times \mathbb{C}^4/\mathbb{Z}_k$. We will then refer to these as primary examples for illustration throughout the remainder of this chapter.

6.1.1.1 Type IIA construction

We start by considering N D2-branes in the background $\mathbb{R}^{1,2} \times C(X_5) \times \mathbb{R}_t$, where $t \in \mathbb{R}$ parametrizes[1] the real line and $C(X_5)$ is a Calabi-Yau three-fold cone singularity. While $C(X_5)$ could be arbitrary, we will illustrate our results with two particularly simple examples, which we refer to as Model I and Model II:

$$\begin{aligned} \text{Model I}: \;& C(X_5)^{\text{I}} = \mathbb{C}^3 \,, \\ \text{Model II}: \;& C(X_5)^{\text{II}} = \{z_1 z_2 = z_3 z_4\} \subset \mathbb{C}^4 \,. \end{aligned} \tag{6.1}$$

Here $C(X_5)^{\text{II}}$ is the well-known conifold singularity with $X_5^{\text{II}} = T^{1,1}$, while the background for Model I is simply flat spacetime with $X_5^{\text{I}} = S^5$. The D2-branes are placed at the conical singularity (which is the origin of $\mathbb{C}^3$, $\mathbb{C}^4$, respectively, in the two models (6.1)), and the origin $t = 0$ of $\mathbb{R}_t$.

The low-energy effective theory on the D2-branes in the $\mathbb{R}^{1,2}$ directions is generically a 3d $\mathcal{N} = 2$ theory. When the singularity $C(X_5)$ admits a resolution to a smooth CY, this effective theory is expected to be described by a quiver gauge theory with superpotential W. For example, this will be the case if $C(X_5)$ is toric, where the gauge group may be taken to be $U(N)^{\mathscr{G}}$ where $\mathscr{G}$ is the Euler number of the CY resolution. For our two examples we have:

Model $\mathbf{I}_0$: $\mathcal{N} = 8$ $U(N)$ SYM. In $\mathcal{N} = 2$ language this is a $U(N)$ vector multiplet, together with three adjoint chiral fields Φ_i, $i = 1, 2, 3$, and superpotential $W = \text{Tr}\,(\Phi_3[\Phi_1, \Phi_2])$.

Model $\mathbf{II}_0$: Klebanov-Witten theory [19]. This is a $U(N)^2$ gauge theory, with bi-fundemental chiral fields A_i, B_i $(i = 1, 2)$, transforming in the $(\mathbf{N}, \overline{\mathbf{N}})$, $(\overline{\mathbf{N}}, \mathbf{N})$ representations, respectively, and superpotential $W = \text{Tr}\,(A_1 B_1 A_2 B_2 - A_1 B_2 A_2 B_1)$.[2]

To obtain the final models that we are interested in, we add two further ingredients:

[1] t is not to be confused with the time direction in $\mathbb{R}^{1,2}$, which will play no particular role here.
[2] The resolved conifold replaces the isolated singular point at the origin of $C(T^{1,1})$ with a copy of $\mathbb{CP}^1 = S^2$.

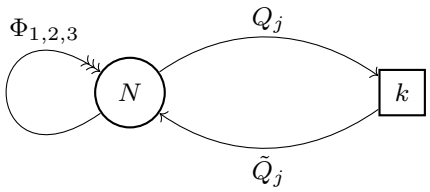


Figure 6.1: Quiver diagram for Model I: the ADHM theory.

D6-branes

We may add D6-branes to the above D2-brane set-up, without breaking any supersymmetry, provided these wrap divisors (complex codimension one submanifolds) in $C(X_5)$. From the low-energy D2-brane worldvolume perspective, this adds chiral matter fields in the fundamental/anti-fundamental representations, corresponding to massless strings stretching between the D2-branes and D6-branes [137, 138]. In particular, we define:

> **Model I**: ADHM theory. We add k pairs of fundamental/anti-fundamental chiral fields $(Q_j, \tilde{Q}_j)$, $j = 1, \ldots, k$ to Model I_0 above, with total superpotential
>
> $$W = \mathrm{Tr}\bigg(\Phi_3[\Phi_1, \Phi_2] + \sum_{j=1}^{k} \tilde{Q}_j \Phi_3 Q_j \bigg) . \tag{6.2}$$
>
> Physically, we added k D6-branes to the original background, located at $\{z_3 = 0\} \subset \mathbb{C}^3$, and at the origin $t = 0$ of $\mathbb{R}_t$. See figure 6.1 for the quiver.

Chern-Simons terms

We may instead add an $\mathcal{N} = 2$ Chern-Simons interaction for each $U(N)$ gauge group factor, proportional to the Chern-Simons levels $k_I \in \mathbb{Z}$, $I = 1, \ldots, \mathscr{G}$. As explained in [139], such Chern-Simons interactions may be induced (via the Wess-Zumino couplings on D-branes) by turning on Ramond-Ramond (RR) fluxes in the original D2-brane background, where the flux threads the various (collapsed) cycles in $C(X_5)$. We assume $\sum_{I=1}^{\mathscr{G}} k_I = 0$, so that the resulting backgrounds admit uplifts to M-theory [140]. For Model II_0 above this leads to:

> **Model II**: ABJM theory [13]. This is the same Model II_0 D2-brane analogue of the

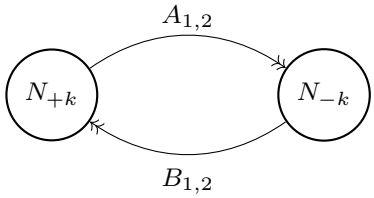


Figure 6.2: Quiver diagram for Model II: the ABJM theory.

Klebanov-Witten theory above, with superpotential

$$W = \mathrm{Tr}\left(A_1 B_1 A_2 B_2 - A_1 B_2 A_2 B_1\right), \tag{6.3}$$

but with Chern-Simons levels $(k_1, k_2) = (k, -k)$. This Chern-Simons coupling is induced by turning on k units of RR two-form flux through the (collapsed) $\mathbb{CP}^1$ at the conifold singularity. The quiver for this theory is shown in Figure 6.2.

More generally, given any $C(X_5)$ one could add D6-branes, introducing fundamental matter in the field theory, and also turn on RR two-form flux, inducing Chern-Simons couplings in the field theory. Both types of deformation fibre the M-theory circle S^1_M over the original type IIA spacetime. The uplifted M-theory solution is then $\mathbb{R}^{1,2} \times C(X_7)$, where $\mathcal{N} = 2$ supersymmetry fixes $C(X_7)$ to be a CY four-fold, with the M-theory circle necessarily complexified into $\mathbb{C}^*_M \equiv \mathbb{R}_t \times S^1_M$, and we may identify $C(X_5) = C(X_7)/\mathbb{C}^*_M$. Both of our models uplift to $\mathbb{R}^{1,2} \times \mathbb{C}^4/\mathbb{Z}_k$, with different $\mathbb{Z}_k$ quotients, as we describe in more detail in section 6.1.1.3.

6.1.1.2 Moduli space of vacua

The class of 3d $\mathcal{N} = 2$ field theories we have introduced have moduli spaces of vacua, and here we briefly comment on a couple of aspects of this which will be relevant for the rest of the chapter. A more complete discussion may be found in the original references [34, 137–139].

The Calabi-Yau geometry $C(X_7)$ probed by the M2-branes appears directly in their vacuum moduli spaces. More specifically, for a single brane that probes $C(X_7)$ as a pointlike object, and is free to move anywhere on $C(X_7)$, by definition $C(X_7)$ should appear as (a component of) the vacuum moduli space of the worldvolume field theory on that brane. Similarly, for N branes the vacuum moduli space should contain a copy of the symmetric product

of N copies of $C(X_7)$, *i.e.* $\mathrm{Sym}^N C(X_7)$. The main point we wish to emphasize here is that the branch of the vacuum moduli space which reproduces $\mathrm{Sym}^N C(X_7)$ has [34]

$$\sigma_1 = \sigma_2 = \cdots = \sigma_{\mathscr{G}} \,, \tag{6.4}$$

where σ_I is the vector multiplet scalar for the I-th gauge group factor in $U(N)^{\mathscr{G}}$. In particular, the matrices σ_I are forced to be diagonal and their N real eigenvalues σ_I^α, where $\alpha = 1, \ldots, N$, may be thought of as parametrizing the positions of the D2/M2-branes along the $\mathbb{R}_t$ direction.

Secondly, in 3d gauge theories one can introduce pointlike *monopole operators*, which by definition create magnetic flux for a gauge field through an S^2_{pt} surrounding that point. For M2-brane theories with gauge group $U(N)^{\mathscr{G}}$ an important role is played by the diagonal monopole operators $T^{(n)}$, which by definition create flux

$$\int_{S^2_{\mathrm{pt}}} \mathrm{Tr}\, F_I = n \in \mathbb{Z} \,, \quad I = 1, \ldots, \mathscr{G} \,. \tag{6.5}$$

Here F_I is the field strength for the I-th gauge field, and it is convenient to further define $T \equiv T^{(1)}$, $\tilde{T} \equiv T^{(-1)}$. In a Chern-Simons theory such monopole operators also carry electric charges under the gauge group. An alternative way to introduce $T, \tilde{T}$ is to first notice that in a quiver gauge theory nothing is charged under the diagonal $U(1)_{\mathrm{diag}} \subset U(N)^{\mathscr{G}}$. This Abelian gauge field may then be dualized to a periodic scalar field τ, with period $2\pi/\mathscr{G}$ [34]. The diagonal monopole operators may then be promoted to complex chiral fields by identifying $T = |T|\, \mathrm{e}^{\mathrm{i}\mathscr{G}\tau}$, $\tilde{T} = |\tilde{T}|\, \mathrm{e}^{-\mathrm{i}\mathscr{G}\tau}$ [137]. For theories without D6-branes, and hence without fundamental/anti-fundamental matter, such as Model II, one can describe the vacuum moduli space without introducing T, $\tilde{T}$;[3] However, for theories that contain fundamental/anti-fundamental matter, the charges of T, $\tilde{T}$ under both gauge and global symmetries in the quantum theory get anomalous contributions from fermion zero modes [137, 138]. The classical vacuum moduli space then gets corrected in the quantum theory, and one necessarily needs to introduce T, $\tilde{T}$ to describe the quantum-corrected moduli space. This leads to:

[3] One can introduce them, but they are immediately redundant, satisfying the trivial relation $T\tilde{T} = 1$.

Model I: The monopole operators satisfy the quantum F-term relation

$$T\tilde{T} = \Phi_3^k \,. \tag{6.6}$$

6.1.1.3 M-theory circle

As already mentioned, adding RR two-form flux and/or D6-branes to a type IIA spacetime fibres the M-theory circle S^1_M, resulting in a 11d spacetime of the form $\mathbb{R}^{1,2} \times C(X_7)$. Equivalently, one can start with the latter and a specific choice of M-theory circle, and then reduce to type IIA. In practice we may fix a Calabi-Yau four-fold $C(X_7)$ and pick a $U(1)_M$ action on it. The flow of the associated Killing vector ζ_M generates the M-theory circle action.

For our models of interest recall that $C(X_7) = \mathbb{C}^4/\mathbb{Z}_k$, where we denote standard complex coordinates on $\mathbb{C}^4$ by $z_a = |z_a|\mathrm{e}^{\mathrm{i}\phi_a}$, and the a-th copy of $\mathbb{C}$ is rotated by ∂_{ϕ_a} with weight one. The $\mathbb{Z}_k$ quotient is precisely along $\mathbb{Z}_k \subset U(1)_M$, but where the M-theory circle action depends on the model. Let us see this explicitly:

Model I: Recall that this theory adds the fundamental/anti-fundamental fields Q_j, $\tilde{Q}_j$, $j = 1, \ldots, k$, to the $\mathcal{N} = 8$ Maxwell theory. The branch of the *classical* vacuum moduli space where $Q_j = 0 = \tilde{Q}_j$ is identical to that for a D2-brane in flat spacetime, namely $\mathbb{C}^*_M \times \mathbb{C}^3$, which has the wrong topology.[4] However, as shown in [137], the quantum-corrected moduli space for this theory may be parametrized by the three complex scalars Φ_1, Φ_2, Φ_3, together with the diagonal monopole operators $T, \tilde{T}$, which recall satisfy the additional quantum constraint (6.6). The latter equation defines an $A_{k-1} = \mathbb{C}^2/\mathbb{Z}_k \subset \mathbb{C}^3$ singularity, where the $\mathbb{C}^3$ here has coordinates $(T, \tilde{T}, \Phi_3)$. We immediately see that the quantum vacuum moduli space is $C(X_7)^{\mathrm{I}} = \mathbb{C}^2/\mathbb{Z}_k \times \mathbb{C}^2$, with (Φ_1, Φ_2) parametrizing the second factor of $\mathbb{C}^2$. We may then identify

$$T = z_1^k \,, \quad \tilde{T} = z_2^k \,, \quad \Phi_1 = z_3 \,, \quad \Phi_2 = z_4 \,, \tag{6.7}$$

[4] There will be an additional "Higgs branch", where Q_j, $\tilde{Q}_j$ may obtain vacuum expectation values, but from the F-term equations $\mathrm{d}W = 0$ this can only happen where $\Phi_3 = 0$, which geometrically is then the D2-branes and D6-brane are coincident. This Higgs branch does not play any role in our discussion.

in terms of the standard coordinates z_a on $\mathbb{C}^4$. The operators above have charges

$$U(1)_M^{\mathrm{I}} : (1, -1, 0, 0)\,, \tag{6.8}$$

under the M-theory circle action $U(1)_M$. The $\mathbb{Z}_k$ quotient is precisely along $\mathbb{Z}_k^{\mathrm{I}} \subset U(1)_M^{\mathrm{I}}$, and we introduce the associated generating vector field $\zeta_M = \frac{1}{k}\,(\partial_{\phi_1} - \partial_{\phi_2})$, whose orbits are precisely the M-theory circles S_M^1 of the quotient. On the other hand, the fixed point set of the circle action $\{z_1 = z_2 = 0\}$ corresponds to the D6-brane locus in the type IIA spacetime.

Model II: There are no quantum corrections in this theory, and we may hence describe the vacuum moduli space without introducing T, $\tilde{T}$. In the Abelian $N = 1$ theory the superpotential W is zero, and the vacuum moduli space is hence parametrized by the four scalar fields

$$A_1 = z_1\,, \quad B_1 = z_2\,, \quad A_2 = z_3\,, \quad B_2 = z_4\,. \tag{6.9}$$

Nothing is charged under the $U(1)_{\mathrm{diag}} \subset U(1)^2$ diagonal gauge group, while we may identify the remaining $U(1)$ (to be concrete, the second $U(1)$ in $U(1)^2$) with the M-theory circle action. Thus the coordinates z_a on $\mathbb{C}^4$ have charges

$$U(1)_M^{\mathrm{II}} : (1, -1, 1, -1)\,. \tag{6.10}$$

The vacuum moduli space is then $C(X_7)^{\mathrm{II}} = \mathbb{C}^4/\mathbb{Z}_k^{\mathrm{II}}$, with the $\mathbb{Z}_k$ quotient along $\mathbb{Z}_k^{\mathrm{II}} \subset U(1)_M^{\mathrm{II}}$, and we correspondingly introduce the vector field $\zeta_M = \frac{1}{k}\,(\partial_{\phi_1} - \partial_{\phi_2} + \partial_{\phi_3} - \partial_{\phi_4})$. In this example the circle action is free, and hence there are no D6-branes. However Kaluza-Klein reduction along $U(1)_M^{\mathrm{II}}$ gives rise to RR fluxes corresponding to Chern Simons coupling in the field theory.

6.1.2 Topologically twisted matrix model

The class of 3d $\mathcal{N} = 2$ Chern-Simons-matter theories we have introduced may be put on $\Sigma_g \times S^1$ with a topological twist along Σ_g, preserving supersymmetry, where Σ_g is a Riemann surface of genus g.[5] The path integral of such a theory is called the topologically twisted index. In the following we review the localization of the latter, which leads to an effective matrix model description whose properties can be extracted in the large N limit. Our discussion follows the original references [56, 141, 142].

The topologically twisted index is a function of the chemical potentials associated to each $U(1)$ global symmetry of the theory as well as the magnetic fluxes of the corresponding background gauge fields. Given each $U(1)$ global symmetry can be though of as rotating a complex scalar by a phase, we can label these with the name of the scalar fields and call them respectively Δ_Φ and $\mathfrak{p}_\Phi$.[6] Such quantities are constrained by[7]

$$\sum_{\Phi \in W} \Delta_\Phi = 2\,, \qquad\qquad \sum_{\Phi \in W} \mathfrak{p}_\Phi = 2g - 2\,. \tag{6.11}$$

where the sum runs over the fields appearing in each monomial of the superpotential. We also introduce the chemical potential for the topological symmetry, which we call Δ_m. Note that formally the chemical potentials can be identified (up to a sign) with the trial R-charges of the same field theories on S^3 (see [4] for more details). This allows us to introduce two formal variables Δ_T and $\Delta_{\tilde{T}}$ associated to the diagonal monopole operators, which satisfy

$$\Delta_m = -\frac{1}{2}(\Delta_T - \Delta_{\tilde{T}})\,. \tag{6.12}$$

6.1.2.1 Localization on $\Sigma_g \times S^1$

The index can be evaluated *exactly* using supersymmetric localization [57]. That is, for BPS observables the path integral is exactly equal to a (finite-dimensional) integral over

[5] From the type IIA perspective, this is achieved by wrapping the D2-branes on Σ_g.

[6] These are the equivalent of Δ_a and $\mathfrak{p}_a$ in the 4d toric setting of section 5.2.1.

[7] Looking only at the constraint on the fugacities it appears that we could have $\sum_\Phi \Delta_\Phi = 2\ell$, $\ell \in \mathbb{Z}$ in general. However it as been argued in [143] that any $\ell \neq 1$ either does not give a consistent solution, or gives a solution related to the $\ell = 1$ solution by discrete symmetries.

certain supersymmetric field configurations, dressed by a one-loop determinant that captures fluctuations. Recall that $\mathcal{N} = 2$ theories have vector multiplets with fields $(A_\mu, \lambda, \sigma, D)$, where A_μ is the gauge field with curvature $F_{\mu\nu}$, λ is an adjoint-valued Dirac fermion, while σ, D are adjoint-valued scalars. The BPS configurations for an $\mathcal{N} = 2$ vector multiplet on $\Sigma_g \times S^1$, denoting the Σ_g directions with orthonormal frame directions e^1, e^2 and the S^1 with e^3, are such that $D = \mathrm{i}F_{12}$, $F_{13} = F_{23} = 0$, while σ and A_3 take constant values along S^1. The BPS moduli space is then characterized by the Cartan-valued variables

$$u = \beta(A_3 + \mathrm{i}\sigma)\,, \qquad \mathfrak{m} = \frac{1}{2\pi}\int_{\Sigma_g} F\,, \tag{6.13}$$

where β is the radius of the S^1 and the gauge magnetic fluxes $\mathfrak{m}$ take values in the co-root lattice of the gauge group. For each $U(N)$ factor in the gauge group, u takes the form of an $N \times N$ matrix, which can be diagonalized by a gauge transformation

$$u_I = \mathrm{diag}(u_I^1, \ldots, u_I^N)\,, \tag{6.14}$$

hence the full BPS moduli space is parametrized by the $\mathscr{G}$ sets of N eigenvalues u_I^α. The localized partition function can then be recast into a contour integral over u_I and a sum over $\mathfrak{m}$

$$Z(\Delta, \mathfrak{p}) = \sum_{\mathfrak{m}} \oint_{\mathcal{C}} Z_{\mathrm{int}}(u, \mathfrak{m}; \Delta, \mathfrak{p})\,. \tag{6.15}$$

We are not interested in the explicit form of the integrand at this stage. Deforming the contour and performing the sum in (6.15), the twisted index reduces to a contour integral with simple poles at $\mathrm{e}^{\mathrm{i}B_I^\alpha} - 1 = 0$ where $\mathrm{e}^{\mathrm{i}B_I^\alpha}$ depends on the field content; explicit rules to build this function can be found in [143]. The index is therefore given by a sum of residues evaluated at the solutions of the so-called Bethe ansatz equations (BAEs)

$$\mathrm{e}^{\mathrm{i}B_I^\alpha} = 1 \quad \Longrightarrow \quad B_I^\alpha + 2\pi n_I^\alpha = 0\,, \tag{6.16}$$

where the variables n_I^α parameterize the phase ambiguities, and are chosen in order to cancel long range forces [56]. Furthermore, the BAEs can be obtained as critical points of a function

known as the Bethe potential $\mathcal{U}$,

$$\text{BAEs}: \qquad \frac{\partial \mathcal{U}}{\partial u_I^\alpha} = 0\,. \tag{6.17}$$

In summary, this reformulates the problem of evaluating the index to the one of extremizing the Bethe potential.

6.1.2.2 The large N limit

In the large N limit, (6.17) can be solved numerically by taking the following ansatz for the eigenvalues, which is partly based on some analytical arguments and on the numerical simulations in [56],

$$u_I^\alpha = \mathrm{i}t^\alpha N^{1/2} + v_I^\alpha\,, \tag{6.18}$$

where t^α, v_I^α are real and taken to be $\mathcal{O}(1)$ in the large N limit. Notice that (6.18) may equivalently be written as

$$\mathrm{Im}\, u_1 = \cdots = \mathrm{Im}\, u_{\mathscr{G}} = \mathrm{diag}(t^1, \cdots, t^N) N^{1/2}\,. \tag{6.19}$$

Note this condition implies that $\sigma_1 = \cdots = \sigma_{\mathscr{G}}$, which is *precisely* the same condition that arises on the vacuum moduli space – see equation (6.4). This is a non-trivial statement: (6.19) describes the large N eigenvalue distribution of the field theory localized on $\Sigma_g \times S^1$, while (6.4) is a statement about the moduli space of the same field theory on flat spacetime $\mathbb{R}^{1,2}$. Recall that in the latter case we interpreted $\sigma_1 = \cdots = \sigma_{\mathscr{G}}$ as the position of the corresponding D2-branes in $\mathbb{R}_t$. We will return to this comment in section 6.3, when we come to interpret the large N saddle point distribution directly in the gravity dual.

The numerical simulations also show that the imaginary parts of the eigenvalues t^α become dense at large N, and are distributed over a finite interval $[t_{\min}, t_{\max}]$. We may order the eigenvalues using Weyl transformations so that t^α are increasing, and introduce the cor-

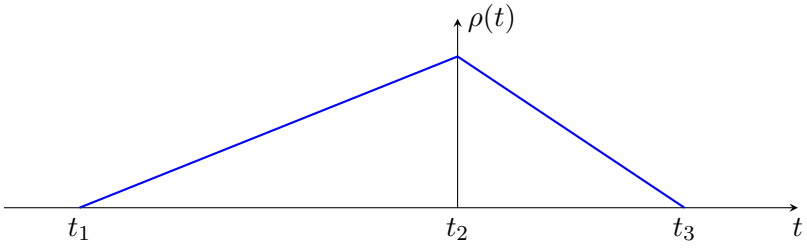


Figure 6.3: Schematic behaviour of the piecewise linear distribution of eigenvalues in the large N limit for the Model I ADHM theory.

responding (discrete) density function

$$\rho(t) = \frac{1}{N}\sum_{\alpha=1}^{N}\delta(t-t^{\alpha})\,, \qquad \int_{t_{\min}}^{t_{\max}} \mathrm{d}t\,\rho(t) = 1\,. \tag{6.20}$$

In the $N \to \infty$ limit the eigenvalues t^{α} become a continuous variable t, with continuous eigenvalue density $\rho(t)$. In particular (6.18) becomes a continuous function

$$u_I(t) = \mathrm{i}tN^{1/2} + v_I(t)\,. \tag{6.21}$$

In fact, the Bethe potential can be formulated in terms of $\rho(t)$ and $v_I(t)$, and the solutions of the BAEs are found by extremizing the potential with respect to these functions. Again there are rules, which can be found in [143], to build $\mathcal{U}$ in terms of these variables directly from the field content of the theory. The normalization of ρ is imposed via the introduction of a Lagrange multiplier μ, and the quantity to extremize is actually

$$\frac{\mathcal{U}}{\mathrm{i}N^{3/2}} - \pi\mu\left(\int \mathrm{d}t\,\rho(t) - 1\right)\,. \tag{6.22}$$

We now present the results of this extremization for model I and model II introduced before, which may be found in [144] and [56] respectively:

Model I: The chemical potentials satisfy the constraints

$$\sum_{i=1}^{3}\Delta_{\Phi_i} = 2\,, \quad \Delta_T + \Delta_{\tilde{T}} = k\Delta_{\Phi_3}\,, \tag{6.23}$$

leaving three independent. The first constraint is simply the superpotential one,

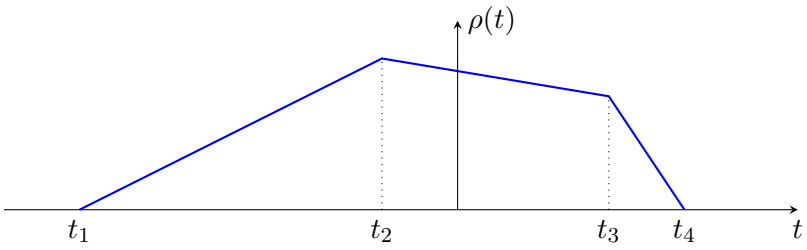


Figure 6.4: Schematic behaviour of the piecewise linear distribution of eigenvalues in the large N limit for the Model II ABJM theory.

where the W is given in (6.2), while the second constraint follows from (6.6). The saddle point eigenvalue density is

$$\rho(t) = \begin{cases} \dfrac{\mu + \Delta_{\tilde{T}} t}{\pi^2 \Delta_{\Phi_1} \Delta_{\Phi_2} \Delta_{\Phi_3}}\,, & t_{\min} < t < 0\,, \\ \dfrac{\mu - \Delta_T t}{\pi^2 \Delta_{\Phi_1} \Delta_{\Phi_2} \Delta_{\Phi_3}}\,, & 0 \leq t < t_{\max}\,, \end{cases} \tag{6.24}$$

where the endpoints are given by

$$t_{\min} = -\frac{\mu}{\Delta_{\tilde{T}}}\,, \qquad t_{\max} = \frac{\mu}{\Delta_T}\,, \tag{6.25}$$

and the extremal value of the Lagrange multiplier is

$$\mu = \pi \sqrt{\frac{2}{k} \Delta_{\Phi_1} \Delta_{\Phi_2} \Delta_T \Delta_{\tilde{T}}}\,. \tag{6.26}$$

In particular, for generic Δ's, $\rho(t)$ is linear in two regions (see figure 6.3).

Model II: The chemical potentials Δ_{A_i}, Δ_{B_i}, $i = 1, 2$, satisfy the single superpotential constraint

$$\Delta_{A_1} + \Delta_{B_1} + \Delta_{A_2} + \Delta_{B_2} = 2\,, \tag{6.27}$$

where W is given by (6.3). Without loss of generality, we may assume that $\Delta_{A_1} \leq$

Δ_{A_2}, $\Delta_{B_1} \leq \Delta_{B_2}$. One finds the following eigenvalue density

$$\rho(t) = \begin{cases} \frac{\mu + k\Delta_{B_1} t}{\pi^2(\Delta_{A_1}+\Delta_{B_1})(\Delta_{A_2}+\Delta_{B_1})(\Delta_{B_2}-\Delta_{B_1})}\,, & t_1 < t < t_2\,, \\ \frac{2\mu + k(\Delta_{B_1}\Delta_{B_2} - \Delta_{A_1}\Delta_{A_2})t}{\pi^2(\Delta_{A_1}+\Delta_{B_1})(\Delta_{A_1}+\Delta_{B_2})(\Delta_{A_2}+\Delta_{B_1})(\Delta_{A_2}+\Delta_{B_2})}\,, & t_2 < t < t_3\,, \\ \frac{\mu - k\Delta_{A_1} t}{\pi^2(\Delta_{A_1}+\Delta_{B_1})(\Delta_{A_1}+\Delta_{B_2})(\Delta_{A_2}-\Delta_{A_1})}\,, & t_3 < t < t_4\,. \end{cases} \tag{6.28}$$

which is linear in the three regions separated by

$$t_1 = -\frac{\mu}{k\Delta_{B_1}}\,, \quad t_2 = -\frac{\mu}{k\Delta_{B_2}}\,, \quad t_3 = \frac{\mu}{k\Delta_{A_2}}\,, \qquad t_4 = \frac{\mu}{k\Delta_{A_1}}\,, \tag{6.29}$$

where $t_{\min} = t_1 < t_2 < t_3 < t_4 = t_{\max}$, as depicted in figure 6.4. The extremal value of the Lagrange multiplier is

$$\mu = \pi\sqrt{2k\Delta_{A_1}\Delta_{A_2}\Delta_{B_1}\Delta_{B_2}}\,. \tag{6.30}$$

The free energy $F = -\log Z$ can also be computed directly from the Bethe potential evaluated on the BAEs solutions [143]

$$\log Z_{\Sigma_g \times S^1}(\Delta, \mathfrak{p}) = \frac{1}{\pi}\sum_{\Phi}\left[\mathfrak{p}_\Phi \frac{\partial \bar{\mathcal{U}}(\Delta)}{\partial \Delta_\Phi}\right], \tag{6.31}$$

$$\bar{\mathcal{U}}(\Delta) \equiv -\mathrm{i}\mathcal{U}|_{\mathrm{BAEs}} = \frac{2\pi\mu}{3}N^{3/2}\,, \tag{6.32}$$

where the sum runs over all the fields and monopole operators in the quiver. For our examples, this recovers some known results:

Model I

$$\log Z^{\mathrm{ADHM}}_{\Sigma_g \times S^1} = \frac{\pi}{3}\sqrt{\frac{2}{k}\Delta_{\Phi_1}\Delta_{\Phi_2}\Delta_T\Delta_{\tilde{T}}}\left(\frac{\mathfrak{p}_{\Phi_1}}{\Delta_{\Phi_1}} + \frac{\mathfrak{p}_{\Phi_2}}{\Delta_{\Phi_2}} + \frac{\mathfrak{p}_T}{\Delta_T} + \frac{\mathfrak{p}_{\tilde{T}}}{\Delta_{\tilde{T}}}\right)N^{3/2}\,, \tag{6.33}$$

and

$$\frac{2}{\pi}\bar{\mathcal{U}}(\Delta) = \frac{4\pi}{3}\sqrt{\frac{2}{k}\Delta_{\Phi_1}\Delta_{\Phi_2}\Delta_T\Delta_{\tilde{T}}}\,N^{3/2} = F^{\mathrm{ADHM}}_{S^3}\,. \tag{6.34}$$

Model II

$$\log Z^{\rm ABJM}_{\Sigma_g\times S^1} = \frac{\pi}{3}\sqrt{2k\Delta_{A_1}\Delta_{A_2}\Delta_{B_1}\Delta_{B_2}}\left(\frac{\mathfrak{p}_{A_1}}{\Delta_{A_1}}+\frac{\mathfrak{p}_{A_2}}{\Delta_{A_2}}+\frac{\mathfrak{p}_{B_1}}{\Delta_{B_1}}+\frac{\mathfrak{p}_{B_2}}{\Delta_{B_2}}\right)N^{3/2}\,, \quad (6.35)$$

and

$$\frac{2}{\pi}\bar{\mathcal{U}}(\Delta) = \frac{4\pi}{3}\sqrt{2k\Delta_{A_1}\Delta_{A_2}\Delta_{B_1}\Delta_{B_2}}N^{3/2} = F^{\rm ABJM}_{S^3}\,. \quad (6.36)$$

There are two things to notice here. First, the similarity of the expressions between the two models. This is easily understood from looking at the dual geometries which we will do in section 6.3.1. Second, that $\bar{\mathcal{U}}$ corresponds to the expression of the free energy on S^3 upon identifying the chemical potential with the R-charges, which has already been noted in [143]. There is no *a priori* reason for these quantities to be related from a purely field theoretic point of view. For some related discussion in the gravity dual, see [119].

Finally we shall also be interested in the expectation values of supersymmetric Wilson loop operators. Recall that a Wilson loop in a representation $\mathcal{R}$ is defined as

$$W_{\mathcal{R}} = {\rm Tr}_{\mathcal{R}}\mathcal{P}\exp\oint {\rm d}\tau\left({\rm i}A_\mu\dot{x}^\mu+\sigma|\dot{x}|\right). \quad (6.37)$$

The Wilson loop is supersymmetric when it wraps the S^1 direction [141]. It then reduces to $W_{\mathcal{R}} = {\rm Tr}_{\mathcal{R}}\exp({\rm i}u)$ with u defined in (6.13). The expectation value is obtained by inserting $W_{\mathcal{R}}$ into the path integral, and normalizing by a factor of $1/Z$. In the large N limit, the factors of the partition function simply cancel. Therefore, in the fundamental representation

$$\langle W_{\rm fund}\rangle = \sum_{I=1}^{\mathscr{G}}\sum_{\alpha=1}^{N} e^{{\rm i}u_I^\alpha} = N\sum_{I=1}^{\mathscr{G}}\int_{t_{\rm min}}^{t_{\rm max}}{\rm d}t\,\rho(t){\rm e}^{-N^{1/2}t+{\rm i}v_I(t)}\,, \quad (6.38)$$

such that at leading order in N

$$\log\langle W_{\rm fund}\rangle = -N^{1/2}t_{\rm min}\,. \quad (6.39)$$

6.2 Near-horizon geometry of non-accelerating black holes

In this section we briefly highlight some of the geometric features of M-theory backgrounds dual to 3d topologically twisted theories. The vacuum $\mathrm{AdS}_4 \times Y_7$ solutions, dual to the same 3d field theories placed on S^3 (the conformal boundary of global Euclidean AdS_4) were already discussed in the introduction 1.2.2. Here we consider inserting a (non-accelerating) magnetically charged black hole with horizon Σ_g into such a background. This is the gravity setting relevant for reproducing the topologically twisted index at large N discussed in section 6.1.2, as the conformal boundary with the insertion of a black hole becomes $\Sigma_g \times S^1$. The near-horizon geometry of such extremal black holes takes the form of $\mathrm{AdS}_2 \times Y_9$ as detailed in 1.2.3, with Y_9 a GK manifold. More specifically Y_9 here is the total space of a fibration such as (2.1), but with the spindle replaced with a Riemann surface Σ_g. Most of the relevant results for such setup can be obtained from their spindle equivalent as in chapters 2 and 3 by setting $m_\pm = 1$ and sending $b_0 \to 0$, however it is worth highlighting a few important points. The original references are [70, 119, 127].

6.2.1 Fibrations over Σ_g

As anticipated, we consider $\mathrm{AdS}_2 \times Y_9$ backgrounds as in (1.35) where Y_9 takes the fibered form

$$X_7 \hookrightarrow Y_9 \to \Sigma_g \,, \tag{6.40}$$

where X_7 is a manifold as in (1.8), albeit with a *a priori* generic Kähler two-form ω instead of the Sasakian ω_S. Differently from the spindle case, here the R-symmetry vector ξ is assumed to be tangent to X_7 since Σ_g does not have any abelian isometry, hence it can be parametrized using only the $U(1)$ isometry generators on the fibre, namely as in (1.11). Physically the fibration (6.40) may be achieved by turning on s $U(1)$ gauge fields A_i supported on Σ_g with integer magnetic fluxes

$$\frac{1}{2\pi}\int_{\Sigma_g} \mathrm{d}A_i = p_i \in \mathbb{Z} \,, \tag{6.41}$$

These are the equivalent of (2.7) and are identified with the magnetic charges of the black hole. The first directon $i = 1$ is singled out and the equivalent of (2.14) is now $p_1 = 2g - 2$.

We can relate explicitly some quantities in the GK geometry with quantities on the fibres X_7. Denoting $\tilde{\psi}$ as the one-form such that locally $\omega = \mathrm{d}\tilde{\psi}$, concretely the fibration amounts to replace

$$\tilde{\eta} \quad \to \quad \tilde{\eta}^{\mathrm{t}} \equiv \tilde{\eta}\,\big|_{\mathrm{d}\varphi_i \to \mathrm{d}\varphi_i + A_i}\,, \tag{6.42}$$

$$\tilde{\psi} \quad \to \quad \tilde{\psi}^{\mathrm{t}} \equiv \tilde{\psi}\,\big|_{\mathrm{d}\varphi_i \to \mathrm{d}\varphi_i + A_i} \tag{6.43}$$

where the superscript t stands for "twisted". One can show that for Y_9 as in (6.40) we have

$$\eta = \tilde{\eta}^{\mathrm{t}} + \text{basic}\,, \tag{6.44}$$

$$J = \mathrm{d}\tilde{\psi}^{\mathrm{t}} + A\,\mathrm{vol}_{\Sigma_g} + \text{basic exact}\,, \tag{6.45}$$

where we take the normalization to be $\int_{\Sigma_g} \mathrm{vol}_{\Sigma_g} = 1$, A is parametrizing the Kähler class of the Riemann surface, and "basic" here is with respect to the R-symmetry foliation $\mathcal{F}_\xi$. Note that the equation $\mathrm{d}\eta = \varrho$ at the cohomology level becomes

$$[\mathrm{d}\tilde{\eta}^{\mathrm{t}}] = [\varrho] \in H^2_B(\mathcal{F}_\xi)\,. \tag{6.46}$$

To summarize: we started from a manifold X_7 with $U(1)^s$ isometry, within which we picked an R-symmetry vector field ξ, parametrized in terms of b_i as in (1.11). Then we built the fibration (6.40) specified by some twisting parameters $p_i \in \mathbb{Z}$. The resulting manifold is a foliation defined by the above choice of ξ, which furthermore depends on the Kähler form of the transverse metric (6.45), which is unspecified up to this point.

6.2.2 Flavour twist

In the remainder of this chapter we will be interested in the "flavour twist" case only, which here amounts to imposing that the Kähler class of the fibre is proportional to its Ricci class

$$[\omega] = \Lambda\,[\tilde{\varrho}]\,. \tag{6.47}$$

The reason we impose this restriction is that this is the case which is under control from the holographic perspective, where a holographic matching of the free energy has been achieved [119, 127]. Note that the full Kähler class $[J]$ is now parameterized by two parameters only: A and Λ. For manifolds X_7 with no baryonic symmetries, *i.e.* $H^2(X_7,\mathbb{R}) = 0$ (such as S^7 and $\mathbb{Z}_k$ quotients thereof, as in our main examples), the condition (6.47) is automatically true.

As explained for the spindle in section 3.2.1, the geometric extremization procedure in the flavour twist case simplifies considerably. We will not go through the steps here but we remind that Kähler class parameter Λ can be obtained by imposing the flux quantization condition (1.29) through a 7-cycle coinciding with the fibre itself, resulting in

$$\Lambda = \frac{(2\pi\ell_p)^3}{\sqrt{24 b_1^3\,\mathrm{Vol}_S(X_7)}}\,N^{1/2}\,. \tag{6.48}$$

Then the remaining equations in (1.28) and (1.29) fix A, and put constraints on the remaining quantized fluxes $\mathcal{N}_\Upsilon$ in terms of the R-symmetry vector b_i and the flavour twisting parameters p_i, and eventually one obtains the trial black hole entropy, which we remind is

$$\mathscr{S}[\xi] = 4\sum_{i=1}^{s} p_i\,\frac{\partial}{\partial b_i}\,F_{\mathrm{grav}}[\xi]\,\Big|_{b_1=1}\,, \tag{6.49}$$

where $F_{\mathrm{grav}}[\xi]$ is the trial free energy (1.19) of the vacuum AdS_4 solution we started with.

Let us also remind that one can introduce the geometric R-charges R_a associated to 5d $U(1)^s$-invariant supersymmetric submanifolds in the fibres $S_a \subset X_7$, which in the flavour twist case are given by

$$R_a = \frac{2\pi}{3b_1}\,\frac{\mathrm{Vol}_S(S_a)}{\mathrm{Vol}_S(X_7)}\,, \tag{6.50}$$

with $R_a > 0$. Other relevant quantities associated to these submanifolds are the quantized

fluxes M_a that are obtained by considering the integral in (1.29) on fibrations $S_a \hookrightarrow \Sigma_a \to \Sigma_g$. These are non-vanishing even if $H_5(X_7, \mathbb{R}) = 0$, and are related to the geometric R-charges R_a via[8]

$$M_a = \frac{N}{2} \sum_{i=1}^{4} p_i \, \frac{\partial}{\partial b_i} \left(b_1 R_a \right) . \tag{6.51}$$

6.2.3 Example: $X_7 = S^7$

It is worth coming back to the example where the fibre X_7 is the 7-sphere S^7, which is the simplest example of the above geometry and will be the relevant one for the holography of model I and model II introduced in section 6.1.

The cone $C(S^7)$ in this case is simply $\mathbb{C}^4$, hence we can introduce four complex coordinates $z_a = |z_a| \mathrm{e}^{\mathrm{i}\phi_a}$, $a = 1, 2, 3, 4$, with ϕ_a having period 2π. The holomorphic form $\Psi_{(4,0)}$ is the standard one on $\mathbb{C}^4$

$$\Psi_{(4,0)} = \mathrm{d}z_1 \wedge \mathrm{d}z_2 \wedge \mathrm{d}z_3 \wedge \mathrm{d}z_4 . \tag{6.52}$$

The standard Kähler form for the flat metric on $\mathbb{C}^4$ is

$$\mathcal{J} = \frac{\mathrm{i}}{2} \sum_{a=1}^{4} \mathrm{d}z_a \wedge \mathrm{d}\bar{z}_a = \sum_{a=1}^{4} \mathrm{d}(\tfrac{1}{2}|z_a|^2) \wedge \mathrm{d}\phi_a = \sum_{a=1}^{4} \mathrm{d}y_a \wedge \mathrm{d}\phi_a , \tag{6.53}$$

where in the last step we introduced the coordinates $y_a = \frac{1}{2}|z_a|^2 \geq 0$. Note that the last form in (6.53) is still valid when we lift the Einstein condition on $\mathbb{C}^4$, though the coordinates y_a are defined differently.

The number of independent $U(1)$ isometries is clearly $s = 4$, hence there has to exist a linear change of variables relating the vector fields ∂_{ϕ_a} rotating the coordinates z_a with weight one with the general basis introduced in (1.11)

$$\partial_{\phi_a} = \sum_{i=1}^{4} v_{ai} \, \partial_{\varphi_i} , \tag{6.54}$$

where v_{ai} are 16 constants. Recalling that we require $\Psi_{(4,0)}$ to have charge one under ∂_{φ_1}

[8] Note how (6.51) can be obtained from (3.28) by setting $m_\pm = 1$ and sending $b_0 \to 0$.

and to be uncharged under the remaining ∂_{φ_i} we can read off

$$v_1 = (1,0,0,0)\,, \quad v_2 = (1,1,0,0)\,, \quad v_3 = (1,0,1,0)\,, \quad v_4 = (1,0,0,1)\,. \tag{6.55}$$

Recall that the Sasakian volume as a function of the R-symmetry vector is given by

$$\mathrm{Vol}_S(S^7) = \frac{\pi^4}{3b_2\,b_3\,b_4\,(b_1-b_2-b_3-b_4)}\,. \tag{6.56}$$

Setting $z_a = 0$ selects a copy of $\mathbb{C}^3 \subset \mathbb{C}^4$ which is the cone over the submanifold S_a. The corresponding Sasakian volumes are given by

$$\mathrm{Vol}_S(S_1) = \frac{\pi^3}{b_2\,b_3\,b_4}, \qquad \mathrm{Vol}_S(S_a) = \frac{\pi^3\,b_a}{b_2\,b_3\,b_4\,(b_1-b_2-b_3-b_4)}\,, \quad a=2,3,4\,. \tag{6.57}$$

From the quantities above we can directly read off the final results for the gravitational free energy of the AdS_4 solution (1.19), and the black hole entropy (6.49), the geometric R-charges (6.50), and the fluxes (6.51) through the submanifolds $\Sigma_a \subset Y_9$ of the AdS_2 solution

$$\begin{aligned}
F_{\mathrm{grav}} &= \frac{\pi}{3}\sqrt{2b_2\,b_3\,b_4\,(b_1-b_2-b_3-b_4)}\,N^{3/2}\,,\\
\mathscr{S} &= \frac{4\pi}{3}\,N^{3/2}\sum_{i=1}^{4} p_i\,\frac{\partial}{\partial b_i}\,\sqrt{2b_2\,b_3\,b_4\,(b_1-b_2-b_3-b_4)}\,,\\
R_1 &= \frac{2}{b_1}\,(b_1-b_2-b_3-b_4)\,, \qquad R_a = \frac{2b_a}{b_1}\,, \quad a=2,3,4\,,\\
M_1 &= N(p_1-p_2-p_3-p_4)\,, \qquad M_a = N\,p_a\,, \quad a=2,3,4\,.
\end{aligned} \tag{6.58}$$

Note that all of these can be obtained from the spindle equivalents in section 3.3.2 by setting $m_\pm = 1$ and sending $b_0 \to 0$. One should then set $b_1 = 1$ and extremize $\mathscr{S}$ in order to obtain the on-shell quantities. Note that we have

$$\sum_{a=1}^{4} R_a = 2\,, \qquad \sum_{a=1}^{4} M_a = (2g-2)N\,. \tag{6.59}$$

It is also convenient to give an expression for the R-symmetry vector in terms of the original

basis ∂_{ϕ_a}. One may check that

$$\xi = \frac{b_1}{2} \sum_{a=1}^{4} R_a \, \partial_{\phi_a} \, . \tag{6.60}$$

Using this expression to compute $\xi \lrcorner \mathcal{J}$ with both (6.53) and (1.9) we find that the radius in the coordinates $\{y_a\}$ is

$$r^2 = \sum_{a=1}^{4} R_a \, y_a \, . \tag{6.61}$$

Later we will be interested in $\mathbb{Z}_k$ quotients of the 7-sphere. This will be reviewed for the two main models of interest in section 6.3.1. However, at the level of the various quantities obtained via integration introduced above, the quotient simply amounts to adding a factor of $k \in \mathbb{Z}$ in the denominator of the volumes (6.56) and (6.57). Moreover, for later purposes it is useful to invert the relations (3.83) and express F_{grav} and $\mathscr{S}$ in terms of the geometric R-charges, so that eventually we have

$$F_{\text{grav}} = \frac{4\pi}{3} \sqrt{2kR_1R_2R_3R_4} \, N^{3/2} \, , \tag{6.62}$$

$$\mathscr{S} = \frac{\pi}{3} \sqrt{2kR_1R_2R_3R_4} \sum_{a=1}^{4} \frac{(M_a/N)}{R_a} N^{3/2} \, , \tag{6.63}$$

where we have already set $b_1 = 4$ in the former and $b_1 = 1$ in the latter. Finally, let us also give an expression for the Kähler class parameter (6.48) in the flavour twist as we will need it many times later

$$\Lambda = \frac{\pi \ell_p^3 \, N^{1/2}}{2} \sqrt{2kR_1R_2R_3R_4} \, . \tag{6.64}$$

6.3 Matrix model geometry

The topologically twisted matrix models described in section 6.1 are dual to the black hole near-horizon geometries presented in section 6.2. Here we make a precise identification of various quantities on both sides of this duality. We start in section 6.3.1 by reviewing the matching between chemical potentials and geometric R-charges, and the free energy with the entropy. In section 6.3.2 then we introduce the M-theory Hamiltonian function, which allows us to give a further geometrical interpretation of the matrix model, in particular its eigenvalue density discussed in section 6.3.3. The relation to probe M2-branes wrapping the

M-theory circle, and their Wilson loop duals, is described in section 6.3.4. Along the way we describe the general matching for any cone $C(X_7)$, but illustrate with our two examples where $C(X_7) = \mathbb{C}^4/\mathbb{Z}_k$; further examples will be discussed in the toric context in section 6.5.

6.3.1 Holography of free energies and R-charges

As already discussed in section 6.1.1.3, given any M-theory solution we may in principle make different choices of M-theory circle $U(1) \equiv U(1)_M$ acting on the spacetime, and reduce in different ways to type IIA. Starting with a given $\mathrm{AdS}_2 \times Y_9$ background, with Y_9 a fibration as in (6.40), different choices of M-theory circle acting on X_7 lead to different field theories on $\Sigma_g \times S^1$. Our principal examples of this are Models I and II, which are both dual to M-theory geometries with $X_7 = S^7/\mathbb{Z}_k$, but with $U(1)_M$ actions given in (6.8) and (6.10) respectively, where the $\mathbb{Z}_k$ quotient is taken along the corresponding M-theory circle.

Having fixed a particular GK geometry and choice of M-theory circle, and hence a choice of UV field theory on $\Sigma_g \times S^1$, we would like to identify variables on each side of the duality. From a geometric engineering point of view, baryonic operators arise from M5-branes wrapping five-dimensional submanifolds $S_\Phi \subset Y_7$. The R-charge of the corresponding field is given in term of $\mathrm{Vol}_S(S_\Phi)$ in the same way we defined the geometrical R-charges in (6.50);[9] this was first studied in the D3-brane holographic context in [145]. Hence we are led to identify

$$\Delta_\Phi = R_\Phi \,. \tag{6.65}$$

Similarly, the field theory fluxes $\mathfrak{p}_\Phi$ are related in the same way to the geometrical fluxes

$$\mathfrak{p}_\Phi = \frac{M(S_\Phi)}{N} \,, \tag{6.66}$$

where $M(S_\Phi)$ is the quantized flux through $S_\Phi \hookrightarrow \Sigma_\Phi \to \Sigma_g$, which is computed via (6.51).

Let us illustrate this for our two models:

Model I: The identifications (6.7) give the relation between the fields in this model

[9] The distinction between S_Φ and S_a is motivated by the fact that in some examples the choice we make in gravity for the S_a does not directly correspond to the S_Φ associated to physical operators but rather to linear combinations thereof. Correspondingly, the same will be true for any other associated quantity *e.g.* R_Φ vs R_a.

and the divisors on $\mathbb{C}^4/\mathbb{Z}_k$. In this case, the submanifolds S_Φ directly correspond to (multiples of) S_a (recall the latter are defined by $\{z_a = 0\}$). Substituting this into (6.65) gives the identifications

$$\Delta_T = kR_1\,, \quad \Delta_{\tilde{T}} = kR_2\,, \quad \Delta_{\Phi_1} = R_3\,, \quad \Delta_{\Phi_2} = R_4\,, \tag{6.67}$$

$$\mathfrak{p}_T = k\,\frac{M_1}{N}\,, \quad \mathfrak{p}_{\tilde{T}} = k\,\frac{M_2}{N}\,, \quad \mathfrak{p}_{\Phi_1} = \frac{M_3}{N}\,, \quad \mathfrak{p}_{\Phi_2} = \frac{M_4}{N}\,. \tag{6.68}$$

Model II: We may again use (6.65) together with the identifications (6.9) to deduce the mapping

$$\Delta_{A_1} = R_1\,, \quad \Delta_{B_1} = R_2\,, \quad \Delta_{A_2} = R_3\,, \quad \Delta_{B_2} = R_4\,, \tag{6.69}$$

$$\mathfrak{p}_{A_1} = \frac{M_1}{N}\,, \quad \mathfrak{p}_{B_1} = \frac{M_2}{N}\,, \quad \mathfrak{p}_{A_2} = \frac{M_3}{N}\,, \quad \mathfrak{p}_{B_2} = \frac{M_4}{N}\,. \tag{6.70}$$

Having made these identifications allows one to then match other physical quantities on both sides of the correspondence. In particular minus the free energy of the field theory on $\Sigma_g \times S^1$ reproduces the entropy $\mathscr{S}$:

$$\log Z_{\Sigma_g \times S^1}[\Delta, \mathfrak{p}] = \mathscr{S}[R, M]\,. \tag{6.71}$$

The matching (6.71) has been verified in multiple examples [56, 119, 127], and is particularly straightforward to see in our main examples. For Model I, using the dictionary (6.67)–(6.68), $\log Z$ in (6.33) matches the entropy (6.63) on S^7. Likewise for Model II, the dictionary (6.69)–(6.70) relates (6.35) with (6.63). In a similar fashion, a well-known matching is that of the free energy on S^3 with F_{grav}, which can be observed explicitly for both models as (6.36) and (6.34) match with (6.62). Interestingly F_{S^3} and F_{grav} are proportional to μ and Λ respectively, such that a direct consequence of their matching is

$$\Lambda = \frac{\ell_p^3 N^{1/2}}{2}\mu\,, \tag{6.72}$$

which is indeed what we observe by comparing (6.64) with (6.26) and (6.30).

6.3.2 M-theory circle moment map

Our aim here is to provide a geometric interpretation of the matrix model described in section 6.1.2.2, or more precisely the large N saddle point distribution. To this end, we start by identifying the variable t from a geometric perspective in M-theory.

Recall that, in the large N limit, the variable t corresponds to the continuum limit of the imaginary parts of the eigenvalues in (6.18). On the other hand, before taking the large N limit the eigenvalues t^α, $\alpha = 1, \ldots, N$, are simply defined as the values of the scalars σ^α (up to an overall proportionality constant). Physically the VEVs of the scalars σ^α also parametrize the position of the N D2-branes in the $\mathbb{R}_t$ direction, as described in section 6.1.1.2. Via this chain of identifications, it is natural to conclude that the matrix model variable t should be related to the coordinate parametrizing $\mathbb{R}_t$ in the type IIA construction. The aim of the rest of this section will be to make this statement precise.

Let us start by considering the uplifted geometry in M-theory without the branes' back-reaction. Recall from section 6.1.1.3 that the Killing vector ζ_M by definition generates the $U(1)_M$ isometry of the M-theory circle action. This $U(1)_M$ action is Hamiltonian on $C(X_7)$, namely there exists a function $\mu_M \colon C(X_7) \to \mathbb{R}$, called the moment map, such that

$$\mathrm{d}\mu_M = -\,\zeta_M \lrcorner\, \mathcal{J}\,, \tag{6.73}$$

where $\mathcal{J}$ is the original Kähler form on $C(X_7)$. The crucial point is that the image of μ_M is precisely identified with the $\mathbb{R}_t$ direction. In fact, from a physical perspective, the D-term equations that fix the VEVs of σ^α (*i.e.* the position of the M2-branes along $\mathbb{R}_t$), correspond geometrically to fixing level sets of the moment map [34]!

Let us illustrate this in the two examples with $C(X_7) = \mathbb{C}^4/\mathbb{Z}_k$. We will focus on the Abelian case ($N = 1$), where note that the Kähler form is given in (6.53).

Model I: From (6.8) we recall that the M-theory circle is given by $\zeta^{\mathrm{I}}_M = \frac{1}{k}\,(\partial_{\phi_1} - \partial_{\phi_2})$. Hence, using the definition (6.73), the moment map in this case is simply

$$\mu^{\mathrm{I}}_M(z_a) = \frac{1}{2k}\left(|z_1|^2 - |z_2|^2\right). \tag{6.74}$$

On the other hand the D-term equation for $k = 1$ reads [137]

$$|T|^2 - |\tilde{T}|^2 = \frac{\sigma}{2\pi}\,, \tag{6.75}$$

and hence from the identifications in (6.7) we can see that the D-term equation for $k = 1$ can be expressed as[10]

$$\mu_M^{\rm I}(z_a) = \frac{\sigma}{\pi}\,. \tag{6.76}$$

Model II: Here, the M-theory circle is in (6.10) and reads $\zeta_M^{\rm II} = \frac{1}{k}\left(\partial_{\phi_1} - \partial_{\phi_2} + \partial_{\phi_3} - \partial_{\phi_4}\right)$. From (6.73) we then read the moment map

$$\mu_M^{\rm II}(z_a) = \frac{1}{2k}\left(|z_1|^2 - |z_2|^2 + |z_3|^2 - |z_4|^2\right). \tag{6.77}$$

The D-term equation for this theory is [13]

$$\frac{1}{k}\left(|A_1|^2 - |B_1|^2 + |A_2|^2 - |B_2|^2\right) = \frac{\sigma}{2\pi}\,. \tag{6.78}$$

From the identifications (6.9) it follows that the D-term equation is again

$$\mu_M^{\rm II}(z_a) = \frac{\sigma}{\pi}\,. \tag{6.79}$$

Our claim is that this picture is "preserved", in a sense that we will specify momentarily, when taking the large N limit in field theory and the near-horizon limit in gravity.

As explained in section 6.1.2.2, in field theory the eigenvalues u_I^α in the large N limit become infinite in number, and continuously distributed, with their imaginary part parametrized by the real variable t which takes values in a finite interval $[t_{\rm min}, t_{\rm max}]$. Moreover, this interval is divided into a certain number of subintervals, on each of which the eigenvalue density $\rho(t)$ is linear; in particular $\rho'(t)$ is discontinuous at the endpoints of each subinterval. The gravity duals are described by the $\mathrm{AdS}_2 \times Y_9$ backgrounds in M-theory described in section 1.2.3. In

[10]Recall that $\mathbb{C}^2/\mathbb{Z}_k \subset \mathbb{C}^4/\mathbb{Z}_k = C(X_7)$ is realized via the embedded equation $T\tilde{T} = \Phi_3^k$ in $\mathbb{C}^3$ (6.6). This means that for $k > 1$ we cannot identify T, $\tilde{T}$ with the coordinates z_1, z_2 on the covering space $\mathbb{C}^2$ of $\mathbb{C}^2/\mathbb{Z}_k$, and correspondingly the classical metric on the field theory moduli space is different from the spacetime metric. However, these comments are only meant to motivate the precise identifications later.

this context, the $U(1)_M$ action on the fibre X_7 is still Hamiltonian, and hence we can define another moment map h_M (now regarded as a function on X_7) via

$$\mathrm{d}h_M = -\,\zeta_M \lrcorner\, \omega\,. \tag{6.80}$$

Recall here that ω is the transverse Kähler form on X_7, and in the flavour twist case this is given by (6.47). From (1.9) and the fact that $\mathrm{d}\tilde{\eta} = \tilde{\varrho}$ it follows that, for the flavour twist case

$$h_M = 2\Lambda\, \mu_M \big|_{r=1} = \Lambda\, \zeta_M \lrcorner\, \tilde{\eta}\,, \tag{6.81}$$

where μ_M is the moment map on the cone $C(X_7)$ introduced above in (6.73). Since h_M is a continuous real function defined on a compact space, its image is an interval

$$h_M(X_7) = [\tau_{\min}, \tau_{\max}] \subset \mathbb{R}\,. \tag{6.82}$$

The function h_M is defined on X_7, rather than directly on a Kähler manifold (which is instead here a transverse Kähler structure), but nevertheless it is straightforward to import some standard results from the symplectic geometry literature (see *e.g.* [146]). Similar reasoning was used in [135]. First, the interval in (6.82) is divided into subintervals whose boundaries are given by the images of the critical points of the moment map, so $\{\mathrm{d}h_M = 0\}$. In turn these are precisely the loci where ζ_M is aligned with the Reeb vector field ξ, so that along such a locus $\zeta_M \lrcorner\, \tilde{\eta}$ is a constant. This includes the special case where ζ_M is zero, which are fixed point sets signalling the presence of D6-branes. We shall return to what distinguishes these subintervals geometrically in the next subsection, while the relation of these points with physical observables will be discussed in section 6.3.4.

We conclude that there must be a holographic map between the field theory variable t and the geometry variable τ parametrizing the image of the moment map. In particular, from the examples we are going to consider shortly and later in section 6.5, we find the precise identification is

$$\tau = \ell_p^3 N^{1/2}\, t\,. \tag{6.83}$$

Let us once again illustrate how this works concretely for the examples with $C(X_7) = \mathbb{C}^4/\mathbb{Z}_k$ *i.e.* $X_7 = S^7/\mathbb{Z}_k$. Recall the radial coordinate on the cone is given by (6.61)

$$r^2 = \sum_{a=1}^{4} R_a \, y_a \, , \tag{6.84}$$

with $y_a \geq 0$. Note that when $R_a = \frac{1}{2}$ for all $a = 1, 2, 3, 4$ we recover the usual radius for a round 7-sphere. Setting $r^2 = 1$ constrains the possible values of y_a, in particular

$$0 \leq y_a \leq \frac{1}{R_a} \, . \tag{6.85}$$

Model I: The moment map on $S^7/\mathbb{Z}_k$ is given by

$$h_M^{\mathrm{I}} = \frac{2\Lambda}{k} \left(y_1 - y_2 \right) \big|_{r^2=1} \, , \tag{6.86}$$

whose image is clearly

$$h_M^{\mathrm{I}}(S^7/Z_k) = \left[-\frac{2\Lambda}{kR_2}, \, \frac{2\Lambda}{kR_1} \right] \, . \tag{6.87}$$

Using (6.64) for the Kähler class parameter, this precisely maps to the interval $[t_{\min}, t_{\max}]$ with extrema (6.25) via (6.83) and the identification among the R-charges (6.67). Moreover, the only other fixed point locus of the $U(1)_M$ action on $S^7/\mathbb{Z}_k$ is $\{z_1 = z_2 = 0 = y_1 = y_2\}$ which reproduces the point $t = 0$, arising from the D6-brane insertion.

Model II: Here we solve the constraint $r^2 = 1$ for one of the coordinates and substitute it back into the moment map. In order to obtain $\tau_{\min}$ it is convenient to solve for y_4, so that

$$h_M^{\mathrm{II}}(y_a) = \frac{2\Lambda}{k} \left[\left(1 + \frac{R_1}{R_4} \right) y_1 - \left(1 - \frac{R_2}{R_4} \right) y_2 + \left(1 + \frac{R_3}{R_4} \right) y_3 \; - \frac{1}{R_4} \right]. \tag{6.88}$$

In field theory we assumed a particular ordering for the chemical potentials which must be mirrored here: $R_1 \leq R_3$ and $R_2 \leq R_4$. As a consequence the coefficient

of y_2 in the expression above is negative, and it is then clear that the minimum of $h_M^{\rm II}(y_a)$ is achieved when

$$y_1 = y_3 = 0\,, \quad y_2 = \frac{1}{R_2} \quad \Longrightarrow \quad \tau_1 \equiv \tau_{\rm min} = -\frac{2\Lambda}{kR_2}\,. \tag{6.89}$$

Similarly, solving for y_3 it is easy to obtain the maximum

$$\tau_4 \equiv \tau_{\rm max} = \frac{2\Lambda}{kR_1}\,. \tag{6.90}$$

Notice that, as explained in general above, $\tau_{\rm min}$ and $\tau_{\rm max}$ are images of loci where ζ_M is aligned with the R-symmetry vector ξ, specifically here where $\{z_1 = z_3 = z_4 = 0\}$ and $\{z_2 = z_3 = z_4 = 0\}$. Indeed, there are other two such loci/image points:

$$\{z_1 = z_2 = z_3 = 0\} \quad \Longrightarrow \quad \tau_2 = -\frac{2\Lambda}{kR_4}\,, \tag{6.91}$$

$$\{z_1 = z_2 = z_4 = 0\} \quad \Longrightarrow \quad \tau_3 = \frac{2\Lambda}{kR_3}\,. \tag{6.92}$$

By virtue of (6.72), (6.69), and (6.83), τ_1, τ_2, τ_3, τ_4 are matched with (6.29).

6.3.3 Eigenvalue density from geometry

Above we identified the variable t in field theory as the value of the moment map associated to the M-theory circle action. We can actually do better and provide a prescription to compute the full eigenvalue density function of the matrix model $\rho(t)$ from the geometry of the near-horizon dual. Note that for a certain set of $\mathrm{AdS}_4 \times X_7$ geometries with toric X_7 some results concerning this very same matter were already found in the past – see appendix C of [134] and section 3.6 of [135]. However, here we will give a much more complete picture which works off-shell and in principle also for non-toric X_7.

We start by using the moment map h_M defined in (6.81) to build a 5d space out of the fibre X_7, by restricting to the level set $h_M^{-1}(\tau) \subset X_7$ and then quotienting by the M-theory circle action

$$X_\tau \equiv h_M^{-1}(\tau)/U(1)_M\,. \tag{6.93}$$

In the special case when X_7 is quasi-regular, namely that $b_i \in \mathbb{Q}$ for all $i = 1, \ldots, s$, so that the orbits of the R-symmetry vector close, X_τ has a particular structure which derives from the following mathematical construction. We first introduce the 6d Kähler base space K_6 obtained by quotienting

$$K_6 \equiv Y_7/U(1)_\xi \,. \tag{6.94}$$

Note that this quotient would be very badly behaved if we did not assume $b_i \in \mathbb{Q}$, because the generic orbits of ξ would then be open. In passing, let us highlight that the critical points of h_M which delimit the subintervals in the image $h_M(X_7)$ correspond precisely to the fixed points of the $U(1)_M$ action on K_6; indeed these are either fixed points on X_7 itself, which are related to D6-brane insertions, or points where ζ_M is aligned with ξ in the ambient space X_7, as in such a situation the former projects to zero in the quotient above. Given that the moment map h_M is independent of ξ, it can be thought as a function on K_6. We can then consider introducing a 4d subspace $K_\tau \subset K_6$ as a symplectic quotient with Fayet-Iliopoulos parameter τ

$$K_\tau \equiv K_6 /\!\!/ U(1)_M \,, \tag{6.95}$$

and by construction K_τ is itself a Kähler space with a Kähler form ω_τ that is inherited from the original ω on K_6. Finally, we restore the $U(1)_\xi$ direction by building the fibration $S^1_\xi \hookrightarrow X_\tau \to K_\tau$.

The induced Kähler class $[\omega_\tau]$ depends linearly on τ, with a different slope in each of the subintervals in the image of h_M delimited by the $U(1)_M$ fixed points [146]; therefore it is quite natural to relate it with $\rho(t)$. Our precise claim is that

$$\rho(t) \propto \frac{\mathrm{d}}{\mathrm{d}\Lambda} \int_{Y_\tau} \eta \wedge \frac{\omega_\tau^2}{2} \bigg|_{\tau = \ell_p^3 N^{1/2}\, t} = \frac{\mathrm{d}}{\mathrm{d}\Lambda} \mathrm{Vol}(X_\tau) \bigg|_{\tau = \ell_p^3 N^{1/2}\, t} . \tag{6.96}$$

The normalization constant is then fixed by requiring $\rho(t)$ to integrate to 1. Finally, in order for the construction above to make sense even when X_7 is irregular ($b_i \notin \mathbb{Q}$), we note that $\mathrm{Vol}(X_\tau)$ depends continuously on the R-symmetry vector b_i, hence its expression can be extended to the general case by continuity.

Next, we will illustrate the above in the two examples with $X_7 = S^7/\mathbb{Z}_k$, but first let

us comment on how to go about computing the volume $\mathrm{Vol}(X_\tau)$. For toric X_7 it is quite straightforward and we will provide a general recipe later in section 6.5. In general, without further assumptions on the geometry of X_7, it may be difficult to produce closed form expressions. We envisage that an approach based on a fixed point formula, such as that in [147], could however be effective.

For $X_7 = S^7/\mathbb{Z}_k$ we use the coordinates $\{y_a, \phi_a\}$ introduced in section 6.2.3. Modulo angles, the space X_τ is described by imposing both $r^2 = 1$ and $h_M(y_a) = \tau$ which result in the two linear equations describing hyperplanes in $\mathbb{R}^4$. Recalling that r^2 is given by (6.84) and that $y_a \geq 0$, the former equation actually defines a tetrahedron with vertices

$$p_a = \frac{1}{R_a}\, e_a \,, \tag{6.97}$$

where e_a is the standard orthonormal basis on $\mathbb{R}^4$. Imposing the moment map level set equation then amounts to slicing this tetrahedron with a hyperplane. The intersection of the two will be a 2d polygon Q_τ, particularly either a triangle or a quadrilateral. For the flavour twist, by definition the following cohomological relation holds

$$[\omega] = \Lambda[\mathrm{d}\tilde{\eta}] = 2\Lambda[\omega_S] \,. \tag{6.98}$$

From (6.53) one can see that the measure induced via ω_S is simply the standard Euclidean measure on $\mathbb{R}^4$ (times a factor k^{-1} which comes from the $\mathbb{Z}_k$ quotient), and correspondingly ω induces $(2\Lambda)^4$ times the Euclidean volume form. It follows that

$$\mathrm{Vol}(X_\tau) = \frac{(2\pi)^3}{k}\,(2\Lambda)^2\,\mathrm{Vol}_E(Q_\tau) \,, \tag{6.99}$$

where Vol_E denotes the Euclidean volume, and the factor $(2\pi)^3$ comes from integrating over the angles.

Let us also introduce a notation for the vectors orthogonal to the two hyperplanes, which are nothing but ξ and ζ_M in coordinates. The former is

$$\boldsymbol{\xi} = \frac{1}{2}\,(R_1, R_2, R_3, R_4) \,, \tag{6.100}$$

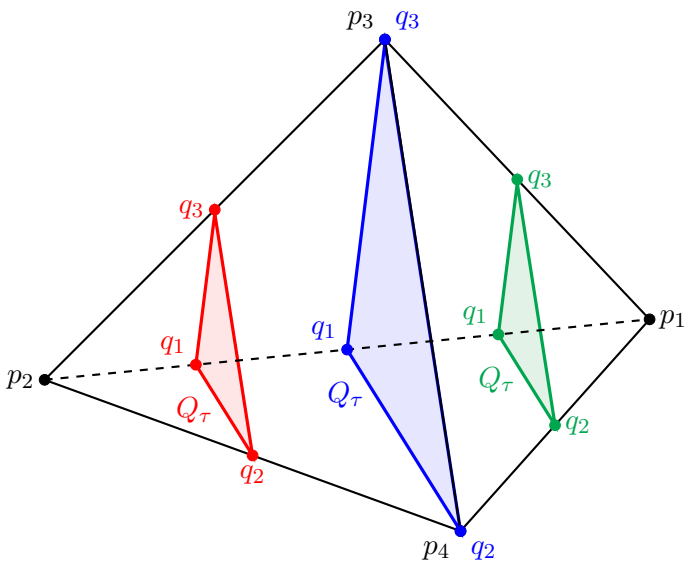


Figure 6.5: Tetrahedron describing S^7 and its slicing corresponding to Model I – ADHM theory. The red slice is for $\tau_{\min} < \tau < 0$, blue slice for $\tau = 0$, and green slice for $0 < \tau < \tau_{\max}$. The perimeter of Q_τ varies with τ qualitatively as ρ in Figure 6.3.

while the latter will depend upon the model we are considering and we will denote it by $\boldsymbol{\zeta}$. It will also be useful to introduce a name for the component of $\boldsymbol{\zeta}$ orthogonal to $\boldsymbol{\xi}$, namely

$$\boldsymbol{\zeta}_\perp \equiv \boldsymbol{\zeta} - \frac{\boldsymbol{\zeta}\cdot\boldsymbol{\xi}}{|\boldsymbol{\xi}|^2}\,\boldsymbol{\xi}\,. \tag{6.101}$$

In both Model Iand II, it turns out the properly normalized $\rho(t)$ is given in gravity by

$$\rho(t) = \frac{1}{32\pi^5 \ell_p^3 N^{1/2}\,|\boldsymbol{\xi}||\boldsymbol{\zeta}_\perp|}\,\frac{\mathrm{d}}{\mathrm{d}\Lambda}\,\mathrm{Vol}(Y_\tau)\Big|_{\tau=\ell_p^3 N^{1/2}\,t}\,. \tag{6.102}$$

Model I: The hyperplane described by the level set equation of the M-theory circle moment map in (6.86) satisfies the equation

$$y_1 - y_2 = \frac{k}{2\Lambda}\,\tau\,, \tag{6.103}$$

with $-\frac{2\Lambda}{kR_2} \le \tau \le \frac{2\Lambda}{kR_1}$, and the vector $\boldsymbol{\zeta}$ is

$$\boldsymbol{\zeta} = \frac{1}{k}\,(1,-1,0,0)\,. \tag{6.104}$$

Note that for $\tau = 0$, both vertices p_3 and p_4 of the tetrahedron belong to $Q_{\tau=0}$, therefore the hyperplane (6.103) is parallel to one of the edges of the tetrahedron. So Q_τ is always a triangle but we have to compute $\mathrm{Vol}_E(Q_\tau)$ separately for $\tau < 0$ and $\tau > 0$, which corresponds to the two subintervals of the image of h_M^{I} that we identified in the previous section (see Figure 6.5). Let us start with $\tau < 0$. By standard linear algebra, one can find that the vertices of Q_τ are

$$\begin{aligned} q_1 &= \left(\frac{2\Lambda + kR_2\tau}{2\Lambda(R_1+R_2)}, \frac{2\Lambda - kR_1\tau}{2\Lambda(R_1+R_2)}, 0, 0 \right), \\ q_2 &= \left(0, -\frac{k\tau}{2\Lambda}, \frac{2\Lambda + kR_2\tau}{2\Lambda R_3}, 0 \right), \\ q_3 &= \left(0, -\frac{k\tau}{2\Lambda}, 0, \frac{2\Lambda + kR_2\tau}{2\Lambda R_4} \right). \end{aligned} \tag{6.105}$$

Given that $\boldsymbol{\xi}$ and $\boldsymbol{\zeta}_\perp$ are both orthogonal to the plane where Q_τ lies, the volume of Q_τ can be related to the volume of the 4d parallelotope whose edges are the aforementioned vectors plus two of the edges of Q_τ. Concretely

$$\begin{aligned} \mathrm{Vol}_E(Q_{\tau<0}) &= \frac{1}{2} \left| \det \left(\frac{\boldsymbol{\xi}}{|\boldsymbol{\xi}|}, \frac{\boldsymbol{\zeta}_\perp}{|\boldsymbol{\zeta}_\perp|}, q_2 - q_1, q_3 - q_1 \right) \right| \\ &= \frac{(2\Lambda + kR_2\tau)^2}{8\Lambda^2 R_3 R_4 (R_1+R_2)} \sqrt{(R_1+R_2)^2 + 2(R_3^2+R_4^2)}\,. \end{aligned} \tag{6.106}$$

Similarly, for $\tau > 0$ we get the vertices

$$\begin{aligned} q_1 &= \left(\frac{2\Lambda + kR_2\tau}{2\Lambda(R_1+R_2)}, \frac{2\Lambda - kR_1\tau}{2\Lambda(R_1+R_2)}, 0, 0 \right), \\ q_2 &= \left(\frac{k\tau}{2\Lambda}, 0, \frac{2\Lambda - kR_1\tau}{2\Lambda R_3}, 0 \right), \\ q_3 &= \left(\frac{k\tau}{2\Lambda}, 0, 0, \frac{2\Lambda - kR_1\tau}{2\Lambda R_4} \right), \end{aligned} \tag{6.107}$$

and therefore the volume

$$\mathrm{Vol}_E(Q_{\tau>0}) = \frac{(2\Lambda - kR_1\tau)^2}{8\Lambda^2 R_3 R_4 (R_1+R_2)} \sqrt{(R_1+R_2)^2 + 2(R_3^2+R_4^2)}\,. \tag{6.108}$$

From (6.106) and (6.108) we can directly compute $\rho(t)$ as explained above. Fixing

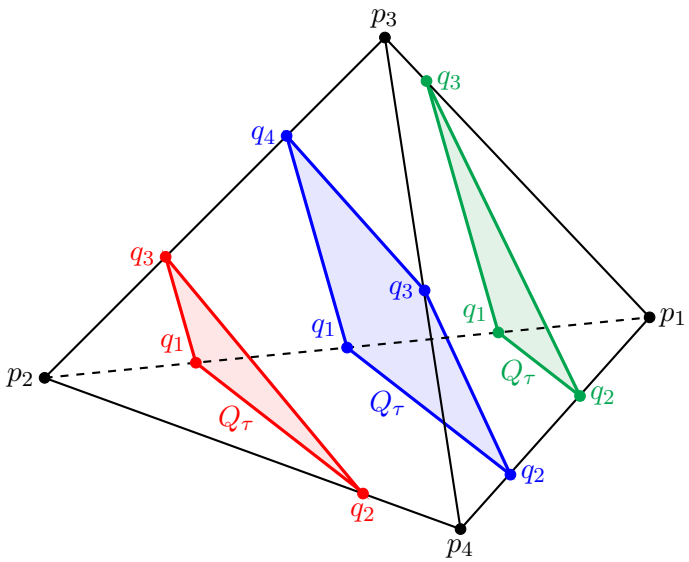


Figure 6.6: Tetrahedron describing S^7 and its slicing corresponding to Model II – ABJM theory. The red slice is for $\tau_1 < \tau < \tau_2$, blue slice for $\tau_2 < \tau < \tau_3$, and green slice for $\tau_3 < \tau < \tau_4$. The perimeter of Q_τ varies with τ qualitatively as ρ in Figure 6.4.

the normalization as in (6.102), we find

$$\rho(t) = \frac{1}{\ell_p^3 N^{1/2}} \left\{ \begin{array}{ll} \dfrac{2\Lambda + kR_2\tau}{\pi^2 R_3 R_4 (R_1+R_2)}\,, & -\dfrac{2\Lambda}{kR_2} < \tau < 0 \\[2ex] \dfrac{2\Lambda - kR_1\tau}{\pi^2 R_3 R_4 (R_1+R_2)}\,, & 0 < \tau < \dfrac{2\Lambda}{kR_1} \end{array} \right| _{\tau = \ell_p^3 N^{1/2}\, t} \,, \tag{6.109}$$

which matches with the eigenvalue distribution (6.24) of the ADHM theory.

Model II: Here the hyperplane corresponding to the moment map level set is described by

$$y_1 - y_2 + y_3 - y_4 = \frac{k}{2\Lambda}\,\tau\,, \tag{6.110}$$

with $-\frac{2\Lambda}{kR_2} \le \tau \le \frac{2\Lambda}{kR_1}$ (recall we assumed $R_1 \le R_3$ and $R_2 \le R_4$), and $\boldsymbol{\zeta}$ is

$$\boldsymbol{\zeta} = \frac{1}{k}\,(1,-1,1,-1)\,. \tag{6.111}$$

In this case there is no value of τ for which both p_3 and p_4 belong to the hyperplane (6.110), hence the latter hyperplane is not parallel to any edge and the situation is as depicted in Figure 6.6. In the intervals $\tau_{\rm min} = \tau_1 < \tau < \tau_2$ and $\tau_3 < \tau < \tau_4 = \tau_{\rm max}$ the

polyhedron Q_τ is a triangle and the computation goes through similarly to Model I. Instead in the interval $\tau_2 < \tau < \tau_3$, Q_τ is a quadrilateral whose vertices are

$$\begin{aligned}
q_1 &= \left(\frac{2\Lambda + kR_2\tau}{2\Lambda(R_1+R_2)}, \frac{2\Lambda - kR_1\tau}{2\Lambda(R_1+R_2)}, 0, 0\right), \\
q_2 &= \left(\frac{2\Lambda + kR_4\tau}{2\Lambda(R_1+R_4)}, 0, 0, \frac{2\Lambda - kR_1\tau}{2\Lambda(R_1+R_4)}\right), \\
q_3 &= \left(0, 0, \frac{2\Lambda + kR_4\tau}{2\Lambda(R_3+R_4)}, \frac{2\Lambda - kR_3\tau}{2\Lambda(R_3+R_4)}\right), \\
q_4 &= \left(0, \frac{2\Lambda - kR_3\tau}{2\Lambda(R_2+R_3)}, \frac{2\Lambda + kR_2\tau}{2\Lambda(R_2+R_3)}, 0\right).
\end{aligned} \tag{6.112}$$

The Euclidean volume of Q_τ can be computed as the sum of the volumes of two triangles, say those with vertices $\{q_1, q_2, q_3\}$ and $\{q_1, q_3, q_4\}$

$$\begin{aligned}
\mathrm{Vol}_E(Q_{\tau_2<\tau<\tau_3}) = \frac{1}{2}\left|\det\left(\frac{\boldsymbol{\xi}}{|\boldsymbol{\xi}|}, \frac{\boldsymbol{\zeta}_\perp}{|\boldsymbol{\zeta}_\perp|}, q_2-q_1, q_3-q_1\right)\right| \\
+ \frac{1}{2}\left|\det\left(\frac{\boldsymbol{\xi}}{|\boldsymbol{\xi}|}, \frac{\boldsymbol{\zeta}_\perp}{|\boldsymbol{\zeta}_\perp|}, q_3-q_1, q_4-q_1\right)\right|.
\end{aligned} \tag{6.113}$$

We do not write the explicit expression as it is long and not particularly insightful. Eventually, fixing the normalization as in (6.102), we find

$$\rho(t) = \frac{1}{\ell_p^3 N^{1/2}} \left\{ \begin{array}{ll} \frac{2\Lambda+kR_2\tau}{\pi^2(R_1+R_2)(R_2+R_3)(R_4-R_2)}\,, & \tau_1<\tau<\tau_2 \\ \frac{4\Lambda+k(R_2R_4-R_1R_3)\tau}{\pi^2(R_1+R_2)(R_2+R_3)(R_1+R_4)(R_3+R_4)}\,, & \tau_2<\tau<\tau_3 \\ \frac{2\Lambda-kR_1\tau}{\pi^2(R_1+R_2)(R_1+R_4)(R_3-R_1)}\,, & \tau_3<\tau<\tau_4 \end{array} \right|_{\tau=\ell_p^3 N^{1/2} t}, \tag{6.114}$$

with

$$\tau_1 = -\frac{2\Lambda}{kR_2}\,, \quad \tau_2 = -\frac{2\Lambda}{kR_4}\,, \quad \tau_3 = \frac{2\Lambda}{kR_3}\,, \quad \tau_4 = \frac{2\Lambda}{kR_1}\,, \tag{6.115}$$

which matches with the eigenvalue distribution (6.28) of the ABJM theory.

6.3.4 M2-branes and Wilson loops

In this section we place probe M2-branes in the black hole backgrounds from section 6.2. In particular, we are interested in M2-branes wrapping AdS_2 and an additional circle $S^1_{\mathrm{M2}} \subset Y_9$

in the internal manifold. When these branes are BPS and wrap a particular S^1 copy, their classical action is related to BPS Wilson loop expectation values in the dual matrix model.

6.3.4.1 BPS probe M2-branes

Since we wish to ultimately match to the Euclidean localized field theory, we need to Wick rotate our background[11]

$$t^{(\mathrm{L})} = -\mathrm{i}t^{(\mathrm{E})}\,, \qquad \mathrm{vol}^{(\mathrm{L})} = -\mathrm{i}\,\mathrm{vol}^{(\mathrm{E})}\,, \qquad \mathrm{i}I^{(\mathrm{L})} = -I^{(\mathrm{E})}\,, \tag{6.116}$$

where the superscripts (L) and (E) denote respectively quantities in Lorentzian and Euclidean signature and I here stands for any action. Consequently, the backgrounds of interest become $\mathrm{EAdS}_2 \times Y_9$. In the rest of the section we will drop the superscripts and work in Euclidean signature unless otherwise stated.

The classical action of a probe M2-brane with worldvolume Σ_{M2} in Euclidean signature is [148][12]

$$I_{\mathrm{M2}} = \frac{1}{(2\pi)^2\ell_p^3}\left[-\mathrm{Vol}\,(\Sigma_{\mathrm{M2}}) - \mathrm{i}\int_{\Sigma_{\mathrm{M2}}} C\right]. \tag{6.117}$$

Note that this formula is gauge-invariant under shifts of the three-form gauge field $C \to C + \mathrm{d}\Omega$, with Ω a two-form such that $\Omega\,|_{\partial\Sigma_{\mathrm{M2}}} = 0$. However, (6.117) requires careful interpretation, as we will discuss next. By virtue of (1.35) and (1.31), we can express C as

$$C = -\mathrm{i}\,\mathrm{vol}_{\mathrm{EAdS}_2} \wedge \mathcal{A} + \mathrm{d}\Omega\,, \tag{6.118}$$

where Ω parametrizes the gauge freedom and we have defined

$$\mathcal{A} = -\psi + \mathrm{e}^{-B}\eta\,, \tag{6.119}$$

with $\mathrm{d}\psi = J$. Notice here that J is closed, so we may always *locally* write $J = \mathrm{d}\psi$, with ψ a transverse one-form (*i.e.* $\xi \lrcorner \psi = 0$), but in general this will not be globally well-defined.

[11] In this instance $t^{(\mathrm{L})}$ is the time coordinate rather than the direction $\mathbb{R}_t$ introduced at the beginning of section 6.1.1.1.

[12] We use the conventions of [149], Wick-rotated as in (6.116).

Indeed, $[J] \in H^2_B(\mathcal{F}_\xi)$ always defines a non-zero basic cohomology class – if it were a basic exact form then using Stokes' theorem the volume of Y_9 would necessarily be zero.[13] Explicitly, recalling (6.45) we can write

$$\mathcal{A} = -(\tilde{\psi}^t + A\,\sigma_{\Sigma_g}) + \mathrm{e}^{-B}\eta + \text{basic exact}\,, \tag{6.120}$$

where both $\tilde{\psi}$ and σ_{Σ_g}, such that $\mathrm{d}\sigma_{\Sigma_g} = \mathrm{vol}_{\Sigma_g}$, are *local* one-forms only. There is no possible choice of gauge fixing that turns the total C-field (6.118) into a globally defined form. However, in the following we will be interested in a particular case where S^1_{M2} is tangent to the fibres X_7. Therefore, if we can turn C into a global form when restricted to the fibres, that would yield a well-defined M2-brane action when substituted into (6.117). Assuming the flavour twist condition (6.47), we can do this by choosing

$$\Omega = -\mathrm{i}\,\mathrm{vol}_{\mathrm{EAdS}_2} \wedge (-\Lambda z)\ , \tag{6.121}$$

so that (6.118) reads (*cf.* (6.44))

$$C = -\mathrm{i}\,\mathrm{vol}_{\mathrm{EAdS}_2} \wedge (-\Lambda\eta - A\,\sigma_{\Sigma_g} + \mathrm{e}^{-B}\eta + \text{basic exact})\,. \tag{6.122}$$

Restricting the above expression to a point on the Riemann surface, the term proportional to σ_{Σ_g} drops out and everything left is proportional to η, which itself is a global one-form since the only class in $H^2_B(\mathcal{F}_\xi)$ that is zero when pulled back to a class in $H^2(Y_9)$ is that generated by $[\varrho]$. In fact as discussed in [68] for the class of GK geometries we are considering $H^2(Y_9) \cong H^2_B(\mathcal{F}_\xi)/[\varrho]$, where $\varrho = \mathrm{d}\eta$ immediately implies that $[\varrho] = 0 \in H^2(Y_9)$.

Substituting (6.122) into (6.117) and recalling we are interested in the case where $\Sigma_{\mathrm{M2}} = \mathrm{EAdS}_2 \times S^1_{\mathrm{M2}}$, we get

$$I_{\mathrm{M2}} = \frac{1}{(2\pi)^2\ell_p^3}\left[(-2\pi)\int_{S^1_{\mathrm{M2}}}\left(-\mathrm{e}^{-2B/3}\,\mathrm{vol}_{S^1_{\mathrm{M2}}} + \Lambda\eta - \mathrm{e}^{-B}\eta\right)\right], \tag{6.123}$$

where the factor (-2π) appearing in front of the first integral comes from the regularized

[13] This is a modification of a standard argument in Kähler geometry, showing that the Kähler class of a compact manifold is always non-zero.

volume of EAdS_2 [150].

We are interested in computing the action (6.123) for BPS M2-branes. In general, a probe M2-brane will break the supersymmetry of the background. However, the M2-brane action possesses another fermionic symmetry, called κ-symmetry [148],[14] which we can use to compensate for the supersymmetry variation. In Appendix A.4 we discuss in some detail the condition to retain some supersymmetry with the M2-brane insertion, and we find that the circle S^1_{M2} needs to be aligned with the R-symmetry circle, *i.e.*

$$\mathrm{vol}_{S^1_{\mathrm{M2}}} = -\mathrm{e}^{-B/3}\,\eta\,. \tag{6.124}$$

Then, in the action (6.123) the first and third terms inside the first integral cancel to give the final result

$$I^{\mathrm{BPS}}_{\mathrm{M2}} = -\frac{\Lambda}{2\pi\ell_p^3}\int_{S^1_{\mathrm{M2}}}\eta\,, \tag{6.125}$$

where Λ is given explicitly in (6.48), and depends on $\mathrm{Vol}_S(X_7)^{-1/2}$ and $N^{1/2}$. Note that this integral is a quantity that will differ from model to model and from point to point and will have to be computed in each example. For ease of notation, we will drop the BPS superscript in the following, and by I_{M2} we will always mean the action of a BPS M2-brane.

Finally, let us make a further comment on the C-field (6.122). This is valid for solutions in the flavour twist class, but outside this class it is not clear how to generalize the gauge-fixing we have carried out and compute well-defined M2-brane actions. Notice that while the action of an M2-brane is invariant under gauge transformations of the C-field, the issue in this case is that we are working with a complex solution, with purely imaginary C-field, and the saddle point solution then in general manifestly depends on the (complex) gauge choice. On the other hand, the holographic matching of quantities in gravity and localized field theory/matrix models only seems to hold for the same flavour twist class, and it is possible that these observations are related.

[14] This is a symmetry of the Green-Schwarz brane action which includes also fermionic degrees of freedom. However, when evaluating the Green-Schwarz action on a classical bosonic background such a contribution vanishes and one is left with the action (6.117).

6.3.4.2 Wilson loop dual

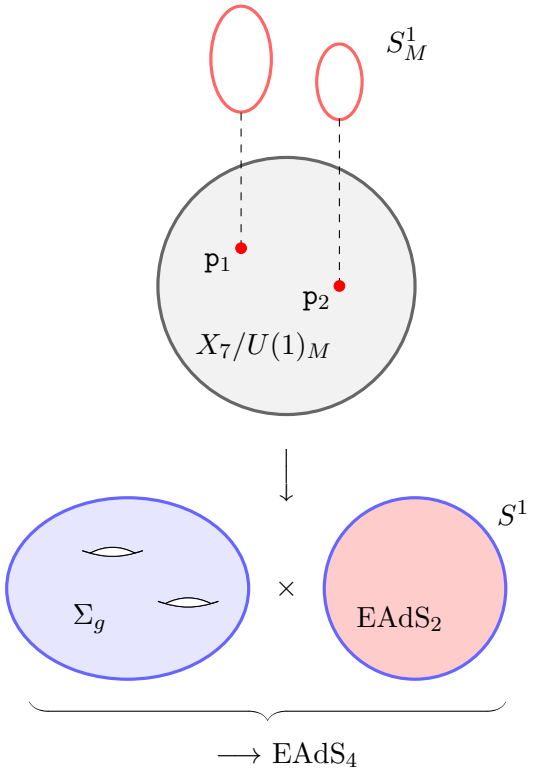


Figure 6.7: We consider an extremal black hole with Euclidean near horizon geometry $\mathrm{EAdS}_2 \times \Sigma_g$ in EAdS_4. The full geometry is $\mathrm{EAdS}_2 \times Y_9$ with Y_9 a fibration of X_7 over Σ_g. The probe M2-branes wrap the EAdS_2 and a copy of the M-theory circle S^1_M at the points $\mathtt{p}_n$ (red) where ζ_M is aligned with the R-symmetry vector ξ. The dual field theory lives on $\Sigma_g \times S^1$ (blue), with S^1 being the boundary of EAdS_2. This S^1 is also the direction wrapped by the Wilson loop, in order for it to be BPS.

In order for the probe M2-branes to be holographically dual to Wilson loops in the fundamental representation, they should wrap $\mathrm{EAdS}_2 \times S^1_M$ – see Figure 6.7.[15,16] Indeed Wilson loops are dual to fundamental strings from the type IIA perspective [151], so we should take $S^1_{\mathrm{M2}} = S^1_M$.[17] In the previous subsection we derived that the M2-branes were BPS for S^1_{M2} aligned with the R-symmetry circle. Then further imposing that they wrap the M-theory circle, the branes are BPS at the points where ζ_M is aligned with the R-symmetry

[15] Similar M2-branes were considered in [135], although without any black hole in AdS_4 present.

[16] Note that we can use a probe approximation because we are interested in Wilson loops in the fundamental representation which are "light", meaning that the corresponding brane has negligible backreaction. The equivalent statement in field theory is that the insertion of the Wilson loop in the path integral does not affect the eigenvalue density itself, to leading order.

[17] Note that, as anticipated, this circle is always tangent to the fibres X_7, hence the expression (6.123) is well-defined.

vector ξ. There are a finite number of such connected loci, which can be determined explicitly for each choice of X_7 together with a $U(1)_M$ action. Let us denote by $\mathtt{p}_n$ a point in the n-th such locus. Holographically the dual Wilson loop expectation value is determined by the M2-brane action evaluated at $\mathtt{p}_n$, where we should sum (or integrate) over all the possible configurations

$$\langle W_{\text{fund}} \rangle = \sum_n \int \mathrm{d}\mathtt{p}_n \, \mathrm{e}^{-I_{\text{M2}}|_{\mathtt{p}_n}} \,. \tag{6.126}$$

Interestingly the value of the action only depends on the locus and not on the specific point within. One should also integrate over the locus, with some measure, although the choice of measure is a subleading effect in N, and we have correspondingly been schematic in writing (6.126). Another interesting point is that the Wilson loop for the class of supersymmetric black holes we are considering is not zero due to integration over gauge-equivalent configurations, discussed in [152]. We refer to [4] for a more detailed discussion of this subtlety.

The ordering of the loci is arbitrary from the geometry point of view, and we order them such that $I_{\text{M2}}|_{\mathtt{p}_n}$ is increasing with n. At large N we only consider the dominant contribution in the sum in (6.126), which comes from the most negative M2-brane action

$$\log \langle W_{\text{fund}} \rangle = -I_{\text{M2}}|_{\mathtt{p}_1} \,. \tag{6.127}$$

Comparing with the expression for the Wilson loop at large N in field theory (6.39), we have a matching $I_{\text{M2}}|_{\mathtt{p}_1} = N^{1/2} t_{\min}$. Our claim is that more is true and actually the M2-brane action reproduces all the points t_n at which the derivative of the eigenvalue density is discontinuous:

$$I_{\text{M2}}|_{\mathtt{p}_n} = N^{1/2} t_n \,. \tag{6.128}$$

Recall that $\mathtt{p}_n$ is a point in the n-th region where ζ_M and ξ are aligned. Let us denote β_n the factor of proportionality at such a point. Then we have

$$\zeta_M = \beta_n \xi \quad \Longrightarrow \int_{S^1_M|_{\mathtt{p}_n}} \eta = -2\pi\beta_n \,, \tag{6.129}$$

as $\xi \lrcorner \, \eta = 1$ and the sign is due to the orientation determined in (6.124). Therefore the action

of a BPS M2-brane dual to a Wilson loop reads

$$I_{\rm M2}|_{\mathtt{p}_n} = \frac{\Lambda}{\ell_p^3}\,\beta_n\,. \tag{6.130}$$

The statement (6.128) is actually equivalent to the argument in section 6.3.2 that the discontinuity points of ρ' are reproduced by the fixed points of the moment map. Indeed recall that $h_M = \Lambda\,\zeta_M \lrcorner\, \eta$, and we already mentioned that the critical points of h_M were those where ζ_M and ξ are aligned. At a point $\mathtt{p}_n$ where $\zeta_M = \beta_n\,\xi$ we have $\tau_n \equiv h_M|_{\mathtt{p}_n} = \Lambda\beta_n$, such that

$$t_n = \frac{\tau_n}{\ell_p^3 N^{1/2}} = \frac{\Lambda\beta_n}{\ell_p^3 N^{1/2}} = \frac{I_{\rm M2}|_{\mathtt{p}_n}}{N^{1/2}}. \tag{6.131}$$

Let us next examine this in our favourite examples. Recall that on $S^7/\mathbb{Z}_k$

$$\xi = \sum_{a=1}^{4} \frac{R_a}{2}\,\partial_{\phi_a}\,. \tag{6.132}$$

Model I: For ADHM

$$\zeta_M^{\rm I} = \frac{1}{k}(\partial_{\phi_1} - \partial_{\phi_2})\,, \tag{6.133}$$

such that $\zeta_M^{\rm I} = \beta_n\xi$ in the regions $\mathtt{p}_1 \in (0, z_2, 0, 0)$, $\mathtt{p}_2 \in (0, 0, z_3, z_4)$, $\mathtt{p}_3 \in (z_1, 0, 0, 0)$, with

$$\beta_1 = -\frac{2}{kR_2}\,, \quad \beta_2 = 0\,, \quad \beta_3 = \frac{2}{kR_1}\,. \tag{6.134}$$

This reproduces the points in (6.25), recalling the relation (6.72) between Λ and μ.

Model II: For ABJM

$$\zeta_M^{\rm II} = \frac{1}{k}(\partial_{\phi_1} - \partial_{\phi_2} + \partial_{\phi_3} - \partial_{\phi_4})\,, \tag{6.135}$$

such that $\zeta_M^{\rm II}$ and ξ are aligned on the regions where only one of the coordinate is non-zero. Ordering them by increasing β_n we denote $\mathtt{p}_1 \in (0, z_2, 0, 0)$, $\mathtt{p}_2 \in (0, 0, 0, z_4)$, $\mathtt{p}_3 \in (0, 0, z_3, 0)$, $\mathtt{p}_4 \in (z_1, 0, 0, 0)$, giving

$$\beta_1 = -\frac{2}{kR_2}\,, \quad \beta_2 = -\frac{2}{kR_4}\,, \quad \beta_3 = \frac{2}{kR_3}\,, \quad \beta_4 = \frac{2}{kR_1}\,, \tag{6.136}$$

which exactly reproduces the subinterval points in (6.29).

In the case where some of the R-charges are equal the regions may change topology. In particular when $R_a = 1/2$ for all a, there are two loci on which $\zeta_M^{\rm II}$ and ξ are aligned, namely $\mathtt{p}_1 \in \{z_1 = z_3 = 0\}$, $\mathtt{p}_2 \in \{z_2 = z_4 = 0\}$, where

$$\beta_1 = -\frac{4}{k}\,, \quad \beta_2 = \frac{4}{k}\,, \tag{6.137}$$

and $\rho(t) = 2\mu/\pi$ is just a constant function between these two points. In our polytope picture this corresponds to the moment map plane being parallel to both the edge between p_1 and p_3 and that between p_2 and p_4, so that Q_τ is always a quadrilateral. In this case, we also have

$$\Lambda = \frac{\pi \ell_p^3 N^{1/2}}{8}\sqrt{2k} = \frac{\pi \ell_p^3 N^{1/2}}{2}\mu\,. \tag{6.138}$$

This particular case describes the so-called universal twist, which is an explicitly known black hole solution of minimal 4d gauged supergravity that uplifts on general classes of internal space X_7 [153], including $S^7/\mathbb{Z}_k$ discussed here.

6.4 Matrix models on the spindle

We now generalize the results obtained so far to the case where the black hole has a further parameter corresponding to the acceleration. In field theory, the observable equivalent to the topologically twisted index is the *spindle index* [93, 94]. The corresponding large N matrix models were studied only recently in [95] and agree with our prediction. Some earlier related work on the "refined twisted index", with which we make contact here, has been carried out in [154], and may be matched to our gravitational formulas too.

6.4.1 Shifted eigenvalue densities

Let us begin by noticing that the geometric characterization of the matrix models we presented in section 6.3 is motivated somewhat heuristically, albeit with concrete computational checks. At this stage we lack a systematic derivation of a similar description for the accel-

erating case, with the spindle replacing the Riemann surface, given the more complicated geometric structure of the fibrations described in chapter 2. Nevertheless, we can exploit the lessons learned with the non-accelerating case to describe some of the features of said matrix models, leaving a more thorough analysis to future work.

First of all, let us notice that at the fixed points of the vector fields $\zeta_\pm$ (*cf.* (2.16)), that is at the respective poles of Σ,[18] the geometry of the internal space becomes equivalent to that described in section 6.2 upon using the shifted R-symmetry vectors $b_i \to b_i^{(\pm)}$. Moreover, the vector field ζ_M generating the $U(1)_M$ action is a characteristic feature of the original geometric engineering set-up, and as such it only rotates directions inside the fibres X_7, and does not act on the spindle itself – that is, it does not have any component along ∂_{φ_0}. Hence it is clear that at the two poles of the spindle the geometric set-up is much the same as what we had before, and thus we can envisage having a doubling of all the quantities associated to the matrix model, with a copy at the "+" pole and another at the "−" pole.

We begin by noting that the $U(1)_M$ action is Hamiltonian on $X_\pm$, and therefore we can define two associated moment maps $h_M^\pm$ at the poles of the spindle to be such that

$$\mathrm{d}h_M^\pm = -\,\zeta_M \lrcorner\, J|_{X_\pm}\,. \tag{6.139}$$

From here, everything goes through as in section 6.3, although with the shifted R-symmetry vector $b_i^{(\pm)}$ and consequently the shifted Kähler class parameters $\Lambda_\pm$ and the shifted R-charges $R_a^\pm$. Parametrizing with τ the images of $h_M^\pm$, we can define two quotients of the fibres $X_\pm$

$$X_\tau^\pm \equiv (h_M^\pm)^{-1}(\tau)/U(1)_M\,. \tag{6.140}$$

The volumes of $X_\tau^\pm$ can be obtained from $\mathrm{Vol}(X_\tau)$, as computed in the Riemann surface case, by shifting the R-symmetry vectors and dividing by a factor $m_\pm$ which accounts for the quotients in writing $X_\pm = X_7/\mathbb{Z}_{m_\pm}$

$$\mathrm{Vol}(X_\tau^\pm) = \frac{1}{m_\pm}\,\mathrm{Vol}(X_\tau)\Big|_{b_i^{(\pm)}}\,. \tag{6.141}$$

[18] Note here $\zeta_\pm$ should not be confused with the M-theory circle action generator ζ_M (or its components $\boldsymbol{\zeta}$).

Note that τ is just a label at this stage, and there is no reason why it should be the same at the two poles, hence we will rename it to $\tau^{\pm}$ respectively. We can correspondingly define two "shifted densities" $\rho_{\pm}(t^{\pm})$ as in (6.96). In particular, denoting with $\rho_{\Sigma_g}(t)$ the eigenvalue density of a certain field theory on Σ_g, the same field theory on the spindle will have

$$\rho_{\pm}(t^{\pm}) = \rho_{\Sigma_g}(t^{\pm})\big|_{b_i^{(\pm)}} \,. \tag{6.142}$$

Moreover, the derivatives $\rho'_{\pm}(t)$ are discontinuous at the critical points of $h_M^{\pm}$, namely where ζ_M is aligned with $\xi_{\pm}$ and are simply given by

$$t_n^{\pm} = t_n|_{b_i^{(\pm)}} \,, \tag{6.143}$$

where t_n are the points of discontinuity of $\rho'_{\Sigma_g}(t)$.

This last point can be corroborated by looking at probe M2-branes in this background. The discussion about supersymmetry we carried out in section 6.3.4.1 goes through without any change as it relies only on the fact that Y_9 is a GK manifold. There we showed that the M2-branes are BPS when ζ_M is aligned with ξ, and from (2.18) we can see that in the loci where $\zeta_{\pm}$ are zero, namely the respective poles of the spindle, this is equivalent to requiring ζ_M to be aligned with $\xi_{\pm}$, as stated above. With suitable tweaks, also the gauge fixing in section 6.3.4 goes through, albeit it has to be done separately at the two poles, and we find that BPS M2-branes wrapping $\mathrm{EAdS}_2 \times S^1_M$ can sit at either poles of Σ, and their action matches (6.143)

$$I_{\mathrm{M2}}|_{\mathfrak{p}_n^{\pm}} = N^{1/2} t_n^{\pm} \,. \tag{6.144}$$

Here $\mathfrak{p}_n^{\pm}$ are points in the n-th locus where $\zeta_M \propto \xi_{\pm}$. Correspondingly, in field theory a Wilson loop in the fundamental representation wrapping the Euclidean time circle is supersymmetric when it sits at either of the two poles, and its expectation value at leading order in N will be

$$\log \langle W^{\pm}_{\mathrm{fund}} \rangle = -I_{\mathrm{M2}}|_{\mathfrak{p}_1^{\pm}} \,. \tag{6.145}$$

All the quantities introduced up to now should then match with corresponding quantities

derived from a purely field theoretic computation. In particular, for 3d $\mathcal{N}=2$ SCFTs on $\Sigma\times S^1$ it is convenient to introduce the shifted chemical potentials (similar to (5.21))

$$\Delta_\Phi^\pm = \Delta_\Phi \pm \frac{\varepsilon}{2}\left(\mathfrak{p}_\Phi \pm \frac{r_\Phi}{2}\,\frac{\sigma m_+ - m_-}{m_+ m_-}\right), \tag{6.146}$$

where ε is an extra parameter which will enter the extremization procedure and the r_Φ are subject to the constraint $\sum_{\Phi\in W} r_\Phi = 2$ but are otherwise free. We expect all physical quantities to have natural expressions in terms of these, and the holographic matching to be achieved by suitably identifying $\Delta_\Phi^\pm$ with linear combinations of $R_a^\pm$ and ε with $2b_0$.

To summarize, the matrix model arising from the large N limit of the localized partition function on $\Sigma\times S^1$ is expected to factorize into two different matrix models, which can be studied independently and result in the densities $\rho_\pm(t^\pm)$ introduced above. We expect that the information contained in said "shifted" densities can be used to recover the total $\rho_\Sigma(t)$, as a function of a single variable t obtained from $t^\pm$. This picture is also motivated by several results in the literature where in different contexts a factorization of physical observables have been observed, ultimately related to a fixed point formula. Of these, the refined twisted index discussed in [154] is directly relevant, and will be discussed in more detail shortly.

Since we left most of the formulas in this section rather implicit, we conclude by presenting the explicit BPS M2-brane actions for the ABJM model on a spindle. There are 4 such BPS M2-branes, wrapping an aligned M-theory circle and R-symmetry vector over each pole of the spindle, giving 8 values in total. From (6.144) and the results in 6.3.4.2 we can write

$$I_{\mathrm{M2}}|_{\mathfrak{p}_a^\pm} = N^{1/2} t_a^\pm\,, \quad a=1,2,3,4\,, \tag{6.147}$$

where

$$t_1^\pm = -\frac{\mu^\pm}{kR_2^\pm}\,, \quad t_2^\pm = -\frac{\mu^\pm}{kR_4^\pm}\,, \quad t_3^\pm = \frac{\mu^\pm}{kR_3^\pm}\,, \quad t_4^\pm = \frac{\mu^\pm}{kR_1^\pm}\,, \tag{6.148}$$

and

$$\mu^\pm = \pi\sqrt{2kR_1^\pm R_2^\pm R_3^\pm R_4^\pm}\,. \tag{6.149}$$

Here the R-charges $R_a^{\pm}$ should be matched to linear combinations of the chemical potential variables $\Delta_\Phi^{\pm}$ in (6.146). We also identify $\epsilon = 2b_0$. This gives a very precise prediction for the large N matrix model behaviour of the ABJM theory on a spindle, with (6.148) giving the points at which the expected eigenvalue density blocks have discontinuities in their derivatives. More physically, as we have explained the least such M2-brane action computes a BPS Wilson loop VEV in the field theory on the spindle.

6.4.2 Connecting to the refined twisted index

To conclude the discussion on the spindle index, we will make contact with the field theory results of [154]. There the authors studied the matrix models arising from the large N limit of the *refined* twisted index $Z_{S^2_\varepsilon \times S^1}$, which is defined for the genus $g = 0$ case as a further refinement of the topologically twisted index with respect to the axial $U(1)$ isometry of the two-sphere (see section 4 of [141]). This index depends on an extra parameter ε, which "rotates" the S^1 relative to the S^2. Holographically, its logarithm has been matched with the entropy of supersymmetric, magnetically charged, and also rotating black holes in AdS_4 [155], with ε identified with the chemical potential conjugate to the angular momentum of the black hole [124].

We shall see in this section that the field theory results of [154] may also be matched to GK geometries for which X_7 is fibred over S^2, and where the R-symmetry vector also rotates the S^2. Specifically, we shall see that the field theory parameter $\varepsilon = 2b_0$, in terms of the component b_0 of ξ that rotates the S^2. A similar matching was pointed out in [2], and also relies on some observations in [89]. In order to explain this, one first observes for the twisted $S^2_\varepsilon \times S^1$, the R-symmetry Killing vector field bilinear for this rigid supersymmetric background is [89, 141][19]

$$K = \bar{\psi}\gamma^\mu \psi \partial_\mu = \partial_\theta + \tfrac{1}{2}\varepsilon\, \partial_{\varphi_0}\,. \tag{6.150}$$

Here ψ is the Killing spinor of the background, θ has period 2π and parametrizes the S^1, while φ_0 parametrizes the axial direction on the S^2 and is also normalized to have canonical

[19] The fugacity was denoted $\mathrm{e}^{\mathrm{i}\epsilon} = \mathrm{e}^{\mathrm{i}\varsigma/2}$ in [141], which explains the factor of $\frac{1}{2}$ in (6.150).

period 2π. The expression (6.150) is a more invariant geometric way to characterize the parameter ε, in terms of specifying the R-symmetry vector field of the background on which one is localizing. On the other hand, the bulk black hole solution inherits the same Killing vector field, and when lifted to 11d M-theory this explains why $\varepsilon = 2b_0$, since by definition b_0 parameterizes the component of the R-symmetry vector of the full solution along the horizon direction Σ. This is all detailed quite explicitly for the class of dyonically charged, accelerating and rotating black holes studied in [48, 89] (which lie in the universal truncation of [156]), but the same arguments should go through also for the more general class of purely magnetically charged black holes considered in this chapter, with general choice of X_7 and magnetic fluxes, but with a trial R-symmetry vector field that also rotates the horizon S^2. We then expect the entropy function in (3.36) to match $\log Z_{S^2_{\tilde{\varepsilon}}\times S^1}$ in the twist case $\sigma = 1$ and in the limit $m_\pm = 1$, which we find is indeed the case. This is then consistent with the conjecture in [2]: that b_0 may be regarded as a chemical potential for angular momentum J, with the entropy of *rotating* versions of the black holes considered here obtained via a Legendre transform. Moreover, given the results presented here, we may go further and also match matrix model quantities in the refined field theory calculation, and GK geometry with $b_0 \neq 0$.

When considering the refined index, the summation over the gauge magnetic fluxes $\mathfrak{m}$ in (6.15) cannot be performed directly and instead one should keep them as variables when taking the large N limit. In particular, in [154] the authors supplement the ansatz (6.18) with[20]

$$\mathfrak{m}_I^\alpha = \mathrm{i}N^{1/2}\,\mathfrak{s}^\alpha + \mathfrak{p}_I^\alpha \quad \longrightarrow \quad \mathfrak{m}_I(t) = \mathrm{i}N^{1/2}\,\mathfrak{s}(t) + \mathfrak{p}_I(t)\,. \tag{6.151}$$

Moreover, the partition function takes the form of a product of holomorphic blocks [157], which at large N can be expressed in terms of shifted Bethe potentials

$$\log Z_{S^2_{\tilde{\varepsilon}}\times S^1} = -\frac{\mathrm{i}}{\pi\varepsilon}\left[\mathcal{U}(\rho_+(t^+), v_I^+(t^+), \Delta_\Phi^+) - \mathcal{U}(\rho_-(t^-), v_I^-(t^-), \Delta_\Phi^-)\right], \tag{6.152}$$

where $\mathcal{U}$ is the same Bethe potential we introduced in section 6.1.2.1 and the various quantities

[20] Our notation differs from that of [154] in the following way: $\mathfrak{s}^{\text{there}} = -\mathfrak{p}$, $\mathfrak{p}^{\text{there}} = \mathfrak{s}$, $\epsilon^{\text{there}} = \pi\varepsilon$, $\Delta^{\text{there}} = \pi\Delta$, $T^{(\pm)}_{\text{there}} = t^\pm$, $\widetilde{\mathcal{W}}^{\text{there}} = -\mathcal{U}$.

appearing are defined as

$$
\begin{aligned}
&t^{\pm} = t \pm \frac{\pi\varepsilon}{2}\,\mathfrak{s}(t)\,, \qquad \rho_{\pm}(t^{\pm}) = \frac{\rho(t)}{1 \pm \frac{\pi\varepsilon}{2}\,\mathfrak{s}'(t)}\,, \qquad v_I^{\pm}(t^{\pm}) = v_I(t) \pm \frac{\pi\varepsilon}{2}\,\mathfrak{p}_I(t)\,, \\
&\Delta_{\Phi}^{\pm} = \Delta_{\Phi} \pm \frac{\varepsilon}{2}\,\mathfrak{p}_{\Phi}\,,
\end{aligned}
\tag{6.153}
$$

and the shifted chemical potentials satisfy the constraints

$$
\sum_{\Phi \in W} \Delta_{\Phi}^{\pm} = 2 \mp \varepsilon\,. \tag{6.154}
$$

Note that the $\Delta_{\Phi}^{\pm}$ introduced for the spindle in (6.146) precisely reduce to those in (6.153) when $\sigma = 1$ and $m_+ = m_- = 1$.

At this point, one should extremize (6.152) with respect to $\rho(t)$, $v_I(t)$, $\mathfrak{s}(t)$, and $\mathfrak{p}_I(t)$, but in [154] the authors observed that this is actually equivalent to extremizing independently the two Bethe potentials with respect to $\rho_{\pm}(t^{\pm})$ and $v_I^{\pm}(t^{\pm})$. With a suitable map between the variables this is equivalent to the unrefined case and therefore the results are the same

$$
\rho_{\pm}(t^{\pm}) = \rho_{\Sigma_g}(t^{\pm})\big|_{\Delta_{\Phi}^{\pm}}\,, \qquad v_I^{\pm}(t^{\pm}) = v_I^{\Sigma_g}(t^{\pm})\big|_{\Delta_{\Phi}^{\pm}}\,. \tag{6.155}
$$

The physical $\rho(t)$ and the other functions of t of the matrix model are then obtained by going backwards through the definitions of the shifted quantities in (6.153) and imposing some consistency conditions which will not be detailed here. Substituting (6.155) into (6.152) one obtains

$$
\log Z_{S^2_{\tilde{\varepsilon}} \times S^1} = \frac{1}{\pi\varepsilon}\left[\bar{\mathcal{U}}(\Delta_{\Phi}^{+}) - \bar{\mathcal{U}}(\Delta_{\Phi}^{-})\right] = \frac{1}{2\varepsilon}\left[F_{S^3}(\Delta_{\Phi}^{+}) - F_{S^3}(\Delta_{\Phi}^{-})\right]. \tag{6.156}
$$

As anticipated, this matches perfectly with the entropy function (3.36) when $\sigma = 1$ and $m_+ = m_- = 1$ if we identify $\varepsilon = 2b_0$ and $\Delta_{\Phi}^{\pm}$ with suitable linear combinations of $R_a^{\pm}(\xi_{\pm})$.[21] Furthermore, notice that the densities (6.155) are exactly the same as those we defined from GK geometry, for the spindle matrix model, in (6.142).

[21] Recall that $F_{S^3} = F_{\rm grav}|_{b_1=4} = 16 F_{\rm grav}|_{b_1=1}$ upon identifying Δ_{Φ} with the same linear combinations of $R_a(\xi)$.

6.5 Matrix models from toric spaces

In this final section we will specify the results of this chapter for generic choices of toric Calabi-Yau cones $C(X_7)$, which are dual to various flavoured variants of the two quivers we already discussed. These are somewhat more involved computationally, but there are no extra ingredients entering the picture besides some toric geometry machinery. We first explain how the extra toric structure provides an algorithmic way to compute both the eigenvalue density and the discontinuity points of its derivative. We then apply the above to the examples where $C(X_7) = \mathbb{C} \times C(T^{1,1})$. Note that here we consider only the non-accelerating case but every result can be extended to the accelerating case via the prescriptions of section 6.4.

6.5.1 Critical points and M2-branes

Recall that the moment map h_M associated to the $U(1)_M$ action defined in (6.81) maps Y_7 to the interval $[\tau_{\min}, \tau_{\max}]$ which gives the support of the eigenvalue density. Let us compute h_M explicitly. Firstly, note that for general toric X_7 we have [70, 132]

$$\partial_{\varphi_i} \lrcorner\, \omega = -\,\mathrm{d}x^i\,, \tag{6.157}$$

where $x^i = (y^i - y^i_*)$ and y^i_* is given by (4.12) without the first coordinate. Defining ζ_i to be the coefficient of the M-theory killing vector ζ_M in the toric basis, *i.e.* $\zeta_M = \sum_{i=1}^4 \zeta_i\, \partial_{\varphi_i}$, it follows that

$$h_M(y^i) = \sum_{i=1}^4 \zeta_i\, (y^i - y^i_*)\,. \tag{6.158}$$

The coefficients ζ_i depend on the particular physical model we consider.

Recall also that the image of h_M is divided in subintervals whose extrema correspond to its value at the critical points, *i.e.* where $\mathrm{d}h_M = 0$. In turn such points are those where ζ_M is proportional to ξ, and we can find them explicitly by employing the following strategy. Define ν_a as the vector fields that shrink on the a-th facet $\mathcal{P}_a$ of the polyhedric cone

$$\nu_a = \sum_{i=1}^4 v_{ai}\, \partial_{\varphi_i}\,. \tag{6.159}$$

Then, we firstly find all the linear combinations of the form

$$\zeta_M = \beta\,\xi + \sum_{a\in F} \alpha_a \nu_a \,, \tag{6.160}$$

where F is any set of toric indices $\{a\}$ such that all the corresponding facets $\{\mathcal{P}_a\}$ have at least one point in common. By definition, in the intersection $\bigcap_{a\in F}\mathcal{P}_a$ all the vectors ν_a with $a \in F$ collapse, and therefore $\zeta_M = \beta\,\xi$ which is precisely the condition for criticality of h_M. Note that here β could also be vanishing, which signals the presence of D6-branes. In all the examples considered, the intersection above is either a single point in the toric polytope or one of its edges. Ultimately, the extrema of the subintervals in the image of h_M are obtained by evaluating

$$h_M(y_F)\,, \qquad y_F \in \bigcap_{a\in F} \mathcal{P}_a \,, \tag{6.161}$$

for each set F defined as above, where note that different sets F do not always lead to different points in the image.

Furthermore, we can directly make contact with the M2-brane discussion of section 6.3.4. In particular, from (6.129) we see that β determines precisely the value of the action of the probe M2-brane, which becomes BPS when it sits at y_F

$$I_{\rm M2} = \frac{\Lambda}{\ell_p^3}\,\beta\,. \tag{6.162}$$

6.5.2 Eigenvalue density

We now want to compute the eigenvalue density as the volume of the quotient space (6.93) for any choice of toric $C(X_7)$. In fact, recall that in section 6.3.3 we stated that

$$\rho(t) \propto \frac{\mathrm{d}}{\mathrm{d}\Lambda}\,\mathrm{Vol}(X_\tau)\,\Big|_{\tau=\ell_p^3 N^{1/2} t}\,, \tag{6.163}$$

where X_τ is defined as a quotient of the τ level set of h_M. In the toric setting we can always follow the strategy we exploited for the two examples considered earlier in section 6.3.3,

and decouple the coordinates $y^i \in \mathbb{R}^4$ with Euclidean metric[22] from the angles $\varphi_i \in U(1)^4$, which simply give a contribution of 2π each. Firstly, we note that the polytope (4.11) is the generalization of the tetrahedron defined by $r^2 = 1$ in section 6.3.3. The shape of such a polytope will depend on the toric data v_a. Saturating the a-th inequality, *i.e.*

$$(y^i - y^i_*)\, v_{ai} = \lambda_a \,, \tag{6.164}$$

defines the plane where the a-th facet $\mathcal{P}_a$ lies, and changing the corresponding Kähler class parameter λ_a amounts to shifting the facet parallel to itself. Upon setting the flavour twist condition $\lambda_a = -\Lambda$, all the facets move together when changing Λ. We then restrict to the level set of the moment map (6.158) imposing

$$(y^i - y^i_*)\, \zeta_i = \tau \,. \tag{6.165}$$

This equation describes a hyperplane in $\mathbb{R}^4$ which slices the polytope $\mathcal{P}$. The intersection of the two will be a polygon $\mathcal{Q}_\tau$ whose shape depends on the value of τ and whose Euclidean area determines directly the volume we are interested in

$$\mathrm{Vol}(X_\tau) = (2\pi)^3\, \mathrm{Vol}_E(\mathcal{Q}_\tau) \,. \tag{6.166}$$

Every time the plane (6.165) crosses a vertex or an edge of the polytope, the expression for $\mathrm{Vol}_E(\mathcal{Q}_\tau)$ changes, hence it is clear that these correspond to the discontinuity points in the derivative of the density, *i.e.* the critical points of the previous subsection. Note that here we have a clear geometric interpretation of what it means taking the derivative with respect to Λ in (6.163): given what we said below (6.164), it is clear that $\frac{\mathrm{d}}{\mathrm{d}\Lambda}\mathrm{Vol}_E(\mathcal{Q}_\tau)$ is (proportional to) the length of the perimeter of the polygon $\mathcal{Q}_\tau$.

In general, for a fixed τ a vertex $q_{ab} \in \mathbb{R}^4$ of $\mathcal{Q}_\tau$ is computed by imposing simultaneously two equations like (6.164) for adjacent facets $\mathcal{P}_a$ and $\mathcal{P}_b$, the Reeb hyperplane condition

[22] Differently from section 6.3.3, here the Kähler class parameter is absorbed into the coordinates y^i. This has some repercussions on the normalization of quantities. In particular, this is why we distinguish $\mathcal{Q}_\tau$ from Q_τ (see (6.166) versus (6.99)) which are otherwise conceptually the same quantity.

$y \in H(b)$, and the moment map level set in (6.165)

$$\begin{aligned}
(q^i_{ab} - y^i_*)\, v_{ai} &= -\Lambda\,, \\
(q^i_{ab} - y^i_*)\, v_{bi} &= -\Lambda\,, \\
(q^i_{ab} - y^i_*)\, b_i &= 0\,, \\
(q^i_{ab} - y^i_*)\, \zeta_i &= \tau\,.
\end{aligned} \tag{6.167}$$

These are four linear equations for four variables q^i_{ab}, $i = 1, \ldots, 4$, hence the vertices of $\mathcal{Q}_\tau$ are uniquely determined in terms of Λ, τ and the b_i (for a given field theory v_a and ζ are fixed). This system should be solved for any pair of adjacent facets. Note that it may not admit any solution, for certain pairs, indicating that the moment map hyperplane cuts the polytope parallel to the edge between these two facets. Further imposing that the solution indeed lies inside the polytope

$$(q^i_{ab} - y^i_*) v_{ci} \geq -\Lambda\,, \quad \forall c = 1, \ldots, d \tag{6.168}$$

gives the range of τ for which q_{ab} is a vertex of $\mathcal{Q}_\tau$. Therefore the set of vertices of $\mathcal{Q}_\tau$, and consequently the expression for its perimeter (which recall is the quantity identified with the eigenvalue density ρ), changes on each such interval of τ. Once the sets of vertices are found, the surface area of $\mathcal{Q}_\tau$ on each interval can be computed by splitting it into triangles and computing the area of each triangle as a determinant as we did in the examples in section 6.3.3. More concretely, let us call $\boldsymbol{\zeta}$ the vector in $\mathbb{R}^4$ with components ζ_i and introduce

$$\boldsymbol{\zeta}_\perp \equiv \boldsymbol{\zeta} - \frac{\boldsymbol{\zeta} \cdot b}{|b|^2}\, b\,. \tag{6.169}$$

This is the equivalent of (6.101) but all the vectors here are expressed in toric coordinates. Then, the area of a triangle with vertices $q_{a_1a_2}, q_{a_3a_4}, q_{a_5a_6} \in \mathbb{R}^4$ can be computed as

$$\frac{1}{2} \left| \det \left(\frac{b}{|b|}, \frac{\boldsymbol{\zeta}_\perp}{|\boldsymbol{\zeta}_\perp|}, q_{a_3a_4} - q_{a_1a_2}, q_{a_5a_6} - q_{a_1a_2} \right) \right|, \tag{6.170}$$

and $\mathrm{Vol}_E(\mathcal{Q}_\tau)$ will be a finite sum of such determinants. Note that it is crucial to have $\boldsymbol{\zeta}_\perp$

rather then $\boldsymbol{\zeta}$ in (6.170) because only $\boldsymbol{\zeta}_\perp$ is orthogonal to both the triangle and to b, so that the volume of the parallelotope computed by the determinant is simply the area of the triangle times the length of the two "heights", which are both 1. We refer the reader to the examples in the next subsection to see how this procedure works more concretely.

Finally, let us highlight that we are now able to justify the normalization in (6.102). Let us compute the integral of the RHS of (6.163)

$$\mathcal{I} \equiv \int_{t_{\min}}^{t_{\max}} \mathrm{d}t \, \frac{\mathrm{d}}{\mathrm{d}\Lambda} \mathrm{Vol}(X_\tau) = \frac{(2\pi)^3}{\ell_p^3 N^{1/2}} \frac{\mathrm{d}}{\mathrm{d}\Lambda} \int_{\tau_{\min}}^{\tau_{\max}} \mathrm{d}\tau \, \mathrm{Vol}_E(\mathcal{Q}_\tau) \,, \tag{6.171}$$

where in the last step we exchanged the integral and the derivative and changed the variable of integration from t to τ. Now the integral above with a suitable measure is nothing but the volume of the entire polytope $\mathcal{P}$, which can be expressed in terms of the master volume $\mathcal{V}_7$

$$\int_{\tau_{\min}}^{\tau_{\max}} \frac{\mathrm{d}\tau}{|\boldsymbol{\zeta}_\perp|} \, \mathrm{Vol}_E(\mathcal{Q}_\tau) = \mathrm{Vol}_E(\mathcal{P}) = \frac{|b|}{(2\pi)^4} \, \mathcal{V}_7 \,. \tag{6.172}$$

Substituting this back into (6.171) we obtain

$$\mathcal{I} = \frac{|b||\boldsymbol{\zeta}_\perp|}{2\pi \ell_p^3 N^{1/2}} \frac{\mathrm{d}\mathcal{V}_7}{\mathrm{d}\Lambda} = \frac{|b||\boldsymbol{\zeta}_\perp|}{2\pi \ell_p^3 N^{1/2}} \, (2\pi \ell_p)^6 N \,, \tag{6.173}$$

where the second equality comes from the flux quantization condition in the flavour twist. Hence, the correct normalization for (6.163) is

$$\rho(t) = \frac{1}{\mathcal{I}} \frac{\mathrm{d}}{\mathrm{d}\Lambda} \mathrm{Vol}(X_\tau) \Big|_{\tau = \ell_p^3 N^{1/2} t} = \frac{1}{32\pi^5 \ell_p^3 N^{1/2} |b||\boldsymbol{\zeta}_\perp|} \frac{\mathrm{d}}{\mathrm{d}\Lambda} \mathrm{Vol}(X_\tau) \Big|_{\tau = \ell_p^3 N^{1/2}\, t} \,, \tag{6.174}$$

which is exactly what we had in (6.102). If X_7 is a quotient space by a $\mathbb{Z}_n$ action, similarly to section 6.3, there is an additional factor of n relating the volumes of X_τ and $\mathcal{Q}_\tau$ (the unquotiented case is $n = 1$), and the final expression for ρ reads

$$\rho(t) = \frac{1}{4\pi^2 \ell_p^3 N^{1/2} |b||\boldsymbol{\zeta}_\perp| n} \frac{\mathrm{d}}{\mathrm{d}\Lambda} \mathrm{Vol}(\mathcal{Q}_\tau) \Big|_{\tau = \ell_p^3 N^{1/2}\, t} \,. \tag{6.175}$$

6.5.3 Example: $C(X_7) = \mathbb{C} \times C(T^{1,1})$

We now illustrate the procedure outlined in the previous subsection on the toric cone $\mathbb{C} \times C(T^{1,1})$, which admits two field theory duals depending on the choice of the M-theory circle action. First let us describe some properties of this geometry. The toric vectors are

$$\begin{aligned} &v_1 = (1,0,0,0)\,, \quad v_2 = (1,0,0,1)\,, \quad v_3 = (1,0,1,1)\,, \\ &v_4 = (1,0,1,0)\,, \quad v_5 = (1,1,0,0)\,, \end{aligned} \tag{6.176}$$

and the corresponding toric diagram is shown in Figure 6.8. A subtle point to address is that the space X_7 has a singularity and therefore computing the master volume naively leads to the wrong result. As discussed in [119] this is fixed by imposing a restriction on the Kähler class parameters

$$\lambda_1 - \lambda_2 + \lambda_3 - \lambda_4 = 0\,. \tag{6.177}$$

Incidentally, this constraint also enforces the flavour twist condition (6.47), which is precisely what we need to compare with field theory results. The Sasakian volume of the link X_7 of $\mathbb{C} \times C(T^{1,1})$ is

$$\mathrm{Vol}_S(X_7) = \frac{\pi^4 (b_1 - b_2)}{3 b_2 b_3 b_4 (b_1 - b_2 - b_3)(b_1 - b_2 - b_4)}\,. \tag{6.178}$$

The geometric R-charges are

$$\begin{aligned} &R_1 = \frac{2(b_1 - b_2 - b_3)(b_1 - b_2 - b_4)}{b_1(b_1 - b_2)}\,, \qquad R_2 = \frac{2b_4(b_1 - b_2 - b_3)}{b_1(b_1 - b_2)}\,, \\ &R_3 = \frac{2b_3 b_4}{b_1(b_1 - b_2)}\,, \qquad R_4 = \frac{2b_3(b_1 - b_2 - b_4)}{b_1(b_1 - b_2)}\,, \qquad R_5 = \frac{2b_2}{b_1}\,, \end{aligned} \tag{6.179}$$

so they satisfy

$$\sum_{a=1}^{5} R_a = 2\,, \qquad R_1 R_3 - R_2 R_4 = 0\,. \tag{6.180}$$

Note that the second constraint implements the partial extremization over the baryonic directions in field theory. Finally, the Kähler class parameter defined in (6.48) can be expressed

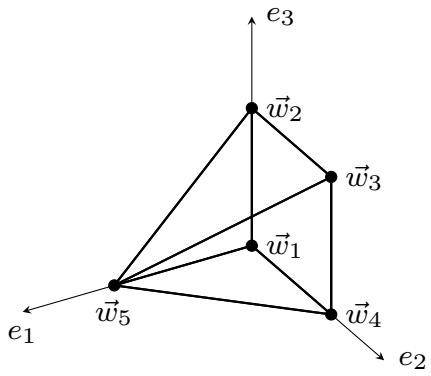


Figure 6.8: Toric diagram for $\mathbb{C} \times C(T^{1,1})$.

in terms of the R-charges as

$$\Lambda = \frac{\ell_p^3 N^{1/2} \pi}{2} \sqrt{\frac{2(R_1+R_2)(R_3+R_4)(R_1+R_4)(R_2+R_3)R_5}{R_1+R_2+R_3+R_4}} \,. \tag{6.181}$$

Notice that the denominator may also be expressed as $2 - R_5$.

6.5.3.1 Flavoured $U(N)$

Geometry The first choice of $U(1)_M$ action we consider has weights $(1, -1, 0, 0, 0)$ on the complex coordinates z_a in the ambient space of the GIT quotient defining $C(X_7)$ (see appendix A.1), which are rotated by $\partial_{\phi_a} \equiv \nu_a = \sum_i v_{ai}\, \partial_{\varphi_i}$ [137]. Using the toric data (6.176), the M-theory circle action therefore reads

$$\zeta_M = -\partial_{\varphi_4} \,. \tag{6.182}$$

For this choice of ζ_M and toric data (6.176), (6.160) admit two non-trivial solutions for β,[23] which we multiply by Λ to obtain τ

$$\tau_{\min} = -\frac{2\Lambda}{R_2+R_3} \,, \qquad \tau_{\max} = \frac{2\Lambda}{R_1+R_4} \,. \tag{6.183}$$

The non-zero α_a coefficients for these solutions are $\{\alpha_1, \alpha_4, \alpha_5\}$ and $\{\alpha_2, \alpha_3, \alpha_5\}$ respectively, which is reflected by the vertices in Figure 6.9. Note that $\beta = \tau/\Lambda = 0$ is also a solution for

[23] In practice we solve the system in terms of b_i and then convert the results in the R_a variables using (6.179).

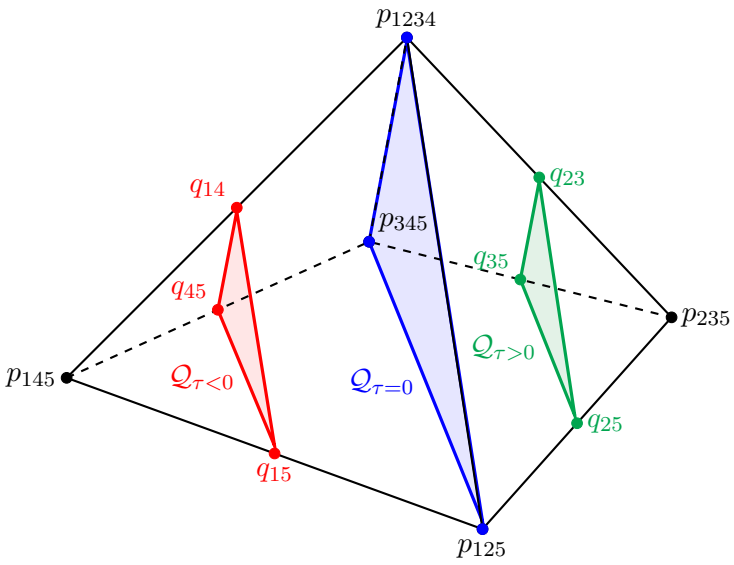


Figure 6.9: Pyramid describing $\mathbb{C} \times C(T^{1,1})$ and its slicing corresponding to flavoured $U(N)$. The red slice is $\mathcal{Q}_\tau$ for $\tau_{\min} < \tau < 0$, the blue slice for $\tau = 0$, and the green slice for $0 < \tau < \tau_{\max}$. Each vertex p_{abc} denotes the intersection of the facets $\mathcal{P}_a$, $\mathcal{P}_b$, $\mathcal{P}_c$, and the Reeb hyperplane. The perimeter of $\mathcal{Q}_\tau$ varies with τ qualitatively as ρ in Figure 6.3.

either $\{\alpha_1, \alpha_2\}$ or $\{\alpha_3, \alpha_4\}$ non-vanishing. Recall that these results also correspond to the action of BPS M2-branes via (6.131).

Next we want to obtain the full distribution ρ by solving the system (6.167). We find solutions for $\{q_{14}, q_{15}, q_{45}, q_{23}, q_{25}, q_{35}\}$. We do not report the explicit expressions of the vertices as they are not particularly insightful. They have a similar structure to the ones presented in the examples of section 6.3.3. Further imposing the inequalities (6.168), we find that the first three solutions are the vertices of $\mathcal{Q}_\tau$ for $\tau \in [\tau_{\min}, 0]$, while the last three define $\mathcal{Q}_\tau$ for $\tau \in [0, \tau_{\max}]$, where we reproduce the expression of $\tau_{\min}$, $\tau_{\max}$ in (6.183). $\mathcal{Q}_\tau$ is therefore a triangle in both regions, and its area can be computed via the determinant (6.170) first for $\{q_{14}, q_{15}, q_{45}\}$ and then for $\{q_{23}, q_{25}, q_{35}\}$, see Figure 6.9. Finally taking the Λ derivative to obtain the perimeter and normalizing by the appropriate factor (6.175) gives the geometrical density

$$\rho(t) = \frac{1}{\ell_p^3 N^{1/2}} \left\{ \begin{array}{ll} \dfrac{2\Lambda + (R_2 + R_3)\tau}{\pi^2 (R_1 + R_2)(R_3 + R_4) R_5}\,, & \tau_{\min} < \tau < 0 \\ \dfrac{2\Lambda - (R_1 + R_4)\tau}{\pi^2 (R_1 + R_2)(R_3 + R_4) R_5}\,, & 0 < \tau < \tau_{\max} \end{array} \right| \Bigg|_{\tau = \ell_p^3 N^{1/2} t} . \tag{6.184}$$

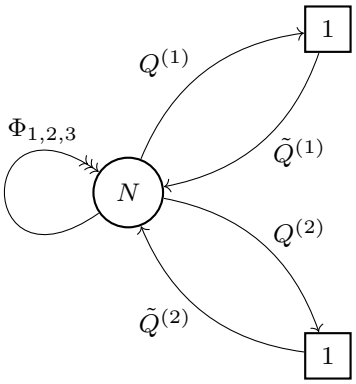


Figure 6.10: Quiver diagram of the flavoured U(N) theory.

Field theory The dual field theory to this geometry is a flavoured $U(N)$ theory which contains two pairs of fundamental chiral fields $\{Q^{(1)}, \tilde{Q}^{(1)}\}$, $\{Q^{(2)}, \tilde{Q}^{(2)}\}$ and three adjoint chiral fields Φ_i, $i = 1, 2, 3$, see Figure 6.10, and has superpotential

$$W = \mathrm{Tr}\left[\Phi_1[\Phi_2, \Phi_3] + \tilde{Q}^{(1)}\Phi_1 Q^{(1)} + \tilde{Q}^{(2)}\Phi_2 Q^{(2)}\right], \tag{6.185}$$

such that

$$T\tilde{T} = \Phi_1\Phi_2 \implies \Delta_T + \Delta_{\tilde{T}} = \Delta_{\Phi_1} + \Delta_{\Phi_2}\,. \tag{6.186}$$

The matrix models quantities were derived in [144] and read

$$t_{\min} = -\frac{\mu}{\Delta_{\tilde{T}}}\,, \qquad t_{\max} = \frac{\mu}{\Delta_T}\,, \tag{6.187}$$

$$\rho(t) = \begin{cases} \dfrac{\mu + \Delta_{\tilde{T}} t}{\pi^2 \Delta_{\Phi_1}\Delta_{\Phi_2}\Delta_{\Phi_3}}\,, & t_{\min} < t < 0\,, \\ \dfrac{\mu - \Delta_T t}{\pi^2 \Delta_{\Phi_1}\Delta_{\Phi_2}\Delta_{\Phi_3}}\,, & 0 < t < t_{\max}\,, \end{cases}, \tag{6.188}$$

with

$$\mu = \pi\sqrt{\frac{2\Delta_{\Phi_1}\Delta_{\Phi_2}\Delta_{\Phi_3}\Delta_T\Delta_{\tilde{T}}}{\Delta_T + \Delta_{\tilde{T}}}}\,. \tag{6.189}$$

Matching The field theory and geometrical parameters are related as [119]

$$\begin{aligned} \Delta_{\Phi_1} = R_1 + R_2\,, \quad \Delta_{\Phi_2} = R_3 + R_4\,, \quad \Delta_{\Phi_3} = R_5\,, \\ \Delta_T = R_1 + R_4\,, \quad \Delta_{\tilde{T}} = R_2 + R_3\,. \end{aligned} \tag{6.190}$$

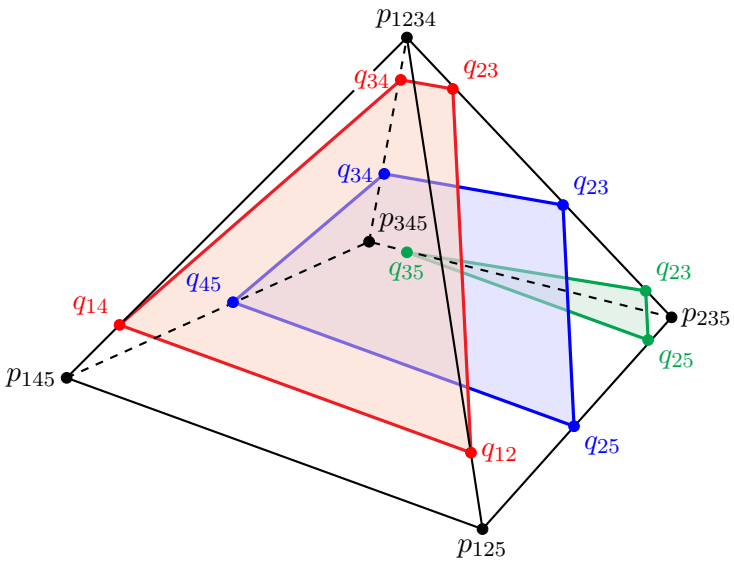


Figure 6.11: Pyramid describing $\mathbb{C}\times C(T^{1,1})$ and its slicing corresponding to flavoured ABJM. The red slice is $\mathcal{Q}_\tau$ for $\tau_1 < \tau < \tau_2$, the blue slice for $\tau_2 < \tau < \tau_3$, and the green slice for $\tau_3 < \tau < \tau_4$. Each vertex p_{abc} denotes the intersection of the facets $\mathcal{P}_a$, $\mathcal{P}_b$, $\mathcal{P}_c$, and the Reeb hyperplane. Note that we do not draw the slice at $\tau = \tau_2 = 0$, where $q_{14} = q_{45} = p_{145}$ and $q_{12} = q_{25} = p_{125}$.

As expected, under this identification, $\mu = 2\Lambda/(\ell_p^3 N^{1/2})$. It is then easy to see that the discontinuity points of $\rho'(t)$ match, and also that we reproduce $\rho(t)$.

6.5.3.2 Flavoured ABJM

Geometry A second possible choice of $U(1)_M$ is to have weights $(1,0,0,0,-1)$ on z_a, which using the toric data (6.176) reads on the cone

$$\zeta_M = -\partial_{\varphi_2}\,. \tag{6.191}$$

In the following we assume $R_4 < R_2$. Solving (6.160) for this choice of M-theory circle gives four solutions (recall $\tau = \Lambda\beta$)

$$\tau_1 = -\frac{2\Lambda}{R_5}\,, \quad \tau_2 = 0\,, \quad \tau_3 = \frac{2\Lambda}{R_1+R_2}\,, \quad \tau_4 = \frac{2\Lambda}{R_1+R_4}\,, \tag{6.192}$$

and associated non-zero α_a, $\{\alpha_1,\alpha_2,\alpha_3,\alpha_4\}$, $\{\alpha_1,\alpha_5\}$, $\{\alpha_3,\alpha_4,\alpha_5\}$ $\{\alpha_2,\alpha_3,\alpha_5\}$, respectively, as clearly appears in Figure 6.11. Physically these results correspond to the value of the

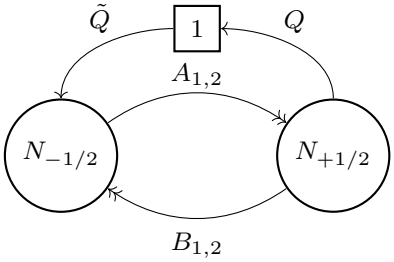


Figure 6.12: Quiver diagram for the flavoured ABJM theory.

action of BPS probe M2-branes.

To reproduce ρ we turn to the system (6.167), which in this case admits solutions for any pair of neighbouring v_a, except for q_{15}. The M-theory hyperplane therefore slices the toric polytope parallel to the edge between $\mathcal{P}_1$ and $\mathcal{P}_5$ as shown in Figure 6.11. Then from the inequalities (6.168), we find that $\mathcal{Q}_\tau$ has vertices $\{q_{12}, q_{23}, q_{34}, q_{14}\}$, $\{q_{25}, q_{23}, q_{34}, q_{45}\}$, $\{q_{25}, q_{23}, q_{35}\}$ in the regions $[\tau_1, \tau_2]$, $[\tau_2, \tau_3]$, $[\tau_3, \tau_4]$ respectively, where we recover the values of τ from (6.192). In the regions where $\mathcal{Q}_\tau$ is quadrilateral the area is computed by splitting into two triangles, and summing the two areas computed via the determinant (6.170). After taking the derivative and normalizing properly, see (6.175), we deduce that the density is given by

$$\rho(t) = \frac{1}{\ell_p^3 N^{1/2}} \left\{ \begin{array}{ll} \frac{4\Lambda+2R_5\tau}{\pi^2(R_2+R_3)(R_3+R_4)(R_1+R_5+R_2)(R_1+R_5+R_4)}\,, & \tau_1<\tau<\tau_2 \\ \frac{4\Lambda-(2R_1+R_2R_4-R_3(R_1+R_5))\tau}{\pi^2(R_2+R_3)(R_3+R_4)(R_1+R_5+R_2)(R_1+R_5+R_4)}\,, & \tau_2<\tau<\tau_3 \\ \frac{2\Lambda-(R_1+R_4)\tau}{\pi^2(R_2-R_4)(R_4+R_3)(R_1+R_5+R_4)}\,, & \tau_3<\tau<\tau_4 \end{array} \right|_{\tau=\ell_p^3 N^{1/2}\, t} . \tag{6.193}$$

Field theory The field theory dual to $\mathbb{C}\times C(T^{1,1})$ equipped with the M-theory circle (6.191) is an instance of the flavoured ABJM theory. That is the Model II with an additional pair of fundamental chiral fields $(Q, \tilde{Q})$ and with Chern-Simons level $(-1/2, 1/2)$ [137].[24] The quiver diagram is shown in Figure 6.12. The superpotential is the ABJM superpotential,

[24]The half-integer level is needed to cancel the parity anomaly due to the additional pair of chiral fields. Note that we exchange k and $-k$ compared to [137], according to the prescription in table 1 of [143].

plus a deformation term

$$W = \mathrm{Tr}\left[A_1 B_1 A_2 B_2 - A_1 B_2 A_2 B_1 + Q A_1 \tilde{Q}\right], \tag{6.194}$$

$$T\tilde{T} = A_1 \implies \Delta_T + \Delta_{\tilde{T}} = \Delta_{A_1}\,. \tag{6.195}$$

The field theory results for this model were derived in [4]. Assuming $\Delta_{B_1} < \Delta_{B_2}$ we have

$$\begin{aligned} t_1 &= -\frac{\mu}{\Delta_{\tilde{T}}}\,, & t_2 &= 0\,, \\ t_3 &= \frac{\mu}{\Delta_T + \Delta_{B_2}}\,, & t_4 &= \frac{\mu}{\Delta_T + \Delta_{B_1}}\,. \end{aligned} \tag{6.196}$$

$$\rho(t) = \begin{cases} \frac{2\mu + 2\Delta_{\tilde{T}} t}{\pi^2 (\Delta_{A_1}+\Delta_{B_1})(\Delta_{A_1}+\Delta_{B_2})(\Delta_{A_2}+\Delta_{B_1})(\Delta_{A_2}+\Delta_{B_2})}\,, & t_1 < t < t_2\,, \\ \frac{2\mu - (2\Delta_T + \Delta_{B_1}\Delta_{B_2} - \Delta_{A_1}\Delta_{A_2})t}{\pi^2 (\Delta_{A_1}+\Delta_{B_1})(\Delta_{A_1}+\Delta_{B_2})(\Delta_{A_2}+\Delta_{B_1})(\Delta_{A_2}+\Delta_{B_2})}\,, & t_2 < t < t_3\,, \\ \frac{\mu - (\Delta_T + \Delta_{B_1})t}{\pi^2 (\Delta_{A_1}+\Delta_{B_1})(\Delta_{A_2}+\Delta_{B_1})(\Delta_{B_2}-\Delta_{B_1})}\,, & t_3 < t < t_4\,. \end{cases} \tag{6.197}$$

$$\mu = \pi \sqrt{\frac{2(\Delta_{A_2}+\Delta_{B_1})(\Delta_{A_2}+\Delta_{B_2})(\Delta_T+\Delta_{B_1})(\Delta_T+\Delta_{B_2})\Delta_{\tilde{T}}}{2-\Delta_{\tilde{T}}}}\,. \tag{6.198}$$

Matching Finally, the parameters on both sides are related by [127][25]

$$\begin{aligned} \Delta_{A_1} = R_1 + R_5\,, \quad \Delta_{A_2} = R_3\,, \quad \Delta_{B_1} = R_4\,, \quad \Delta_{B_2} = R_2\,, \\ \Delta_T = R_1\,, \quad \Delta_{\tilde{T}} = R_5\,, \end{aligned} \tag{6.199}$$

such that again, $\mu = 2\Lambda/(\ell_p^3 N^{1/2})$, t and τ match and we exactly reproduce ρ in the geometry. Note that the orderings we assumed on each side, namely $R_4 < R_2$ and $\Delta_{B_1} < \Delta_{B_2}$, are equivalent.

[25] Note we used a different toric basis from [127]. In particular, we have $R_1 = \Delta_1^{\text{there}}$, $R_2 = \Delta_3^{\text{there}}$, $R_3 = \Delta_5^{\text{there}}$, $R_4 = \Delta_2^{\text{there}}$, $R_5 = \Delta_4^{\text{there}}$.

Chapter 7

Discussion and outlook

In this thesis we studied generic AdS_3 and AdS_2 solutions arising from wrapping D3-branes and M2-branes respectively on a spindle and can be interpreted as the near-horizon geometry of accelerating black strings and black holes. These general classes of solutions include some explicit examples that have been found earlier in lower dimensional gauged supergravity and then uplifted to type IIB or 11d supergravity. Thanks to various geometric techniques applied to the extremal problem defined in GK geometry we were able to derive general features of such geometries and exploit them in the study of their holographic dual theories. One of our main results is the formula (3.1) which, in particular, gives rise to the gravitational block form for the supersymmetric action as given in (3.11). By setting $m_\pm = 1$, this formula is also valid if the spindle is replaced with a two-sphere, giving a new perspective on some of the results on GK geometry presented in [70, 119, 127, 132, 158]. These results provide a concrete demonstration that gravitational blocks appear very generally in the context of M2 and D3-branes reduced on two-dimensional spaces with an azimuthal symmetry.

A crucial point that our extremal problem analysis does not touch upon is that of the existence of such solutions. Indeed, a key assumption of our results is that the corresponding AdS solutions exist but there may be obstructions to this. Ultimately, one needs an existence result for the corresponding PDE (1.24), possibly resulting in additional constraints on physical quantities such as the geometric R-charges. One may hope to gain insights to this end by looking at explicit spindle solutions in lower dimensional gauged supergravities which uplift on X_{2n-1}. Therefore, finding new such solutions and comparing them with the results presented here could be a very useful endeavour for future studies. Moreover, as a further reseach direction along these lines, it would be extremely important to find solutions for the full black holes/strings. This would serve to corroborate our claim that the geometries studied in this thesis describe their near-horizon region - especially in the black string case for which no explicit accelerating solution is know to date.

Other intriguing directions for future work would involve attempting a similar analysis with different physical setups. For example, a certain class of $\mathrm{AdS}_3 \times M_8$ solutions of M-theory, which was described in [159], gives rise to 2d $\mathcal{N} = (0, 2)$ SCFTs too and it is conceivable that a geometric extremization principle dual to c-extremization exist there too.[1] In particular, when M_8 is a fibration over a spindle (for example a 4-sphere fibered over a product of a spindle and Riemann surface as in the M5 solution in [1]) we expect the central charge to likewise get contributions from two blocks. Another interesting case would be that of $\mathrm{AdS}_2 \times Y_9$ solutions with the internal space fibered over AdS_2 [160] which from a physical perspective would amount to considering black holes in AdS_4 that are rotating and/or electrically charged too.

A further interesting development could be extend the analysis to subleading orders in the large N expansion. Precision holography has had many interesting developments over the last few years, both on the gravity and the field theory side [161–164]. In particular, in gravity these subleading contributions to physical observables arise from higher curvature terms in the supergravity action. This means that one would have to check whether the GK backgrounds are solutions of the higher derivative theory, and in case they are not modify them accordingly. Unfortunately, not all corrections to type IIB and 11d supergravity are currently known, so it is difficult to reach any conclusion on this matter at the moment.

For the $\mathrm{AdS}_3 \times Y_7$ class of toric GK geometries in type IIB string theory discussed in chapter 5, we have obtained a general proof that our off-shell supersymmetric action agrees with the off-shell trial c-function in field theory, thus obtaining a very general exact result in AdS/CFT. It would be interesting to extend this result to the non-toric setting, which would likely require a reformulation of the quantized fluxes discussion in terms of equivariant cohomology as explained in appendix A.2.

For the $\mathrm{AdS}_2 \times Y_9$ class of GK geometries in M-theory discussed in chapter 6, we identified the imaginary part t of the continuously distributed eigenvalues in the dual matrix model, and their density function $\rho(t)$, with natural geometric quantities associated with the M-theory circle action $U(1)_M$ on Y_9. Moreover, we argued that the points where $\rho'(t)$ is discontinuous

[1] Some work in this direction, albeit with a different approach based on equivariant localization in supergravity, was carried out recently (see [101, 102]).

match with the classical action of BPS probe M2-branes wrapping AdS_2 and the M-theory circle. These results provide an interesting extension of the holographic dictionary. Perhaps the most interesting open question is to further match quantities in the matrix model to quantities in gravity. For example, it seems likely that there is also a simple geometric characterization of the fluxes $\mathfrak{s}(t)$ that appear in the refined/spindle case. One also expects a more direct holographic interpretation of these variables, and of the density function $\rho(t)$. Our analysis suggests a somewhat direct physical interpretation on the gravity side. Specifically, the near-horizon solutions are sourced by N M2-branes, where in AdS/CFT the brane sources disappear and are replaced by N units of dissolved flux over the internal space. On the other hand, in type IIA we have N D2-branes, where $h_M \sim t$ is the location of the D2-branes (before the back-reaction and near-horizon limit). This suggests that the eigenvalue density $\rho(t)$ is also playing the role of a density function directly in the gravity dual, describing how the dissolved D2/M2-branes are distributed in the internal space. We leave this speculation for future work.

Other extensions of our geometric interpretation of the matrix models involve a generalization to different setups. Firstly, one could ask what happens when the flavour twist condition (6.47) is lifted and therefore the transverse Kähler class is allowed to be very general. However, for this setup it is currently not even understood how to match the black hole entropy to a localization computation in field theory. In fact, in this thesis we found a new related puzzle in interpreting correctly the action of probe M2-branes as soon as we are outside the flavour twist - see the discussion at the end of section 6.3.4.1. Understanding how to properly treat this case would certainly be illuminating. Secondly, one could try to use our gravitational analysis to gain insights into chiral field theories. Such theories result in localized matrix models where long-range interactions among eigenvalues do not cancel out and therefore it has so far been impossible to find any eigenvalue density [165]. On the other hand, the gravity duals are not any different from those we talked about in this thesis - for example the case with $X_7 = M^{1,1,1}$ gives rise to a $U(N)^3$ gauge theory with nine bi-fundamental fields which is chiral.[2] Therefore, all of our discussion in gravity goes through unchanged and a $\rho(t)$ could be defined from the volume of the Kähler quotient as

[2]This example was considered from a geometric extremization perspective in [166].

in (6.102). Finally, there are certain 3d field theories with a free energy that, at large N, scales as $N^{5/3}$ rather than $N^{3/2}$. Such theories are dual to AdS_2 backgrounds in massive type IIA supergravity and therefore they do not admit any uplift to 11d and no M-theory circle is present. However, from a purely field theory perspective the corresponding matrix models are not particularly different from those considered in the present thesis, thus one might expect a similar geometric construction to be possible in that context.

Appendix A

Appendices

A.1 Delzant construction

To see that the toric data (4.22) describes a fibration (4.19), we can utilize the Delzant construction for toric cones (see *e.g.* [27]). We first recall this construction for $C(X_{2n-1})$ where, for simplicity, we assume X_{2n-1} is simply-connected. There is a linear map

$$\mathcal{A}^{(n)} : \mathbb{R}^d \to \mathbb{R}^n \ , \qquad \mathcal{A}^{(n)}(e_a) = v_a \in \mathbb{R}^n \ , \tag{A.1}$$

where $\{e_a\}$ denotes the standard orthonormal basis for $\mathbb{R}^d$, with components $e_{ab} = \delta_{ab}$, and $v_a = (v_{ai})_{i=1}^n$ are the toric data for X_{2n-1}, where in what follows it will be convenient to suppress the vector index i on v_a (which are the components of v_a in a basis for the Lie algebra of $U(1)^n$). Since $\mathcal{A}^{(n)}$ maps $\mathbb{Z}^d$ to $\mathbb{Z}^n$, there is an induced map of tori $U(1)^d = \mathbb{R}^d/\mathbb{Z}^d \to \mathbb{R}^n/\operatorname{span}_{\mathbb{Z}}\{v_a\}$, with a kernel $U(1)^{d-n}$.The latter is generated by an integer $d \times (d-n)$ matrix q_I^a, $I = 1, \ldots, d-n$, satisfying

$$\sum_{a=1}^{d} q_I^a \, v_{ai} = 0 \, , \qquad i = 1, \ldots, n \, , \tag{A.2}$$

which specifies the embedding $U(1)^{d-n} \subset U(1)^d$. The toric $U(1)^n$ action on $C(X_{2n-1})$ is then via the quotient $U(1)^n = U(1)^d/U(1)^{d-n}$. In physics language, the above construction describes a gauged linear sigma model (GLSM) with d complex fields and $U(1)^{d-n}$ charges specified by q_I^a, with $C(X_{2n-1})$ being the vacuum moduli space (see *e.g.* [27]).

For a toric $C(Y_{2n+1})$ there is then a similar construction, with linear map

$$\mathcal{A}^{(n+1)} : \mathbb{R}^D \to \mathbb{R}^{n+1} \ , \qquad \mathcal{A}^{(n+1)}(e_A) = v_A \in \mathbb{R}^{n+1} \ , \tag{A.3}$$

with standard orthonormal basis $\{e_A\}$ of $\mathbb{R}^D$, with components $e_{AB} = \delta_{AB}$, toric data $v_A =$

$(v_{A\mu})_{\mu=0}^{n}$ for $C(Y_{2n+1})$, and with a kernel specified by an integer $D\times(D-n-1)$ matrix $Q_{\hat{I}}^{A}$, $\hat{I}=0,1,\ldots,d-n$, satisfying

$$\sum_{A=1}^{D} Q_{\hat{I}}^{A}\, v_{A\mu} = 0\,, \qquad \mu = 0,1,\ldots,n\,. \tag{A.4}$$

From (4.22), which recall relates the toric data for $C(Y_{2n+1})$ in terms of that for $C(X_{2n-1})$, the spindle data $m_{\pm}$, and the twisting variables p_i, $a_{\pm}$, we identify part of this kernel:

$$Q_I = (0,0,q_I^1,\ldots,q_I^d)\ , \qquad I=1,\ldots,d-n\,. \tag{A.5}$$

Note here that this satisfies (A.4) by virtue of (A.2), where $v_a=(1,\vec{w}_a)$. Since $\hat{I}$ takes $D-n-1=d+1-n$ values and $I=1,\ldots,d-n$, there is one more kernel vector to identify, which we label as the $\hat{I}=0$ component of $Q_{\hat{I}}^{A}$. We write this charge vector as

$$Q_0 = (m_-,\sigma m_+,q_0^1,\ldots,q_0^d)\ . \tag{A.6}$$

Notice here that the first two entries are fixed by the 0-th components of the vectors in (4.22). From (4.22) and (A.4) we see that Q_0 is a kernel vector provided that the vector q_0^a satisfies

$$\sum_{a=1}^{d} q_0^a\, v_{ai} \;=\; p_i\ , \qquad i=1,\ldots,n\,, \tag{A.7}$$

where we recall from (4.20) that $p_1=-(m_-+\sigma m_+)$, with $\sigma=+1$ being the twist, and $\sigma=-1$ being the anti-twist. In fact the above equations are precisely describing the fibration (4.19) in a two step process, as we now describe.

To begin, recall that to fibre $C(X_{2n-1})$ over a spindle $\Sigma=\mathbb{WCP}^1_{[m_-,m_+]}$, we may first fibre $\mathbb{C}^d$ over Σ. To do so we must first lift the $U(1)^n$ action on $C(X_{2n-1})$ to $\mathbb{C}^d$, which means specifying n vectors $\alpha^i=(\alpha_a^i)_{a=1}^d\in\mathbb{Z}^d$, $i=1,\ldots,n$ satisfying

$$\mathcal{A}^{(n)}(\alpha^i)=e_i\in\mathbb{Z}^n\ , \tag{A.8}$$

where $\{e_i\}$ is the standard orthonormal basis for $\mathbb{R}^n$. In components this condition reads

$$\sum_{a=1}^{d} v_{ai}\, \alpha_a^j = \delta_i^j \ . \tag{A.9}$$

Of course the choice of each $\alpha^i \in \mathbb{Z}^d$, $i = 1, \ldots, n$, is unique only up to the kernel of $\mathcal{A}^{(n)}$, generated by q_I^a. Geometrically, this is because $C(X_{2n-1})$ is precisely a Kähler quotient of $\mathbb{C}^d$ via the torus $U(1)^{d-n}$ generated by this kernel. Put more simply, the charge of the a-th coordinate z^a of $\mathbb{C}^d$ under the i-th $U(1) \subset U(1)^n$ is precisely α_a^i.

With this in hand, we now re-examine (A.7) and the kernel $Q_{\hat{I}}^A$. We first consider the twist case. The GLSM for $C(Y_{2n+1})$ begins with $\mathbb{C}^D = \mathbb{C}^{d+2}$. Taking the quotient by $U(1)$ with charge vector Q_0 given by (A.6) then describes the total space of a $\mathbb{C}^d$ bundle over Σ, where the charge vector q_0^a describes the twisting. That is, as a first step we construct the $(d+1)$-dimensional space

$$Z \ \equiv \ \mathcal{O}(q_0^a)_\Sigma \times_{U(1)^d} \mathbb{C}^d \ . \tag{A.10}$$

Here the notation means we twist the a-th coordinate of $\mathbb{C}^d$ by the line bundle $O(q_0^a)_\Sigma$. The 0-th component of the condition (A.7) then simply says that Z is a Calabi-Yau $(d+1)$-fold. Notice here that $q_0^a < 0$ is necessary for the convex toric geometry description we have given to be applicable, although the space Z defined by (A.10) exists as a complex manifold with zero first Chern class irrespective of the signs of the charges.

In the anti-twist case, with $\sigma = -1$, the charge of the second coordinate on $\mathbb{C}^D = \mathbb{C}^{d+2}$ under Q_0 in (A.6) is negative. Taking the Kähler quotient by this $U(1)$ then does not result in a space with the topology given in (A.10). Formally, we may complex conjugate the second coordinate on $\mathbb{C}^D$, to see that topologically Z given by (A.10) is a partial resolution of the conical geometry in the anti-twist case. However, the space Z is then no longer Calabi-Yau, since $\sum_{a=1}^d q_0^a$ is not equal to $-(m_- + m_+)$ when $\sigma = -1$.[1] This lack of any clear relation to a partially resolved Calabi-Yau geometry, with a blown up copy of Σ on which the branes may wrap, is one reason why the anti-twist solutions are more difficult to interpret physically.

[1] This was discussed in some details in [71] for various solutions where $d = n$ and $C(X_{2n-1}) = \mathbb{C}^n$.

Returning to the twist case with $\sigma = +1$, at this stage we have quotiented by $U(1)$ out of $U(1)^{d+1-n}$ to obtain a Calabi-Yau $(d+1)$-fold Z, which is a $\mathbb{C}^d$ fibration over the spindle Σ. Quotienting by the remaining $U(1)^{d-n} = U(1)^{d+1-n}/U(1)$ then precisely turns the fibre $\mathbb{C}^d$ into $C(X_{2n-1})$ – this is clear from (A.5), which only acts on the $\mathbb{C}^d$ fibre direction of Z. Since $\mathbb{C}^d$ is fibred non-trivially over the spindle, the $C(X_{2n-1})$ will also be fibred, and equation (A.7) is telling us how. Specifically, this condition is solved by writing

$$q_0^a = \sum_{i=1}^{n} p_i \, \alpha_a^i \ . \tag{A.11}$$

The fact this solves (A.7) follows from (A.9):

$$\sum_{a=1}^{d} q_0^a \, v_{ai} = \sum_{a=1}^{d} \sum_{j=1}^{n} p_j \, \alpha_a^j \, v_{ai} = p_i \ , \qquad i = 1, \ldots, n \, . \tag{A.12}$$

Geometrically, recall that α_a^i gives the charge of the a-th coordinate on $\mathbb{C}^d$ under the i-th $U(1)$ in $U(1)^n$. Thus $\vec{p} = (p_2, \ldots, p_n)$ precisely has the interpretation of twisting $\mathbb{C}^d$ by the line bundle $O(\vec{p})_\Sigma$, so that we may also write

$$Z = O(\vec{p})_\Sigma \times_{U(1)^n} \mathbb{C}^d \ , \tag{A.13}$$

where q_0 in (A.10) is specified by (A.11). The vacuum moduli space with the full quotient is

$$O(\vec{p})_\Sigma \times_{U(1)^n} C(X_{2n-1}) \ . \tag{A.14}$$

In the anti-twist case this last quotient of $\mathbb{C}^d$ by $U(1)^{d-n}$ to obtain the Calabi-Yau cone fibres $C(X_{2n-1})$ is still valid, but the space in (A.14), while being a partial resolution of $C(Y_{2n+1})$, is no longer Calabi-Yau.

A.2 Fluxes from Kaluza-Klein reduction

In this appendix we expand further on how flavour and baryonic fluxes arise from Kaluza-Klein reduction in $\mathrm{AdS}_4 \times X_7/\mathrm{AdS}_5 \times X_5$ solutions with $n = 4$, $n = 3$, respectively, and

in particular analyze the relation (4.55) for the toric fluxes M_a from this point of view. This expands on the discussion in [167] (see also [168, 169]), to make contact with some flux formulas that appear in this thesis. Here we relate fluxes in a linearized Kaluza-Klein analysis around $\mathrm{AdS}_4\times X_7/\mathrm{AdS}_5\times X_5$ solutions, to fluxes in near horizon $\mathrm{AdS}_2\times Y_9/\mathrm{AdS}_3\times Y_7$ solutions – while one cannot directly compare the solutions at this level, the fluxes are quantized, and hence one should be able to make such a matching; and indeed, we find a consistent picture.

Let us consider Kaluza-Klein reduction of, respectively, Type IIB and 11d supergravity on a Sasaki-Einstein manifold X_{2n-1} with $U(1)^s$ isometry. As explained in [167], we obtain a supergravity theory with an $\mathrm{AdS}_5/\mathrm{AdS}_4$ vacuum, with massless gauge fields A_a, where a runs from 1 to $d \equiv s + b_{2n-3}$, where b_{2n-3} is the $(2n-3)$-th Betti number *i.e.* $b_{2n-3} \equiv \dim H_{2n-3}(X_{2n-1}, \mathbb{R})$. Such gauge fields appear in the expansion of the $(2n-2)$-form potential

$$C_{2n-2} = \left[\frac{2\pi}{V}\,\mathrm{vol}_{X_{2n-1}} + \sum_{a=1}^{d} A_a \wedge \omega_a + \cdots\right] \frac{\nu_n L^{2n-2}}{(5-n)2\pi} N\,. \tag{A.15}$$

Here $V \equiv \mathrm{Vol}_{SE}(X_{2n-1})$ and $\mathrm{vol}_{X_{2n-1}}$ is the volume form on X_{2n-1}, coming from the AdS background, and the terms in the $\cdots$ are not relevant for our discussion. The remaining term $\sum_{a=1}^{d} A_a \wedge \omega_a$ is the KK fluctuation term, where ω_a are $(2n-3)$-forms satisfying [167]

$$\mathrm{d}\omega_a = \sum_{i=1}^{s} v_{ai}\, \partial_{\varphi_i} \lrcorner\, \mathrm{vol}_{X_{2n-1}}\,, \tag{A.16}$$

$$\mathrm{d} *_{2n-1} \omega_a = 0\,. \tag{A.17}$$

The v_{ai} are constants, and in the case that X_{2n-1} is toric, *i.e.* $s = n$, they are precisely the toric data [167]. While we expect everything in this appendix to be true in general, for concreteness we assume that X_{2n-1} is toric so as to be able to make use of various toric formulas that appear in the main text, and appendix A.1.

In general, quantities labelled by the index a can be split into linear combinations of quantities labelled by an index i, $i = 1, \ldots, s$, and those labelled by an index I, $I = 1, \ldots, b_{2n-3}$.

We thus begin by writing

$$A_a = \sum_{i=1}^{s} \alpha_a^i \, A_i + \sum_{I=1}^{b_{2n-3}} q_I^a A_I \, , \tag{A.18}$$

$$\omega_a = \sum_{i=1}^{s} v_{ai} \, \omega_i + \sum_{I=1}^{b_{2n-3}} m_I^a \, \omega_I \, . \tag{A.19}$$

Here in (A.18) we take α_a^i and the baryonic charge matrix q_I^a to be the quantities introduced in appendix A.1. This is then precisely what one means by a splitting into "flavour" and "baryonic" symmetries: by definition α_a^i is the charge of the a-th coordinate z^a of the GLSM $\mathbb{C}^d$ under the i-th $U(1) \subset U(1)^s$, while q_I^a is the charge of this coordinate under the I-th baryonic symmetry. By definition, these then couple to the flavour gauge field A_i and baryonic gauge field A_I, respectively, as in (A.18). Similarly, in (A.19) we take the ω_I to be harmonic $(2n-3)$-forms, constituting a basis of $H^{2n-3}(X_{2n-1}, \mathbb{R})$ and such that $\int_{\mathcal{C}_I} \omega_J = \delta_{IJ}$ for $\mathcal{C}_I$ a basis for the free part of $H_{2n-3}(X_{2n-1}, \mathbb{Z})$, while ω_i satisfy

$$\mathrm{d}\omega_i = \partial_{\varphi_i} \lrcorner \, \mathrm{vol}(X_{2n-1}) \, . \tag{A.20}$$

This then ensures that (A.16) holds. Moreover, taking the v_{ai} and m_I^a to satisfy the relations

$$\sum_{a=1}^{d} v_{ai} \, \alpha_a^j = \delta_i^j \, , \qquad \sum_{a=1}^{d} v_{ai} \, q_I^a = 0 \, , \tag{A.21}$$

$$\sum_{a=1}^{d} q_I^a \, m_J^a = \delta_{IJ} \, , \qquad \sum_{a=1}^{d} \alpha_a^i \, m_I^a = 0 \, , \tag{A.22}$$

then gives the projections

$$A_i = \sum_{a=1}^{d} v_{ai} \, A_a \, , \qquad A_I = \sum_{a=1}^{d} m_I^a A_a \, , \tag{A.23}$$

$$\omega_i = \sum_{a=1}^{d} \alpha_a^i \, \omega_a \, , \qquad \omega_I = \sum_{a=1}^{d} q_I^a \, \omega_a \, . \tag{A.24}$$

The forms ω_i and ω_I are then precisely the projections onto flavour and baryonic directions, respectively. The relations in (A.21) are precisely those in appendix A.1, where v_{ai} give the

toric data for X_{2n-1}. In particular, recall that α_a^j are not unique, precisely due to the kernel generated by q_I^a. On the other hand, in the first equation in (A.22) the baryonic charges q_I^a, $I = 1, \ldots, b_{2n-3}$, are by definition linearly independent, and m_J^a is simply a choice of inverse. Due to the second equation in (A.21) we are free to shift $m_I^a \to m_I^a - \sum_{i=1}^s c_i^I v_{ai}$, and using this freedom one can then always impose the second equation in (A.22). Notice, however, that we are still free to make the following simultaneous shifts, without changing A_a and ω_a:

$$A_I \;\to\; A_I - \sum_{i=1}^{s} c_i^I \, A_i \,, \qquad \omega_i \;\to\; \omega_i + \sum_{I=1}^{b_{2n-3}} c_i^I \, \omega_I \,, \tag{A.25}$$

$$\alpha_a^i \;\to\; \alpha_a^i + \sum_{I=1}^{b_{2n-3}} c_i^I \, q_I^a \,, \qquad m_I^a \;\to\; m_I^a - \sum_{i=1}^{s} c_i^I \, v_{ai} \,, \tag{A.26}$$

where c_i^I are arbitrary constants. This is the same freedom discussed in section 4.2.3. With these decompositions, we can then rewrite (A.15) as

$$C_{2n-2} = \left[\frac{2\pi}{V} \operatorname{vol}(X_{2n-1}) + \sum_{i=1}^{s} A_i \wedge \omega_i + \sum_{I=1}^{b_{2n-3}} A_I \wedge \omega_I + \cdots \right] \frac{\nu_n L^{2n-2}}{(5-n)2\pi} N \,. \tag{A.27}$$

Up to now, all we did was expanding upon the KK analysis discussed in [167]. However, consider now putting the lower-dimensional theory on a spindle, fibering the internal manifold X_{2n-1} over it and building an $(2n+1)$-dimensional internal space $X_{2n-1} \hookrightarrow Y_{2n+1} \to \Sigma$. As explained in section 2.1.2, this is achieved by turning on the flavour magnetic charges

$$\frac{1}{2\pi} \int_\Sigma \mathrm{d}A_i = \frac{p_i}{m_+ m_-} \,, \tag{A.28}$$

Next consider integrating $\mathrm{d}C_{2n-2}$ over supersymmetric $(2n-1)$-submanifolds Σ_a, that are fibrations $S_a \hookrightarrow \Sigma_a \to \Sigma$, where S_a is defined to be the (toric) submanifold such that $\int_{S_a} \omega_b = \delta_{ab}$ (see (3.16) in the main text). Such integrals give the fluxes M_a

$$M_a = \frac{5-n}{\nu_n L^{2n-2}} \int_{\Sigma_a} \mathrm{d}C_{2n-2} \,. \tag{A.29}$$

These fluxes depend only on the homology classes of Σ_a in Y_{2n+1} which, as explained in section 4.2.3, may be decomposed in terms of the homology classes of the cycles Σ_I obtained

by fibering $\mathcal{C}_I$ over the spindle plus that of the fibre X_{2n-1} itself as

$$[\Sigma_a] = \frac{q_0^a}{m_+ m_-}[X_{2n-1}] + \sum_{I=1}^{b_{2n-3}} q_I^a [\Sigma_I] = \frac{1}{m_+ m_-} \sum_{i=1}^{s} p_i \, \alpha_a^i \, [X_{2n-1}] + \sum_{I=1}^{b_{2n-3}} q_I^a [\Sigma_I] \, . \tag{A.30}$$

In particular this is the homology content of the last equation in (4.52), where $[X_{2n-1}]$ is the class of the fibre in $H_{2n-1}(Y_{2n+1}, \mathbb{Z})$. However, note that given the homology class $[\mathcal{C}_I] \in H_{2n-3}(X_{2n-1}, \mathbb{Z})$ in the fibre, the homology class $[\Sigma_I] \in H_{2n-1}(Y_{2n+1}, \mathbb{Z})$ in the total space is not uniquely identified but it depends on the specific representative we use for $[\mathcal{C}_I]$, because these will be twisted in different ways by the fibration. Indeed, in order for $[\Sigma_a]$ to be invariant under the shift of α_a^i in (A.25), correspondingly there must be a shift in $[\Sigma_I]$

$$[\Sigma_I] \, \to \, [\Sigma_I] - \frac{1}{m_+ m_-} \sum_{i=1}^{s} p_i \, c_i^I \, [X_{2n-1}] \, , \tag{A.31}$$

which is exactly what parametrizes the ambiguity in choosing a representative for $[\mathcal{C}_I]$.

We now have everything we need to compute the fluxes (A.29):

$$\begin{aligned} M_a &= \frac{5-n}{\nu_n L^{2n-2}} \left[\frac{1}{m_+ m_-} \sum_{i=1}^{s} p_i \, \alpha_a^i \int_{X_{2n-1}} \mathrm{d}C_{2n-2} + \sum_{I=1}^{b_{2n-3}} q_I^a \int_{\Sigma_I} \mathrm{d}C_{2n-2} \right] \\ &= \frac{N}{m_+ m_- V} \sum_{i=1}^{s} p_i \, \alpha_a^i \int_{X_{2n-1}} \mathrm{vol}(X_{2n-1}) + \sum_{I=1}^{b_{2n-3}} q_I^a \, \mathcal{N}_I \\ &= \frac{N}{m_+ m_-} \sum_{i=1}^{s} p_i \, \alpha_a^i + \sum_{I=1}^{b_{2n-3}} q_I^a \, \mathcal{N}_I \, , \end{aligned} \tag{A.32}$$

where, in agreement with (1.32), (1.36), we introduced

$$\begin{aligned} \mathcal{N}_I \equiv \frac{5-n}{\nu_n L^{2n-2}} \int_{\Sigma_I} \mathrm{d}C_{2n-2} &= \frac{N}{2\pi} \left[\sum_{i=1}^{s} \int_{\Sigma} \mathrm{d}A_i \int_{\mathcal{C}_I} \omega_i + \sum_{J=1}^{b_{2n-3}} \int_{\Sigma} \mathrm{d}A_J \int_{\mathcal{C}_I} \omega_J \right] \\ &= \frac{N}{m_+ m_-} \sum_{i=1}^{s} p_i \int_{\mathcal{C}_I} \omega_i + N \int_{\Sigma} \frac{\mathrm{d}A_I}{2\pi} \, . \end{aligned} \tag{A.33}$$

In particular this gives a formula for the "baryonic fluxes" $\mathcal{N}_I$ in terms of the KK reduction. Notice that the second term $N \int_\Sigma \mathrm{d}A_I/2\pi$ is what one would naturally call the "baryonic flux", but that in general also the first term contributes, coming from the flavour twisting p_i.

Equation (A.32) shows how to split the fluxes M_a into a "flavour" part and a "baryonic" part. It is clear that, while the fluxes M_a are unambiguous and dictate how the fields are twisted over the spindle in the dual field theory[2], on the other hand applying the shift invariance (A.25) to (A.32) results in an ambiguity in the flavour/baryonic splitting

$$\begin{aligned} \mathcal{N}_I &\to \mathcal{N}_I - \frac{N}{m_+ m_-} \sum_{i=1}^{s} c_i^I \, p_i \,, \\ \alpha_a^i &\to \alpha_a^i + \sum_{I=1}^{b_{2n-3}} c_i^I \, q_I^a \,. \end{aligned} \tag{A.34}$$

The transformations above encode the freedom to choose $s \cdot b_{2n-3}$ constants c_i^I. Given that there are b_{2n-3} fluxes $\mathcal{N}_I$, we can always choose them in such a way to fix the $\mathcal{N}_I$ to whatever we want (*e.g.* to zero) and we will actually still have some freedom left, parametrized by $(s-1)\, b_{2n-3}$ constants. The shift in the $\mathcal{N}_I$ can also be understood from (A.33) by noting that $\mathrm{d}C_{2n-2}$ is invariant under (A.25) but the cycle Σ_I is not, and transforms as (A.31).[3]

A.3 Matching GK geometry for $\mathrm{AdS}_3 \times Y_7$ with field theory

Here we consider GK geometry for toric Y_7 comprised of toric X_5 fibred over a spindle. We show that the off-shell central charge $\mathscr{Z}$ for the $\mathrm{AdS}_3 \times Y_7$ solution matches with the off-shell central charge $c_{\mathrm{trial}}|_{\mathrm{baryonic}}$ in the field theory, where the extremization over the baryonic directions has been carried out. The proof strategy is inspired by some results of [158].

It will be convenient to use different choices of gauge for the Kähler class parameters λ^A. Recall the master volume $\mathcal{V}_7$ is invariant under the gauge transformations given in (4.14):

$$\lambda_A \to \lambda_A + \sum_{\mu=0}^{3} \gamma^\mu (v_{A\mu} b_1 - b_\mu) \,. \tag{A.35}$$

Although γ^μ has four components only three of them yield a non-trivial transformation since

[2] In the toric case there is a general prescription to identify M_a with the twisting of the dual gauge theory, since this has a known relation to the GLSM. No such general prescription is known for the non-toric setting. Presumably, it is possible to define a set of "equivariant" fluxes via a form of equivariant cohomology that generalizes toric geometry appropriately, so that flavour and baryonic charges may be combined naturally.

[3] One cannot see the shift in $\mathcal{N}_I$ directly from the final line of (A.33), as the information on how the cycle $\mathcal{C}_I$ has been fibred over Σ has been lost in this expression.

the dependence on γ^1 drops out. Any function which is homogeneous in λ_A is invariant under (A.35) and, in particular, $\mathcal{V}_7$, $\mathcal{V}_5^\pm$, $R_a^\pm$, and $\mathscr{Z}$ are all gauge-invariant quantities.

We will use three different gauge choices. Noting that the transformation of $\lambda_a^{(+)}$ only depends on γ^2, γ^3, we can choose these to set two of the $\lambda_a^{(+)}$ to vanish, for example

$$\textit{Plus gauge:} \qquad \lambda_1^{(+)} = \lambda_2^{(+)} = 0\,. \tag{A.36}$$

Similarly, we can instead choose γ^2, γ^3 to set two of the $\lambda_a^{(-)}$ to vanish, for example

$$\textit{Minus gauge:} \qquad \lambda_1^{(-)} = \lambda_2^{(-)} = 0\,. \tag{A.37}$$

Finally, the transformation of $\lambda_\pm$ depends on $\gamma^0, \gamma^2, \gamma^3$ we can choose γ^2, γ^3 (say) to obtain

$$\textit{Symmetric gauge:} \qquad \lambda_+ = \lambda_- = 0 \quad \Rightarrow \quad \lambda_a^{(\pm)} = \lambda_a\,. \tag{A.38}$$

Note that all these gauge choices leave a residual one-parameter gauge invariance parametrized by γ^0, which we will not need to fix.

A.3.1 $\mathscr{Z}$ as a function of $R_a^\pm$

The master volume for toric X_5 is homogeneous of degree 2 in the λ_a and hence we can write

$$\mathcal{V}_5^\pm = \frac{1}{2}\sum_{a=1}^{d} \frac{\partial \mathcal{V}_5^\pm}{\partial \lambda_a}\,\lambda_a^{(\pm)} = -\frac{N\nu_3}{4}\sum_{a=1}^{d} R_a^\pm\,\lambda_a^{(\pm)}\,, \tag{A.39}$$

where we used the expressions for $R_a^\pm$ given in (4.60). We now show that we can express $\lambda_a^{(\pm)}$ in (A.39) in terms of $R_a^\pm$ and obtain an expression for the off-shell central charge $\mathscr{Z}$. We will use different gauges to treat the $\pm$ cases, but the final results are gauge invariant.

It is helpful to recall the explicit formula for $\mathcal{V}_5 = \mathcal{V}_5(\vec{b}; \{\lambda_a\})$ given in (1.3) of [70]:[4]

$$\mathcal{V}_5 = \frac{(2\pi)^3}{2}\sum_{a=1}^{d} \lambda_a\, \frac{\lambda_{a-1}(\vec{v}_a, \vec{v}_{a+1}, \vec{b}) - \lambda_a(\vec{v}_{a-1}, \vec{v}_{a+1}, \vec{b}) + \lambda_{a+1}(\vec{v}_{a-1}, \vec{v}_a, \vec{b})}{(\vec{v}_{a-1}, \vec{v}_a, \vec{b})(\vec{v}_a, \vec{v}_{a+1}, \vec{b})}\,. \tag{A.40}$$

[4]Throughout this appendix we will use the arrow notation for 3d vectors with an i index (*e.g.* v_{ai} will be denoted with $\vec{v}_a$) unless otherwise stated.

We now define

$$J_{ab} \equiv \frac{\partial \mathcal{V}_5}{\partial\lambda_a \partial\lambda_b}\,, \qquad J^{\pm}_{ab} \equiv J_{ab}\big|_{\vec{b}=\vec{b}^{(\pm)}}\,, \tag{A.41}$$

with J_{ab} independent of λ_a and $\vec{b} = (b_1, b_2, b_3)$. The only non-vanishing components of the matrix J_{ab} are J_{aa} and $J_{a,a+1} = J_{a+1,a}$ given by

$$J_{aa} = -(2\pi)^3 \frac{(\vec{v}_{a-1}, \vec{v}_{a+1}, \vec{b})}{(\vec{v}_{a-1}, \vec{v}_a, \vec{b})(\vec{v}_a, \vec{v}_{a+1}, \vec{b})}\,, \qquad J_{a,a+1} = (2\pi)^3 \frac{1}{(\vec{v}_a, \vec{v}_{a+1}, \vec{b})}\,. \tag{A.42}$$

The homogeneity of the master volume $\mathcal{V}_5$ implies that we can recast $R^{\pm}_a$ in (4.60) as

$$\begin{aligned} R^{\pm}_a &= -\frac{2}{N\nu_3} \sum_{b=1}^{d} J^{\pm}_{ab}\, \lambda^{(\pm)}_b\,, \\ &= -\frac{16\pi^3}{N\nu_3} \left[\frac{\lambda_{a-1}}{(\vec{v}_{a-1}, \vec{v}_a, \vec{b}^{(\pm)})} - \frac{(\vec{v}_{a-1}, \vec{v}_{a+1}, \vec{b}^{(\pm)})\, \lambda_a}{(\vec{v}_{a-1}, \vec{v}_a, \vec{b}^{(\pm)})(\vec{v}_a, \vec{v}_{a+1}, \vec{b}^{(\pm)})} + \frac{\lambda_{a+1}}{(\vec{v}_a, \vec{v}_{a+1}, \vec{b}^{(\pm)})} \right]. \end{aligned} \tag{A.43}$$

We now focus on the + case and choose the "plus gauge" (A.36), $\lambda^{(+)}_1 = \lambda^{(+)}_2 = 0$. We have

$$\begin{aligned} R^{+}_1 &= -\frac{2}{N\nu_3} \left(J^{+}_{1d}\, \lambda^{(+)}_d \right), \\ R^{+}_2 &= -\frac{2}{N\nu_3} \left(J^{+}_{23}\, \lambda^{(+)}_3 \right), \\ R^{+}_3 &= -\frac{2}{N\nu_3} \left(J^{+}_{33}\, \lambda^{(+)}_3 + J^{+}_{34}\, \lambda^{(+)}_4 \right), \\ R^{+}_4 &= -\frac{2}{N\nu_3} \left(J^{+}_{43}\, \lambda^{(+)}_3 + J^{+}_{44}\, \lambda^{(+)}_4 + J^{+}_{45}\, \lambda^{(+)}_5 \right), \\ &\cdots \quad , \end{aligned} \tag{A.44}$$

and these equations can be solved recursively for the $\lambda^{(+)}_a$ to get (as in [158])

$$\lambda^{(+)}_a = -\frac{N\nu_3}{16\pi^3} \sum_{b=2}^{a} (\vec{v}_b, \vec{v}_a, \vec{b}^{(+)})\, R^{+}_b, \qquad a = 3, \ldots, d\,. \tag{A.45}$$

The identity for R^{+}_a given in (4.64) ensures that the expression for $\lambda^{(+)}_d$ we get from the first equation in (A.44) is consistent with (A.45). Substituting (A.45) back into (A.39) we get

$$\mathcal{V}^{+}_5 = \frac{N^2\nu_3^2}{64\pi^3} \sum_{a=3}^{d} \sum_{b=2}^{a} (\vec{v}_b, \vec{v}_a, \vec{b}^{(+)}) R^{+}_a\, R^{+}_b\,, \tag{A.46}$$

and then after again using the identity (4.64) we can write

$$\mathcal{V}_5^+ = \frac{N^2\nu_3^2 b_1}{128\pi^3}\sum_{a=3}^{d}\sum_{b=2}^{a}\sum_{c=1}^{d}(\vec{v}_b,\vec{v}_a,\vec{v}_c)R_a^+R_b^+R_c^+ = \frac{N^2\nu_3^2 b_1}{128\pi^3}\sum_{a<b<c}(\vec{v}_a,\vec{v}_b,\vec{v}_c)\,R_a^+R_b^+R_c^+\,. \quad \text{(A.47)}$$

This expression does not depend on the gauge choice and hence it holds in all gauges.

Analogously, for the $-$ case we can utilise the "minus gauge" (A.37), and obtain an equivalent expression for $\mathcal{V}_5^-$ in terms of R_a^-. We can then write the supersymmetric action (4.45) and hence the trial central charge $\mathscr{Z}$ defined in (1.34) in the form

$$\mathscr{Z} = \frac{3N^2b_1^2}{4b_0}\sum_{a<b<c}(\vec{v}_a,\vec{v}_b,\vec{v}_c)\left(R_a^+R_b^+R_c^+ - R_a^-R_b^-R_c^-\right). \quad \text{(A.48)}$$

In this expression we note that $R_a^\pm$ has to be viewed as functions of b_μ and the fluxes M_A (after eliminating the λ's via the last two lines of (4.17) or, equivalently, (4.49) and (4.50)).

We now observe that after setting $b_1 = 2$, which is required in the GK extremization procedure, the expression for $\mathscr{Z}$ in (A.48) has precisely the same form as the field theory expression for the central charge (5.20) using the dictionary between field theory and geometric quantities discussed in section 5.2.2:

$$\varepsilon = b_0\,, \qquad \Delta_a^\pm\big|_{\text{baryonic}} = R_a^\pm\,. \quad \text{(A.49)}$$

We also identify the rank of the field theory gauge group, N, with the flux $N \equiv m_+M_+ = \sigma m_-M_-$ and the background magnetic fluxes for the SCFT $\mathfrak{p}_a$ with the five-from fluxes via $\mathfrak{p}_a \equiv \frac{M_a}{N}$ as in (5.28).

We now argue that the identification (A.49) is possible. On the GK geometry side we have three independent variables, b_0, b_2, b_3. We also have three independent variables on the field theory side, the $d+1$ variables ε, Δ_a satisfying the $d-2$ constraints

$$\sum_{a=1}^{d}\Delta_a = 2\,, \qquad \sum_{a=1}^{d}q_I^a\,\frac{\partial c_{\text{trial}}}{\partial\Delta_a} = 0\,, \qquad I = 1,\ldots,d-3\,. \quad \text{(A.50)}$$

Interestingly, we will show below (see (A.56)) that the latter constraints are actually $d-2$ linear constraints in terms of the variables Δ_a, ε. We will also show in section A.3.3 that

the $R_a^\pm$, after eliminating the λ_a variables, are linear functions of b_2, b_3 and b_0. Thus, (A.49) is $2d+1$ linear equations for 3 variables and hence the system seems to be overdetermined. However, only 3 of the equations are independent, and the other $2d-2$ can be obtained as linear combinations of these. To see this, we introduce the notation

$$E_a^\pm \equiv \Delta_a^\pm\big|_{\text{baryonic}} - R_a^\pm \,, \tag{A.51}$$

so that the $2d$ linear equations in the second line of (A.49) are simply $E_a^\pm = 0$. Then, combining the identities (4.62) and the definition (5.21), we conclude

$$E_a^+ - E_a^- = 0 \,, \tag{A.52}$$

which eliminates d equations, say those encoded by E_a^-, from the original system. Another equation can be eliminated because

$$\sum_{a=1}^{d} E_a^+ = 0 \,, \tag{A.53}$$

where we used (4.61) and (5.24). Finally, the last set of $d-3$ linear constraints comes from the baryonic extremization condition in (A.50). To see this we will show below that

$$\sum_{a=1}^{d} q_I^a \left.\frac{\partial c_{\text{trial}}}{\partial \Delta_a}\right|_{\Delta_a^\pm = R_a^\pm(b_\mu, M_A)} = 0 \,, \qquad I = 1, \ldots, d-3 \,. \tag{A.54}$$

Furthermore, to do so we will also prove that the baryonic extremization condition (A.50) can be re-expressed in the equivalent form

$$\sum_{b=1}^{d}\sum_{a=1}^{b}\sum_{c=1}^{d} q_I^a(\vec{v}_a, \vec{v}_b, \vec{v}_c)\left(\Delta_b^+\Delta_c^+ - \Delta_b^-\Delta_c^-\right) = 0 \,. \tag{A.55}$$

Writing (A.55) purely in terms of Δ_a^+, say, yields

$$\sum_{b=1}^{d}\sum_{a=1}^{b}\sum_{c=1}^{d} q_I^a(\vec{v}_a, \vec{v}_b, \vec{v}_c)\left(\mathfrak{p}_b\Delta_c^+ + \mathfrak{p}_c\Delta_b^+ + \varepsilon\,\mathfrak{p}_b\mathfrak{p}_c\right) = 0 \,, \tag{A.56}$$

from which we see that the baryonic constraints are linear in the Δ_a and ε as noted above. Hence, given (A.54), the baryonic extremization condition implies that the system of linear equations E_a^+ is, indeed, also subject to $d-3$ linear constraints

$$\sum_{b=1}^{d}\sum_{a=1}^{b}\sum_{c=1}^{d} q_I^a(\vec{v}_a,\vec{v}_b,\vec{v}_c)\left(\mathfrak{p}_b E_c^+ + \mathfrak{p}_c E_b^+\right) = 0\,. \tag{A.57}$$

Thus, the linear identifications (A.49) are actually not overdetermined. In practice we can take the identification to be, for example,

$$\varepsilon = b_0\ , \qquad \Delta_1^+\big|_{\text{baryonic}} = R_1^+\,, \qquad \Delta_2^+\big|_{\text{baryonic}} = R_2^+\,. \tag{A.58}$$

A.3.2 Proof of baryonic extremization conditions

We now prove (A.54) and (A.55). We begin with the latter. Let us start by using the expression for c_{trial} in (5.20) to write

$$\sum_{a=1}^{d} q_I^a \frac{\partial c_{\text{trial}}}{\partial \Delta_a} = \frac{3}{\varepsilon}\sum_{e<b<c}(\vec{v}_e,\vec{v}_b,\vec{v}_c)\left[q_I^e\Delta_b^+\Delta_c^+ + q_I^b\Delta_e^+\Delta_c^+ + q_I^c\Delta_b^+\Delta_e^+ - (+\leftrightarrow -)\right]\,. \tag{A.59}$$

We can rewrite the triple sum in the following way

$$\sum_{e<b<c} = \sum_{e=1}^{d}\sum_{b=e}^{d}\sum_{c=b}^{d} = \sum_{b=1}^{d}\sum_{e=1}^{b}\sum_{c=b}^{d}\,, \tag{A.60}$$

where due to the asymmetry of the determinant the sum gets no contribution if we set any two of e,b,c equal. Using (A.2), we can rewrite the third term in (A.59) as

$$-\sum_{b=1}^{d}\sum_{e=1}^{b}\sum_{c=1}^{b}(\vec{v}_e,\vec{v}_b,\vec{v}_c)q_I^c\Delta_b^+\Delta_e^+ = \sum_{b=1}^{d}\sum_{e=1}^{b}\sum_{c=1}^{b}(\vec{v}_e,\vec{v}_b,\vec{v}_c)q_I^e\Delta_b^+\Delta_c^+\,, \tag{A.61}$$

where we swapped the indices e and c to get the second expression. Hence, summing the first and the third term of (A.59) yields

$$\sum_{b=1}^{d}\sum_{e=1}^{b}\sum_{c=1}^{d}(\vec{v}_e,\vec{v}_b,\vec{v}_c)q_I^e\Delta_b^+\Delta_c^+\,. \tag{A.62}$$

For the second term in (A.59), we can exploit the skew-symmetry of the summand to extend the range of c and then massage it via some relabelling and again using (A.2) to find

$$\begin{aligned}\sum_{b=1}^{d}\sum_{e=1}^{b}\sum_{c=b}^{d}(\vec{v}_e,\vec{v}_b,\vec{v}_c)q_I^b\Delta_e^+\Delta_c^+ &= \sum_{b=1}^{d}\sum_{e=1}^{b}\sum_{c=1}^{d}(\vec{v}_e,\vec{v}_b,\vec{v}_c)q_I^b\Delta_e^+\Delta_c^+ \\ &= \sum_{e=1}^{d}\sum_{b=e}^{d}\sum_{c=1}^{d}(\vec{v}_e,\vec{v}_b,\vec{v}_c)q_I^b\Delta_e^+\Delta_c^+ = -\sum_{e=1}^{d}\sum_{b=1}^{e}\sum_{c=1}^{d}(\vec{v}_e,\vec{v}_b,\vec{v}_c)q_I^b\Delta_e^+\Delta_c^+ \\ &= \sum_{b=1}^{d}\sum_{e=1}^{b}\sum_{c=1}^{d}(\vec{v}_e,\vec{v}_b,\vec{v}_c)q_I^e\Delta_b^+\Delta_c^+ \,. \end{aligned} \tag{A.63}$$

Hence we find that the second term in (A.59) is equal to the sum of the first and the third. We can obtain a similar result for the terms involving Δ_a^- and hence we have proven (A.55).

We now prove (A.54):

$$\sum_{a=1}^{d} q_I^a \left.\frac{\partial c_{\text{trial}}}{\partial\Delta_a}\right|_{\Delta_a^\pm = R_a^\pm(b_\mu, M_A)} = 0\,, \qquad I = 1,\ldots,d-3\,. \tag{A.64}$$

Using what we just proved in (A.55), as well as the conditions satisfied by $R_a^\pm$ given in (4.64) to carry out the sum over c, this condition can be written equivalently as

$$W \equiv \sum_{a=1}^{d}\sum_{b=a}^{d} q_I^a\left[(\vec{v}_a,\vec{v}_b,\vec{b}^{(+)})R_b^+ - (\vec{v}_a,\vec{v}_b,\vec{b}^{(-)})R_b^-\right] = 0\,, \tag{A.65}$$

where we have also swapped the sums over a and b. To proceed we exploit the determinant identity $(\vec{a},\vec{b},\vec{c}) = \vec{a}\cdot(\vec{b}\wedge\vec{c})$ to write W in the form

$$W = \sum_{a=1}^{d} q_I^a\,\vec{v}_a\cdot\vec{u}_a\,, \qquad \vec{u}_a \equiv \sum_{b=a}^{d}\left[(\vec{v}_b\wedge\vec{b}^{(+)})R_b^+ - (\vec{v}_b\wedge\vec{b}^{(-)})R_b^-\right]. \tag{A.66}$$

Note that the expression for W is unchanged under the following shift of the vectors $\vec{u}_a$:

$$\vec{u}_a \to \vec{u}'_a = \vec{u}_a + \vec{v}_a\wedge\vec{z}_a\,, \tag{A.67}$$

for an arbitrary vector $\vec{z}_a$. The strategy is to show that we can choose $\vec{z}_a$ in such a way that

all of the $\vec{u}'_a$ are actually the same vector $\vec{u}$, since if this is the case we then have

$$W = \sum_{a=1}^{d} q_I^a \, \vec{v}_a \cdot \vec{u}'_a = \sum_{a=1}^{d} q_I^a \, \vec{v}_a \cdot \vec{u} = 0 \,, \tag{A.68}$$

where in the last step we again used (A.2). We now show that such a choice of $\vec{z}_a$ is possible. We first compute the difference between two adjacent $\vec{u}'_a$ vectors:

$$\vec{u}'_{a+1} - \vec{u}'_a = -(\vec{v}_a \wedge \vec{b}^{(+)})R_a^+ + (\vec{v}_a \wedge \vec{b}^{(-)})R_a^- + \vec{v}_{a+1} \wedge \vec{z}_{a+1} - \vec{v}_a \wedge \vec{z}_a \,. \tag{A.69}$$

We thus want to choose the variables $\vec{z}_a$, $a = 1, \ldots, d$ to solve the system of equations

$$-\vec{v}_a \wedge \left[\vec{b}^{(+)}R_a^+ - \vec{b}^{(-)}R_a^- + \vec{z}_a\right] + \vec{v}_{a+1} \wedge \vec{z}_{a+1} = 0 \,, \qquad a = 1, \ldots, d \,, \tag{A.70}$$

where the indices are identified cyclically *i.e.* $d + 1 = 1$. Since $\vec{v}_a$ and $\vec{v}_{a+1}$ are not parallel this is solved if both terms are proportional to $\vec{v}_a \wedge \vec{v}_{a+1}$, which implies that we can write

$$\begin{aligned} \vec{b}^{(+)}R_a^+ - \vec{b}^{(-)}R_a^- + \vec{z}_a &= k_a \vec{v}_{a+1} + k'_a \vec{v}_a \,, \\ \vec{z}_{a+1} &= -k_a \vec{v}_a + k''_{a+1} \vec{v}_{a+1} \,, \end{aligned} \tag{A.71}$$

for some real constants k_a, k'_a, and k''_a, $a = 1, \ldots, d$. This is equivalent to

$$\begin{aligned} \vec{z}_a &= k_a \vec{v}_{a+1} + k'_a \vec{v}_a - \vec{b}^{(+)}R_a^+ + \vec{b}^{(-)}R_a^- \,, \\ \vec{z}_a &= -k_{a-1} \vec{v}_{a-1} + k''_a \vec{v}_a \,. \end{aligned} \tag{A.72}$$

Now recall from (A.67) that $\vec{z}_a$ can be shifted by a vector proportional to $\vec{v}_a$ without changing $\vec{u}'_a$. Hence, we can reabsorb, for example, the term $k''_a \vec{v}_a$ inside $\vec{z}_a$ with an associated redefinition of k'_a. Thus, consistency of the two expressions for each $\vec{z}_a$ in (A.72) amounts to solving the following system of equations for k_a and k'_a

$$k_a \vec{v}_{a+1} + k'_a \vec{v}_a + k_{a-1} \vec{v}_{a-1} = \vec{b}^{(+)}R_a^+ - \vec{b}^{(-)}R_a^- \,, \qquad a = 1, \ldots, d \,. \tag{A.73}$$

This is $3(d-1)$ independent equations for $2d$ variables k_a, k'_a. A solution can exist provided that a set of $d-3$ constraints are satisfied. Let us introduce the notation

$$\vec{b}^{(+)}R_a^+ - \vec{b}^{(-)}R_a^- \equiv (\beta_a^1,\, \vec{\beta}_a)\,, \tag{A.74}$$

where $\vec{\beta}_a$ is a two dimensional vector. Then the first component of (A.73) can be used to solve for k'_a as follows

$$k'_a = \beta_a^1 - k_a - k_{a-1}\,. \tag{A.75}$$

Substituting this back into (A.73) we get the set of two-dimensional equations

$$k_a(\vec{w}_{a+1} - \vec{w}_a) - k_{a-1}(\vec{w}_a - \vec{w}_{a-1}) = \vec{\beta}_a - \beta_a^1\vec{w}_a\,. \tag{A.76}$$

Now if we project this 2d equation onto vectors orthogonal to $(\vec{w}_{a+1} - \vec{w}_a)$ and $(\vec{w}_a - \vec{w}_{a-1})$, we get two simple linear equations for k_{a+1} and k_a respectively.[5] We therefore deduce

$$\begin{aligned} k_a\left[(\vec{w}_{a+1},\vec{w}_a) - (\vec{w}_{a+1},\vec{w}_{a-1}) + (\vec{w}_a,\vec{w}_{a-1})\right] &= (\vec{\beta}_a,\vec{w}_a) - (\vec{\beta}_a,\vec{w}_{a-1}) + \beta_a^1(\vec{w}_a,\vec{w}_{a-1})\,,\\ -k_{a-1}\left[(\vec{w}_a,\vec{w}_{a+1}) - (\vec{w}_{a-1},\vec{w}_{a+1}) + (\vec{w}_{a-1},\vec{w}_a)\right] &= (\vec{\beta}_a,\vec{w}_{a+1}) - (\vec{\beta}_a,\vec{w}_a) - \beta_a^1(\vec{w}_a,\vec{w}_{a+1})\,, \end{aligned} \tag{A.77}$$

where here $(\vec{a},\vec{c})$ denotes the determinant of the 2×2 matrix built with the vectors $\vec{a}$ and $\vec{c}$. So, we obtain two different expressions for k_a and the constraint is that they must be equal

$$\frac{(\vec{\beta}_a,\vec{w}_a) - (\vec{\beta}_a,\vec{w}_{a-1}) + \beta_a^1(\vec{w}_a,\vec{w}_{a-1})}{(\vec{w}_{a+1},\vec{w}_a) - (\vec{w}_{a+1},\vec{w}_{a-1}) + (\vec{w}_a,\vec{w}_{a-1})} = -\frac{(\vec{\beta}_{a+1},\vec{w}_{a+2}) - (\vec{\beta}_{a+1},\vec{w}_{a+1}) - \beta_{a+1}^1(\vec{w}_{a+1},\vec{w}_{a+2})}{(\vec{w}_{a+1},\vec{w}_{a+2}) - (\vec{w}_a,\vec{w}_{a+2}) + (\vec{w}_a,\vec{w}_{a+1})}\,. \tag{A.78}$$

We are left to show that β_a^1 and $\vec{\beta}_a$ are such that (A.78) is satisfied. Notice that this equation can be rewritten in terms of 3×3 determinants as

$$\frac{(\vec{v}_a,\vec{v}_{a-1},\vec{b}^{(+)})R_a^+ - (\vec{v}_a,\vec{v}_{a-1},\vec{b}^{(-)})R_a^-}{(\vec{v}_{a+1},\vec{v}_a,\vec{v}_{a-1})} = \frac{(\vec{v}_{a+2},\vec{v}_{a+1},\vec{b}^{(+)})R_{a+1}^+ - (\vec{v}_{a+2},\vec{v}_{a+1},\vec{b}^{(-)})R_{a+1}^-}{(\vec{v}_{a+2},\vec{v}_{a+1},\vec{v}_a)}\,. \tag{A.79}$$

[5] Note that we can do this since by construction $(\vec{w}_{a+1} - \vec{w}_a)$ and $(\vec{w}_a - \vec{w}_{a-1})$ are linearly independent.

This equation is gauge invariant, so we can choose a convenient gauge to show that it is satisfied. In particular it is convenient to pick the "symmetric gauge" (A.38) such that $\lambda_a^{(\pm)} = \lambda_a$. We substitute the expression (A.43) for $R_a^{\pm}$ into (A.79). The terms involving λ_{a-1} and λ_{a+2} cancel and we are left with an expression involving λ_a and λ_{a+1} given by[6]

$$\begin{aligned}
&\lambda_a\Bigg[\frac{(\vec{v}_{a-1},\vec{v}_{a+1},\vec{b}^{(+)})(\vec{v}_a,\vec{v}_{a+1},\vec{b}^{(-)})-(\vec{v}_{a-1},\vec{v}_{a+1},\vec{b}^{(-)})(\vec{v}_a,\vec{v}_{a+1},\vec{b}^{(+)})}{(\vec{v}_{a+1},\vec{v}_a,\vec{v}_{a-1})}\\
&\qquad-\frac{(\vec{v}_{a+2},\vec{v}_{a+1},\vec{b}^{(+)})(\vec{v}_a,\vec{v}_{a+1},\vec{b}^{(-)})-(\vec{v}_{a+2},\vec{v}_{a+1},\vec{b}^{(-)})(\vec{v}_a,\vec{v}_{a+1},\vec{b}^{(+)})}{(\vec{v}_{a+2},\vec{v}_{a+1},\vec{v}_a)}\Bigg]\\
+&\lambda_{a+1}\Bigg[\frac{(\vec{v}_a,\vec{v}_{a-1},\vec{b}^{(+)})(\vec{v}_a,\vec{v}_{a+1},\vec{b}^{(-)})-(\vec{v}_a,\vec{v}_{a-1},\vec{b}^{(-)})(\vec{v}_a,\vec{v}_{a+1},\vec{b}^{(+)})}{(\vec{v}_{a+1},\vec{v}_a,\vec{v}_{a-1})}\\
&\qquad-\frac{(\vec{v}_a,\vec{v}_{a+2},\vec{b}^{(+)})(\vec{v}_a,\vec{v}_{a+1},\vec{b}^{(-)})-(\vec{v}_a,\vec{v}_{a+2},\vec{b}^{(-)})(\vec{v}_a,\vec{v}_{a+1},\vec{b}^{(+)})}{(\vec{v}_{a+2},\vec{v}_{a+1},\vec{v}_a)}\Bigg]=0\,. \qquad \text{(A.80)}
\end{aligned}$$

We can show that both the terms inside the square brackets vanish independently as a result of the vector quadruple product identity. Specifically for any four vectors $\vec{a},\vec{b},\vec{c},\vec{d}$ in $\mathbb{R}^3$ we have

$$\vec{a}(\vec{b},\vec{c},\vec{d})-\vec{b}(\vec{c},\vec{d},\vec{a})+\vec{c}(\vec{d},\vec{a},\vec{b})-\vec{d}(\vec{a},\vec{b},\vec{c})=0\,, \qquad \text{(A.81)}$$

which immediately implies the following identity involving products of determinants:

$$(\vec{a},\vec{d},\vec{e})(\vec{b},\vec{d},\vec{c})+(\vec{b},\vec{d},\vec{e})(\vec{c},\vec{d},\vec{a})+(\vec{c},\vec{d},\vec{e})(\vec{a},\vec{d},\vec{b})=0\,. \qquad \text{(A.82)}$$

Using this identity we can write

$$\begin{aligned}
&(\vec{v}_{a-1},\vec{v}_{a+1},\vec{b}^{(+)})(\vec{v}_a,\vec{v}_{a+1},\vec{b}^{(-)})-(\vec{v}_{a-1},\vec{v}_{a+1},\vec{b}^{(-)})(\vec{v}_a,\vec{v}_{a+1},\vec{b}^{(+)})\\
&\qquad=(\vec{v}_{a+1},\vec{v}_a,\vec{v}_{a-1})(\vec{v}_{a+1},\vec{b}^{(-)},\vec{b}^{(+)})\,,\\
&(\vec{v}_{a+2},\vec{v}_{a+1},\vec{b}^{(+)})(\vec{v}_a,\vec{v}_{a+1},\vec{b}^{(-)})-(\vec{v}_{a+2},\vec{v}_{a+1},\vec{b}^{(-)})(\vec{v}_a,\vec{v}_{a+1},\vec{b}^{(+)})\\
&\qquad=(\vec{v}_{a+2},\vec{v}_{a+1},\vec{v}_a)(\vec{v}_{a+1},\vec{b}^{(-)},\vec{b}^{(+)})\,, \qquad \text{(A.83)}
\end{aligned}$$

which implies that the coefficient of λ_a in (A.80) vanishes. A similar argument shows that

[6] We could in principle have exploited the residual gauge invariance to set *e.g.* $\lambda_{a+1}=0$ but this is not necessary to conclude the proof.

the coefficient of λ_{a+1} in (A.80) also vanishes and this concludes the proof of (A.64).

A.3.3 $R_a^{\pm}$ as functions of b_2, b_3

Here we show that $R_a^{\pm}$, after eliminating the λ_a variables, are linear functions of b_2, b_3 and b_0. This shows that the second line in (A.49) are linear equations in these variables and also that (A.56), after substituting $\Delta_a^+ \to R_a^+$, are linear constraints.

The key equation from the previous subsection is (A.79). After eliminating R_a^- via (4.62) and using also (2.20), we find (A.79) can be rewritten as

$$\frac{(\vec{v}_a, \vec{v}_{a-1}, \vec{p})\frac{R_a^+}{m_+m_-} + (\vec{v}_a, \vec{v}_{a-1}, \vec{b}^{(-)})\frac{M_a}{N}}{(\vec{v}_{a+1}, \vec{v}_a, \vec{v}_{a-1})} = \frac{(\vec{v}_{a+2}, \vec{v}_{a+1}, \vec{p})\frac{R_{a+1}^+}{m_+m_-} + (\vec{v}_{a+2}, \vec{v}_{a+1}, \vec{b}^{(-)})\frac{M_{a+1}}{N}}{(\vec{v}_{a+2}, \vec{v}_{a+1}, \vec{v}_a)} \,. \tag{A.84}$$

Schematically we can write this in the form

$$R_a^+ = R_{a+1}^+ A_a + B_a \,, \tag{A.85}$$

where A_a is independent of b_2, b_3 and b_0, while B_a is linear in b_2, b_3 and b_0. By recursively substituting the expression for R_{a+1}^+ into the expression for R_a^+, we can eventually express all R_a^+ in terms of the last one, R_d^+, as

$$R_a^+ = R_d^+ A'_a + B'_a \,, \tag{A.86}$$

with A'_a, B'_a having the same properties. Next we can use (4.61) to find

$$R_d^+ = \left(\sum_{a=1}^{d} A'_a\right)^{-1} \left[2 - \frac{b_0}{m_+} - \sum_{a=1}^{d} B'_a\right] \,, \tag{A.87}$$

to conclude that R_d^+ is a linear function of b_2, b_3 and b_0. From (A.85) we find that all of the R_a^+ are linear functions of b_2, b_3 and b_0 and, recalling that R_a^- are related to R_a^+ via (3.19), the same is true for R_a^-.

A.4 BPS condition for M2-branes

In the following we denote with $M = (0, 1, m)$ the 11d spacetime index and with $\mathsf{A} = (0, 1, \mathsf{a})$ the 11d frame indices, and we introduce a local orthonormal frame e^{A} for the metric (1.35) such that $e^{10} = \mathrm{e}^{-B/3}\,\eta$. If ϵ is the Killing spinor of the background, an M2-brane whose configuration is described by the embedding coordinates X^M does not break supersymmetry if it is such that ϵ satisfies the following Euclidean projection condition [170]

$$\mathbb{P}\,\epsilon = 0, \qquad \text{with} \qquad \mathbb{P} \equiv \frac{1}{2}\left(1 - \frac{\mathrm{i}}{3!}\,\varepsilon^{ijk}\,\partial_i X^M \partial_j X^N \partial_k X^P\,\Gamma_{MNP}\right). \tag{A.88}$$

Here i, j, k are worldvolume indices, ε^{ijk} is the 3d Levi-Civita tensor, and Γ_{MNP} are antisymmetric products of the 11d gamma matrices in curved space, *i.e.* $\Gamma_M = \Gamma_{\mathsf{A}}\,e^{\mathsf{A}}{}_M$. The configuration of branes we are interested in is wrapping EAdS_2 (*i.e.* the (0,1) directions) and S^1_{M2}, which we take to be a generic linear combination of the directions in Y_9, *i.e.*[7]

$$\mathrm{vol}_{S^1_{\mathrm{M2}}} = \sum_{\mathsf{a}=2}^{10} c_{\mathsf{a}}\,e^{\mathsf{a}}\,, \qquad c_{\mathsf{a}} \in \mathbb{R}\,. \tag{A.89}$$

We choose a parametrization where

$$\begin{aligned} \partial_0 X^0 = \partial_1 X^1 = 1\,, \quad (\partial_3 X^m)\,e^{\mathsf{a}}{}_m = c_{\mathsf{a}}\,, \\ \partial_0 X^m = \partial_1 X^m = \partial_3 X^0 = \partial_3 X^1 = 0\,. \end{aligned} \tag{A.90}$$

Then the only non-zero contributions in the sum in $\mathbb{P}$ are those for which $(M, N, P) = (0, 1, m)$ or permutations, yielding

$$\mathbb{P}\,\epsilon = 0, \qquad \text{with} \qquad \mathbb{P} = \frac{1}{2}\left(1 - \mathrm{i}\sum_{\mathsf{a}=2}^{10} c_{\mathsf{a}}\,\Gamma_0\Gamma_1\Gamma_{\mathsf{a}}\right). \tag{A.91}$$

The next step is to decompose this projection on our $\mathrm{AdS}_2 \times Y_9$ background. Following the conventions of [37,149] but rotated to Euclidean signature, as those are compatible with our GK backgrounds, we split the 11d gamma matrices as $\Gamma_{\mathsf{A}} = (\beta_0 \otimes \mathbb{I}_9,\, \beta_1 \otimes \mathbb{I}_9,\, \beta_* \otimes \gamma_{\mathsf{a}})$, where

[7] Of course the fact that S^1_{M2} must be a circle will in principle put restrictions on the coefficients c_{a}, but we will not need them as the projection condition (A.88) is enough to fix all the coefficients.

$\beta_0 = \sigma_2$ and $\beta_1 = \sigma_1$ are Pauli matrices, $\beta_* = -\mathrm{i}\beta_0\beta_1 = -\sigma_3$ is the chiral gamma matrix in 2d, and γ_{a} generates the 9d Clifford algebra. This gives

$$\mathbb{P} = \frac{1}{2}\left(\mathbb{I}_2 \otimes \mathbb{I}_9 - \mathrm{i}\beta_0\beta_1\beta_* \otimes \sum_{\mathsf{a}=2}^{10} c_{\mathsf{a}}\gamma_{\mathsf{a}}\right) = \frac{1}{2}\,\mathbb{I}_2 \otimes \left(\mathbb{I}_9 + \sum_{\mathsf{a}=2}^{10} c_{\mathsf{a}}\gamma_{\mathsf{a}}\right), \tag{A.92}$$

where we used the fact that $\mathrm{i}\beta_0\beta_1\beta_* = -\mathbb{I}_2$. Notice that in order for $\mathbb{P}$ to be a well-defined projector we have to ensure that $\mathbb{P}^2 = \mathbb{P}$, which implies that $\sum_{\mathsf{a}=2}^{10} c_{\mathsf{a}}^2 = 1$. Splitting also the 11d Killing spinor as $\epsilon = \theta \otimes \chi + c.c.$, where θ is a Killing spinor on AdS_2 and χ on Y_9, the condition $\mathbb{P}\,\epsilon = 0$ results in the following equation involving the 9d spinor only

$$\sum_{\mathsf{a}=2}^{10} c_{\mathsf{a}}\gamma_{\mathsf{a}}\chi = -\chi\,. \tag{A.93}$$

Finally, taking χ to be normalized as $\bar{\chi}\chi = 1$, it can be shown that for a GK geometry the 1-form η is given by the bilinear [36]

$$\eta = \mathrm{e}^{B/3}\,\bar{\chi}\gamma_{\mathsf{a}}\chi\, e^{\mathsf{a}}\,, \tag{A.94}$$

but recall that by definition of the frame $\eta = \mathrm{e}^{B/3}e^{10}$, so that χ necessarily satisfies

$$\gamma_{10}\chi = \chi\,, \qquad\qquad \bar{\chi}\gamma_{\mathsf{a}}\chi = 0\,, \quad \mathsf{a} \neq 10\,. \tag{A.95}$$

These equations tell us that χ is an eigenvector of γ_{10} with unit eigenvalue and $\gamma_{\mathsf{a}}\chi$ is orthogonal to $\bar{\chi}$ when $\mathsf{a} \neq 10$. Similarly, the Kähler 2-form of the GK background is given by

$$J = -\frac{\mathrm{i}}{2}\,\bar{\chi}\gamma_{\mathsf{ab}}\chi\, e^{\mathsf{a}} \wedge e^{\mathsf{b}}\,, \tag{A.96}$$

where $\gamma_{\mathsf{ab}} = \gamma_{[\mathsf{a}}\gamma_{\mathsf{b}]}$. However, one can always choose a frame such that

$$J = e^2 \wedge e^3 + e^4 \wedge e^5 + e^6 \wedge e^7 + e^8 \wedge e^9\,, \tag{A.97}$$

so that $\mathrm{i}\gamma_{23}\chi = \mathrm{i}\gamma_{45}\chi = \mathrm{i}\gamma_{67}\chi = \mathrm{i}\gamma_{89}\chi = \chi$ and $\bar{\chi}\gamma_{\mathsf{ab}}\chi = 0$ for any other combination of indices a, b. As a consequence, one may check that the two sets of spinors

$$\{\chi, \gamma_2\chi, \gamma_4\chi, \gamma_6\chi, \gamma_8\chi\} \quad \text{and} \quad \{\chi, \gamma_3\chi, \gamma_5\chi, \gamma_7\chi, \gamma_9\chi\} \tag{A.98}$$

are both linearly independent. Combining (A.95) with (A.98), we find that (A.93) is solved by setting

$$\begin{cases} c_{\mathsf{a}} = 0\,, \quad \mathsf{a} \neq 10 \\ c_{10} = -1 \end{cases} \qquad \Longrightarrow \qquad \mathrm{vol}_{S^1_{\mathrm{M2}}} = -e^{10} = -\mathrm{e}^{-B/3}\,\eta\,. \tag{A.99}$$

We thus conclude that an M2-brane wrapping $\mathrm{EAdS}_2 \times S^1_{\mathrm{M2}}$ is supersymmetric precisely when the circle direction is aligned with the R-symmetry circle.

Bibliography

[1] A. Boido, J. M. P. Ipiña, and J. Sparks, "Twisted D3-brane and M5-brane compactifications from multi-charge spindles," *JHEP* **07** (2021) 222, arXiv:2104.13287 [hep-th].

[2] A. Boido, J. P. Gauntlett, D. Martelli, and J. Sparks, "Entropy Functions For Accelerating Black Holes," *Phys. Rev. Lett.* **130** no. 9, (2023) 091603, arXiv:2210.16069 [hep-th].

[3] A. Boido, J. P. Gauntlett, D. Martelli, and J. Sparks, "Gravitational Blocks, Spindles and GK Geometry," *Commun. Math. Phys.* **403** no. 2, (2023) 917–1003, arXiv:2211.02662 [hep-th].

[4] A. Boido, A. Lüscher, and J. Sparks, "Matrix models from black hole geometries," *JHEP* **05** (2024) 226, arXiv:2312.11640 [hep-th].

[5] G. 't Hooft, "A Planar Diagram Theory for Strong Interactions," *Nucl. Phys. B* **72** (1974) 461.

[6] J. Polchinski, "Dirichlet Branes and Ramond-Ramond charges," *Phys. Rev. Lett.* **75** (1995) 4724–4727, arXiv:hep-th/9510017.

[7] J. M. Maldacena, "The Large N limit of superconformal field theories and supergravity," *Adv. Theor. Math. Phys.* **2** (1998) 231–252, arXiv:hep-th/9711200.

[8] S. S. Gubser, I. R. Klebanov, and A. M. Polyakov, "Gauge theory correlators from noncritical string theory," *Phys. Lett. B* **428** (1998) 105–114, arXiv:hep-th/9802109.

[9] E. Witten, "Anti-de Sitter space and holography," *Adv. Theor. Math. Phys.* **2** (1998) 253–291, arXiv:hep-th/9802150.

[10] O. Aharony, S. S. Gubser, J. M. Maldacena, H. Ooguri, and Y. Oz, "Large N field theories, string theory and gravity," *Phys. Rept.* **323** (2000) 183–386, arXiv:hep-th/9905111.

[11] H. Nastase, *Introduction to the ADS/CFT Correspondence.* Cambridge University Press, 9, 2015.

[12] J. Penedones, "TASI lectures on AdS/CFT," in *Theoretical Advanced Study Institute in Elementary Particle Physics: New Frontiers in Fields and Strings*, pp. 75–136. 2017. arXiv:1608.04948 [hep-th].

[13] O. Aharony, O. Bergman, D. L. Jafferis, and J. Maldacena, "N=6 superconformal Chern-Simons-matter theories, M2-branes and their gravity duals," *JHEP* **10** (2008) 091, arXiv:0806.1218 [hep-th].

[14] E. Witten, "Some comments on string dynamics," in *STRINGS 95: Future Perspectives in String Theory*, pp. 501–523. 7, 1995. arXiv:hep-th/9507121.

[15] P. Claus, R. Kallosh, and A. Van Proeyen, "M five-brane and superconformal (0,2) tensor multiplet in six-dimensions," *Nucl. Phys. B* **518** (1998) 117–150, arXiv:hep-th/9711161.

[16] J. P. Gauntlett, D. Martelli, S. Pakis, and D. Waldram, "G structures and wrapped NS5-branes," *Commun. Math. Phys.* **247** (2004) 421–445, arXiv:hep-th/0205050.

[17] J. P. Gauntlett and S. Pakis, "The geometry of D = 11 Killing spinors," *JHEP* **04** (2003) 039, arXiv:hep-th/0212008.

[18] J. P. Gauntlett, J. B. Gutowski, and S. Pakis, "The Geometry of D = 11 null Killing spinors," *JHEP* **12** (2003) 049, arXiv:hep-th/0311112.

[19] I. R. Klebanov and E. Witten, "Superconformal field theory on three-branes at a Calabi-Yau singularity," *Nucl. Phys. B* **536** (1998) 199–218, arXiv:hep-th/9807080.

[20] B. S. Acharya, J. M. Figueroa-O'Farrill, C. M. Hull, and B. J. Spence, "Branes at conical singularities and holography," *Adv. Theor. Math. Phys.* **2** (1999) 1249–1286, arXiv:hep-th/9808014.

[21] D. R. Morrison and M. R. Plesser, "Nonspherical horizons. 1.," *Adv. Theor. Math. Phys.* **3** (1999) 1–81, arXiv:hep-th/9810201.

[22] J. P. Gauntlett, D. Martelli, J. Sparks, and D. Waldram, "Sasaki-Einstein metrics on S**2 x S**3," *Adv. Theor. Math. Phys.* **8** no. 4, (2004) 711–734, arXiv:hep-th/0403002.

[23] J. P. Gauntlett, D. Martelli, J. F. Sparks, and D. Waldram, "A New infinite class of Sasaki-Einstein manifolds," *Adv. Theor. Math. Phys.* **8** no. 6, (2004) 987–1000, arXiv:hep-th/0403038.

[24] M. Cvetic, H. Lu, D. N. Page, and C. N. Pope, "New Einstein-Sasaki spaces in five and higher dimensions," *Phys. Rev. Lett.* **95** (2005) 071101, arXiv:hep-th/0504225.

[25] D. Martelli and J. Sparks, "Toric Sasaki-Einstein metrics on S**2 x S**3," *Phys. Lett. B* **621** (2005) 208–212, arXiv:hep-th/0505027.

[26] M. Cvetic, H. Lu, D. N. Page, and C. N. Pope, "New Einstein-Sasaki and Einstein spaces from Kerr-de Sitter," *JHEP* **07** (2009) 082, arXiv:hep-th/0505223.

[27] D. Martelli and J. Sparks, "Toric geometry, Sasaki-Einstein manifolds and a new infinite class of AdS/CFT duals," *Commun. Math. Phys.* **262** (2006) 51–89, arXiv:hep-th/0411238.

[28] S. Benvenuti, S. Franco, A. Hanany, D. Martelli, and J. Sparks, "An Infinite family of superconformal quiver gauge theories with Sasaki-Einstein duals," *JHEP* **06** (2005) 064, arXiv:hep-th/0411264.

[29] A. Butti, D. Forcella, and A. Zaffaroni, "The Dual superconformal theory for L**pqr manifolds," *JHEP* **09** (2005) 018, arXiv:hep-th/0505220.

[30] S. Franco, A. Hanany, K. D. Kennaway, D. Vegh, and B. Wecht, "Brane dimers and quiver gauge theories," *JHEP* **01** (2006) 096, arXiv:hep-th/0504110.

[31] S. Gukov, C. Vafa, and E. Witten, "CFT's from Calabi-Yau four folds," *Nucl. Phys. B* **584** (2000) 69–108, arXiv:hep-th/9906070. [Erratum: Nucl.Phys.B 608, 477–478 (2001)].

[32] D. Fabbri, P. Fre', L. Gualtieri, C. Reina, A. Tomasiello, A. Zaffaroni, and A. Zampa, "3-D superconformal theories from Sasakian seven manifolds: New nontrivial evidences for AdS(4) / CFT(3)," *Nucl. Phys. B* **577** (2000) 547–608, arXiv:hep-th/9907219.

[33] M. Billo, D. Fabbri, P. Fre, P. Merlatti, and A. Zaffaroni, "Rings of short N=3 superfields in three-dimensions and M theory on AdS(4) x N**(0,1,0)," *Class. Quant. Grav.* **18** (2001) 1269–1290, arXiv:hep-th/0005219.

[34] D. Martelli and J. Sparks, "Moduli spaces of Chern-Simons quiver gauge theories and AdS(4)/CFT(3)," *Phys. Rev. D* **78** (2008) 126005, arXiv:0808.0912 [hep-th].

[35] N. Kim, "AdS_3 solutions of IIB supergravity from D3-branes," *JHEP* **01** (2006) 094, arXiv:hep-th/0511029 [hep-th].

[36] N. Kim and J.-D. Park, "Comments on AdS(2) solutions of D = 11 supergravity," *JHEP* **09** (2006) 041, arXiv:hep-th/0607093.

[37] J. P. Gauntlett and N. Kim, "Geometries with Killing Spinors and Supersymmetric AdS Solutions," *Commun. Math. Phys.* **284** (2008) 897–918, arXiv:0710.2590 [hep-th].

[38] J. P. Gauntlett, O. A. P. Mac Conamhna, T. Mateos, and D. Waldram, "Supersymmetric AdS(3) solutions of type IIB supergravity," *Phys. Rev. Lett.* **97** (2006) 171601, arXiv:hep-th/0606221 [hep-th].

[39] F. Benini, N. Bobev, and P. M. Crichigno, "Two-dimensional SCFTs from D3-branes," *JHEP* **07** (2016) 020, arXiv:1511.09462 [hep-th].

[40] J. M. Maldacena and C. Nunez, "Supergravity description of field theories on curved manifolds and a no go theorem," *Int.J.Mod.Phys.* **A16** (2001) 822–855, arXiv:hep-th/0007018 [hep-th].

[41] J. P. Gauntlett, N. Kim, and D. Waldram, "M-fivebranes wrapped on supersymmetric cycles," *Phys. Rev.* **D63** (2001) 126001, arXiv:hep-th/0012195.

[42] D. Gaiotto and J. Maldacena, "The Gravity duals of N=2 superconformal field theories," *JHEP* **10** (2012) 189, arXiv:0904.4466 [hep-th].

[43] M. T. Anderson, C. Beem, N. Bobev, and L. Rastelli, "Holographic Uniformization," *Commun. Math. Phys.* **318** (2013) 429–471, arXiv:1109.3724 [hep-th].

[44] E. Witten, "Topological Quantum Field Theory," *Commun. Math. Phys.* **117** (1988) 353.

[45] M. Bershadsky, C. Vafa, and V. Sadov, "D-branes and topological field theories," *Nucl. Phys. B* **463** (1996) 420–434, arXiv:hep-th/9511222.

[46] G. Festuccia and N. Seiberg, "Rigid Supersymmetric Theories in Curved Superspace," *JHEP* **06** (2011) 114, arXiv:1105.0689 [hep-th].

[47] P. Ferrero, J. P. Gauntlett, J. M. Pérez Ipiña, D. Martelli, and J. Sparks, "D3-Branes Wrapped on a Spindle," *Phys. Rev. Lett.* **126** no. 11, (2021) 111601, arXiv:2011.10579 [hep-th].

[48] P. Ferrero, J. P. Gauntlett, J. M. P. Ipiña, D. Martelli, and J. Sparks, "Accelerating black holes and spinning spindles," *Phys. Rev. D* **104** no. 4, (2021) 046007, arXiv:2012.08530 [hep-th].

[49] J. D. Bekenstein, "Black holes and the second law," *Lett. Nuovo Cim.* **4** (1972) 737–740.

[50] J. D. Bekenstein, "Black holes and entropy," *Phys. Rev. D* **7** (1973) 2333–2346.

[51] J. M. Bardeen, B. Carter, and S. W. Hawking, "The Four laws of black hole mechanics," *Commun. Math. Phys.* **31** (1973) 161–170.

[52] S. W. Hawking, "Particle Creation by Black Holes," *Commun. Math. Phys.* **43** (1975) 199–220. [Erratum: Commun.Math.Phys. 46, 206 (1976)].

[53] A. Sen, "Extremal black holes and elementary string states," *Mod. Phys. Lett. A* **10** (1995) 2081–2094, arXiv:hep-th/9504147.

[54] A. Strominger and C. Vafa, "Microscopic origin of the Bekenstein-Hawking entropy," *Phys. Lett. B* **379** (1996) 99–104, arXiv:hep-th/9601029.

[55] J. Kinney, J. M. Maldacena, S. Minwalla, and S. Raju, "An Index for 4 dimensional super conformal theories," *Commun. Math. Phys.* **275** (2007) 209–254, arXiv:hep-th/0510251.

[56] F. Benini, K. Hristov, and A. Zaffaroni, "Black hole microstates in AdS_4 from supersymmetric localization," *JHEP* **05** (2016) 054, arXiv:1511.04085 [hep-th].

[57] V. Pestun, "Localization of gauge theory on a four-sphere and supersymmetric Wilson loops," *Commun. Math. Phys.* **313** (2012) 71–129, arXiv:0712.2824 [hep-th].

[58] V. Pestun *et al.*, "Localization techniques in quantum field theories," *J. Phys. A* **50** no. 44, (2017) 440301, arXiv:1608.02952 [hep-th].

[59] A. Zaffaroni, "AdS black holes, holography and localization," *Living Rev. Rel.* **23** no. 1, (2020) 2, arXiv:1902.07176 [hep-th].

[60] A. H. Chamseddine and W. A. Sabra, "Magnetic strings in five-dimensional gauged supergravity theories," *Phys. Lett. B* **477** (2000) 329–334, arXiv:hep-th/9911195.

[61] D. Klemm and W. A. Sabra, "Supersymmetry of black strings in D = 5 gauged supergravities," *Phys. Rev. D* **62** (2000) 024003, arXiv:hep-th/0001131.

[62] J. Brown and M. Henneaux, "Central Charges in the Canonical Realization of Asymptotic Symmetries: An Example from Three-Dimensional Gravity," *Commun. Math. Phys.* **104** (1986) 207–226.

[63] K. A. Intriligator and B. Wecht, "The Exact superconformal R symmetry maximizes *a*," *Nucl. Phys.* **B667** (2003) 183–200, arXiv:hep-th/0304128 [hep-th].

[64] D. L. Jafferis, "The Exact Superconformal R-Symmetry Extremizes Z," *JHEP* **05** (2012) 159, arXiv:1012.3210 [hep-th].

[65] F. Benini and N. Bobev, "Exact two-dimensional superconformal R-symmetry and c-extremization," *Phys. Rev. Lett.* **110** no. 6, (2013) 061601, arXiv:1211.4030 [hep-th].

[66] D. Martelli, J. Sparks, and S.-T. Yau, "The Geometric dual of a-maximisation for Toric Sasaki-Einstein manifolds," *Commun. Math. Phys.* **268** (2006) 39–65, arXiv:hep-th/0503183 [hep-th].

[67] D. Martelli, J. Sparks, and S.-T. Yau, "Sasaki-Einstein manifolds and volume minimisation," *Commun. Math. Phys.* **280** (2008) 611–673, arXiv:hep-th/0603021 [hep-th].

[68] C. Couzens, J. P. Gauntlett, D. Martelli, and J. Sparks, "A geometric dual of c-extremization," *JHEP* **01** (2019) 212, arXiv:1810.11026 [hep-th].

[69] J. Sparks, "Sasaki-Einstein Manifolds," *Surveys Diff. Geom.* **16** (2011) 265–324, arXiv:1004.2461 [math.DG].

[70] J. P. Gauntlett, D. Martelli, and J. Sparks, "Toric geometry and the dual of c-extremization," *JHEP* **01** (2019) 204, arXiv:1812.05597 [hep-th].

[71] P. Ferrero, J. P. Gauntlett, and J. Sparks, "Supersymmetric spindles," *JHEP* **01** (2022) 102, arXiv:2112.01543 [hep-th].

[72] F. Benini and N. Bobev, "Two-dimensional SCFTs from wrapped branes and c-extremization," *JHEP* **06** (2013) 005, arXiv:1302.4451 [hep-th].

[73] S. M. Hosseini, K. Hristov, and A. Zaffaroni, "Rotating multi-charge spindles and their microstates," *JHEP* **07** (4, 2021) 182, arXiv:2104.11249 [hep-th].

[74] I. Arav, J. P. Gauntlett, M. M. Roberts, and C. Rosen, "Leigh-Strassler compactified on a spindle," *JHEP* **10** (2022) 067, arXiv:2207.06427 [hep-th].

[75] M. Suh, "Baryonic spindles from conifolds," arXiv:2304.03308 [hep-th].

[76] A. Amariti, N. Petri, and A. Segati, "$T^{1,1}$ truncation on the spindle," *JHEP* **07** (2023) 087, arXiv:2304.03663 [hep-th].

[77] P. Ferrero, M. Inglese, D. Martelli, and J. Sparks, "Multicharge accelerating black holes and spinning spindles," *Phys. Rev. D* **105** no. 12, (2022) 126001, arXiv:2109.14625 [hep-th].

[78] C. Couzens, K. Stemerdink, and D. van de Heisteeg, "M2-branes on discs and multi-charged spindles," *JHEP* **04** (2022) 107, arXiv:2110.00571 [hep-th].

[79] C. Couzens, "A tale of (M)2 twists," *JHEP* **03** (2022) 078, arXiv:2112.04462 [hep-th].

[80] M. Suh, "Spindle black holes and mass-deformed ABJM," *JHEP* **05** (2024) 267, arXiv:2211.11782 [hep-th].

[81] K. Hristov and M. Suh, "Spindle black holes in $AdS_4\times$ SE_7," *JHEP* **10** (2023) 141, arXiv:2307.10378 [hep-th].

[82] P. Ferrero, J. P. Gauntlett, D. Martelli, and J. Sparks, "M5-branes wrapped on a spindle," *JHEP* **11** (2021) 002, arXiv:2105.13344 [hep-th].

[83] M. Suh, "M5-branes and D4-branes wrapped on a direct product of spindle and Riemann surface," *JHEP* **02** (2024) 205, arXiv:2207.00034 [hep-th].

[84] C. Couzens and K. Stemerdink, "Universal spindles: D2's on Σ and M5's on $\Sigma \times \mathbb{H}^3$," arXiv:2207.06449 [hep-th].

[85] A. Amariti, S. Mancani, D. Morgante, N. Petri, and A. Segati, "BBBW on the spindle," arXiv:2309.11362 [hep-th].

[86] F. Faedo and D. Martelli, "D4-branes wrapped on a spindle," *JHEP* **02** (2022) 101, arXiv:2111.13660 [hep-th].

[87] S. Giri, "Black holes with spindles at the horizon," *JHEP* **06** (2022) 145, arXiv:2112.04431 [hep-th].

[88] P. Ferrero, "D6 branes wrapped on a spindle and $Y^{p,q}$ manifolds," *JHEP* **05** (2024) 182, arXiv:2403.03988 [hep-th].

[89] D. Cassani, J. P. Gauntlett, D. Martelli, and J. Sparks, "Thermodynamics of accelerating and supersymmetric AdS4 black holes," *Phys. Rev. D* **104** no. 8, (2021) 086005, arXiv:2106.05571 [hep-th].

[90] H. Kim, N. Kim, Y. Lee, and A. Poole, "Thermodynamics of accelerating AdS_4 black holes from the covariant phase space," *Eur. Phys. J. C* **83** no. 12, (2023) 1095, arXiv:2306.16187 [hep-th].

[91] F. Faedo, A. Fontanarossa, and D. Martelli, "Branes wrapped on orbifolds and their gravitational blocks," *Lett. Math. Phys.* **113** no. 3, (2023) 51, arXiv:2210.16128 [hep-th].

[92] S. M. Hosseini, "Gravitational blocks: Symplectic covariance unveiled," *Phys. Lett. B* **843** (2023) 138044, arXiv:2303.07365 [hep-th].

[93] M. Inglese, D. Martelli, and A. Pittelli, "Supersymmetry and Localization on Three-Dimensional Orbifolds," arXiv:2312.17086 [hep-th].

[94] M. Inglese, D. Martelli, and A. Pittelli, "The spindle index from localization," *J. Phys. A* **57** no. 8, (2024) 085401, arXiv:2303.14199 [hep-th].

[95] E. Colombo, S. M. Hosseini, D. Martelli, A. Pittelli, and A. Zaffaroni, "Microstates of accelerating and supersymmetric AdS_4 black holes from the spindle index," arXiv:2404.07173 [hep-th].

[96] K. C. M. Cheung, J. H. T. Fry, J. P. Gauntlett, and J. Sparks, "M5-branes wrapped on four-dimensional orbifolds," *JHEP* **08** (2022) 082, arXiv:2204.02990 [hep-th].

[97] C. Couzens, H. Kim, N. Kim, Y. Lee, and M. Suh, "D4-branes wrapped on four-dimensional orbifolds through consistent truncation," *JHEP* **02** (2023) 025, arXiv:2210.15695 [hep-th].

[98] F. Faedo, A. Fontanarossa, and D. Martelli, "Branes wrapped on quadrilaterals," arXiv:2402.08724 [hep-th].

[99] A. Pittelli, "Orbifold Indices in Four Dimensions," arXiv:2403.12318 [hep-th].

[100] P. Benetti Genolini, J. M. Perez Ipiña, and J. Sparks, "Localization of the action in AdS/CFT," *JHEP* **10** (2019) 252, arXiv:1906.11249 [hep-th].

[101] P. Benetti Genolini, J. P. Gauntlett, and J. Sparks, "Equivariant Localization in Supergravity," *Phys. Rev. Lett.* **131** no. 12, (2023) 121602, arXiv:2306.03868 [hep-th].

[102] D. Martelli and A. Zaffaroni, "Equivariant localization and holography," *Lett. Math. Phys.* **114** no. 1, (2024) 15, arXiv:2306.03891 [hep-th].

[103] E. Colombo, F. Faedo, D. Martelli, and A. Zaffaroni, "Equivariant volume extremization and holography," *JHEP* **01** (2024) 095, arXiv:2309.04425 [hep-th].

[104] P. Benetti Genolini, J. P. Gauntlett, and J. Sparks, "Localizing wrapped M5-branes and gravitational blocks," *Phys. Rev. D* **108** no. 10, (2023) L101903, arXiv:2308.10933 [hep-th].

[105] P. Benetti Genolini, J. P. Gauntlett, Y. Jiao, A. Lüscher, and J. Sparks, "Localization and attraction," *JHEP* **05** (2024) 152, arXiv:2401.10977 [hep-th].

[106] C. Couzens and A. Lüscher, "A geometric dual of F-maximization in massive type IIA," arXiv:2406.15547 [hep-th].

[107] P. Benetti Genolini, J. P. Gauntlett, Y. Jiao, A. Lüscher, and J. Sparks, "Localization of the free energy in supergravity," arXiv:2407.02554 [hep-th].

[108] I. Bah, F. Bonetti, R. Minasian, and E. Nardoni, "Holographic Duals of Argyres-Douglas Theories," *Phys. Rev. Lett.* **127** no. 21, (2021) 211601, arXiv:2105.11567 [hep-th].

[109] I. Bah, F. Bonetti, R. Minasian, and E. Nardoni, "M5-brane sources, holography, and Argyres-Douglas theories," *JHEP* **11** (2021) 140, arXiv:2106.01322 [hep-th].

[110] M. Suh, "D3-branes and M5-branes wrapped on a topological disc," *JHEP* **03** (2022) 043, arXiv:2108.01105 [hep-th].

[111] M. Suh, "D4-branes wrapped on a topological disk," *JHEP* **06** (2023) 008, arXiv:2108.08326 [hep-th].

[112] P. Karndumri and P. Nuchino, "Five-branes wrapped on topological disks from 7D N=2 gauged supergravity," *Phys. Rev. D* **105** no. 6, (2022) 066010, arXiv:2201.05037 [hep-th].

[113] C. Couzens, H. Kim, N. Kim, and Y. Lee, "Holographic duals of M5-branes on an irregularly punctured sphere," *JHEP* **07** (2022) 102, arXiv:2204.13537 [hep-th].

[114] P. Bomans, C. Couzens, Y. Lee, and S. Ning, "Symmetry breaking and consistent truncations from M5-branes wrapping a disc," *JHEP* **01** (2024) 088, arXiv:2308.08616 [hep-th].

[115] C. Couzens, M. J. Kang, C. Lawrie, and Y. Lee, "Holographic duals of Higgsed $\mathcal{D}_p^b(BCD)$," arXiv:2312.12503 [hep-th].

[116] P. Bomans and C. Couzens, "On the Class $\mathcal{S}$ Origin of Spindle Solutions," arXiv:2404.08083 [hep-th].

[117] M. Gutperle and N. Klein, "A note on co-dimension 2 defects in N=4,d=7 gauged supergravity," *Nucl. Phys. B* **984** (2022) 115969, arXiv:2203.13839 [hep-th].

[118] M. Gutperle, N. Klein, and D. Rathore, "Holographic 6d co-dimension 2 defect solutions in M-theory," *JHEP* **11** (2023) 191, arXiv:2304.12899 [hep-th].

[119] J. P. Gauntlett, D. Martelli, and J. Sparks, "Toric geometry and the dual of $\mathcal{I}$-extremization," *JHEP* **06** (2019) 140, arXiv:1904.04282 [hep-th].

[120] J. P. Gauntlett, N. Kim, and D. Waldram, "Supersymmetric AdS(3), AdS(2) and Bubble Solutions," *JHEP* **04** (2007) 005, arXiv:hep-th/0612253 [hep-th].

[121] M. Cvetic *et al.*, "Embedding AdS black holes in ten and eleven dimensions," *Nucl. Phys.* **B558** (1999) 96–126, arXiv:hep-th/9903214.

[122] H. K. Kunduri and J. Lucietti, "Near-horizon geometries of supersymmetric AdS(5) black holes," *JHEP* **12** (2007) 015, arXiv:0708.3695 [hep-th].

[123] I. Bah, C. Beem, N. Bobev, and B. Wecht, "Four-Dimensional SCFTs from M5-Branes," *JHEP* **1206** (2012) 005, arXiv:1203.0303 [hep-th].

[124] S. M. Hosseini, K. Hristov, and A. Zaffaroni, "Gluing gravitational blocks for AdS black holes," *JHEP* **12** (2019) 168, arXiv:1909.10550 [hep-th].

[125] S. M. Hosseini, I. Yaakov, and A. Zaffaroni, "The joy of factorization at large N: five-dimensional indices and AdS black holes," *JHEP* **02** (2022) 097, arXiv:2111.03069 [hep-th].

[126] K. Hristov, "4d $\mathcal{N} = 2$ supergravity observables from Nekrasov-like partition functions," *JHEP* **02** (2022) 079, arXiv:2111.06903 [hep-th].

[127] S. M. Hosseini and A. Zaffaroni, "Geometry of $\mathcal{I}$-extremization and black holes microstates," *JHEP* **07** (2019) 174, arXiv:1904.04269 [hep-th].

[128] D. Martelli and J. Sparks, "AdS_4/CFT_3 duals from M2-branes at hypersurface singularities and their deformations," *JHEP* **12** (2009) 017, arXiv:0909.2036 [hep-th].

[129] S. Franco, A. Hanany, D. Martelli, J. Sparks, D. Vegh, and B. Wecht, "Gauge theories from toric geometry and brane tilings," *JHEP* **01** (2006) 128, arXiv:hep-th/0505211 [hep-th].

[130] A. Butti and A. Zaffaroni, "R-charges from toric diagrams and the equivalence of a-maximization and Z-minimization," *JHEP* **11** (2005) 019, arXiv:hep-th/0506232 [hep-th].

[131] D. Martelli and J. Sparks, "Notes on toric Sasaki-Einstein seven-manifolds and AdS(4) / CFT(3)," *JHEP* **11** (2008) 016, arXiv:0808.0904 [hep-th].

[132] J. P. Gauntlett, D. Martelli, and J. Sparks, "Fibred GK geometry and supersymmetric *AdS* solutions," *JHEP* **11** (2019) 176, arXiv:1910.08078 [hep-th].

[133] S. M. Hosseini, K. Hristov, Y. Tachikawa, and A. Zaffaroni, "Anomalies, Black strings and the charged Cardy formula," *JHEP* **09** (2020) 167, arXiv:2006.08629 [hep-th].

[134] D. R. Gulotta, C. P. Herzog, and S. S. Pufu, "Operator Counting and Eigenvalue Distributions for 3D Supersymmetric Gauge Theories," *JHEP* **11** (2011) 149, arXiv:1106.5484 [hep-th].

[135] D. Farquet and J. Sparks, "Wilson loops and the geometry of matrix models in AdS_4/CFT_3," *JHEP* **01** (2014) 083, arXiv:1304.0784 [hep-th].

[136] D. Farquet and J. Sparks, "Wilson loops on three-manifolds and their M2-brane duals," *JHEP* **12** (2014) 173, arXiv:1406.2493 [hep-th].

[137] F. Benini, C. Closset, and S. Cremonesi, "Chiral flavors and M2-branes at toric CY4 singularities," *JHEP* **02** (2010) 036, arXiv:0911.4127 [hep-th].

[138] D. L. Jafferis, "Quantum corrections to $\mathcal{N} = 2$ Chern-Simons theories with flavor and their AdS_4 duals," *JHEP* **08** (2013) 046, arXiv:0911.4324 [hep-th].

[139] M. Aganagic, "A Stringy Origin of M2 Brane Chern-Simons Theories," *Nucl. Phys. B* **835** (2010) 1–28, arXiv:0905.3415 [hep-th].

[140] D. Gaiotto and A. Tomasiello, "The gauge dual of Romans mass," *JHEP* **01** (2010) 015, arXiv:0901.0969 [hep-th].

[141] F. Benini and A. Zaffaroni, "A topologically twisted index for three-dimensional supersymmetric theories," *JHEP* **07** (2015) 127, arXiv:1504.03698 [hep-th].

[142] F. Benini and A. Zaffaroni, "Supersymmetric partition functions on Riemann surfaces," *Proc. Symp. Pure Math.* **96** (2017) 13–46, arXiv:1605.06120 [hep-th].

[143] S. M. Hosseini and A. Zaffaroni, "Large N matrix models for 3d $\mathcal{N} = 2$ theories: twisted index, free energy and black holes," *JHEP* **08** (2016) 064, arXiv:1604.03122 [hep-th].

[144] S. M. Hosseini and N. Mekareeya, "Large N topologically twisted index: necklace quivers, dualities, and Sasaki-Einstein spaces," *JHEP* **08** (2016) 089, arXiv:1604.03397 [hep-th].

[145] D. Berenstein, C. P. Herzog, and I. R. Klebanov, "Baryon spectra and AdS /CFT correspondence," *JHEP* **06** (2002) 047, arXiv:hep-th/0202150 [hep-th].

[146] F. Kirwan, "Momentum maps and reduction in algebraic geometry," *Differential Geometry and its Applications* **9** no. 1, (1998) 135–171.

[147] S.-y. Wu, "An Integration formula for the square of moment maps of circle actions," *Lett. Math. Phys.* **29** (1993) 311–328, arXiv:hep-th/9212071.

[148] E. Bergshoeff, E. Sezgin, and P. K. Townsend, "Supermembranes and Eleven-Dimensional Supergravity," *Phys. Lett. B* **189** (1987) 75–78.

[149] J. P. Gauntlett, "Branes, calibrations and supergravity," arXiv:hep-th/0305074 [hep-th].

[150] L.-Y. Hung, R. C. Myers, M. Smolkin, and A. Yale, "Holographic Calculations of Renyi Entropy," *JHEP* **12** (2011) 047, arXiv:1110.1084 [hep-th].

[151] J. M. Maldacena, "Wilson loops in large N field theories," *Phys. Rev. Lett.* **80** (1998) 4859–4862, arXiv:hep-th/9803002.

[152] E. Witten, "Anti-de Sitter space, thermal phase transition, and confinement in gauge theories," *Adv. Theor. Math. Phys.* **2** (1998) 505–532, arXiv:hep-th/9803131.

[153] F. Azzurli, N. Bobev, P. M. Crichigno, V. S. Min, and A. Zaffaroni, "A universal counting of black hole microstates in AdS_4," *JHEP* **02** (2018) 054, arXiv:1707.04257 [hep-th].

[154] S. M. Hosseini and A. Zaffaroni, "The large N limit of topologically twisted indices: a direct approach," *JHEP* **12** (2022) 025, arXiv:2209.09274 [hep-th].

[155] K. Hristov, S. Katmadas, and C. Toldo, "Rotating attractors and BPS black holes in AdS_4," *JHEP* **01** (2019) 199, arXiv:1811.00292 [hep-th].

[156] J. P. Gauntlett and O. Varela, "Consistent Kaluza-Klein Reductions for General Supersymmetric AdS Solutions," *Phys. Rev.* **D76** (2007) 126007, arXiv:0707.2315 [hep-th].

[157] C. Beem, T. Dimofte, and S. Pasquetti, "Holomorphic Blocks in Three Dimensions," *JHEP* **12** (2014) 177, arXiv:1211.1986 [hep-th].

[158] S. M. Hosseini and A. Zaffaroni, "Proving the equivalence of c-extremization and its gravitational dual for all toric quivers," *JHEP* **03** (2019) 108, arXiv:1901.05977 [hep-th].

[159] A. Ashmore, "N = (2, 0) AdS_3 solutions of M-theory," *JHEP* **05** (2023) 101, arXiv:2209.10680 [hep-th].

[160] C. Couzens, E. Marcus, K. Stemerdink, and D. van de Heisteeg, "The Near-Horizon Geometry of Supersymmetric Rotating AdS_4 Black Holes in M-theory," arXiv:2011.07071 [hep-th].

[161] N. Bobev, A. M. Charles, K. Hristov, and V. Reys, "The Unreasonable Effectiveness of Higher-Derivative Supergravity in AdS_4 Holography," *Phys. Rev. Lett.* **125** no. 13, (2020) 131601, arXiv:2006.09390 [hep-th].

[162] N. Bobev, A. M. Charles, K. Hristov, and V. Reys, "Higher-derivative supergravity, AdS_4 holography, and black holes," *JHEP* **08** (2021) 173, arXiv:2106.04581 [hep-th].

[163] N. Bobev, J. Hong, and V. Reys, "Large N Partition Functions, Holography, and Black Holes," *Phys. Rev. Lett.* **129** no. 4, (2022) 041602, arXiv:2203.14981 [hep-th].

[164] N. Bobev, J. Hong, and V. Reys, "Large N partition functions of 3d holographic SCFTs," *JHEP* **08** (2023) 119, arXiv:2304.01734 [hep-th].

[165] D. L. Jafferis, I. R. Klebanov, S. S. Pufu, and B. R. Safdi, "Towards the F-Theorem: N=2 Field Theories on the Three-Sphere," *JHEP* **06** (2011) 102, arXiv:1103.1181 [hep-th].

[166] H. Kim and N. Kim, "Black holes with baryonic charge and $\mathcal{I}$-extremization," *JHEP* **11** (2019) 050, arXiv:1904.05344 [hep-th].

[167] S. Benvenuti, L. A. Pando Zayas, and Y. Tachikawa, "Triangle anomalies from Einstein manifolds," *Adv. Theor. Math. Phys.* **10** no. 3, (2006) 395–432, arXiv:hep-th/0601054.

[168] I. Bah, F. Bonetti, R. Minasian, and E. Nardoni, "Anomalies of QFTs from M-theory and Holography," *JHEP* **01** (2020) 125, arXiv:1910.04166 [hep-th].

[169] I. Bah, F. Bonetti, R. Minasian, and P. Weck, "Anomaly Inflow Methods for SCFT Constructions in Type IIB," *JHEP* **02** (2021) 116, arXiv:2002.10466 [hep-th].

[170] K. Becker, M. Becker, and A. Strominger, "Five-branes, membranes and nonperturbative string theory," *Nucl. Phys. B* **456** (1995) 130–152, arXiv:hep-th/9507158.